Biennial Report

Zweijahresbericht 2018/2019

Leibniz Association

TROPOS

Leibniz Institute for Tropospheric Research

Leibniz Institute for
Tropospheric Research

Leibniz
Association

Imprint

Published by
TROPOS
Leibniz Institute for Tropospheric Research
Leibniz-Institut für Troposphärenforschung e.V. Leipzig
Member of the Leibniz Association (WGL)

Permoserstraße 15
04318 Leipzig
Germany

Phone: ++49 (341) 2717-7060
Fax: ++49 (341) 2717-99-7060
Email: info@tropos.de
Internet: http://www.tropos.de

Copy editors
Katja Schmieder, Konstanze Kunze, Kerstin Müller,
Heike Scherf, Beate Richter, Tilo Arnhold (Photographer)

Editorial board
Andres Macke, Hartmut Herrmann, Ina Tegen,
Ulla Wandinger, Alfred Wiedensohler

Photo and illustration credits © TROPOS / as described in the captions
p. 1: top - M. Pedoussaut / ESA
middle - Tilo Arnhold / TROPOS
bottom - Esther Horvath / Alfred-Wegener-Institut
p. 37: top - Alfred-Wegener-Institut / Stephan Schön, Sächsische Zeitung
middle - Dietrich Althausen / TROPOS
bottom - Tilo Arnhold / TROPOS
p. 145: top - Tilo Arnhold / TROPOS
middle - Tilo Arnhold / TROPOS
bottom - Ronny Engelmann / TROPOS

Table of contents

Table of contents

Introduction / Einleitung

Overview / Übersicht

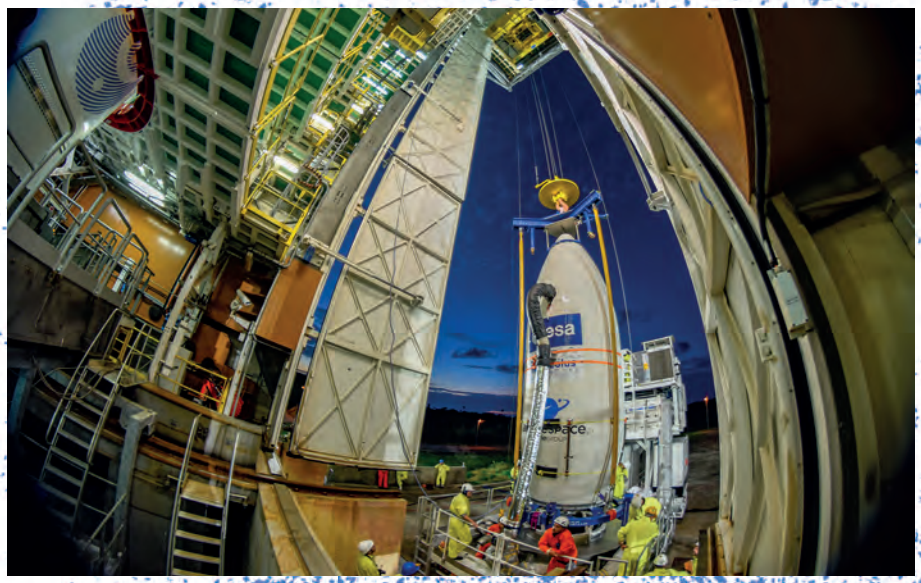

Introduction

Since 1992 the Leibniz Institute for Tropospheric Research (TROPOS) is located in the “Research Park Leipzig/Permoserstraße” close to the Helmholtz Centre for Environmental Research, the Leibniz-Institute for Surface Modification and other research institutions. Its name identifies TROPOS as a member of the Leibniz Association. The institute is funded by

Fig. / Abb. 1: TROPOS main building. / TROPOS-Hauptgebäude. (Photo: Patric Seifert / TROPOS)

the Free State of Saxony and the Federal Ministry of Education and Research with a basic budget of approx. 10.164 million euros, approx. 7 million euros per year are raised in third-party funds. TROPOS employs a total of 158 people, 75 of whom are scientists.

The institute was founded to research physical and chemical processes in the polluted troposphere. Over the years a well-defined and globally unique research profile of TROPOS emerged. Today, the focus is on the physical and chemical interactions between atmospheric small airborne particles (aerosol particles) and cloud particles. Despite their minute absolute amount, aerosol and cloud particles are essential parts of the atmosphere because

Fig. / Abb. 2: The new TROPOS chemistry laboratory. / Des neue TROPOS-Chemielaborgebäudes. (Photo: Tilo Arnhold / TROPOS)

Einleitung

Im Wissenschaftspark Leipzig/Permoserstraße befindet sich seit 1992 das Leibniz-Institut für Troposphärenforschung e. V. (TROPOS) in Nachbarschaft zum Helmholtz-Zentrum für Umweltforschung, zum Leibniz-Institut für Oberflächenmodifizierung sowie weiteren Einrichtungen. Sein Name weist es als Mitglied der Wissenschaftsgemeinschaft Gottfried Wilhelm Leibniz aus.

Das Institut wird vom Freistaat Sachsen und dem Bundesministerium für Bildung und Forschung mit einem Grundetat von ca. 10,164 Millionen Euro gefördert, ca. 7 Millionen pro Jahr werden an Drittmitteln eingeworben.

Am TROPOS sind insgesamt 158 Mitarbeitende beschäftigt, davon 75 Wissenschaftlerinnen und Wissenschaftler. Gegründet wurde das TROPOS zur Erforschung physikalischer und chemischer Prozesse in der belasteten Troposphäre.

Das TROPOS hat ein klares und weltweit einzigartiges Forschungsprofil herausgebildet, in dessen Mittelpunkt heute die physikalischen und chemischen Wechselwirkungen zwischen atmosphärischen

Fig. / Abb. 3: TROPOS cloud laboratory. / TROPOS-Wolkenlabor. (Photo: Tilo Arnhold / TROPOS)

Schwebeteilchen (Aerosolpartikeln) und Wolkenpartikeln stehen. Trotz geringster absoluter Mengen sind diese Partikel wesentliche Bestandteile der Atmosphäre, weil sie den Energie-, Wasser- und Spurenstoffhaushalt des Erdsystems beeinflussen. Menschliche Aktivitäten können die Eigenschaften dieser hochdispersen Systeme verändern und damit sowohl direkt als auch indirekt auf den Menschen zurückwirken. Beispielhaft seien hier die gesundheitliche Wirkung eingeatmeter Partikel und Nebeltröpfchen und die regionalen und globalen Klimaänderungen genannt.

Trotz dieser wichtigen Beziehungen zwischen Mensch auf der einen sowie Aerosolen und Wolken auf der anderen Seite müssen die

Fig. / Abb. 4: The first station in Central Asia within the global dust belt of the worldwide atmosphere network PollyNet started operations in Dushanbe, the capital of Tajikistan. / Die erste Station des weltweiten Atmosphärennetzwerks PollyNet in Zentralasien und damit innerhalb des globalen Staubgürtels nahm in Duschanbe, der Hauptstadt Tadschikistans, ihren Betrieb auf. (Photo: Dietrich Althausen / TROPOS)

they control the budgets of energy, water and trace substances of the Earth System. Human activities can change these highly disperse systems and thus directly as well as indirectly feedback on human beings. This occurs for example via health effects caused by inhaled particles and fog droplets and also through regional and global climate change.

Despite these strong connections between human beings, aerosols, and clouds, the important physico-chemical processes of aerosol and cloud formation and the relationships with climate and health still need to be investigated to a large extent. This is mainly due to difficulties with analysing the very small samples and because of the complex behaviour of tropospheric multiphase systems, in which individual processes seldom can clearly be distinguished. In climate research this limitation is reflected in much larger uncertainties in predicted anthropogenic aerosol and cloud effects in comparison to the greenhouse effects of gases.

To gain rapid advances in our process understanding of the tropospheric multiphase system and to improve the application of this process understanding in the prediction of human impacts in this system field studies, laboratory and model studies are developed and performed. These three approaches for the investigation of aerosols and clouds are closely coordinated and constitute an overall process understanding of atmospheric multiphase systems.

The long-term measurements, to a large extend initiated by TROPOS, increasingly enable the identification of trends in regional and large-scale aerosol distribution.

physiko-chemischen Prozesse von Aerosol- und Wolkenbildung und die Wechselwirkungen mit Gesundheit und Klima zu einem großen Teil noch erforscht werden. Gründe dafür sind Schwierigkeiten bei der Analyse der beteiligten kleinsten Stoffmengen und das komplexe Verhalten atmosphärischer Mehrphasensysteme, deren Einzelprozesse in der Atmosphäre nicht klar getrennt beobachtet werden können. Im gegenwärtigen Sachstand zum globalen Klimawandel spiegelt sich diese Komplexität in den sehr viel größeren Unsicherheiten in allen zu Aerosol- und Wolkenwirkung veröffentlichten Zahlen im Vergleich zu den Treibhauseffekten der Gase wieder.

Um raschen Zuwachs im Prozessverständnis troposphärischer Mehrphasenprozesse zu erreichen und dessen Anwendung auf die Vorhersage der Folgen menschlicher Eingriffe zu verbessern, werden am TROPOS aufeinander abgestimmte Feld-, Labor und Modellstudien zur Untersuchung von Aerosolpartikeln und Wolken entwickelt und durchgeführt, so dass sie den Rahmen für ein umfassendes Prozessverständnis atmosphärischer Multiphasensysteme bilden. Die vom TROPOS maßgeblich initiierten Langzeitmessungen erlauben mehr und mehr auch die Erfassung von Trends in der regionalen und großräumigen Aerosolverteilung.

Feldexperimente und Prozessstudien

Die Feldexperimente des Instituts dienen der Aufklärung des atmosphärischen Kreislaufs der Aerosol- und Wolkenpartikel und der damit

Fig. / Abb. 5: During leg 2 of the MOSAiC expedition, PhD student Hannes Griesche is in charge of the OCEANET container on Polarstern and thus the TROPOS lidar. He replaced Dr. Ronny Engelmann in mid-December 2019 and will experience the coldest time of the Arctic expedition until the next change in mid-February. / Doktorand Hannes Griesche betreut während Fahrtabschnitt 2 der MOSAiC-Expedition den OCEANET-Container auf der Polarstern und damit das TROPOS-Lidar. Er hat Mitte Dezember 2019 Dr. Ronny Engelmann abgelöst und wird die kälteste Zeit der Arktis-Expedition erleben bis zum nächsten Wechsel Mitte Februar. (Photo: Ronny Engelmann/TROPOS)

Field experiments and process studies

Field experiments elucidate the atmospheric life cycle and related processes of aerosol and cloud particles. The complexity of this system is reflected in the fact that atmospheric aerosols and cloud particle exist with diameter from nano- to micrometer spanning more than six orders of magnitude. Furthermore, many of the condensable substances of the Earth system can be found in the aerosol and a large number of them effect climate and biosphere in turn. As a result of this diversity and mass-related analytical difficulties, essential global aerosol and cloud properties are still known to a small extend only.

This uncertainty already begins with particle sources, which are research efforts of TROPOS as well. The combustion of fossil and renewable fuels is a significant aerosol source. Measurements of the institute at many urban and rural background stations show that emissions of particles and their precursor gases are followed by strong physical and chemical transformations that need to be investigated with high-resolution sensors in order to identify the underlying processes. Despite extensive legal measures air pollution still exists in Germany and Europe with its consequences for morbidity and mortality of the respective population.

Also the conurbation Leipzig and the background station Melpitz is in the focus of investigations on air pollution with emphasis on aerosol particles, often conducted in collaboration with the Saxon State Agency for Environment and Geology (LfULG). The

Fig. / Abb. 6: Dr. Khanneh Wadinga Fomba is investigating the role of phosphorus in the complex interactions between ocean and atmosphere at PHOSDMAP. For this purpose he took samples at the CVAO in Cape Verde and at the Gobabeb Training and Research Centre in the Namib Desert in Namibia. / Die Rolle von Phosphor in den komplexen Wechselwirkungen zwischen Ozean und Atmosphäre untersucht Dr. Khanneh Wadinga Fomba bei PHOSDMAP. Dazu nahm er Proben am CVAO auf den Kapverden und am Gobabeb Training and Research Centre in der Namib-Wüste in Namibia. (Photo: Khanneh Wadinga Fomba / TROPOS)

Fig. / Abb. 7: TROPOS is investigating the influence of wood heating on air quality in Melpitz near Torgau by comparing measurements from a measuring container in the village centre with those from the station on the outskirts of the village. / Den Einfluss von Holzheizungen auf die Luftqualität untersucht TROPOS in Melpitz bei Torgau und vergleicht dazu Messungen aus einem Messcontainer im Ortskern mit denen aus der Station am Rande des Orts. (Photo: Gerald Spindler / TROPOS)

verbundenen Prozesse. Die Komplexität dieses Systems wird dabei unter anderem dadurch bestimmt, dass in der Atmosphäre Partikel und Tropfen auftreten, deren Durchmesser sich vom Nano- bis zum Mikrometerbereich um mehr als sechs Größenordnungen unterscheiden. Außerdem kann man in den Aerosolpartikeln viele der kondensationsfähigen Stoffe des Erdsystems finden, von denen wiederum eine große Zahl Einfluss auf das Klima und die Biosphäre haben kann. Als Folge dieser Vielfalt und der mengenbedingten analytischen Schwierigkeiten sind wesentliche globale Aerosol- und Wolkeneigenschaften noch wenig bekannt.

Diese Unsicherheit beginnt schon bei den Partikelquellen, die ebenfalls Forschungsgegenstand am TROPOS sind. Die Verbrennung fossiler und nachwachsender Brennstoffe zur Energieerzeugung und im Verkehr ist eine maßgebliche Aerosolquelle. Messungen des Instituts an vielen urbanen Messstellen und kontinentalen Hintergrundstationen zeigen, dass den Emissionen von Partikeln und deren Vorläufern enorme physikalische und chemische Umwandlungen folgen, die mit hoher zeitlicher Auflösung analysiert werden müssen, um die beteiligten Prozesse aufzuklären.

Auch der Ballungsraum Leipzig mit der Hintergrundstation Melpitz steht hier immer wieder im Fokus für Untersuchungen zur Luftverschmutzung mit dem Schwerpunkt auf Partikeln, die oft in Kooperation mit dem Sächsischen Landesamt für Umwelt und Geologie (LfULG) durchgeführt werden. Trotz sehr weitgehender gesetzlicher Regelungen existiert in Deutschland und Europa immer noch Luftverschmutzung mit ihren Folgen für Morbidität und Mortalität in der betroffenen Bevölkerung. Die Forschungsstation

Fig. / Abb. 8: Smog in La Paz (bottom) and its iconic mountain Illimani (6439m asl, on top). / Smog in La Paz (unten) und dahinter der markante Gipfel des Illimani (6439m). (Photo: Ever Veimar Huanca Lucero)

Melpitz research station is more and more applied to specific measurement campaigns with national and international partners. Hereby the high-resolution physical-chemical characterization on the ground is combined with other in-situ and remote sensing measurements of the entire column ("Melpitz-Column").

Even the strongest polluted regions over North America, Europe, Asia with priority on China, Africa, the Indian subcontinent, and South America are far from being sufficiently characterized in terms of aerosol burdens and ensuing climate effects. Subsequently the institute focuses its participation in international field campaigns and dedicated long-term studies in Asia, South America and the Mediterranean area. But also the marine troposphere over the clean southern and the polluted northern Atlantic is observed by long-term measurements for a better understanding aerosol cloud interactions.

Fig. / Abb. 9: Citizens were able to research fine dust and soot in Leipzig in several field phases of the WTimpact project. Dr. Denise Assmann demonstrates the measuring backpack developed for this purpose. / Bürgerinnen und Bürger konnten in mehreren Feldphasen des Projekts WTimpact Feinstaub und Ruß in Leipzig erforschen. Dr. Denise Assmann demonstriert den dafür entwickelten Messrucksack. (Photo: Tilo Arnhold / TROPOS)

Melpitz wird zunehmend für fokussierte Messkampagnen mit nationalen und internationalen Partnern genutzt, auch um die physikalisch-chemisch hoch aufgelöste In-situ-Charakterisierung am Boden mit In-situ- und Fernerkundungsmessungen der gesamten Säule zu kombinieren („Melpitz-Säule").

Die am höchsten belasteten Regionen in Nordamerika, Europa, Asien mit dem Schwerpunkt China, Afrika, dem indischen Subkontinent und Südamerika sind bei weitem noch nicht hinreichend bezüglich ihrer Aerosolbelastungen und den daraus resultierenden Klimawirkungen untersucht. Auf diese Regionen konzentrieren sich daher in internationaler Zusammenarbeit die Feldexperimente des TROPOS, u. a. in Form von Messkampagnen und Langzeitmessungen in Asien, Südamerika und dem mediterranen Bereich. Aber auch die maritime Troposphäre über dem sauberen südlichen und dem belasteten nördlichen Atlantik wird langfristig vermessen, um Aerosol-Wolken-Wechselwirkungen besser zu verstehen. Untersuchungen zum Mineralstaub und marinen Aerosolpartikeln und deren Wirkungen auf den Strahlungshaushalt, die Wolkenbildung und die atmosphärische Eisbildung bleiben ein Kernbestandteil der Arbeiten am TROPOS. Hierzu werden vermehrt Untersuchungen im zentralasiatischen und mediterranem Raum vorgenommen. Durch Nutzung eines kommerziellen Verkehrsflugzeuges der Lufthansa werden im Rahmen der Europäischen Forschungsinfrastruktur IAGOS auch Aerosolverteilungen in der oberen Troposphäre auf regelmäßig beflogenen interkontinentalen Routen gemessen und analysiert.

Am TROPOS werden verschiedene bodengebundene Fernerkundungsverfahren gekoppelt, um so zu einem synergetischen Bild der vertikalen Verteilung von Aerosolen und Hydrometeoren sowie deren Prozessierung zu gelangen. Das hierzu entwickelte

Fig. / Abb. 10: Polarstern in polar night during the MOSAiC expedition in the Central Arctic. / Die Polarstern in der Polarnacht während der MOSAiC-Expedition in der zentralen Arktis. (Photo: Ronny Engelmann / TROPOS)

Investigations on mineral dust and marine aerosol particles and its impact on the radiation budget, cloud formation processes and the atmospheric ice nucleation remain a core component of the institute's research. To this end, investigations in the Central Asian and the Mediterranean region will be intensified.

In the framework of the European infrastructure IAGOS the aerosol distribution in the upper troposphere is measured and analysed using a commercial Lufthansa aircraft operated on frequent intercontinental routes.

At TROPOS different ground-based remote sensing methods are coupled in order to achieve a synergetic picture of the vertical distribution of clouds and aerosols as well as their processing. The Leipzig Aerosol and Cloud Remote Observation System (LACROS), that has been developed to this end, will be further extended towards a European network prototype instrument.

On smaller scales, investigations concerning new particle formation, the interactions between aerosol particles and clouds, and the influences of turbulent mixing processes on cloud development are carried out with help of the helicopter-borne measurement platform ACTOS. In addition, process studies are conducted at suitable locations such as mountain observatories to investigate particle nucleation, particle processing through clouds, and the influence of aerosol particles on the development and freezing of clouds.

TROPOS leads several regional, national and European measurement networks to monitor atmospheric aerosols and cloudiness. In the framework of the Global Atmospheric Watch (GAW) programme of the WMO, TROPOS hosts the World Calibration Centre for physical in-situ aerosol measurement (WCCAP) to assure high quality standards at national and international observatories.

Leipzig Aerosol and Cloud Remote Observation System (LACROS) wird darüberhinaus zu einem Prototyp-Instrument eines europäischen Messnetzes erweitert.

Auf kleineren Skalen werden Untersuchungen zur Partikelbildung und Wechselwirkung zwischen Aerosolpartikeln und Wolken und der Einfluss turbulenter Mischungsprozesse auf die Wolkenentwicklung mit Hilfe der hubschraubergetragenen Messplattform ACTOS durchgeführt. Zusätzlich werden Bergstationen zu Prozessstudien genutzt, die sich dem Verständnis von Einzelprozessen, wie der Partikelneubildung, der physiko-chemischen Veränderung der Aerosolpartikel beim Wolkendurchgang und dem Einfluss von Aerosolpartikeln auf die Entwicklung und das Gefrieren von Wolken widmen.

TROPOS ist maßgeblich an regionalen, nationalen und Europäischen Messnetzen zur Erfassung

Fig. / Abb. 11: Pyranometer installation during the measurement campaign within the joint project "MetPVNet" in Allgäu, 2018 / Pyranometer-Installation während der Messkampagne im Rahmen des Verbundprojekts „MetPVNet" im Allgäu, 2018. (Photo: Jonas Witthuhn / TROPOS).

Fig. / Abb. 12: For the first time, an international team has reconstructed ice nuclei (INP) from clouds of the Arctic of the past 500 years. For this purpose, the samples from two ice cores from Svalbard and Greenland were examined at TROPOS. / Ein internationales Team hat erstmals Eiskeime von Wolken der Arktis der vergangenen 500 Jahre rekonstruiert. Dazu wurden die Rückstellproben von zwei Eisbohrkernen aus Spitzbergen und Grönland gelangten am TROPOS untersucht. (Photo: Tilo Arnhold / TROPOS)

Further on TROPOS is primary responsible for the development and operation of the European and national measurement network for the observation of aerosols, clouds and trace gases (ACTRIS) to ensure, besides process understanding, a basis for the long-term characterisation of short-lifed climate components.

Field campaigns are supported and complemented by analyses based on meteorological satellites. In particular satellite products provide the spatio-temporal development of clouds and their interaction with radiation, as well as transport paths of aerosols. Especially the geostationary European weather satellite Meteosat is applied to this end.

Laboratory experiments

In atmospheric research, physico-chemical models for the description of the most relevant process are continuously developed. These models are based on process parameters that need to be determined in laboratory experiments under controlled environmental conditions.

Laboratory experiments cover the development of a large number of methods to characterize atmospheric particles in ground-based or airborne field measurement campaigns. This work includes for example the improvement of aerosol size spectrometers as well as collection systems for the physical and chemical characterization of cloud droplets and the interstitial aerosol that means those aerosol particles that are suspended in the gas phase inside the cloud along with the cloud particles.

des atmosphärischen Aerosols und der Bewölkung beteiligt. Das Institut betreibt im Rahmen des Global Atmospheric Watch (GAW) Programmes der WMO das Weltkalibrierzentrum für physikalische Aerosolmessungen (WCCAP) mit dem Ziel der Qualitätssicherung von In-situ-Messungen an nationalen und internationalen Messstationen.

TROPOS ist weiterhin federführend an der Entwicklung und dem Betrieb des europäischen und nationalen Messnetzes zur Erfassung von Aerosolen, Wolken und Spurengasen (ACTRIS) beteiligt, um neben Prozessverständnis auch die Basis für eine langfristige Charakterisierung der kurzlebigen Klimabestandteile zu liefern.

Feldexperimente werden durch Analysen, basierend auf meteorologischen Satelliten, unterstützt und erweitert. Insbesondere wird mit Satellitenprodukten die raumzeitliche Entwicklung von Wolken und deren Strahlungsantrieb untersucht, ebenso wie die Transportwege von Aerosolen.

Laborexperimente

In der Atmosphärenforschung werden kontinuierlich physikalisch-chemische Modelle zur Beschreibung der wesentlichen Prozesse entwickelt. Grundlage derartiger Modelle sind stets Prozessparameter, die in Laborexperimenten unter bekannten Umgebungsbedingungen ermittelt werden.

In Laborexperimenten werden zahlreiche Messmethoden entwickelt, die zur Partikelcharakterisierung in boden- und luftgestützten Feldmesskampagnen eingesetzt werden. Diese Arbeiten beinhalten z. B. die Weiterentwicklung von Aerosolgrößenspektrometern sowie Sammelsysteme zur physikalischen

Fig. / Abb. 13: Inter comparison measurements for quality insurance of particle mobility size spectrometer measurements in the World Calibration Center for Aerosol Physics (WCCAP) at TROPOS. / Vergleichsmessungen zur Qualitätssicherung von Partikelgrößenspektrometer-Messungen im Labor des Weltkalibrierzentrums für Aerosolphysik (WCCAP) am TROPOS. (Photo: Tilo Arnhold / TROPOS)

Optical measurement techniques are developed and applied to determine the extinction coefficient of aerosol particles. Multi-wavelength lidar systems and a wind lidar are further developed in the laboratory and applied in the field to determine aerosol properties, aerosol fluxes and meteorological parameters such as temperature, relative humidity and wind. The amount of black carbon and mineral aerosol components in the aerosol samples are quantified with spectral absorption measurements.

Research at the Leipzig Aerosol Cloud Simulator LACIS addresses the activation of cloud droplets and primarily the heterogeneous formation of ice under realistic surrounding conditions. These investigations aim at a better understanding of the underlying fundamental processes, the identification of critical and controlling parameters, and the development of parameterizations to characterize droplet and ice formation processes for applications in dynamical models.

Gas phase reactions of various radicals are being investigated in flow reactors and in the double chamber ACD-C. These reactions are important for ozone and particle formation caused by anthropogenic or biogenic volatile hydrocarbons. The generated particles are also investigated with regard to hygroscopic growth and cloud droplet activation behaviour. In single drop experiments, investigations on phase transfer parameters of trace gases and radicals are being conducted. The determination of phase transfer parameters and reactive uptake coefficients hereby is being extended to previously not considered chemical species and complex surfaces.

In the field of liquid phase mechanisms reactions of primarily radical oxidants are investigated with time-resolved optical detection techniques.

Fig. / Abb. 14: The samples of the surface film are collected for the ensuing laboratory investigations during the Spanish Antarctic expedition PI-ICE. / Probenahme des Oberflächenfilms für anschließende Laboruntersuchungen während der spanischen Antarktis-Expedition PI-ICE. (Photo: Manuela van Pixteren / TROPOS)

Fig. / Abb. 15: Start of the second aerosol chamber for parallel measurements with the new double chamber ACD-C in the laboratory building for atmospheric chemistry. / Inbetriebnahme der zweiten Aerosolkammer für Parallelmessungen mit der neuen Doppelkammer ACD-C im Laborgebäude für Chemie der Atmosphäre. (Photo: Tilo Arnhold / TROPOS)

und chemischen Charakterisierung von Wolkentröpfchen und dem interstitiellen Aerosol, also denjenigen Aerosolpartikeln, die innerhalb von Wolken neben den Wolkenpartikeln selbst in der Gasphase suspendiert sind.

Optische Messmethoden werden zur Bestimmung des Extinktionskoeffizienten von Partikeln entwickelt und angewendet. Mehrwellenlängenlidare und ein Windlidar werden zur Bestimmung von Aerosoleigenschaften, Aerosolflüssen und meteorologischen Parametern wie Temperatur, Feuchte und Wind im Labor weiterentwickelt und im Feld eingesetzt. Die Bestimmung der Anteile „schwarzen Kohlenstoffs“ und mineralischer Aerosolkomponenten in Aerosolproben erfolgt durch spektrale Absorptionsmessungen.

Die Arbeiten am Strömungsreaktor LACIS betreffen die Aktivierung von Wolkentröpfchen und schwerpunktmäßig die heterogene Eisbildung unter realistischen Umgebungsbedingungen. Ziele dieser Untersuchungen sind die Erlangung eines besseren Prozessverständnisses auf fundamentaler Ebene, die Identifikation kritischer und kontrollierender Parameter und die Entwicklung geeigneter Parametrisierungen zur Beschreibung von Tröpfchen- und Eisbildung in dynamischen Modellen.

Gasphasenreaktionen verschiedener Radikale werden in Strömungsreaktoren und der Doppelkammer ACD-C untersucht. Diese Reaktionen sind von Interesse für die Ozon- und Partikelbildung, verursacht durch anthropogene oder biogene flüchtige Kohlenwasserstoffe. Die erzeugten Partikel werden auch hinsichtlich ihres Feuchtewachstums- und Aktivierungsverhaltens untersucht.

In Einzeltropfenexperimenten werden Untersuchungen bzgl. der Phasentransferparameter für

These reactions proceed within haze particles, fog and cloud droplets as well as in deliquescent aerosol particles.

For the understanding of the oxidation of organic trace gases in the tropospheric multiphase system, a large number of reactions with various radicals are being studied as well as reactions of halogenated oxidants. The latter species are of interest for the emission of reactive halogen compounds from sea salt particles, the so-called halogen activation.

The liquid phase laboratory for the investigation of tropospheric liquid phase processes is an important centre for these research activities. The process studies result in the improvement of chemical mechanisms, which can be applied to the self-developed model mechanism CAPRAM.

In the field of analytic measurement technology laboratory experiments are dedicated to improve and test methods for the chemical characterization of organic aerosol components. These methods are mostly based on mass spectrometric processes, which are deployed in various coupling techniques.

In the field of sampling techniques the "Atmospheric Chemistry Department" closely collaborates with the "Experimental Aerosol and Cloud Microphysics Department" on the development of the specific segregation of aerosol particles of a distinct size and their chemical analysis and also on the development of inlet systems and reactors.

Spurengase und Radikale durchgeführt. Die Bestimmung von Phasentransferparametern und reaktiven Aufnahmekoeffizienten wird dabei auf bisher nicht betrachtete chemische Spezies und komplexe Oberflächen ausgeweitet.

Im Bereich von Flüssigphasenmechanismen werden Reaktionen von vorwiegend radikalischen Oxidantien mit zeitaufgelösten optischen Nachweistechniken untersucht. Diese Reaktionen laufen in den Tröpfchen von Wolken, Regen und Nebel sowie in wässrigen Aerosolpartikeln ab. Hier werden zum Verständnis der Oxidation organischer Spurengase im troposphärischen Mehrphasensystem eine Vielzahl von Reaktionen verschiedener Radikale sowie Reaktionen von halogenhaltigen Oxidantien untersucht. Letztere Spezies sind von Interesse bei der Freisetzung von Halogenverbindungen aus maritimen Seesalzpartikeln, der so genannten Halogenaktivierung.

Das Flüssigphasen-Laserlabor zur Untersuchung der troposphärischen Flüssigphasenprozesse ist ein wichtiges Zentrum dieses Forschungsbereiches. Aus den Prozessuntersuchungen resultieren Verbesserungen chemischer Mechanismen, die in der Modellierung mit dem eigenen Mechanismus CAPRAM angewendet werden.

In der analytischen Messtechnik werden in Laborexperimenten Verfahren zur besseren chemischen Charakterisierung der organischen Bestandteile von Aerosolpartikeln entwickelt und getestet.

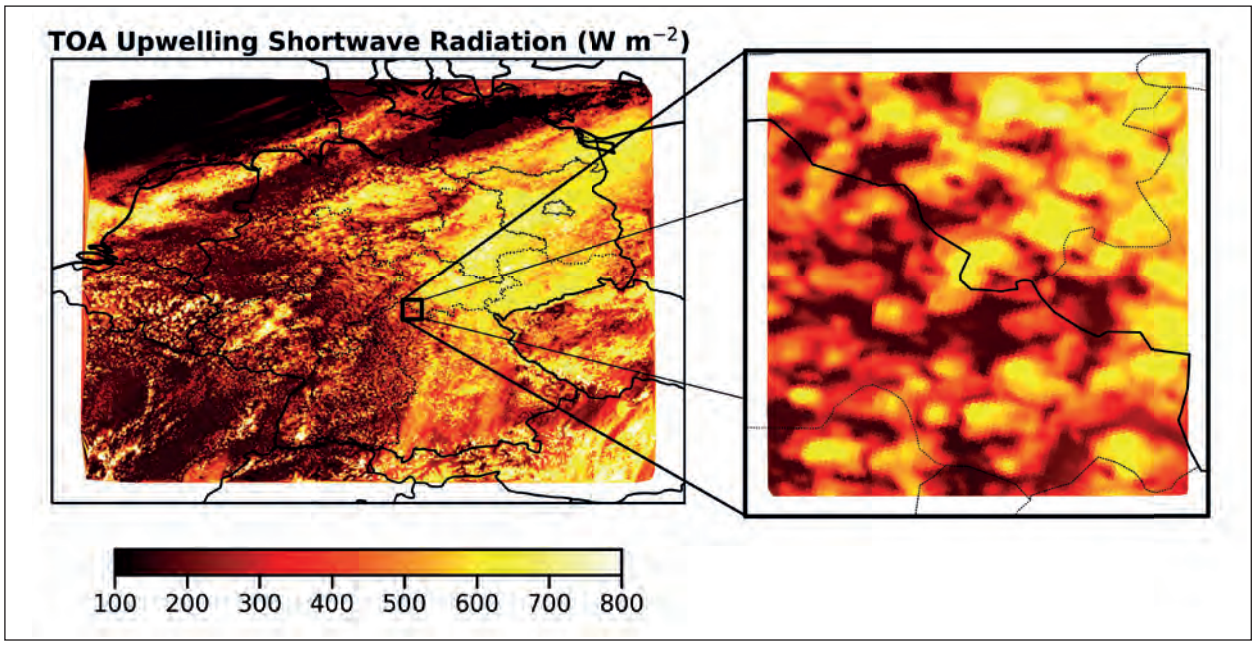

Fig. / Abb. 16: Top-of-the-atmosphere (TOA) upwelling shortwave fluxes simulated with ICON-LEM and 300 m grid spacing. The high-resolution ICON simulations are needed to assess the impact of absorbing aerosol on indirect changes of the TOA radiation budget. / Nach oben gerichtete, kurzwellige Strahlungsflüsse am Oberrand der Atmosphäre simuliert mit ICON und 300 m Gittermaschenweite. Die hochaufgelösten ICON-Simulationen werden gebraucht, um den Einfluss von absorbierendem Aerosol auf indirekte Änderungen der Strahlungsbilanz abzuschätzen.

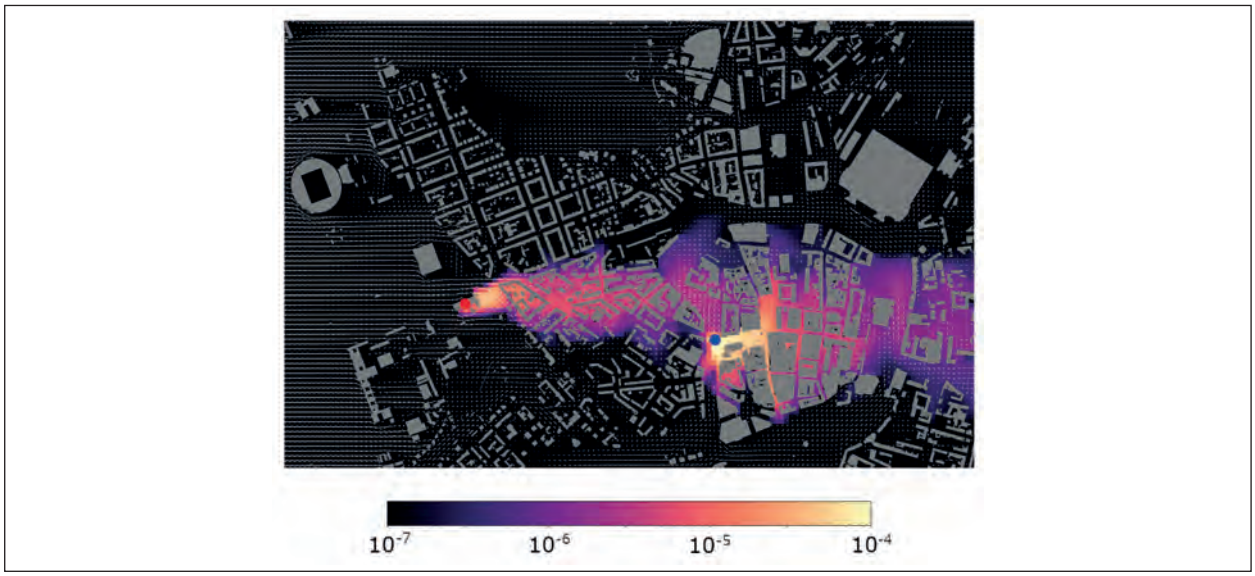

Fig. / Abb. 17: 1st-layer concentration of two test tracers over Leipzig after 1 hour simulation with the new CDF model. Buildings are represented by permeability fields at 20-m grid spacing. A uniform wind of (5 m/s, 270°) was imposed at the lateral boundaries. / Oberflächennahe Konzentration zweier Test-Tracer über Leipzig nach 1-stündiger Simulation mit dem neuen CDF-Modell. Gebäude werden bei 20 m Gitterweite durch Permeabilitätsfelder beschrieben. An den Domainrändern wurde ein gleichmäßiger Wind von (5 m/s, 270°) angenommen.

Modeling

Aerosol and cloud processes are investigated at TROPOS with model studies at different scales. This includes the development and testing of improved process parameterizations considering detailed chemical mechanisms and spectrally resolved microphysics, calculations of mesoscale transport processes with realistic meteorology for direct evaluation of model results with field measurements, and finally the estimation of the effect of simplified versions of the updated aerosol process parameterizations in an aerosol climate model. For this purpose, measurement data from field studies are used for model evaluation and various laboratory data are used as input parameters for the parameterization of aerosol processes.

A main research focus is the investigation of control factors and effects of natural aerosols like mineral dust or organic aerosol from plant emissions. Due to its direct radiative effect and its function as an ice-forming particle in mixed-phase clouds, mineral dust is an important climate factor. The investigation of the atmospheric dust life cycle has a special focus on calculations of dust emissions using regional and global simulations. Further model studies deal with controlling factors of the distribution of urban particulate matter for air quality studies, and with the investigation of cloud processes using spectral aerosol cloud modeling in particular for understanding ice formation in clouds.

In order to answer questions on the understanding of life cycles and interactions of

Diese Techniken beruhen zumeist auf massenspektrometrischen Verfahren, die in verschiedenen Kopplungstechniken eingesetzt werden. Im Bereich der Probenahmetechniken gibt es auch hier eine enge Kooperation mit der Abteilung „Experimentelle Aerosol- und Wolkenmikrophysik“ zur Entwicklung einer gezielten Abscheidung von Partikeln bestimmter Größe und deren chemischer Analyse aber auch zur Entwicklung von Einlasssystemen und Reaktoren.

Modellierung

Aerosol- und Wolkenprozesse werden am TROPOS mit Modellstudien auf verschiedenen Skalenbereichen untersucht. Dazu gehören die Entwicklung und Erprobung verbesserter Prozessparametrisierungen unter Berücksichtigung detaillierter chemischer Mechanismen und spektral aufgelöster Mikrophysik, Berechnungen mesoskaliger Transportprozesse mit realistischer Meteorologie zum direkten Vergleich von Modellergebnissen mit Feldmessungen und schließlich die Abschätzung der Wirkung vereinfachter Versionen der aktualisierten Aerosolprozessparametrisierungen in einem Aerosol-Klimamodell. Dazu werden Messdaten aus Feldstudien zur Modellauswertung und diverse Labordaten als Eingangsparameter für die Parametrisierung von Aerosolprozessen verwendet.

Ein Forschungsschwerpunkt ist die Untersuchung von Kontrollfaktoren und Effekten natürlicher Aerosole wie Mineralstaub oder organischem Aerosol aus Pflanzenemissionen. Mineralstaub ist aufgrund

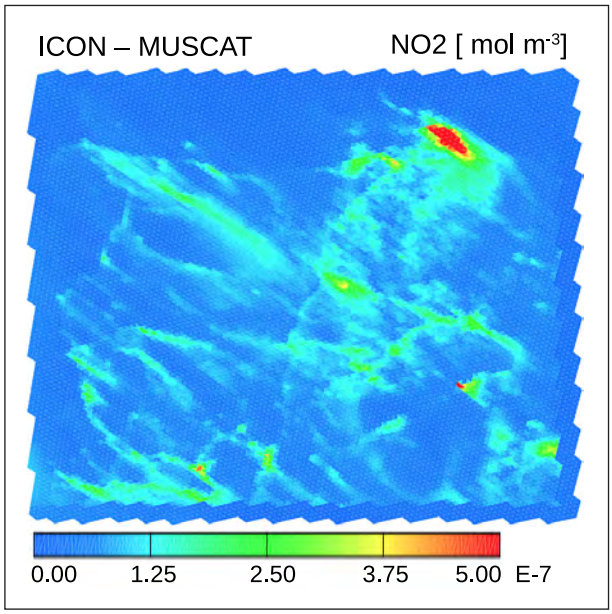

Fig. / Abb. 18: ICON-MUSCAT: Transport, chemie and Emissions for nitrogen dioxide (NO_2) in the area of central Germany. 72 hours were simulated for the mid of July 2018 with 2.5 km gris spacing. / ICON-MUSCAT: Transport, Chemie und Emissionen für Stickstoffdioxid (NO_2) im Bereich Mitteldeutschland. Simuliert wurden 72 Stunden für Mitte Juli 2018 mit 2.5 km Gitterweite.

anthropogenic and natural aerosol, the online-coupled meteorology-aerosol model system COSMO-MUSCAT was developed at TROPOS. The model calculates the effects of aerosol particles on radiation and clouds, and allows the use of mechanisms of liquid phase chemistry. For studies on urban air quality, high-resolution detailed urban structures were implemented in the model for the city of Leipzig to investigate the effects of changes in emissions and urban structures on air quality. The global aerosol climate model ECHAM-HAMMOZ is used to investigate the role of aerosol processes in the climate system. A considerable part of the aerosol processes is described in a similar way in the aerosol modules MUSCAT and HAMMOZ, which allows the investigation of aerosol-climate interactions with well-tested aerosol parameterizations. In addition to the global and regional models, the detailed air parcel model SPACCIM is used to describe spectral microphysics coupled with complex multiphase chemistry e.g. for the generation and conversion of secondary organic aerosols. A detailed description of cloud microphysics is performed with the SPECS model, in which the size spectra of aerosol particles and cloud droplets can develop freely.

In the coming years these model investigations will be performed on different scales with the coupled model systems ICON-MUSCAT and ICON-HAMMOZ. Ideally, these developments will provide a uniform framework for studying the life cycles of aerosol and clouds and their effects on air quality and climate.

seiner direkten Strahlungswirkung und seiner Funktion als eisbildendes Partikel in Mischphasenwolken ein wichtiger Klimafaktor. Die Untersuchung des atmosphärischen Staub-Lebenszyklus hat einen besonderen Schwerpunkt auf Berechnungen von Staubemissionen mit regionalen und globalen Simulationen. Weitere Modellstudien befassen sich mit Kontrollfaktoren der Verteilung von städtischem Feinstaub für Luftqualitätsstudien und mit der Untersuchung von Wolkenprozessen mit Hilfe spektraler Aerosolwolkenmodellierung insbesondere zum Verständnis der Eisbildung in Wolken.

Um Fragen zum Verständnis der Lebenszyklen und Wechselwirkungen von anthropogenem und natürlichem Aerosol zu beantworten, wurde an TROPOS das online-gekoppelte Meteorologie-Aerosol-Modellsystem COSMO-MUSCAT entwickelt. Das Modell berechnet die Auswirkungen von Aerosolpartikeln auf Strahlung und Wolken und erlaubt die Nutzung von Mechanismen der Flüssigphasenchemie. Für Studien zur städtischen Luftqualität wurden im Modell für die Stadt Leipzig hochauflösende, detaillierte Stadtstrukturen implementiert, um die Auswirkungen von Änderungen der Emissionen und der städtischen Strukturen auf die Luftqualität zu untersuchen. Das globale Aerosol-Klimamodell ECHAM-HAMMOZ wird zur Untersuchung der Rolle von Aerosolprozessen im Klimasystem eingesetzt. Ein erheblicher Teil der Aerosolprozesse wird in ähnlicher Weise in den Aerosolmodulen MUSCAT und HAMMOZ beschrieben, was die Untersuchung von Aerosol-Klima-Wechselwirkungen mit gut getesteten Aerosolparametrisierungen ermöglicht. Zusätzlich zu den globalen und regionalen Modellen wird das detaillierte Luftpaketmodell SPACCIM zur Beschreibung der spektralen Mikrophysik in Verbindung mit komplexer Mehrphasenchemie z.B. für die Erzeugung und Umsetzung von sekundären organischen Aerosolen verwendet. Eine detaillierte Beschreibung der Wolkenmikrophysik erfolgt mit dem SPECS-Modell, in dem sich die Größenspektren von Aerosolpartikeln und Wolkentropfen frei entwickeln können.

In den kommenden Jahren werden diese Modelluntersuchungen auf verschiedenen Skalen mit den gekoppelten Modellsystemen ICON-MUSCAT und ICON-HAMMOZ durchgeführt. Im Idealfall bieten diese Entwicklungen einen einheitlichen Rahmen für die Untersuchung der Lebenszyklen von Aerosol und Wolken und deren Auswirkungen auf Luftqualität und Klima.

Overview of the individual contributions

This biennial report presents selected TROPOS work from 2018 to 2019 in four longer and 20 short articles. The contributions focus on the evaluation of campaigns that took place in the previous reporting period. However, the entire spectrum of laboratory, field and modelling work is also covered in the articles. TROPOS continues to cover a wide range of applications always with the strategic goals towards both process understanding of the chemical and physical mechanisms in aerosols and aerosol-cloud interactions and the detection of climatic and anthropogenic induced variability. The latter is achieved by regional and worldwide field campaigns with more and more increasing measurement duration, the former by elaborated laboratory and model studies under the most realistic environmental conditions possible. Once again, new mechanisms have been discovered. Again, observations have been made that require a deeper understanding of the processes involved. The active involvement of the interested public in our work is a new component that will continue to accompany the transfer activities of TROPOS in the future.

Long contributions

Although as a result of clean air measures air quality in Europe has improved considerably in recent years to decades, urban areas continue to be heavily polluted due to numerous local sources. This pollution is extremely variable in space and time due to complex thermodynamic, dynamic, transport and transformation processes. While it is almost impossible to capture this variability even approximately by in-situ measurements, high-resolution models are able to investigate spatio-temporal distributions as well as their causes in urban areas. **Heinold et al.** have now succeeded in providing street-level predictions of air quality in the urban area of Leipzig by combining high-resolution regional modelling and downscaling using a fluid-dynamic model. A particularly interesting aspect is the consideration of the influence of urban vegetation on the development of biogenic volatile organic compounds. The mobile particulate matter sensors, which have just been developed in the citizen science project WTimpact, will for the first time provide observational data that will allow a limited comparison with the particulate matter variability modelled here physico-chemically-dynamically.

Also, the large-scale distribution of the aerosol is difficult to measure. Satellite measurements only provide indirect information with corresponding

Übersicht der Einzelbeiträge

Der vorliegende Zweijahresbericht stellt in vier längeren und 20 Kurzbeiträgen ausgewählte Arbeiten des TROPOS im Zeitraum 2018 bis 2019 vor. Die Beiträge haben einen Schwerpunkt auf der Auswertung von Kampagnen, die im vorherigen Berichtszeitraum stattgefunden haben. Aber auch das ganze Spektrum von Labor-, Feld- und Modellierungsarbeiten ist in den Beiträgen abgebildet. TROPOS gelingt weiterhin ein weites Anwendungsspektrum, das aber stets die strategischen Ziele im Auge hat: sowohl die Prozessuntersuchung der chemischen und physikalischen Mechanismen in Aerosolen und Aerosol-Wolkenwechselwirkungen als auch die Erfassung der klimatisch und anthropogen bedingten Variabilität. Letzteres wird durch regionale und weltweite Feldkampagnen mit zunehmender Messdauer ermöglicht. Ersteres durch aufwändige Labor- und Modellstudien unter möglichst realen Umgebungsbedingungen. Wieder ist es gelungen, neue Mechanismen zu entdecken. Wieder sind Beobachtungen gemacht worden, die ein tieferes Prozessverständnis erfordern. Die aktive Einbindung interessierter Öffentlichkeit in unsere Arbeiten ist eine neue Komponente, die auch in Zukunft die Transferaktivitäten des TROPOS begleiten wird.

Langbeiträge

Auch wenn sich die Luftqualität in Europa in den letzten Jahren bis Dekaden durch Reinhaltemaßnahmen erheblich verbessert hat, herrscht in urbanen Regionen aufgrund zahlreicher lokaler Quellen weiterhin eine starke Luftbelastung vor. Diese ist bedingt durch komplexe thermodynamische, dynamische, Transport- und Umwandlungsprozesse raumzeitlich extrem variabel. Während es für In-situ-Messungen nahezu unmöglich ist, diese Variabilität auch nur annäherungsweise zu erfassen, sind hochaufgelöste Modelle in der Lage, sowohl raumzeitliche Verteilungen als auch deren Ursachen im urbanen Raum zu untersuchen. **Heinold et al.** ist es nun gelungen, durch die Kombination hochaufgelöster Regionalmodellierung und Niederskalierung mittels eines fluid-dynamischen Modells straßenaufgelöste Vorhersagen der Luftqualität im Stadtgebiet Leipzig zu ermöglichen. Ein besonders interessanter Aspekt dabei ist die Berücksichtigung des Einflusses städtischer Vegetation auf die Entwicklung biogener flüchtiger organischer Bestandteile. Die gerade im Bürgerforschungsprojekt WTimpact entwickelten mobilen Feinstaubsensoren werden erstmalig Beobachtungsdaten liefern, die im begrenzten Maße einen Vergleich mit der hier

uncertainties. In-situ measurements are not possible on those scales. TROPOS has therefore made the strategic decision to carry out long-term to permanent measurements of aerosol and aerosol-cloud interaction at exemplary global "hot spots". **Baars et al.** present the latest developments of the lidar network PollyNET, in which dedicated vertically resolved aerosol and cloud properties and from their combination aerosol-cloud interactions can be explored. The examples given range from Canadian forest fires with effects into the stratosphere (analogous to the current Australian forest fires), to Central Asian mineral dust and specific plans for measuring sites on Cyprus and Cape Verde Islands in order to be able to detect variability and trends in the northern hemispheric dust belt in the best possible way by means of ground-based remote sensing. The TROPOS stations are part of the European and national ACTRIS Roadmap program with a perspective duration until 2030 and possibly beyond.

While PollyNET can in principle detect the influence of aerosol on the formation of liquid water and ice under real conditions, only laboratory measurements are able to investigate the physical and chemical processes of aerosol and cloud interaction under controlled environmental conditions. **Niedermeier et al.** now present an important step towards a better comparability of real and laboratory measurements by introducing the turbulent cloud channel LACIS-T. For the first time, it is now possible at TROPOS to specify not only aerosol properties and thermodynamic boundary conditions but also realistic fluctuations of humidity and temperature in a controlled manner. This makes it possible, for example, to compare the influence of turbulence on droplet and ice formation with that of physical and chemical properties of aerosol particles. An essential aspect of this is the accompanying high-resolution numerical simulation, which allows a well-founded interpretation of the results. First results indicate an influence of turbulent humidity fluctuations on droplet formation. Future work will investigate this aspect and the influence of turbulence on heterogeneous ice formation.

In addition to the physical processes of cloud and ice formation, which can only be captured with considerable effort in the field, laboratory and model, especially due to the complex turbulent environmental conditions mentioned above, there is an incredible variety of chemical processes in the aqueous solutions that make up aerosol and cloud particles. It is precisely these particles that enable a multitude of chemical reaction paths that are not possible in the "dry" atmosphere. These include numerous oxidation processes of organic compounds, which are of great importance for the self-cleaning of the troposphere.

physikalisch-chemisch-dynamisch modellierten Feinstaubvariabilität ermöglichen.

Auch die großräumige Verteilung des Aerosols ist messtechnisch nur schwer zu erfassen. Satellitenmessungen liefern nur indirekt Informationen mit entsprechenden Unsicherheiten, In-situ-Messungen sind auf den Skalen nicht möglich. TROPOS hat sich daher strategisch entschieden, an exemplarischen globalen „Hot-Spots" längerfristige bis dauerhafte Erfassungen des Aerosols und der Aerosol-Wolken-Wechselwirkung durchzuführen. **Baars et al.** stellen die jüngsten Entwicklungen des Lidarnetzwerkes PollyNET vor, in dem dezidierte vertikal aufgelöste Aerosol- und Wolkeneigenschaften und aus der Kombination deren Wechselwirkungen erkundet werden können. Die angeführten Bespiele reichen von kanadischen Waldbränden mit Auswirkungen bis in die Stratosphäre (analog zu den aktuellen australischen Waldbränden) über zentral-asiatischen Mineralstaub bis zu konkreten Plänen für Messstandorte auf Zypern und den Kapverden, um Variabilität und Trends im nordhemisphärischen Staubgürtel mittels bodengebundener Fernerkundung bestmöglich erfassen zu können. Die TROPOS-Stationen sind Bestandteil des europäischen und nationalen ACTRIS-Roadmap-Programms mit einer perspektivischen Laufzeit bis 2030 und evtl. darüber hinaus.

Während PollyNET den Einfluss des Aerosols auf die Bildung von Flüssigwasser und Eis unter realen Bedingungen prinzipiell erfassen kann, sind nur Labor-Messungen in der Lage, die physikalischen und chemischen Prozesse der Aerosol- und Wolkenwechselwirkung unter kontrollieren Umgebungsbedingungen zu untersuchen. Einen wichtigen Schritt zur besseren Vergleichbarkeit von Real- und Labor-Messungen präsentieren nun **Niedermeier et al.** mit der Vorstellung des turbulenten Wolkenkanals LACIS-T. Hiermit ist es erstmalig am TROPOS möglich, neben den Aerosoleigenschaften und thermodynamischen Randbedingungen auch realistische Fluktuationen von Feuchte und Temperatur kontrolliert vorzugeben. Damit gelingt es z.B. den Einfluss von Turbulenz auf Tröpfchen- und Eisbildung mit dem der physikalischen und chemischen Eigenschaften der Aerosolpartikel zu vergleichen. Ein wesentlicher Aspekt dabei ist die begleitende hoch aufgelöste numerische Simulation, die eine grundierte Interpretation der Ergebnisse ermöglicht. Erste Ergebnisse weisen auf einen Einfluss turbulenter Feuchteschwankungen auf die Tröpfchenbildung hin. Zukünftige Arbeiten werden diesen Aspekt sowie den Einfluss von Turbulenz auf die heterogene Eisbildung untersuchen.

Neben den physikalischen Prozessen zur Wolken- und Eisbildung, die insbesondere aufgrund der genannten komplexen turbulenten

Schaefer et al. are investigating a particularly interesting mechanism in which so-called photosensitizers are excited by light to produce reactive molecules and can thus accelerate the oxidation processes and thus particle growth. In elaborate laboratory studies quantum yield, lifetime and molar attenuation coefficients of 16 different photosensitizers are investigated. The results indicate that especially products from biomass combustion in aerosol particles may be suitable compounds for photochemically induced oxidation acceleration.

Short contributions

With the completion of the national BMBF project HD(CP)^2, ICON is now a national community model for atmospheric modelling from the mesoscale to the global scale, which can be used to investigate in particular organisational processes in large-scale cloud structures. **Senf** uses HD(CP)^2 results to show the influence of such processes on precipitation formation and cloud radiation budget. In addition to the direct influence of aerosols on cloud formation, the so-called semi-direct effect leads to a considerable indirect influence on cloudiness and radiation budget through absorption of solar radiation by soot and mineral dust and the associated change in atmospheric stability. With a global aerosol climate model **Tegen and Heinold** succeeds in estimating more precisely the interplay of superimposed layers of soot and mineral dust in the global determination of the semi-direct effect. Soot and mineral dust are increasingly introduced into the free troposphere by vegetation fires (keyword “pyrocene”). **Wagner and Schepanski** use high-resolution Large Eddy simulations to show that the heat effect of wild fires increases the dust input due to increased horizontal and vertical winds massively and requires novel parameterizations in aerosol climate models. The spatial distribution of dust sources also influences the wind induced input of mineral dust into the troposphere. **Feuerstein and Schepanski** succeed in a more precise mapping of alluvial sediments, which contribute significantly to dust emission, by combining satellite data of spectral ground reflectivity and a digital elevation model flow accumulation data set. The combination of the thermal emission channels of the SEVIRI radiometer on Meteosat provides an impressive survey of the spatio-temporal distribution of tropospheric mineral dust. Conversely, a radiative transfer model can be used to simulate such measurements from dust model results. **Banks et al**. were able to identify meteorological situations in which dust detection from SEVIRI is particularly feasible or particularly difficult.

Umgebungsbedingungen nur mit erheblichem Aufwand in Feld, Labor und Modell zu erfassen sind, existiert eine unglaubliche Vielfalt chemischer Prozesse in den wässrigen Lösungen, die Aerosol- und Wolkenpartikel ausmachen. Gerade diese Partikel ermöglichen eine Vielzahl chemischer Reaktionswege, die in der „trockenen“ Atmosphäre nicht möglich sind. Hierzu gehören zahlreiche Oxidationsprozesse von organischen Verbindungen, die von großer Bedeutung für die Selbstreinigung der Troposphäre sind. Einen besonders interessanten Mechanismus untersuchen **Schaefer et al.**, bei dem sogenannte Photosensibilatoren durch Licht angeregt zu reaktiven Molekülen werden und so die Oxidationsprozesse und damit das Partikelwachstum beschleunigen können. In aufwändigen Laborstudien werden Quantenausbeute, Lebenszeit und molare Abschwächungskoeffizienten von 16 verschiedenen Photosensibilatoren untersucht. Die Ergebnisse weisen darauf hin, dass insbesondere Produkte aus Biomasseverbrennung in Aerosolpartikeln geeignete Verbindungen für eine photochemisch induzierte Oxidationsbeschleunigung sein können.

Kurzbeiträge

Mit dem Abschluss des nationalen BMBF-Projektes HD(CP)^2 existiert nun mit ICON ein nationales Community-Modell für Atmosphärenmodellierung von der Mesoskala bis zur globalen Skala, mit der insbesondere Organisationsprozesse in großräumigen Wolkenstrukturen untersucht werden können. **Senf** zeigt anhand von HD(CP)^2-Ergebnissen, welchen Einfluss derartige Prozesse auf die Niederschlagsbildung und die Wolkenstrahlungsbilanz haben. Neben dem unmittelbaren Einfluss von Aerosolen auf Wolkenbildung führt der sogenannte semi-direkte Effekt zu einem erheblichen mittelbaren Einfluss auf Bewölkung und Strahlungsbilanz durch Absorption solarer Strahlung an Ruß und Mineralstaub und damit verbundener Änderung der atmosphärischen Stabilität. **Tegen und Heinold** gelingt mit einem globalen Aerosol-Klimamodell eine genauere Abschätzung des Wechselspiels von übereinander gelagerten Ruß- und Mineralstaubschichten in der globalen Bestimmung des semi-direkten Effektes. Ruß und Mineralstaub werden zunehmend durch Vegetationsbrände in die freie Troposphäre eingetragen (Stichwort „Pyrozäen“). **Wagner und Schepanski** zeigen mittels hochaufgelöster Large Eddy Simulationen, dass der Hitzeeffekt von Flächenbränden durch erhöhte Horizontal- und Vertikalwinde den Staubeintrag massiv erhöht und neuartige Parametrisierungen in Aerosol-Klimamodellen erfordert. Auch die räumliche Verteilung von Staubquellen beeinflusst

Overview of the individual contributions / Übersicht der Einzelbeiträge

While Meteosat has been the workhorse of atmospheric remote sensing for many years, last year saw the launch of AEOLUS, a new type of satellite instrument for lidar-based wind and aerosol measurements. **Baars et al.** report how TROPOS uses its worldwide distributed stations for ground-based remote sensing complemented by additional own radiosonde ascents to validate and improve the Aeolus products. An evaluation of satellite-borne measurements of aerosol-optical thickness (AOD) as well as AOD distributions from model calculations was performed by ship-borne sun photometer measurements. **Witthuhn et al.** could show that satellite data are usually closer to ship observations than model re-analyses and that satellite products show a systematic difference especially for mineral dust situations, which indicates a systematic error in the satellite algorithm. Especially for the Arctic, the small-scale spatial distribution of solar irradiance over the sea ice was recorded for the first time during the Polarstern expedition PASCAL. **Barrientos et al.** were able to show with the measurements that the spatial irradiance variability can be assigned to certain cloud types. For optical reasons, lidar-based measurements of the aerosol profile cannot capture the near surface area. This gap is closed by the horizontally oriented spectral extinction measurement SAEMS developed at TROPOS. **Skupin et al**. present the first mobile SAEMS measurements within the scope of a measurement campaign in Košetice (Czech Republic). Progress in the application of cloud radar and lidar measurements to detect the complex interaction between aerosol, vertical wind and the properties of mixed phase clouds under ambient conditions is discussed by **Seifert et al.**. Particularly noteworthy is the closure between derived concentrations of ice-nucleating particles (INP) and those of ice crystals in cirrus and mixed-phase clouds, made possible for the first time by the new techniques.

The highlight of the atmospheric measurements during the Polarstern expedition PASCAL was the use of the TROPOS tethered balloon with various instruments to study the Arctic boundary layer. **Egerer et al.** thereby uncovered layers of increased humidity above Arctic boundary layer clouds, which probably contribute to the longevity of these clouds by turbulent entrainment. TROPOS has been active for years in the in-situ detection of ice-nucleating particles in characteristic climatic regions. **Wex et al.** have now compiled a summary of these measurements and have been able to show that high INP concentrations are generally of terrestrial origin and that local marine sources only contribute significantly to INP availability in remote polar regions. **Sun et al.** have also

den windinduzierten Eintrag von Mineralstab in die Troposphäre. **Feuerstein und Schepanski** gelingt durch die Kombination von Satellitendaten der spektralen Bodenreflektivität und eines orographischen Fluss-Akkumulationsdatensatzes eine genauere Kartierung von Schwemmsedimenten, die maßgeblich zur Staubemission beitragen. Eine beeindruckende Erfassung der raumzeitlichen Verteilung des troposphärischen Mineralstaubs liefert die Kombination der thermischen Emissionskanäle des SEVIRI-Radiometers auf Meteosat. Umgekehrt lassen sich mithilfe eines Strahlungstransportmodelles derartige Messungen aus Staub-Modellergebnissen simulieren. Hiermit konnten **Banks et al.** meteorologische Situationen identifizieren, unter denen die Stauberkennung aus SEVIRI besonders gut machbar bzw. besonders schwierig ist.

Während Meteosat seit vielen Jahres das Arbeitspferd der Atmosphärenfernerkundung ist, startete im letzten Jahr mit AEOLUS ein neuartiges Satelliteninstrumentarium zur lidarbasierten Wind- und Aerosolmessung. **Baars et al.** berichten, wie TROPOS mit dessen weltweit verteilten Stationen zur bodengebundenen Fernerkundung und durch zusätzliche eigene Radiosondenaufstiege zur Validierung und Verbesserung der Aeolus-Produkte beiträgt. Eine Evaluierung satellitengetragener Messungen der Aerosol-optischen Dicke (AOD) sowie von AOD-Verteilungen aus Modellrechnungen wurde durch schiffsgetragene Sonnenphotometermessungen erbracht. **Witthuhn et al.** konnten zeigen, dass Satellitendaten in der Regel näher an den Schiffsbeobachtungen liegen als Modell-Reanalysen und das Satellitenprodukte insbesondere für Mineralstaubsituationen einen systematischen Unterschied zeigen, der auf einen systematischen Fehler im Satellitenalgorithmus hinweist. Speziell für die Arktis wurde im Rahmen der Polarsternexpedition PASCAL erstmalig die kleinskalige räumliche Verteilung der solaren Einstrahlung über dem Meereis erfasst. **Barrientos et al.** konnten mit den Messungen zeigen, dass sich die räumliche Einstrahlungsvariabilität bestimmten Bewölkungstypen zuordnen lässt. Lidarbasierte Messungen des Aerosolsprofils können aus abbildungstechnischen Gründen den bodennahen Bereich nicht erfassen. Diese Lücke schließt die am TROPOS entwickelte horizontal ausgerichtete spektrale Extinktionsmessung SAEMS. **Skupin et al.** stellen die ersten mobilen SAEMS-Messungen im Rahmen einer Messkampagne in Košetice (Tschechien) vor. Fortschritte in der Anwendung von Wolkenradar- und Lidarmessungen zur Erfassung der komplexen Wechselwirkung zwischen Aerosole, Vertikalwind und den Eigenschaften von Mischphasenwolken

conducted a long-term study, but now on a national level and in relation to ultra-fine particulate matter, which is highly relevant for air pollution. On the basis of 16 stations and 10 years of data from the German Ultrafine Aerosol Network GUAN, a general decrease in particulate matter in Germany was found, presumably due to reduction measures in the European region. A major component of particulate matter is soot. The geometric complexity of typical soot particle aggregates makes it difficult to calculate their optical properties. **Romshoo et al.** combined a fractal aggregation model with complex light scattering models to parameterize the optical properties of soot as a function of size and morphology. The greatest health impact of air pollution occurs indoors. To quantify this, TROPOS has recorded particle size distributions in 40 households in Leipzig, both indoors and outdoors. **Zhao et al.** confirm that indoor sources in particular are responsible for the highest levels of pollution.

Air pollution from wood-burning ovens has increased significantly in Germany in recent years. On the basis of long-term measurements in the centre of Melpitz and at the more remote Melpitz observatory of TROPOS, **van Pinxteren et al.** had already found a 60% increase in the PM mass from wood combustion in the centre of the village compared to the background pollution already for the relatively warm winter 2018/19. Air pollution is also reflected in organically bound sulphur, so-called organosulphates. By means of high-resolution mass spectrometry and skilful analytical approaches, **Brüggemann et al.** were able to determine for the first time the concentrations of terpenoid organosulphates in PM10 from Germany (Melpitz) and the northern Chinese plain and to prove that particle acidity plays a decisive role in organosulphate formation. The largest biogenic sulphur source in the atmosphere is dimethyl sulphide (DMS) emitted from the oceans. **Berndt et al.** were able to demonstrate in experiments the dominant process in the gas phase oxidation of the DMS, which is decisive for the formation of natural aerosol and associated cloud formation. Besides DMS, a variety of organic materials are emitted from the sea surface. The complete process chain from enrichment at the ocean surface film and emission into the atmosphere to aerosol formation and cloud influence is investigated by **van Pinxteren et al.** within the SAW project MarParCloud. The article gives a first brief overview of the results obtained. They show that there is a clear link between the ocean and the atmosphere, as substances from the oceans are transported up to cloud heights and are sometimes present in cloud water with high concentration. However, the marine contribution to cloud condensation and ice nucleation nuclei is small, unter Umgebungsbedingungen diskutieren **Seifert et al.**. Besonders erwähnenswert ist die durch die neuen Techniken erstmalig ermöglichte Schließung zwischen abgeleiteten Konzentrationen eisnukleierender Partikel (INP) und denen von Eiskristallen in Zirren und Mischphasenwolken.

Das Highlight der Atmosphärenmessungen während der Polarsternexpedition PASCAL war der Einsatz des TROPOS-Fesselballons mit diversen Instrumenten zur Erfassung der arktischen Grenzschicht. **Egerer et al.** entdeckten damit über den arktischen Grenzschichtwolken Schichten mit erhöhter Feuchte, die vermutlich durch turbulente Einmischung zur Langlebigkeit dieser Wolken beitragen. Seit Jahren ist TROPOS in der In-situ-Erfassung eisnukleierender Partikel in charakteristischen Klimaregionen aktiv. **Wex et al.** haben nun eine Zusammenschau dieser Messungen vorgenommen und konnten zeigen, dass hohe INP-Konzentrationen in der Regel terrestrischen Ursprungs sind und das nur in abgelegenen polaren Regionen lokale marine Quellen signifikant zur INP-Verfügbarkeit beitragen. Eine ebenfalls langangelegte Studie, nun aber national und bezogen auf den für Luftverschmutzung hochrelevanten Ultrafeinstaub, werten **Sun et al.** aus. Auf der Basis von 16 Stationen und 10 Jahren Daten des German Ultrafine Aerosol Networks GUAN ergibt sich dabei eine generelle Abnahme des Feinstaubs in Deutschland, vermutlich aufgrund von Minderungsmaßnahmen in der Europäischen Region. Eine wesentliche Komponente des Feinstaubs ist Ruß. Die geometrische Komplexität von typischen Rußpartikel-Aggregaten erschwert die Berechnung ihrer optischen Eigenschaften. **Romshoo et al.** kombinierte ein fraktales Aggregierungsmodell mit komplexen Lichtstreumodellen, um die optischen Eigenschaften des Rußes als Funktion der Größe und Morphologie zu parametrisieren. Die größte Gesundheitsbelastung durch Luftverschmutzung vollzieht sich in Innenräumen. Um dies zu quantifizieren hat TROPOS in 40 Haushalten in Leipzig Partikelgrößenverteilungen sowohl im Innen- als auch im Außenbereich erfasst. **Zhao et al**. bestätigen, dass insbesondere Innenraumquellen für die stärksten Belastungen verantwortlich sind.

Die Luftbelastung durch Holzofenverbrennung hat in Deutschland in den letzten Jahren stark zugenommen. Anhand von Langzeitmessungen im Ortszentrum Melpitz und an dem mehr abseits gelegenen Melpitz-Observatorium des TROPOS mussten **van Pinxteren et al.** bereits für den relative warmen Winter 2018/19 für das Ortszentrum eine 60%-ige Zunahme der PM-Masse aus Holzverbrennung im Vergleich zur Hintergrundbelastung feststellen.

at least in the subtropical ocean. In close cooperation with MarParCloud, the joint project MARSU is moving towards a more international and transfer-oriented study of marine aerosol and its impact on air pollution. **Fomba et al.** present the first results of the cooperation of scientific and industrial partners from seven nations with field campaigns in Morocco and Cape Verde.

Luftbelastung spiegelt sich auch in organisch gebundenem Schwefel, sogenannten Organosulfaten, wider. Mittels hochaufgelöster Massenspektrometrie und geschickten analytischen Ansätzen konnten **Brüggemann et al.** erstmalig die Konzentrationen von terpenoiden Organosulfaten in PM_{10} aus Deutschland (Melpitz) und der nordchinesischen Ebene ermitteln und nachweisen, dass die Partikelazidität eine entscheidende Rolle in der Organosulfatbildung spielt. Die größte biogene Schwefelquelle in der Atmosphäre stellt das aus den Ozeanen emittierte Dimethylsulfid (DMS) dar. **Berndt et al.** konnten im Experiment den dominanten Prozess in der Gasphasenoxidation des DMS nachweisen, der maßgeblich für die Bildung von natürlichem Aerosol und damit verbundener Wolkenbildung ist. Neben DMS werden eine Vielzahl organischer Materialien aus der Meeresoberfläche emittiert. Die komplette Prozesskette von der Anreicherung am Ozeanoberflächenfilm über die Emission in die Atmosphäre bis zur Aerosolbildung und Wolkenbeeinflussung untersuchen **van Pinxteren et al.** im Rahmen des SAW-Projektes MarParCloud. Der Artikel gibt eine erste kurze Übersicht über die gewonnenen Ergebnisse. Diese zeigen, dass es eine deutliche Verbindung zwischen Ozean und Atmosphäre gibt, da Substanzen aus den Ozeanen bis in Wolkenhöhen transportiert werden und teilweise im Wolkenwasser stark angereichert vorliegen. Allerdings ist der marine Beitrag zu Wolkenkondensations- und Eisnukleationskernen zumindest im subtropischen Ozean gering. In enger Zusammenarbeit mit MarParCloud geht das Verbundprojekt MARSU in eine stärkere international und Transfer-geprägte Untersuchung des marinen Aerosols und dessen Auswirkung auf Luftverschmutzung. **Fomba et al.** stellen die ersten Ergebnisse der Kooperation wissenschaftlicher und industrieller Partner aus sieben Nationen mit Feldkampagnen in Marokko und den Kapverden vor.

Transfer in science and society – overview

Knowledge transfer and public visibility

TROPOS research for the expert public. On account of the application oriented fundamental research of the Institute, its scientific knowledge is mainly transferred through scientific publications and conference contributions (see list, p. 147).

During the reporting period the following conferences with TROPOS contribution are highlighted:

The institutes participating in the Leibniz network "Mathematical Modelling and Simulation" (WIAS, IOM and TROPOS) jointly organised the network meeting "3rd Leibniz MMS Days" in Leipzig with 50 participants in February 2018. In the same year, the plenary meeting of the Leibniz research network INFECTIONS'21 and a symposium of the network with 50 participants took place in Leipzig, organized by Dr. Kerstin Schepanski of the Department Modelling of Atmospheric Processes.

The 16th event of the workshop series "Atmospheric Chemistry and Air Quality: Progress, Challenges, and Multiphase Aspects" was held with international participation in October 2018 in Leipzig, led by the department "Chemistry of the Atmosphere", and offerred an annual compilation of current results in the research field and ongoing projects. In the field of atmospheric chemistry, the "Sino-European School on Atmospheric Chemistry" (SESAC 4, 04.-15.11.2019), which has now been held for the fourth time with 100 PhD students, is also an important interdisciplinary school for young scientists working on the effects of chemical processes in the atmosphere on air quality and climate. TROPOS participated in this international event in Shanghai with several researchers.

The workshop "Synergy of physical, biological, and biogeochemical Arctic observations – from recent Arctic expeditions towards MOSAiC 2018" also had an inter-disciplinary focus. It was a follow-up to the Polarstern expedition "PASCAL" within the SFB "Arctic Amplification". About 45 participants from the disciplines of atmospheric physics, marine biology and biogeochemistry exchanged ideas in Delmenhorst in October 2018.

With the "Forum Wissenschaftsmanagement Leipzig" (FoWi), the four research institutions of the Science Park Leipzig (DBFZ, UFZ, TROPOS and IOM) launched a new conference format in 2018, which addresses questions of administrative science management relating to personnel, research infrastructure, purchasing and finance.

Due to its special importance, a separate article of this report is dedicated to the first conference on

Transfer in Wissenschaft und Gesellschaft – Überblick

Wissenstransfer und Außenwirkung

TROPOS-Forschung für Fachpublikum. Auf Grund der Ausrichtung des Institutes als anwendungsorientiertes Grundlagenforschungsinstitut erfolgt die Verwertung hauptsächlich in Fachpublikationen und Konferenzbeiträgen (siehe Liste, S. 147).

Aus den wissenschaftlichen Tagungen, an denen TROPOS beteiligt war, stechen im Berichtszeitraum folgende heraus:

Die Institute im Leibniz-Netzwerk „Mathematische Modellierung und Simulation" (WIAS, IOM und TROPOS) organisierten im Februar 2018 das Netzwerktreffen „3rd Leibniz MMS Days" mit 50 Teilnehmenden in Leipzig. Im gleichen Jahr fanden, organisiert durch Dr. Kerstin Schepanski der Abteilung Modellierung atmosphärischer Prozesse, die Vollversammlung des Leibniz-Forschungsverbundes INFECTIONS'21 und ein Symposium des Verbundes mit ebenfalls 50 Teilnehmenden in Leipzig statt.

Die 16. Veranstaltung der Workshop-Serie „Atmospheric Chemistry and Air Quality: Progress, Challenges, and Multiphase Aspects" wurde mit internationaler Beteiligung im Oktober 2018 in Leipzig, federführend von der Abteilung „Chemie der Atmosphäre" durchgeführt und bietet eine jährliche Zusammenstellung aktueller Ergebnisse im Forschungsbereich und laufender Projekte. Im Bereich der Atmosphärenchemie ist auf internationaler Ebene auch die inzwischen zum vierten Mal für 100 Promovierende gehaltene „Sino-European School on Atmospheric Chemistry" (SESAC 4, 04.-15.11.2019) eine wichtige interdisziplinäre Schule für Nachwuchswissenschaftlerinnen und -wissenschaftler, die sich mit der Wirkung chemischer Prozesse der Atmosphäre auf Luftqualität und Klima beschäftigen. TROPOS beteiligte sich mit mehreren Forschenden an dieser internationalen Veranstaltung in Shanghai.

Ebenfalls interdisziplinär ausgerichtet war der Workshop „Synergy of physical, biological, and biogeochemical Arctic observations – From recent Arctic expeditions towards MOSAiC 2018" in Nachfolge der Polarstern-Expedition „PASCAL" im Rahmen des SFB „Arctic Amplification". Circa 45 Teilnehmende der Disziplinen Atmosphärenphysik, Meeresbiologie und Biogeochemie tauschten sich im Oktober 2018 in Delmenhorst aus.

Mit dem „Forum Wissenschaftsmanagement Leipzig" (FoWi) starteten die vier Forschungseinrichtungen aus dem Wissenschaftspark Leipzig (DBFZ, UFZ, TROPOS und IOM) 2018 ein neues Konferenzformat, das Fragen des administrativen

Transfer in science and society – overview / Transfer in Wissenschaft und Gesellschaft – Überblick

Central Asian dust "CADUC-1", which could be realised in Tajikistan in April 2019 (see p. 31).

Selected topics and activities for policy and society. Results from TROPOS research contributes to policy advice in the environmental sector. For example, for the Land of Saxony and the Federal Environmental Agency (UBA) or also the Berlin Senate Administration, practise oriented investigations regarding the behaviour and the future development of air pollutants in the atmosphere are conducted. In the framework of projects in collaboration with the Environmental Agency and the Saxon State Office for the Environment, Agriculture and Geology (LfULG) measurement data of fine and ultrafine particles are collected, evaluated and provided for further interpretation of the concentration and chemical composition of these particles.

In the field of clean-air policy-advice TROPOS also contributes with its own studies, which are used for air directive discussions and the implementation of clean-air strategies. This includes for example the engagement in respective advisory boards and events on the topic of air quality, like in the following examples: A global initiative by the National Academies of Science and Medicine from South Africa, Brazil, Germany and the USA to reduce the health effects of air pollution, urged the United Nations to launch a global pact against air pollution, when handing over their report in New York on 19 June 2019. Prof. Dr. Alfred Wiedensohler of TROPOS was also involved in the preparation of the report, which proposes measures in policy, legislation, regulation, standards and enforcement in combination with the introduction of new technologies and the strengthening of social awareness to solve the air problems.

The DECHEMA Special Colloquium "Mobility of the Future in the Light of Air Quality and Climate Change: An Opportunity for the Diesel?", held in Frankfurt am Main on 13 December 2018, discussed, among other things, the so-called "E-Fuels" as an alternative to diesel and the future of this widely used driving technology. The GDCh working group "Atmospheric Chemistry" under the management of Prof. Dr. Hartmut Herrmann from TROPOS was also involved in the preparations.

At the expert hearing on ultra-fine particulate matter on 22/23 August 2019 in Frankfurt am Main, leading experts from Germany – including Prof. Dr. Alfred Wiedensohler and Dr. Dominik van Pinxteren from TROPOS – were invited on the initiative of the Forum Airport and Region (FFR) and the Hessian State Agency for Nature Conservation, Environment and Geology (HLNUG). The hearing marked the start of further intensive investigations into ultra-fine dust

Wissenschaftsmanagements rund um die Bereiche Personal, Forschungsinfrastruktur, Einkauf und Finanzen thematisiert.

Der ersten Konferenz zum zentralasiatischen Staub „CADUC-1", die im April 2019 in Tadschikistan realisiert werden konnte, ist aufgrund ihrer besonderen Bedeutung ein eigener Artikel gewidmet (s. S. 31).

Ausgewählte Themen und Aktivitäten für Politik und Gesellschaft. Die Forschungsergebnisse des TROPOS dienen auch als ein Beitrag zur Politikberatung im Umweltbereich. So werden für das Land Sachsen und das Umweltbundesamt (UBA) oder auch für die Berliner Senatsverwaltung praxisrelevante Untersuchungen zum Verhalten und zur künftigen Entwicklung von Schadstoffen in der Atmosphäre durchgeführt. Außerdem werden im Rahmen von Auftragsprojekten für das UBA und das Sächsische Landesamt für Umwelt und Geologie (LfULG) über längere Zeiträume Messdaten zu den Konzentrationen feiner und ultrafeiner Aerosolpartikel sowie zur chemischen Partikelzusammensetzung in der Atmosphäre erhoben, ausgewertet und diesen Institutionen zur weiteren Nutzung zur Verfügung gestellt.

Im Bereich der Luftreinhaltung trägt TROPOS zur Politikberatung auch durch eigene Forschungsergebnisse bei, die in der Richtliniendiskussion und bei der Erstellung von Luftreinhalteplänen verwendet werden.

Fig. / Abb. 1: Every two years the LfULG status colloquium provides an overview of "Air quality in Saxony". TROPOS experts regularly take part in this public event and report on the latest results of their projects. In 2019, Dr. Falk Mothes informed about the influence of wood heating systems on air quality (photo) and Dr. Dominik van Pinxteren about the influence of weather on air quality. / Das LfULG-Statuskolloquium gibt aller zwei Jahre einen Überblick zur „Luftqualität in Sachsen". Experten von TROPOS beteiligen sich regelmäßig an dieser öffentlichen Veranstaltung und berichten über aktuelle Ergebnisse aus ihren Projekten. 2019 informierte Dr. Falk Mothes über den Einfluss von Holzheizungen auf die Luftqualität (Foto) und Dr. Dominik van Pinxteren über den Einfluss der Witterung auf die Luftqualität. (Photo: Tilo Arnhold / TROPOS)

pollution in the region around Frankfurt Airport, in which TROPOS is also participating.

The 5th LfULG status colloquium "Air Quality in Saxony" on 4thDecember 2019 in Dresden summarised the current knowledge in the state – this year with lectures by Dr. Falk Mothes on wood heating systems and Dr. Dominik van Pinxteren on the influence of weather on air quality, among others.

The DECHEMA Special Colloquium "Mobility Turnaround for Climate Protection: Battery or Fuel Cell - or "Diesel"?" took place on the occasion of the GDCh Carl Duisberg award handed over to Professor Reinhard Zellner on December 4, 2019 in Frankfurt am Main. The event was prepared by the working committees "Chemistry, Air Quality and Climate" and "Fine Dust" of DECHEMA, VGI-GVC, GDCh, DBG and VDI/KRdL, and by Prof. Dr. Hartmut Herrmann of TROPOS.

The public final event of the EU project "OdCom" – "Objectification of odor complaints in the Saxon-Czech border area" took place on 20 May 2019 in the Hygiene Museum Dresden. Within the scope of the project, a detailed documentation of odor events, the testing of innovative measuring techniques and a data evaluation with regard to odor episodes, air quality and toxic risk potential took place. Objective data contributed to the information of the population about the perceived odour pollution and health consequences. Dr. Maik Merkel provided information about

Fig. / Abb. 2: On 17 December 2019, around 40 Leipzig citizens experienced the polar time performance of the Schaubühne Lindenfels at the Natural History Museum in Leipzig and listened intently to the telephone conversation with Polarstern in the Arctic. Dr. Ronny Engelmann from TROPOS reported via satellite telephone about life and work during the polar night of the MOSAiC expedition. / Rund 40 Leipzigerinnen und Leipziger erlebten am 17. Dezember 2019 die Polarzeit-Performance der Schaubühne Lindenfels im Naturkundemuseum Leipzig und hörten gespannt beim Telefonat mit der Polarstern in der Arktis zu. Dr. Ronny Engelmann vom TROPOS berichtete dabei via Satellitentelefon vom Leben und Arbeiten in der Polarnacht bei der MOSAiC-Expedition.. (Photo: Tilo Arnhold / TROPOS)

Dazu zählt unter anderem das Engagement in entsprechenden Gremien und Veranstaltungen zum Thema Luftqualität wie in folgenden Beispielen dargestellt:

Eine globale Initiative zur Reduktion der Gesundheitsauswirkungen von Luftverschmutzung durch die Nationalakademien der Wissenschaften und der Medizin aus Südafrika, Brasilien, Deutschland und den USA hat bei der Übergabe ihres Berichts am 19.06.2019 in New York die Vereinten Nationen aufgefordert, einen globalen Pakt gegen die Luftverschmutzung zu starten. An der Erarbeitung des Berichts, der zur Lösung der Luftprobleme eine Kombination aus Politik, Gesetzgebung, Regulierung, Normen und Durchsetzung in Verbindung mit der Einführung neuer Technologien und der Stärkung des sozialen Bewusstseins vorschlägt, war auch Prof. Dr. Alfred Wiedensohler vom TROPOS beteiligt.

Das DECHEMA-Sonderkolloquium „Mobilität der Zukunft im Lichte von Luftqualität und Klimawandel: Eine Chance für den Diesel?" diskutierte am 13.12.2018 in Frankfurt am Main u.a. über die sogenannten „E-Fuels" als Alternative zum Diesel und die Zukunft dieser weit verbreiteten Antriebstechnologie. In die Vorbereitung war auch der GDCh-Arbeitskreis „Atmosphärenchemie" mit Vorsitz von Prof. Dr. Hartmut Herrmann vom TROPOS involviert.

Die Expertenanhörung Ultrafeinstaub am 22./23.08.2019 in Frankfurt am Main hatte auf Initiative des Forums Flughafen und Region (FFR) und des Hessischen Landesamtes für Naturschutz, Umwelt und Geologie (HLNUG) führende Experten aus Deutschland eingeladen – darunter auch Prof. Dr. Alfred Wiedensohler und Dr. Dominik van Pinxteren des TROPOS. Die Anhörung bildete den Auftakt für weitere intensive Untersuchungen zur Ultrafeinstaubbelastung in der Region um den Frankfurter Flughafen, an denen sich auch TROPOS beteiligt.

Das 5. LfULG-Statuskolloquium „Luftqualität in Sachsen" am 04.12.2019 in Dresden brachte das aktuelle Wissen im Freistaat auf den Punkt – dieses Jahr u.a. mit Vorträgen von Dr. Falk Mothes zu Holzheizungen und Dr. Dominik van Pinxteren zum Einfluss der Witterung auf die Luftqualität.

Das DECHEMA-Sonderkolloquium „Mobilitätswende für den Klimaschutz: Batterie oder Brennstoffzelle – oder doch „Diesel"?" fand anlässlich der Verleihung der Carl-Duisberg-Plakette der GDCh an Professor Reinhard Zellner am 04.12.2019 in Frankfurt am Main statt. Vorbereitet wurde die Veranstaltung durch die Arbeitsausschüsse „Chemie, Luftqualität und Klima" sowie „Feinstäube" von DECHEMA, VGI-GVC, GDCh, DBG und VDI/KRdL u.a. von Prof. Dr. Hartmut Herrmann vom TROPOS.

Transfer in science and society – overview / Transfer in Wissenschaft und Gesellschaft – Überblick

Fig. / Abb. 3: The MOSAiC expedition was present at the UN climate conference COP25 in Madrid - via satellite telephone. TROPOS had organised a side event on aerosol-cloud interactions in the "German Science Hour" of the BMBF. / Die MOSAiC-Expedition war auf der UN-Klimakonferenz COP25 in Madrid dabei - via Satellitentelefon. TROPOS hatte ein Side Event zu Aerosol-Wolken-Wechselwirkungen in der „German Science Hour" des BMBF organisiert. (Photo: Konstantin Engelbrecht, BMZ)

TROPOS measurements of ultra-fine dust and soot in the Saxon-Czech border region

Prof. Dr. Andreas Macke and Dr. Dominik van Pinxteren represented the Institute at "Leibniz im Bundestag" on 5/6 June 2018 in a discussion with members of the German Bundestag on the topic of "Air quality: Environmental zones and diesel driving prohibitions".

TROPOS was also engaged in the field of air quality on an international level: Together with partners from FZ Jülich, IASS Potsdam and the World Federation of Engineers (WFEO), the Institute organized a side event in the European Union pavilion at the UN Climate Conference "COP24" in Katowice, Poland. The scientists presented current research results on air pollution and discussed sustainable solutions on December 3, 2018. The aim of the researchers of the German Climate Consortium (DKK) was to draw attention to the global dimension of air pollution and to promote joint solutions for air and climate protection. In this context Prof. Dr. Hartmut Herrmann from TROPOS informed among other things about the importance of the EU networks ACTRIS and EUROCHAMP-2020.

In addition to the Institute's competence in urban air quality (particulate matter and low emission zones), especially climate relevant expertise about cloud formation processes or the impact of dust in the atmosphere became more important.

As part of the German Science Hour, TROPOS researchers provided information on the significance of aerosols and clouds in the climate system at the UN Climate Conference "COP25" in Madrid on 12 December 2019. The side event "Aerosol-cloud

Die öffentliche Abschlussveranstaltung des EU-Projektes „OdCom" – „Objektivierung der Geruchsbeschwerden im sächsisch-tschechischen Grenzgebiet" fand am 20.05.2019 im Hygienemuseum Dresden statt. Im Rahmen des Projekts erfolgten eine detaillierte Dokumentation von Geruchsereignissen, die Erprobung innovativer Messtechnik und eine Datenauswertung hinsichtlich der Geruchsepisoden, Luftqualität und des toxischen Risikopotentials. Objektive Daten trugen hierbei zur Aufklärung der Bevölkerung über die wahrgenommene Geruchsbelastung und gesundheitlichen Folgen bei. Dr. Maik Merkel informierte dabei über die Messungen des TROPOS zu Ultrafeinstaub und Ruß im sächsisch-tschechischen Grenzgebiet.

Im Deutschen Bundestag aktiv waren Prof. Andreas Macke und Dr. Dominik van Pinxteren, die das Institut bei „Leibniz im Bundestag" am 05./06.06.2018 im Gespräch mit Mitgliedern des Deutschen Bundestages zum Thema „Luftqualität: Umweltzonen und Dieselfahrverbote" vertraten.

Auch auf internationaler Ebene war TROPOS im Bereich Luftqualität aktiv: Zusammen mit Partnern vom FZ Jülich, dem IASS Potsdam sowie dem Weltverband der Ingenieure (WFEO) organisierte das Institut ein Side Event im Pavillon der Europäischen Union auf der UN-Klimakonferenz „COP24" im polnischen Katowice. Die Wissenschaftler stellten dabei am 03.12.2018 aktuelle Forschungsergebnisse zum Thema Luftverschmutzung vor und diskutierten nachhaltige Lösungen. Ziel der Forschenden des Deutschen Klimakonsortiums (DKK) war es, auf die globale Dimension der Luftverschmutzung aufmerksam zu machen und für gemeinsame Lösungen zum Luft- und Klimaschutz zu werben. Prof. Dr. Hartmut Herrmann vom TROPOS informierte dabei u.a. über die Bedeutung der EU-Netzwerke ACTRIS und EUROCHAMP-2020.

Neben der Kompetenz zur urbanen Luftqualität (Feinstaub und Umweltzonen) gewann besonders klimarelevantes Wissen über Prozesse wie Wolkenbildung oder die Auswirkungen von Staub in der Atmosphäre an Bedeutung. Im Rahmen der German Science Hour informierten Forschende des TROPOS auf der UN-Klimakonferenz „COP25" am 12.12.2019 in Madrid über die Bedeutung von Aerosolen und Wolken im Klimasystem. Das Side Event „Aerosol-cloud interaction in a changing climate: chance or threat" erklärte unterhaltsam die physikalischen Prozesse. Experten und Expertinnen, die mittels Liveübertragungen zu Messstationen an Schlüsselorten in Chile, Zypern, Zentralasien und auf dem Forschungsschiff „Polarstern" in der Arktis zugeschaltet wurden, stellten den Einfluss sich ändernder Luftverschmutzung auf das Wetter vor Ort und den globalen Klimawandel vor.

interaction in a changing climate: chance or threat" explained physical processes in an entertaining way. Experts, who were connected via live transmissions to measuring stations at key locations in Chile, Cyprus, Central Asia and on the research vessel "Polarstern" in the Arctic, presented the influence of changing air pollution on local weather and global climate change.

TROPOS research results for the public at large. TROPOS seeks dialogue with the public using print media, radio and TV. The number of press releases published was increased to 34 in 2018/19 (22 releases 2016/17). In addition, there are online published short news and press releases from partner institutions with TROPOS reference (7). This resulted in over 321 media releases in 2018. In 2019 there were 140 publications (to our knowledge).

Numerous radio and television reports on arctic warming should be particularly emphasized: The preparations for the one-year MOSAiC expedition with TROPOS participation, the launch and first news from on board were followed by various print media (above all Sächsische Zeitung). Three radio reports (MDR, WDR) and three television reports on MDR, 3sat and ARD accompanied the events around MOSAiC.

The media discussion on the BMBF project WTimpact and its part "Luft in Leipzig" (Air in Leipzig), in which interested citizens can observe fine dust and soot themselves using a measuring backpack, received a great response. Among others, television reports on MDR, RTL, n-tv and ZDF-KIKA as well as various newspaper and radio reports reported on the project.

The distribution of wood combustion aerosol during the reporting period, especially the smoke from Canadian forest fires, and also volcanic dust, regularly attracts media interest. As TROPOS has its own measurements and expertise the Institute's scientists are available for enquiries and provide measurement results. Various online media worldwide and for example "Spiegel.de" reported on this topic in 2018. A great media interest was also generated by the support of the new ESA wind satellite Aeolus by the TROPOS Lidar Group, for example a "Deutsche Welle" broadcast and others.

Under the headline "Why clouds are important", an article on the importance of clouds was published nationwide by the news agency "dpa" in its news for children, which led to about 210 appearances in various German-language newspapers. In 2018/19, several magazine articles were also dedicated in detail to cloud research, e.g. the "Lufthansa Magazin" and "Bild der Wissenschaft". Among the many articles, a feature by SWR2 stood out in 2018, which was dedicated to the controversial topic of climate engineering

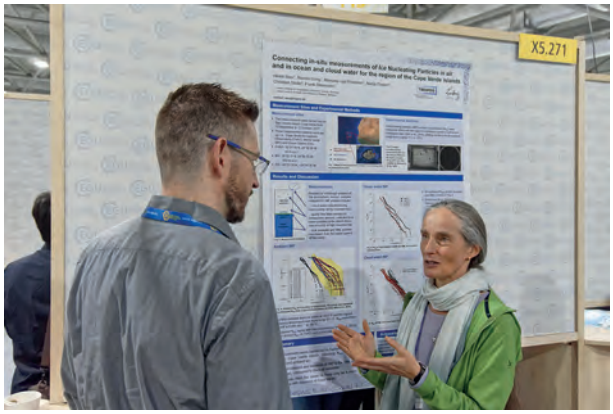

Fig. / Abb. 4: In 2019, many TROPOS researchers again actively participated with talks and posters in the annual General Assembly of the European Union of Geosciences (EGU) in Vienna, one of the largest conferences of its kind. / Viele TROPOS-Forschende beteiligten sich auch 2019 wieder aktiv mit Vorträgen und Postern an der jährlich in Wien stattfindenden Generalversammlung der Europäische Union der Geowissenschaften (EGU), eine der größten Konferenzen ihrer Art. (Photo: Tilo Arnhold / TROPOS)

TROPOS-Forschung für die breite Öffentlichkeit. TROPOS steht im Dialog mit der Öffentlichkeit – u.a. auch über Printmedien sowie Hör- und Fernsehfunk. Die Veröffentlichung von Mitteilungen wurde 2018/19 auf 34 Pressemitteilungen erhöht (22 Mitteilungen 2016/17). Dazu kommen online veröffentlichte Kurzmitteilungen und Pressemitteilungen von Partner-institutionen mit TROPOS-Erwähnung (7). Daraus resultierten im Jahr 2018 über 321 Medienveröffentlichungen (soweit bekannt). Im Jahr 2019 waren es 140 Veröffentlichungen (soweit bekannt).

Besonders hervorzuheben sind zahlreiche Radio- und Fernsehbeiträge zur Erwärmung der Arktis: Die Vorbereitungen für die einjährige MOSAiC-Expedition mit TROPOS-Beteiligung, der Start und erste Nachrichten von Bord wurden durch verschiedene Printmedien (v.a. Sächsische Zeitung) verfolgt. Drei Radiobeiträge (MDR, WDR) sowie drei Fernsehbeiträge beim MDR, 3sat und in der ARD begleiteten das Geschehen rund um MOSAiC.

Große Resonanz fand das Mediengespräch zum BMBF-Projekt WTimpact und dessen Teilprojekt „Luft in Leipzig", bei dem Interessierte selber Feinstaub und Ruß per Messrucksack erfassen können. Darüber berichteten u.a. Fernsehbeiträge im MDR, RTL, n-tv und ZDF-KIKA sowie diverse Zeitungs- und Radioberichte.

Die Themen Verbreitung von Waldbrandaerosol, hier im Berichtszeitraum vor allem der Rauch kanadischer Waldbrände, und auch Vulkanstaub finden regelmäßiges Medieninteresse, da TROPOS durch eigene Messungen mit Expertise für Anfragen bereitsteht und über Messergebnisse verfügt. Diverse Online-Medien, wie z.B. Spiegel.de berichteten 2018

under the title “Gutes Klima in Teufels Küche?” and spoke with researchers from the atmosphere chambers at TROPOS.

Of local importance was a cover story in the city magazine “der kreuzer”, which dealt with the problem of air pollution in Leipzig on 7 pages, and in detail with TROPOS’ investigations of the environmental zone.

The website addresses research partners as well as the public at large. The section “Discover” aims at presenting TROPOS research for the interested public.

On the occasion of the “World Meteorology Day 2019”, an overview of research projects in which the sun and its radiation play a role was created under the topic “The sun, the earth and the weather”. To illustrate scientific work on the website, scientists increasingly perform picture reports from their work around the world. For this purpose the section “Measurement campaigns” was installed under the menu point “Current issues”, where impressions and reports from measurement campaigns, like “MetPVNet 2018/19” in Allgäu or “PAMARCMiP 2018” on Greenland can be found. One of the focal points (analogous to the Polarstern expedition PS106/PASCAL 2017) is the blog on the drift of Polarstern during the MOSAiC expedition 2019/20 in the central Arctic, in which TROPOS is participating for one year.

With the Twitter channels “@TROPOS_de” & “@TROPOS_eu” the institute is also social media active in German and English. The German-language channel primarily addresses the general public in Germany; the English-language channel is also used for networking within the scientific community, such as ACTRIS. About 666 and 375 persons and institutions respectively have subscribed to the channel (“followers”). On average, the reports are viewed about 50,000 or 20,000 times per month (“Impressions”). This means that, compared to the previous period, the distribution has approximately doubled.

Events. In January 2018, Leipzig’s Science Cinema presented the global topic of air pollution: the arte documentary “Dicke Luft. Wenn Städte ersticken” showed the effects in different regions of the world. After the movie, the 200 visitors discussed the problem with the experts. TROPOS was represented by Prof. Dr. Hartmut Herrmann and Prof. Dr. Alfred Wiedensohler. The panel was completed by Prof. Dr. Jean-Francois Doussin (Laboratoire Interuniversitaire des Systèmes Atmosphériques LISA, Paris), with whom there is close cooperation through the EUROCHAMP project. The event was organised by TROPOS in cooperation with the museum

weltweit darüber. Ebenfalls auf große Resonanz in den Medien stieß die Unterstützung des neue ESA-Windsatelliten „Aeolus“ durch die Lidar-Gruppe am TROPOS, worüber u.a. die Deutsche Welle berichtete.

Unter der Überschrift „Wieso Wolken wichtig sind“ fand ein Artikel zur Bedeutung der Wolken deutschlandweite Verbreitung, den die Nachrichtenagentur dpa in ihren Kindernachrichten veröffentlichte und der zu ca. 210 Erscheinungen in diversen deutschsprachigen Zeitungen führte. Auch 2018/19 widmeten sich mehrere Magazin-Beiträge ausführlich der Wolkenforschung, so z.B. das „Lufthansa-Magazin“ und „Bild der Wissenschaft“. Aus der Vielzahl der Beiträge stach 2018 auch ein Feature von SWR2 hervor, dass sich unter dem Titel „Gutes Klima in Teufels Küche?“ mit dem umstrittenen Thema Climate Engineering beschäftigte und dazu mit Forschenden der Atmosphärenkammern am TROPOS sprach.

Von lokaler Bedeutung war eine Titelgeschichte im Stadtmagazin Kreuzer, die sich auf 7 Seiten dem Problem der Luftverschmutzung in Leipzig befasste und dabei ausführlich auf die Untersuchungen von TROPOS zur Umweltzone einging.

Das Internetangebot richtet sich neben Forschenden zugleich an die breite Öffentlichkeit. Die Rubrik „Entdecken“ hat daher zum Ziel, die Forschung für alle Interessierten zu erläutern. Zum „Welttag der Meteorologie 2019“ entstand dabei anlässlich des Themas „Die Sonne, die Erde und das Wetter“ ein Überblick zu Forschungsprojekten, in denen die

Fig. / Abb. 5: TROPOS experts Prof. Alfred Wiedensohler and Prof. Hartmut Herrmann, together with their French colleague Prof. Jean-François Doussin (LISA, Paris), discussed the global problem of air pollution at the science cinema “Thick air - when cities suffocate” on 24 January 2018 at the Zeitgeschichtliches Forum Leipzig. / Beim Wissenschaftskino „Dicke Luft – Wenn Städte ersticken“ diskutierten am 24.1.2018 im Zeitgeschichtlichen Forum Leipzig die TROPOS-Experten Prof. Alfred Wiedensohler und Prof. Hartmut Herrmann zusammen mit ihrem französischen Kollegen Prof. Jean-François Doussin (LISA, Paris) über das globale Problem Luftverschmutzung. (Photo: Beate Richter / TROPOS)

Zeitgeschichtliches Forum, the city of Leipzig and the Institut Français Leipzig.

Together with 60 other institutions, TROPOS took part in the "Long Night of the Sciences" on 22 June 2018, which takes place every two years in Leipzig. The event offered insights into laboratories, lecture halls, institutes, clinics, magazines and archives and thus also into the laboratories of TROPOS. On the occasion of the expedition "PS106/PASCAL/ACLOUD" within the SFB "Arctic Amplification", the Leipzig Institute of Meteorology and TROPOS jointly presented an Arctic programme: In addition to lectures by expedition participants, visitors were able to gain impressions from the accompanying exhibition by painter Kerstin Heymach and a multimedia presentation of the editor and also expedition participant Stephan Schön of the newspaper Sächsische Zeitung. In addition to this programme in the university's "Augusteum", there was also a tour through the city centre with a measuring backpack for particulate matter and laboratory visits at the institute. TROPOS also had the opportunity to take part in the Dresden Science Night in 2018 and 2019 and provided information on air quality and climate at its cooperation partner LfULG.

In the series "Studium Universale" of the University of Leipzig, TROPOS contributed with a lecture by Prof. Dr. Alfred Wiedensohler on the Leipzig environmental zone. For the young audience, the topic climate change and CO_2 emissions were prepared in a child-friendly manner with experiments in the children's university.

Fig. / Abb. 6: For the Long Night of Sciences 2018 in Leipzig, TROPOS and the Institute of Meteorology organised lectures and exhibitions on Arctic warming in the Augusteum of the Leipzig University. In the foyer, a city tour "On the trail of particles with a measuring backpack" started. / Zur Langen Nacht der Wissenschaften 2018 in Leipzig organisierte TROPOS zusammen mit dem Institut für Meteorologie Vorträge und Ausstellungen über die arktische Klimaerwärmung im Augusteum der Universität Leipzig. Im Foyer startete ein Stadtrundgang „Mit Messrucksack den Partikeln auf der Spur". (Photo: Tilo Arnhold / TROPOS)

Sonne und ihre Strahlung eine Rolle spielten. Um Wissenschaft anschaulicher zu machen, kommen auf www.tropos.de zunehmend Forschende zu Wort, die auch selbst von den Messkampagnen in aller Welt berichten. Dazu wurde unter dem Menüpunkt „Aktuelles" die Rubrik „Messkampagnen" ausgebaut, in der z. B. Berichte und Fotos von Kampagnen und Expeditionen wie „MetPVNet 2018/19" im Allgäu oder „PAMARCMiP 2018" auf Grönland zu finden sind. Einen Schwerpunkt dabei bildet (analog zur Polarstern-Expedition PS106/PASCAL 2017) dabei der Blog zur Drift der „Polarstern" während der MOSAiC-Expedition 2019/20 in der zentralen Arktis, an der TROPOS ein Jahr lang teilnimmt.

Mit den Twitter-Kanälen „@TROPOS_de" & „@TROPOS_eu" ist das Institut auch in den sozialen Medien auf deutsch bzw. englisch aktiv. Der deutschsprachige Kanal richtet sich primär an die breite Öffentlichkeit in Deutschland; der englischsprachige dient auch der Vernetzung innerhalb der wissenschaftlichen Community wie u.a. bei ACTRIS. Circa 666 bzw. 375 Personen und Institutionen haben den Kanal abonniert („Follower"). Im Schnitt werden die Meldungen ca. 50.000 bzw. 20.000 Mal pro Monat betrachtet („Impressions"). Damit konnte die Verbreitung im Vergleich zum vorigen Zeitraum etwa verdoppelt werden.

Veranstaltungen. Das Leipziger Wissenschaftskino zeigte im Januar 2018 das globalen Thema Luftverschmutzung: Die arte-Dokumentation „Dicke Luft. Wenn Städte ersticken" stellte die Auswirkungen in verschiedenen Regionen der Welt dar. Im Anschluss an den Film diskutierten die 200 Besucherinnen und Besucher mit Experten über die Problematik. TROPOS war dabei durch Prof. Dr. Hartmut Herrmann und Prof. Dr. Alfred Wiedensohler vertreten. Die Runde komplettierte Prof. Jean-Francois Doussin (Laboratoire Interuniversitaire des Systèmes Atmosphériques LISA, Paris), mit dem über EUROCHAMP eine enge Kooperation besteht. Die Veranstaltung wurde von TROPOS in Kooperation mit dem Zeitgeschichtlichen Forum, der Stadt Leipzig und dem Institut français Leipzig organisiert.

Zusammen mit 60 anderen Institutionen beteiligte sich TROPOS an der alle zwei Jahre in Leipzig stattfindenden „Langen Nacht der Wissenschaften" am 22. Juni 2018, die Einblicke in Labore, Hörsäle, Institute, Kliniken, Magazine und Archive bot und damit auch in die Labore des TROPOS. Anlässlich der Expedition „PS106/PASCAL/ACLOUD" im Rahmen des SFB „Arktische Verstärkung" präsentierten das Leipziger Institut für Meteorologie und TROPOS gemeinsam ein arktisches Programm: Neben Vorträgen von Expeditionsteilnehmenden konnten die Besucher auch

Transfer in science and society – overview / Transfer in Wissenschaft und Gesellschaft – Überblick

Fig. / Abb. 7: In August 2018, Prof. Dr. Alfred Wiedensohler informed at the Leipzig-based association Ökolöwe Umweltbund Leipzig e.V. about the "Effects of the Leipzig Low Emission Zone on air quality". / Im August 2018 informierte Prof. Dr. Alfred Wiedensohler beim Leipziger Verein Ökolöwe Umweltbund Leipzig e.V. über die „Effekte der Leipziger Umweltzone auf die Luftqualität". (Photo: Tilo Arnhold / TROPOS)

TROPOS is actively participating in the public relations work of the German Climate Consortium (DKK), the "Klimanavigator" and the Leibniz Association.

The BMBF project WTimpact, launched in September 2017, is a new approach to develop collaborative knowledge development as a transfer instrument and to move from knowledge transfer to knowledge exchange: In this project, Leipzig residents were able to measure particulate matter and soot in the city by means of mobile devices. For several field phases of the "Air in Leipzig" project, TROPOS had recruited volunteers who were interested in air quality and how it is investigated. Equipped with a new type of measuring backpack and intensively supervised by TROPOS, they spent a week taking a closer look at the air in Leipzig. The citizen scientists evaluated their measurements in the data portal https://www.luft-leipzig.de, set up especially for this purpose. This process was accompanied by educational and communication researchers. A total of four institutes of the Leibniz Association are thus investigating new methods of knowledge transfer.

Equal opportunities and promotion of young researchers

Equal opportunities are implemented as a leading principle at TROPOS. The institute fulfils the equal opportunity standards of the Leibniz Association, which were worked out by a presidential project group and presented in front of the General Assembly of members 2016.

Already during recruiting processes measures for the absolutely non-discriminatory collaboration are

Eindrücke durch die begleitende Ausstellung der Zeichnerin Kerstin Heymach sowie eine Präsentation der Multimedia-Arbeit des Redakteurs und ebenfalls Expeditionsteilnehmers Stephan Schön der Sächsischen Zeitung gewinnen. Neben diesem Programm im „Augusteum" der Universität fand im Stadtzentrum ein Rundgang mit Feinstaub-Messrucksack statt sowie Laborbesichtigungen am Institut. 2018 und 2019 hatte TROPOS ebenfalls die Möglichkeit bei der Dresdener Wissenschaftsnacht mitzuwirken und informierte beim Kooperationspartner LfULG über Luftqualität sowie Klima.

In der Reihe „Studium Universale" der Universität Leipzig trug TROPOS mit einem Vortrag durch Prof. Dr. Alfred Wiedensohler zur Umweltzone Leipzig bei; für das junge Publikum wurde der $C0_2$-Ausstoß kindgerecht mit Experimenten in einer Veranstaltung der Kinder-Uni aufbereitet.

Außerdem ist TROPOS an den Öffentlichkeitsaktionen des Deutschen Klimakonsortiums (DKK), des Klimanavigators und der Leibniz-Gemeinschaft aktiv beteiligt.

Neue Wege geht das im September 2017 gestartete BMBF-Projekt WTimpact, um die kollaborative Wissensentwicklung als ein Transferinstrument zu entwickeln und vom Wissenstransfer zum Wissensaustausch zu gelangen: Leipzigerinnen und Leipziger konnten dabei selbst mobil Feinstaub und Ruß in der Stadt messen. Für mehrere Feldphasen des Projekts „Luft in Leipzig" hatte TROPOS Freiwillige akquiriert, die sich für die Luftqualität interessieren und dafür, wie diese untersucht wird. Ausgestattet mit einem neuartigen Messrucksack und intensiv betreut durch TROPOS nahmen sie jeweils eine Woche lang die Luft in Leipzig genauer unter die Lupe. Im eigens dazu aufgebauten Datenportal https://www.luft-leipzig.de werteten die Bürger ihre Messungen aus. Dieser Prozess wird durch Bildungs- und Kommunikationsforschende begleitet. Insgesamt untersuchen vier Institute der Leibniz-Gemeinschaft neue Methoden des Wissenstransfers auf diese Art.

Chancengleichheit und Nachwuchsförderung

Gleichstellung ist am TROPOS als Leitprinzip implementiert. Das Institut erfüllt damit die Gleichstellungsstandarts der Leibniz-Gemeinschaft, die von einer präsidentiellen Projektgruppe erarbeitet und 2016 der Mitgliederversammlung vorgestellt wurden. Am TROPOS werden Maßnahmen zur absolut diskriminierungsfreien Zusammenarbeit am Institut bereits im Einstellungsverfahren angewendet und fortlaufend verbessert. Das Institut ist weiterhin bestrebt, den Anteil an internationalen Wissenschaftlerinnen und Wissenschaftlern zu erhöhen.

applied at the institute and are improved constantly. TROPOS intends to further increase the proportion of international researchers.

Following the so-called Leibniz cascade model TROPOS also intends to increase the proportion of women, especially in post-doc and leading positions. Therefore, a stage-model was implemented in 2012, which was defined according the current structure of employees at the institute. Particularly worth mentioning here is the SAW funded junior research group "Dust at the interface" led by Dr. habil. Kerstin Schepanski and "MARPARCLOUD" led by Dr. Manuela van Pinxteren.

Audit "berufundfamilie". An important prerequisite for equal opportunities and career orientation is the reconciliation of career and family, especially for the promotion of young researchers. On May 25, 2011 the TROPOS efforts in this direction were internally and externally manifested in the certificate for the "career and family audit" and the respective measures are applied.

As a result of a re-auditing procedure TROPOS received the certificate for the audit once again on 29 June, 2015. During the following consolidation phase, TROPOS continued to implement family-friendly measures in accordance with the target agreement in the audit and received the third certificate on 27 June, 2018.

Promotion of young researchers. TROPOS actively promotes young researchers in the bachelor and master education at the Leipzig University as well as during and after doctoral research projects. The institute is involved in the development and implementation of the new bachelor and master programmes and is exclusively responsible for four modules and partially responsible for further two modules.

Highly qualified scientists of the Institute contribute to teaching activities in cooperation with the Leipzig University as joint appointments. In addition to meteorology students also chemistry and physics students are trained at TROPOS (see list, p. 164).

The institute offers young researchers an individualized realization of their dissertation projects supported by the supervision committee in the framework of a structured doctoral training programme. TROPOS scientists give lectures at the universities of Jena, Beijing, Jinan, and Shanghai, Helsinki and Stockholm, in international summer and winter schools, training courses and networks (see list, p. 162).

The 2012 founded Leipzig Graduate School on "Aerosols, Clouds and Radiation" provided together with the University Leipzig a solid basis for the

Fig. / Abb. 8: On 27 June 2018 TROPOS received the "berufundfamilie" audit for the third time: TROPOS head of administration Claudia Kostka (3rd from left) accepted the award from Federal Minister of Family Affairs Franziska Giffey (left). / Am 27. Juni 2018 erhielt das TROPOS zum dritten Mal das Audit „berufundfamilie": TROPOS-Verwaltungsleiterin Claudia Kostka (3.v.l.) nahm die Auszeichnung von Bundesfamilienministerin Franziska Giffey (links) entgegen. (Photo: berufundfamilie, Thomas Ruddies / Christoph Petras)

TROPOS will den Anteil von Frauen, vor allem in wissenschaftlichen Führungspositionen, weiter erhöhen und verfolgt dabei das so genannte Kaskadenmodell nach den Empfehlungen der Leibniz-Gemeinschaft, wobei ein an die momentane institutsspezifische Stellensituation angepasstes Stufenmodell im Jahr 2012 definiert wurde. Speziell erwähnt sei hier die Leitung der SAW-geförderten Nachwuchsgruppe „Interdust" durch Frau Dr. habil. Kerstin Schepanski und „MARPARCLOUD" durch Dr. Manuela van Pinxteren.

Nachwuchsförderung. TROPOS fördert aktiv den wissenschaftlichen Nachwuchs in der Bachelor- und Masterausbildung, während der Promotionsvorhaben und darüber hinaus. Das Institut ist eng in die Entwicklung und in die Durchführung der Bachelor- und Masterstudiengänge an der Universität Leipzig eingebunden und ist für vier Module exklusiv und für zwei weitere Module teilweise verantwortlich.

Hochqualifizierte Mitarbeiterinnen und Mitarbeiter beteiligen sich als gemeinsame Berufungen an der Lehre der Universität Leipzig. Neben Studierenden der Meteorologie werden am TROPOS auch Chemie- und Physikstudierende ausgebildet (siehe Liste, S. 164).

Das Institut bietet jungen Wissenschaftlerinnen und Wissenschaftlern eine individuell abgestimmte und von einem Betreuungsteam begleitete Realisierung ihrer Promotionen im Rahmen der strukturierten Promovendenausbildung. Mitarbeitende des TROPOS halten Kurse an den Universitäten von Jena, Peking, Jinan und Shanghai, Helsinki und Stockholm und bei

doctoral training at TROPOS and combines the expertise of both partners within the coupled research fields "aerosols, clouds, and radiation". By now the Graduate School has 40 members and is located in the Research Academy Leipzig (RAL).

Create future. TROPOS is a partner within the MINT-Individual network to inspire and generate interest in technical and natural science studies, and especially shows career perspectives in tropospheric research. Students get to know research work in a playful manner and have the possibility to directly talk to scientists from the MINT field. In the framework of this initiative the institute regularly participates in the Girls' Day (girls future day). In 2018 and 2019 interested female students could gain insight into laboratories and career opportunities as scientists and other professions at TROPOS.

A total of seven educational and information events for school children, two for students and 12 for adults, including two teacher training courses, were held in both years. TROPOS also supported the regional competition of "Jugend forscht".

In the reporting period, the scientific departments of TROPOS supervised 10 student internships and one BELL project, which won the Saxon Geography Prize of the Saxony regional association (see Prizes, p. 167). As part of Scientists for Future, TROPOS researchers supported the climate action week initiated by Fridays for Future at the University of Leipzig with lectures on the scientific principles of climate change and by providing information on the subject to school classes in a way that was suitable for children. As in the last years TROPOS will continue to finance an apprentice position.

Cooperations and networking

Numerous grown networks within the Leibniz Association, with Universities, with Max Planck Institutes, with institutes of the Helmholtz Society, and collaborations at the international level demonstrate the actual level of TROPOS networking in the field of interdisciplinary aerosol and cloud research. Similar alike TROPOS is networked on the European and global level and actively develops research programmes (see list, p. 179).

Technological developments at TROPOS lead to international standards in the experimental direct and indirect acquisition of aerosols and hydrometeors from ground up to the high atmosphere as well as in model-based descriptions of the complex multiphase system.

internationalen Sommerschulen, Ausbildungskursen und -netzwerken (siehe Liste, S. 162).

Die im Juli 2012 gegründete Leibniz-Graduiertenschule zu „Wolken, Aerosolen und Strahlung" hat die Promovendenausbildung am TROPOS gemeinsam mit der Universität Leipzig auf eine solide Grundlage gestellt und bündelt die gemeinsame Expertise in den gekoppelten Bereichen „Aerosole-Wolken-Strahlung". Sie ist mit nunmehr 40 Mitgliedern in der „Research Academy Leipzig" (RAL) verortet.

Zukunft schaffen. TROPOS unterstützt den Weg zum naturwissenschaftlichen Studium, indem berufliche Perspektiven im Bereich der Atmosphärenforschung aufgezeigt werden. Schülerinnen und Schüler lernen die Forschungsarbeit auf spielerische Art kennen und kommen mit Forschenden aus dem MINT-Bereich ins Gespräch. Im Rahmen der MINT-Initiative, die zum Ziel hat, Jugendliche für einen Beruf in den Fächern Mathematik, Informatik, Naturwissenschaften und Technik zu begeistern, beteiligt sich TROPOS auch am Zukunftstag Girls' Day. In den Jahren 2018 und 2019 konnten sich an diesem Tag interessierte Schülerinnen in den Laboren über Ausbildungsmöglichkeiten informieren. Insgesamt wurden in beiden Jahren sieben Bildungs- und Informationsveranstaltungen für Schulkinder, zwei für Studierende und 12 für Erwachsene, darunter zwei Lehrerfortbildungen, durchgeführt. Außerdem unterstützte TROPOS den Regionalwettbewerb von „Jugend forscht".

Im Berichtszeitraum wurden von den wissenschaftlichen Abteilungen des TROPOS 10

Fig. / Abb. 9: Team of the campaign GreenEquityHEALTH at a temperature/humidity measuring station in the Friedenspark Leipzig. The 2-week campaign is accompanied by mobile air quality measurements of TROPOS. / Team der Kampagne GreenEquityHEALTH an einer Temperatur/Luftfeuchtemessstation im Friedenspark Leipzig. Die 2-wöchige Kampagne wird durch mobile Luftqualitätsmessungen des TROPOS begleitet. (Photo: Jens Voigtländer / TROPOS)

In the framework of the Leibniz competition funds cooperation is extended among the Leibniz Association and with university institutes. The TROPOS is associated with numerous international institutions through cooperation agreements (see list, p. 179) and plays a leading role in the European research infrastructure network ACTRIS (Aerosols, Clouds, and Trace gases Research InfraStructure Network). In September 2019, the German contribution "ACTRIS-D" was added to the National Roadmap for Research Infrastructures. Nearly all major players in German atmospheric research – including universities, non-university research institutions and public authorities – work together in ACTRIS-D. The German part of the European research infrastructure is coordinated by TROPOS. At European level, more than 120 institutions in over 20 countries are already involved. Such a large concentration of resources has never been reached in atmospheric research before.

The ground-based remote sensing and in-situ measurement activities of TROPOS are also integrated into ESA policy advice. The in-situ measurements of aerosol particles are part of the EMEP and WMO GAW networks.

In Cyprus, the ERATOSTHENES Centre of Excellence (ECoE) has been launched, which is to become a leading digital innovation centre (DIH) for Earth observation and geodata over the next seven years. TROPOS is also participating in the new remote sensing centre for the eastern Mediterranean, Middle East and North Africa region, in order to better investigate global change in climate, land use and the

Fig. / Abb. 10: Opening ceremony of the ERATOSTHENES Centre of Excellence (ECoE) at the Cyprus University of Technology in Limassol with the President of the Republic of Cyprus, Nikos Anastasiadis (2nd from right). / Feierliche Eröffnung des ERATOSTHENES Centre of Excellence (ECoE) an der Cyprus University of Technology in Limassol mit dem Präsidenten der Republik Zypern, Nikos Anastasiadis (2.v.r.). (Photo: Patric Seifert / TROPOS)

Schülerpraktika und eine BELL- Arbeit betreut, die den Sächsischen Geopreis des Landesverbandes Sachsen gewinnen konnte (s. Preise, S. 167). Forschende des TROPOS unterstützten im Rahmen von „Scientists for Future" die von „Fridays for Future" initiierte Klimaaktionswoche an der Universität Leipzig mit Vorträgen über wissenschaftliche Grundlagen zum Klimawandel sowie informierten in Schulklassen kindgerecht zum Thema.

TROPOS wird auch in den nächsten Jahren mindestens einen Lehrlingsausbildungsplatz aus Haushaltsmitteln finanzieren.

Bedeutende Kooperationen und Vernetzung in der Forschung

Zahlreiche bisher gewachsene Vernetzungen innerhalb der Leibniz-Gemeinschaft, mit Universitäten, mit Max-Planck-Instituten, mit Instituten der Helmholtz-Gemeinschaft sowie auf internationaler Ebene zeigen den derzeitigen Stand der Vernetzung des TROPOS in der interdisziplinären Aerosol- und Wolkenforschung. Ähnlich ist TROPOS auf der europäischen und weltweiten Ebene vernetzt und entwickelt hier aktiv Forschungsprogramme (siehe Liste, S. 179).

Technologische Entwicklungen am TROPOS führen zu internationalen Standards in der experimentellen direkten und indirekten Erfassung von Aerosolen und Hydrometeoren vom Boden bis zur hohen Atmosphäre sowie in der modellmäßigen Beschreibung des komplexen Multiphasensystems.

Im Rahmen des Wettbewerbsfonds der Leibniz-Gemeinschaft werden die Kooperationsmöglichkeiten innerhalb der Leibniz-Gemeinschaft und mit Universitätsinstituten ausgebaut. Durch Kooperationsvereinbarungen ist das Institut mit zahlreichen internationalen Einrichtungen verbunden (siehe Liste, S. 179).

TROPOS spielt eine führende Rolle im Netzwerk der europäischen Forschungsinfrastruktur ACTRIS (Aerosols, Clouds, and Trace gases Research InfraStructure Network). Im September 2019 wurde der deutsche Beitrag „ACTRIS-D" auf die Nationale Roadmap für Forschungsinfrastrukturen aufgenommen. In ACTRIS-D arbeiten nahezu alle bedeutenden Akteure der deutschen Atmosphärenforschung zusammen – darunter Universitäten, außeruniversitäre Forschungseinrichtungen und Behörden. Koordiniert wird der deutsche Teil der europäischen Forschungsinfrastruktur durch TROPOS. Auf europäischer Ebene sind bereits mehr als 120 Institutionen in über 20 Ländern beteiligt. Eine so große Bündelung von Ressourcen hat es bisher in der Atmosphärenforschung noch nicht gegeben.

associated social challenges in the eastern Mediterranean from space and from the ground. At the end of November, the President of the Republic of Cyprus, Nikos Anastasiadis, also took part in the ceremonial launch of the centre in Limassol, which is being funded by the EU EXCELSIOR project.

On August 22, 2018, the European Space Agency ESA launched a new type of wind satellite into space. "Aeolus" is to create vertical wind profiles by 2021 using a modern and powerful laser system. Its goal is to close large data gaps and thus improve weather forecasting. In addition to technical know-how in the production of the satellite, a great deal of experience in the investigation of the atmosphere by laser light will also be incorporated into the project from Germany. This lidar technology (light detection and ranging) has been used from the ground for many years. The knowledge gathered will help to interpret the data from Aeolus in the coming years. In this framework Experts from several German research institutes met at the Leibniz Institute for Tropospheric Research (TROPOS) in Leipzig at the end of July.

Die bodengebundenen Fernerkundungs- und In-situ-Messungen sind international eingebunden in die langfristigen ACTRIS-Arbeiten und in Beratungstätigkeiten für die ESA. Die In-situ-Aerosolaktivitäten sind international in den EMEP- und WMO-GAW-Netzwerken eingebunden.

In Zypern ist der Startschuss für das ERATOSTHENES Centre of Excellence (ECoE) gefallen, dass in den nächsten sieben Jahren zu einem führenden digitalen Innovationszentrum (DIH) für Erdbeobachtung und Geodaten werden soll. An dem neuen Fernerkundungszentrum für die Region im östlichen Mittelmeer, dem Nahen Osten und Nordafrika beteiligen sich aus Deutschland auch TROPOS, um den globalen Wandel in Klima, Bodennutzung und den damit verbundenen gesellschaftlichen Herausforderungen im östlichen Mittelmeer aus dem All und vom Boden aus besser untersuchen zu können. Am feierlichen Startschuss für den Aufbau des vom EU-Projekt EXCELSIOR geförderten Zentrums in der Hafenstadt Limassol nahm Ende November auch der Präsident der Republik Zypern, Nikos Anastasiadis, teil.

Am 22.08.2018 hat die Europäische Weltraumagentur ESA einen neuartigen Windsatelliten ins All gesendet. „Aeolus" soll bis 2021 mit einem modernen und leistungsstarken Laser-System vertikale Windprofile erstellen. Sein Ziel: Große Datenlücken schließen und so die Wettervorhersage verbessern. In das Projekt fließen aus Deutschland neben technischem Know-how bei der Produktion des Satelliten auch viele Erfahrungen mit der Untersuchung der Atmosphäre per Laserlicht ein. Diese Lidar-Technik (Light Detection and Ranging) wird seit vielen Jahren vom Boden aus genutzt. Das gesammelte Wissen soll in den nächsten Jahren helfen, die Daten von Aeolus zu interpretieren. Ende Juli trafen sich dazu Expertinnen und Experten mehrerer deutscher Forschungsinstitute am Leibniz-Institut für Troposphärenforschung (TROPOS) in Leipzig.

Conference Highlight: CADUC – Central Asian DUst Conference / Konferenzhöhepunkt: CADUC – Zentralasiatische Staubkonferenz

CADUC – 1. conference regarding atmospheric dust in Tajikistan

Dietrich Althausen and Julian Hofer

Highlight 1: Location and Organization

This meeting was the first meeting of its kind in Tajikistan. It was initiated by TROPOS, organized, and managed by TROPOS and the Academy of sciences of Tajikistan in Dushanbe from 8 to 12 April 2019. CADUC was funded by and thus made possible through the Volkswagen Foundation. The 79 participants came from 17 countries on three continents: Asia (West to East Asia), Europe, and America.

Highlight 2: Conference content

Under the topic "Desert Dust in West, Central and East Asia", the international conference brought together contributions on general and regionally relevant research findings. The submitted abstracts have undergone a peer-review process and are published as a conference proceeding under the open-access policy.

Highlight 3: Future

The conference was considered as very successful and significant by the participants. The wish was expressed to hold a follow-up meeting in Central Asia. TROPOS has received in total 12 letters of support from internationally well renown scientists expressing support for this.

CADUC – 1. Konferenz zum atmosphärischen Staub in Tadschikistan

Dietrich Althausen und Julian Hofer

Highlight 1: Ort und Organisation

Die CADUC Konferenz war die erste Tagung ihrer Art in Tadschikistan. Sie wurde von TROPOS initiiert und zusammen mit der Akademie der Wissenschaften von Tadschikistan organisiert und vom 8. – 12. April 2019 in Duschanbe durchgeführt. CADUC wurde vollständig von der Volkswagenstiftung finanziert und damit erst ermöglicht. Die 79 TeilnehmerInnen kamen aus 17 Ländern von drei Kontinenten: Asien (West- bis Ostasien), Europa und Amerika.

Highlight 2: Tagungsinhalt

Unter dem Thema „Wüstenstaub in West-, Zentral- und Ostasien" behandelte die internationale Konferenz wegweisende Beiträge zu allgemeinen und regional relevanten Erkenntnissen. Die eingereichten Abstracts haben einen peer-review Prozess durchlaufen und sind als Tagungsband unter der open-access policy veröffentlicht.

Highlight 3: Zukunft

Die Tagung wurde von den Teilnehmern als sehr erfolgreich und bedeutend eingeschätzt. Es wurde der Wunsch zur Ausrichtung einer Folgetagung in Zentralasien formuliert. Dazu wurden dem Organisator vom TROPOS 12 Unterstützungsschreiben von international anerkannten Wissenschaftlern zugeschickt.

Fig. / Abb. 1: CADUC logo. / CADUC-Logo. (Graphic: Dietrich Althausen / TROPOS)

Conference Highlight: CADUC – Central Asian DUst Conference / Konferenzhöhepunkt: CADUC – Zentralasiatische Staubkonferenz

Fig. / Abb. 2: Dust Belt. / Staubgürtel. (Graphic: adapted from Hofer et al., 2017, https://doi.org/10.5194/acp-17-14559-2017)

Highlight 1: Location and Organization

Tajikistan, with its capital Dushanbe, is located in Central Asia in the middle of the vast dust belt that stretches from the Sahara in the west through the Middle East and Central Asia to the Gobi Desert in the east (Fig. 2).

Desert dust, emitted in the Sahara, the Middle East, and other areas in Asia has many ecological, economic, social, natural and health consequences, especially in Central Asia, which affect people's lives. Some of them in extreme ways. Despite the regional significance of dust aerosol, there has not yet been a major international conference on atmospheric dust in Central Asia.

Motivated by the fruitful cooperation in the framework of the project Central Asian Dust EXperiment (CADEX) run by TROPOS and the Academy of Sciences of Tajikistan, the idea of an international conference in Dushanbe grew. An idea that was finally made possible by the approval of a conference project through the Volkswagen Foundation. This way, the conference could cover the financial costs of air travel, accommodation and meal expenses of the participants and the costs of the conference in Tajikistan itself. It was an important financial contribution that secured the participation of scientists independent of the financial possibilities of their home institutes and thus allowed to in particular invite scientists from low-income countries. Overall, this was seen as a huge contribution to the positive outcome of CADUC.

Scientists from 17 countries attended the conference. They appreciated the high scientific level of the meeting and expressed great interest in future joint scientific work on the various aspects of dust.

Zum Highlight 1: Ort und Organisation

Tadschikistan mit seiner Hauptstadt Duschanbe liegt in Zentralasien inmitten des ausgedehnten Staubgürtels, der sich von der Sahara im Westen über den Nahen Osten und Zentralasien bis zur Wüste Gobi im Osten erstreckt (Abb. 2).

Mit dem atmosphärischen Staub, der in den Wüsten der Sahara, im Nahen Osten, und in anderen Gebieten Asiens emittiert wird, sind besonders in Zentralasien viele ökologische, ökonomische, soziale Natur- und Gesundheitsfolgen verbunden, die in teilweise extremer Art das Leben der Menschen beeinflussen. Trotz der regionalen Bedeutung vom Staubaerosol gab es bisher keine große internationale Tagung zum atmosphärischen Staub in Zentralasien.

Motiviert durch die produktive Zusammenarbeit im Projekt Central Asian Dust EXperiment (CADEX) von TROPOS und der Akademie der Wissenschaften von Tadschikistan wuchs die Idee einer internationalen Tagung in Duschanbe, welche schließlich durch die Bewilligung eines Tagungs-Projekts von der Volkswagenstiftung ermöglicht wurde. Nur so konnten die Finanzierung der Flüge und Aufenthalte der Teilnehmer und die Tagungskosten in Tadschikistan sichergestellt werden. Dieses war ein wichtiger finanzieller Beitrag, der insbesondere auch die Teilnahme von Wissenschaftlern unabhängig der finanziellen Möglichkeiten ihrer Heimatinstitute sicherte.

An der Tagung nahmen Wissenschaftler aus 17 Ländern teil. Sie haben das wissenschaftliche Niveau der Tagung sehr hoch eingeschätzt und danach großes Interesse an zukünftigen gemeinsamen Arbeiten zu den verschiedenen Aspekten des Staubs geäußert.

Conference Highlight: CADUC – Central Asian DUst Conference / Konferenzhöhepunkt: CADUC – Zentralasiatische Staubkonferenz

Highlight 2: Conference content

Session 1: Atmospheric dust at source regions. Noteworthy and of particular interest to the conference's audience were the presentations on inventories of dust sources, which change over time, and their conceptual designs. Many of the analyses are based on satellite-based measurements, but approaches using in-situ measurements have also been presented, namely the estimate of dust emission fluxes in a Mongolian desert or the characterization of the developing dust sources in Iran (e.g., Urmia Lake and Sistan Basin area). It was generally found that the salty dust storms are recently becoming more frequently, which has been linked to the dehydration of large lake areas in particular and to the Asian soil conditions in general. According to prevailing geographical and meteorological conditions, dust suspended in the atmosphere is transported along certain pathways. These transport paths essentially link source regions to remote areas, where, e.g., suspended dust decreases air quality. Exemplarily, this was studied for western Asia (Kuwait). Furthermore, dust aerosol can be associated with the transport of bacteria. In a nutshell, further scientific work is inevitably to more comprehensively and thus more accurate describe the sources of dust by their intrinsic, relevant parameters and - associated with them - by appropriate methods and techniques.

Session 2: Atmospheric dust during transport (dust properties at transport). During an 1.5-year series of measurement carried out in the framework

Zum Highlight 2: Tagungsinhalt

Session 1: atmosphärischer Staub in den Quellgebieten (atmospheric dust at source regions). Besonders interessant waren die unterschiedlichen Beiträge zu den neuen Analysen (Inventories) der Staubquellen, die sich zeitlich verändern. Viele der Analysen beruhen auf satellitengestützte Messungen, es wurden aber auch In-situ-Messungen vorgestellt, wie z.B. die Bestimmung des Staubflusses in einer mongolischen Wüste oder Charakteristiken der sich entwickelnden Staubquellen im Iran (z.B. Urmia See und Sistan-Gebiet). Generell wurde festgestellt, dass die Salz-Staubstürme zunehmen, was mit der Austrocknung von großen See-Bereichen und mit der asiatischen Bodenbeschaffenheit zu tun hat. Entsprechend der geographischen und meteorologischen Gegebenheiten kann sich der Staub entlang bestimmter Pfade ausbreiten, die z.B. in Westasien (Kuwait) untersucht wurden. Mit dem Staub kann der Transport von Bakterien verbunden sein. Weitere wissenschaftliche Arbeiten sind erforderlich, um die Staubquellen durch ihre intrinsischen, wichtigen Parameter und, damit verbunden, durch geeignete Methoden zu beschreiben.

Session 2: atmosphärischer Staub während des Transports (dust properties at transport). Während der 1,5-jährigen Messkampagne im Rahmen des CADEX-Projekts wurde durch ein TROPOS-Lidar in Dushanbe, Tadschikistan, erstmals Staub in Zentralasien in Höhen bis zu 12 km über N.N. nachgewiesen. Diese Messungen suggerieren,

Fig. / Abb. 3: Conference attendees and in the background the fortress of Hissor in Tajikistan. / Konferenzteilnehmer und im Hintergrund die Festung von Hissor in Tadschikistan. (Photo: Attendee / CADUC)

of the CADEX project, for the first time, a TROPOS lidar detected dust in Central Asia at altitudes up to 12 km a.s.l. in Dushanbe, Tajikistan. These observations illustrate that the dust detected in East Asia can also originate from western Asia and, furthermore, that the Pamir Mountains do not form a natural boundary for atmospheric dust being transported from East to West Asia. The typical ranges of altitudes of atmospheric dust are seasonally varying. Especially in spring, the dust layers are at rather high attitude. Dust aerosol particles change their physico-chemical properties during their stay in the atmosphere as they are mixing with other particles and aging. This raises the questions to which parameters and which value ranges of these parameters are suitable for the different investigation methods aiming at identifying dust suspended in the atmosphere. During the conference, vertically resolved measurements and soil measurements on dust over West Asia (Israel) and Central Asia were presented and discussed. Likewise intriguing were Japanese measurements of Saharan dust from Africa highlighting possible transport paths via Central Asia to Japan. Revealing were also the presentation of measurements from the satellite-based Cloud-Aerosol LIdar with Orthogonal Polarization (CALIOP) instrument. With measurements covering several years, it was possible to estimate that the dust export had actually decreased for certain regions in Asia. A scientific presentation on a study elaborating the electrostatic charging of dust particles during atmospheric transport was pointing towards new approached investigating the atmospheric life-time of dust particles. Up to now, it is not clear to what extent this electrostatic charge modulates dust transport and changes the particles' properties. Whereas predominant dust transport pathways are obvious, one study presented proved Central Asian dust to be transported towards Moscow, which is thousands of kilometers away from the sources and not an obvious destination for desert dust. Modelling studies of atmospheric dust, in summary, show the relatively low dust emissions in Central Asia compared to deserts in North Africa and East Asia, but they also illustrate the high atmospheric dust loads in Central Asia due to dust being advected from various western source areas.

Session 3: Atmospheric dust at its sink areas. Although studied in detail since a while, there is still no general overview of all mineral components of atmospheric dust. This is, of course, due to the continuous step-by-step development of suitable sampling devices and analysis techniques, but also due to the sometimes-challenging sampling environment in the deposition areas. Hence, particularly valuable work was presented at CADUC on the chemical and

dass der in Ostasien nachgewiesene Staub auch aus Westasien stammen kann und dass z.B. das Pamir-Gebirge keine natürliche Grenze für den atmosphärischen Staub bildet. Die Transporthöhen des atmosphärischen Staubs sind naturgemäß saisonal unterschiedlich und besonders im Frühjahr sehr hoch. Der Staub ändert während seines Aufenthalts in der Atmosphäre seine Eigenschaften. Dies geschieht insbesondere durch Mischung mit anderen Partikeln und durch Alterung. Damit ergibt sich die Frage, welche Parameter und welche Wertebereiche dieser Parameter für die unterschiedlichen Untersuchungsmethoden zur Identifikation von Staub in der Atmosphäre geeignet sind. Während der Tagung wurden vertikal aufgelöste Messungen und Bodenmessungen zum Staub über Westasien (Israel) und Zentralasien vorgestellt und diskutiert. Interessante Einblicke in die Verbreitungswege von Wüstenstaub gewährten auch japanische Messungen zum Saharastaub aus Afrika und dessen mögliche Transportwege über Asien, Zentralasien und Ostasien. Ebenso erkenntnisreich waren die Messungen vom satellitengestützten Cloud-Aerosol LIdar with Orthogonal Polarization (CALIOP) Instrument. Mit diesen jahrelangen Messungen konnte für bestimmte Regionen in Asien abgeschätzt werden, dass sich der Staubexport sogar verringert hat. Neue Ansätze zeigte auch ein Beitrag zur elektrostatischen Aufladung der Staubpartikel beim atmosphärischen Transport auf. Es ist noch nicht klar, inwieweit diese Aufladung dann wieder auf den Staubtransport rückwirkt und inwieweit diese elektrostatische Aufladung andere Partikeleigenschaften verändert. Ein interessantes und auf den ersten Blick nicht zu erwartendes Ergebnis einer Präsentation war, dass zentralasiatischer Staub in Moskau – d.h. tausende Kilometer von den Quellen entfernt – nachgewiesen wurde. Modellierungen zum atmosphärischen Staub zeigen die relativ geringen Staubemissionen in Zentralasien, aber auch die hohen Staubbelastungen in Zentralasien durch Staub von verschiedenen westlichen gelegenen Quellbereichen.

Session 3: atmosphärischer Staub in den Depositionsbereichen. Es gibt noch keine allgemeine Übersicht über alle mineralischen und anderen Bestandteile des atmosphärischen Staubs, was natürlich zum einen auf die Entwicklung der Untersuchungsmethoden, aber auch auf die teilweise schwer zugänglichen Probennahmen in den Depositionsgebieten zurückzuführen ist. Auch deshalb sind die auf der CADUC vorgestellten Arbeiten zu den chemischen und mineralogischen Bestandteilen des zentralasiatischen Staubs und deren Vergleich mit Ergebnissen vom Saharastaub, zu dem bereits viele Studien publiziert sind, besonders wertvoll. Zum

mineralogical components of Central Asian dust and their comparison with Saharan dust that is already described in a variety of publications. On the other hand, it had to be noted that the description of the individual mineralogical components in deposition areas depends on various parameters, such as particle size distribution, contributing source areas, atmospheric transport paths, mixing ratios of minerals and elements, atmospheric residence time, measurement routine, type of deposition (e.g., wet or dry). The man-made transformation of the Aral Sea area from a lake into a desert not only generates a larger dust source area, it also leads to an increased dust deposition flux in this area. Finding from studies on Central Asian dust in remote areas such as Georgia and Siberia were presented in this session too, which once again underlines and makes the extensive importance of dust investigations apparent.

Session 4: Impacts of atmospheric dust. The richly detailed presentation of the various, possibly dangerous and highly interfering effects of atmospheric dust (such as soil loss, spread of diseases, economic losses in e.g. solar energy production, plant destruction, drinking water contamination) clearly showed that dust suspended in the atmosphere is of concern for the humanity and that its relevance certainly will increase in future. In addition to the manifold effects of dust on human well-being and global governance, desert dust modulates the global radiation budget and impacts on cloud and precipitation formation processes ultimately stimulating the water cycle and the Earth thermostat. With the development of the innovative measurement techniques, fundamental relations were discovered, proposed, and discussed in a collaborative manner. Health impacts of dust are particularly important in Central Asia due to the presence of high near-surface dust concentrations, which may, for instance, contain toxic metals. Additionally, recent studies showed that the dust aerosol may carry bacteria from their source regions to remote areas and dust deposited on plants is further expected to negatively affect plant growth and bioproductivity.

General information about the conference is available via https://www.e3s-conferences.org/caduc-2019. The submitted abstracts are double peer-reviewed by the scientific committee and published as proceedings under the open-access policy: https://www.e3s-conferences.org/articles/e3sconf/abs/2019/25/contents/contents.html. A general conference report was also published in EOS https://eos.org/meeting-reports/scientists-share-results-of-dust-belt-research.

anderen musste festgestellt werden, dass die Beschreibung der Bestandteile des Staubs in seinen Depositionsbereichen von vielen Parametern abhängt, unter anderem: Größenverteilung, Quellenbereiche, Ausbreitungspfade, wichtige Mischungsverhältnisse von Mineralien und Elementen, Zeit zwischen Emission und Deposition, Tagesgang der Depositionsmessungen, Art der Deposition. Der menschengemachte Wandel des Aralsee-Bereichs von einem See zu einer Wüste führt auch zur verstärkten Staubdeposition in diesem Quellenbereich. Auch in dieser Session wurden Untersuchungen von zentralasiatischem Staub in den weit entfernten Gebieten Georgien und Sibirien vorgestellt, was die weitreichende Bedeutung der Staubuntersuchungen offensichtlich macht.

Session 4: Auswirkungen des atmosphärischen Staubs. Die sehr ausführliche Darstellung der verschieden, unter Umständen bedrohlichen und sehr beeinträchtigenden Auswirkungen des atmosphärischen Staubs (wie z.B. Verlust von Mutterboden, Krankheiten, ökonomische Probleme wie Solarenergiegewinnung, Pflanzenzerstörung, Trinkwasserkontamination u.v.m.) zeigte deutlich, dass Staub in der Atmosphäre ein wichtiges Thema für die Menschheit ist und seine Bedeutung in Zukunft zunehmen wird. Neben den vielfältigen Auswirkungen des Staubs auf die Menschen gibt es auch meteorologische Auswirkungen wie z.B. die auf den globalen Strahlungshaushalt (auch durch Staubschichten in der Atmosphäre, die sich über anderen Partikelschichten befinden können) oder die auf die Tropfen- und Eiskristallbildung in der Atmosphäre und damit auf die Wolkenbildung und den Wasserkreislauf. Mit Entwicklung der Messtechnik wurden solche wichtigen Zusammenhänge teilweise erstmalig diskutiert, da sie z.T. erst seit kurzem untersuchbar sind. In Zentralasien sind durch die hohen Staubkonzentrationen auch gesundheitsrelevante Aspekte von Staub am Boden wie z.B. toxische Metalle im Staub besonders wichtig. Neuere Untersuchungen zeigen, dass mit dem Staub ein Bakterientransport erfolgt und wie das Pflanzenwachstums durch atmosphärischen Staub beeinflusst wird.

Allgemeine Informationen zur Konferenz sind über https://www.e3s-conferences.org/caduc-2019 verfügbar, die proceedings wurden durch das wissenschaftliche Komitee doppelt peer-reviewed und sind über https://www.e3s-conferences.org/articles/e3sconf/abs/2019/25/contents/contents.html zugänglich. Ein allgemeiner Konferenzreport wurde auch in EOS (https://eos.org/meeting-reports/scientists-share-results-of-dust-belt-research) veröffentlicht.

Facts and figures / Zahlen und Fakten

	2018 / 2019
158 / 58 female	**2 / 5**
Employees	Doctoral theses
75 / 22 female	**8 / 5**
Scientists	Master of Science
38 / 13 female	**1 / 2**
Doctoral candidates	Bachelor of Sciences

17.325 Mio €

Budget in total

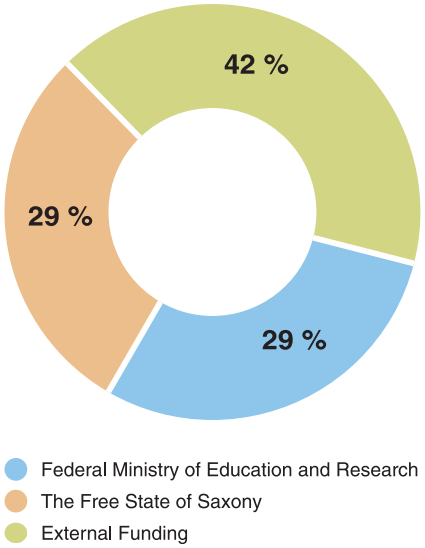

2018 / 2019	2018 / 2019	2018 / 2019	2018 / 2019
88 / 85	**6 / 5**	**42 / 46**	**12 / 25**
Publications (peer-reviewed)	National campaigns	National cooperations	Public events
214 / 171	**15 / 22**	**61 / 67**	**14 / 20**
Reviews	International campaigns	International cooperations	Press releases
15 / 23	**4 / 5**	**33**	**321 / 143**
Scientific events	Long-term measurements	General cooperations	Media publications

Articles

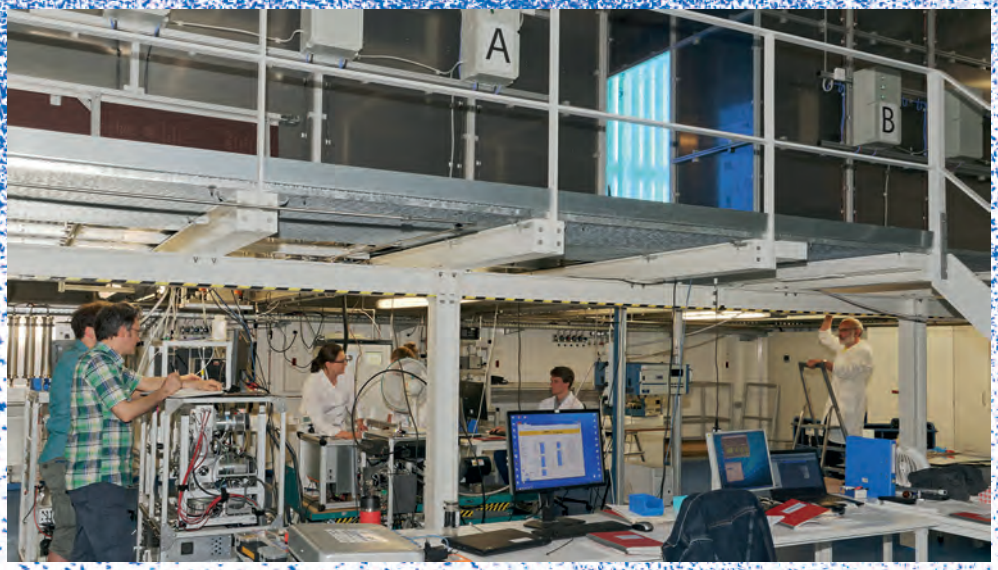

Urban air-quality modelling

Bernd Heinold, Michael Weger, Ralf Wolke, Marie Luttkus, Oswald Knoth, Marcel König

Urbane Luftverschmutzung ist ein Gesundheitsrisiko für eine wachsende Bevölkerung in Städten. Die zeitlich-räumliche Verteilung der Luftschadstoffe ist äußerst variabel und unterliegt komplexen Einflüssen der städtischen Grenzschicht. Zur Untersuchung urbaner Luftverschmutzung und relevanter Prozesse wird am TROPOS an Modellen verschiedener Auflösungen gearbeitet. In diesem Beitrag werden die neuesten Entwicklungen zur Modellierung städtischer Luftqualität vorgestellt: ein Vorhersagesystem zur kleinräumigen Schadstoffprognose für Leipzig und andere Städte, das auf dem Chemie-Transport-Modell des TROPOS basiert, erste hochauflösende Simulationen mit einem am TROPOS entwickelten CFD-Modell und dem neuen Stadtklimamodell PALM-4U sowie eine Studie zum Einfluss biogener Emissionen auf die Luftqualität in der Stadt Leipzig.

Introduction

Air quality has improved significantly in Europe and other developed regions during recent decades. For a growing population in cities, however, high levels of urban air pollution are still considered a threat to public health and well-being, as well as a cause of significant harm to ecosystems. In particular, exposures to ultrafine and fine particulate matter, soot, nitrogen oxides, and ozone have been shown to be health-relevant [*EEA*, 2019]. In urban areas, the concentration of air pollutants generally varies greatly depending on a number of different factors like the distribution of emissions, transport and physical/chemical transformations of trace gases and aerosol. These processes are strongly non-linear and affected by complex building structures and traffic situation, urban radiation and heat budget, as well as long-range transboundary air mass transport.

At TROPOS, sophisticated and numerically efficient models are developed, which allow for process studies and air-quality simulations across scales from regional background to neighbourhood and pedestrian level. The aim is to investigate and better understand air pollution in cities and its small-scale variability and controls from emissions to exposure. The model development goes hand in hand with the current substantial development and exploration of the potential of mobile sensors to achieve a higher spatial density of measurements in addition to the permanent measuring sites operated by TROPOS in the city of Leipzig. Combining detailed air quality measurements and model simulations will advance understanding of the links between air pollution and urban microclimate and related processes. In addition, this will enable to support city authorities in developing and evaluating air-pollution reduction scenarios.

Here, ongoing projects related to urban modelling in Leipzig are presented. This includes the development of a new, flexible multi-scale system for air-quality modelling, which is based on the TROPOS chemistry-transport model (CTM) COSMO-MUSCAT and was first applied for campaign-based forecast for Leipzig and eastern central Germany within the project WT!mpact. Furthermore, different models for street-level simulations are currently being developed and evaluated regarding their potential as downscaling approach for the multi-scale air-quality modelling framework. Another project deals with the intriguing topic of the relationship between biogenic emissions from trees and plants and the urban air pollution through impacts on atmospheric oxidants and secondary organic aerosol (SOA) formation.

Multi-scale air-quality modelling framework

A flexible multi-scale system for air-quality modelling is currently being developed for Leipzig and surroundings, which could potentially be applied in other cities. The core is an urbanised version of the model system COSMO-MUSCAT (COSMO: Consortium for Small-scale Modelling model – MUSCAT: MUltiScale Chemistry-Aerosol-Transport model), which has been developed and used at TROPOS

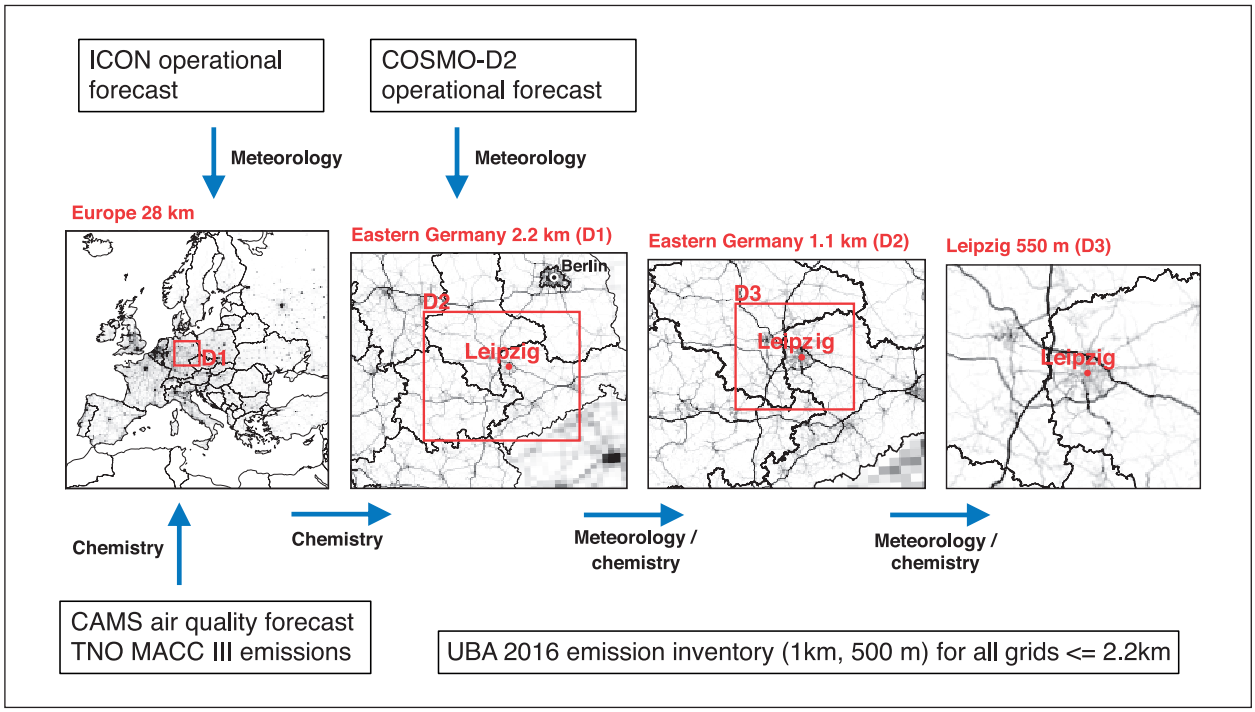

Fig. 1: Nested domains of the COSMO-MUSCAT air-quality forecast for the city of Leipzig and surroundings.

for aerosol and chemistry process studies for many years [e.g., *Wolke et al.*, 2012]. The model performed well in inter-comparison studies [e.g., *Kioutsioukis et al.*, 2016] and has been evaluated with a wide range of measurements in the framework of various field experiments.

Driven by the meteorological model COSMO, MUSCAT treats the atmospheric transport as well as chemical transformations for several gas-phase species and particle populations. An on-line feedback allows to also consider the impacts of aerosol on radiation and cloud microphysics. The model system includes up-to-date production parameterizations for natural aerosol, including an advanced scheme for biogenic emissions and SOA formation, and considers complex multiphase chemistry processes. Anthropogenic air pollutant emissions are prescribed from latest inventories.

Here, COSMO-MUSCAT has been set up for applications in urban areas below the 1-km scale. Since the impact of the city morphology on air flow and radiation still remains subgrid-scale, the model has been equipped with the Double Canyon Effect Parametrization (DCEP) by *Schubert et al.* [2012]. Urban surfaces are represented by two neighbouring street canyons with a characteristic orientation, building and street width, and building height distribution. The DCEP scheme closes the surface energy balance for road, wall and roof surfaces at different heights within the urban canopy, including the radiative interaction of roofs with other urban surfaces, and computes the exchange of momentum and heat with the atmosphere for the urban fraction of respective grid cells. The required statistical input is calculated from a detailed building dataset in CityGML format, using flexible pre-processor tools in Python language.

The application of an urban parameterization leads to a more realistic description of the dynamics and heat exchange in a city, with a significant increase of urban surface temperatures (urban heat island effect), a reduction of specific humidity and mean wind speed, and an increase of vertical turbulent mixing. Several modelling studies over urban areas, however, also stress the importance of a realistic representation of emission fluxes at this scale and their diurnal variability [e.g. *Huszar et al.*, 2018]. A further element of model development has been the visualization of model results using interactive online mapping on an internet platform (e.g., project websites). The system can be run in quasi-operational mode, which allows to accompany field campaigns on request.

The multi-scale modelling framework recently was first tested in hindcast mode for the hot summer 2018, and as 48-h forecast for the 2019 field phases of the knowledge transfer project WT!mpact, funded by the Federal Ministry of Education and Research (Bundesministerium für Bildung und Forschung, BMBF). Long-term stationary observations at four sites in the city of Leipzig and extensive mobile measurements from the WT!mpact field campaigns are available for the upcoming evaluation. The simulations

are realised with a nesting chain, where the horizontal resolution is gradually increased from 28 km over Europe to about 550 m over the city area (Fig. 1). The outer domain, which provides the background concentrations of aerosol and chemical species over Germany, is driven by the global ICON forecast of DWD. Copernicus Atmosphere Monitoring Service (CAMS) forecasts provide the input for the aerosol and gas boundary conditions of the coarse domain. The meteorological initial and boundary data for the German domain come from the DWD COSMO-D2 forecast. The subsequent domains use the boundary conditions of the respective coarser model run. For the European domain, TNO-CAMS emissions are used, while for Germany, point as well as detailed area (550 m native resolution) and road emissions are available from the German Environment Agency (Umweltbundesamt, UBA). The forecast system provides the distribution of health-relevant parameters like fine particulate matter (PM_{10}, $PM_{2.5}$), soot (BC), nitrogen oxides (NO, NO_2), and ozone (O_3), as well as various precursors for 48 hours on everyday basis. The first comparison of the model results from the innermost domain to the monitoring station measurements shows a reasonably good agreement for the temporal evolution of PM_{10}, NO_2, and O_3 at all sites. The levels of PM_{10} and NO_2 are matched well by the model at the urban background stations, as well as

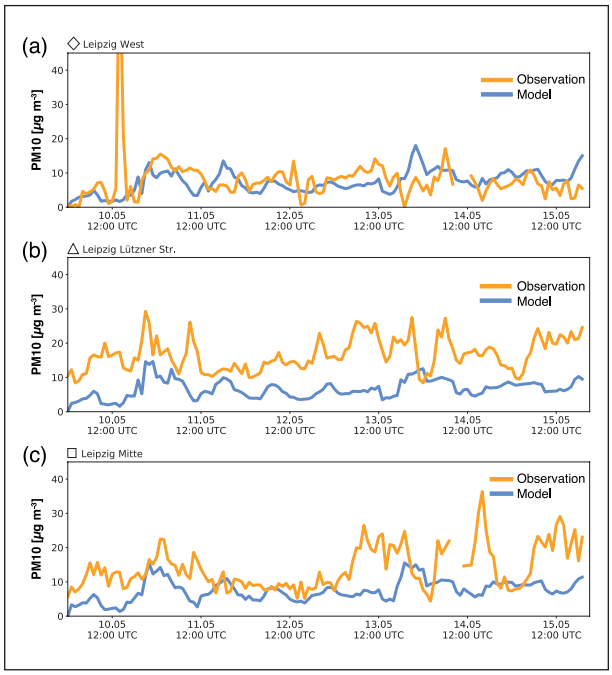

Fig. 2: PM_{10} concentration at Leipzig's air quality monitoring stations (a) Leipzig West (urban background), (b) Lützner Str. (high traffic road), and (c) City Centre for 10 – 15 May 2019. Compared are observations (orange line) and COSMO-MUSCAT model results at 550-m spatial resolution (blue line).

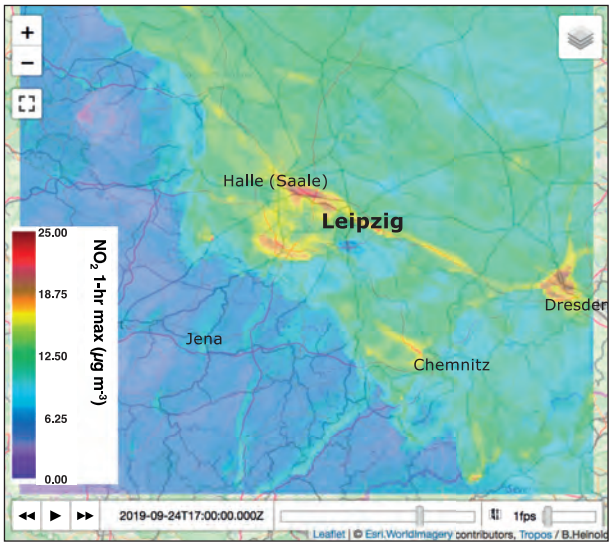

Fig. 3: Maximum hourly NO_2 concentration at surface as forecasted with COSMO-MUSCAT for Leipzig on 24 September 2019, 1700 UTC. Screenshot of the interactive web map as provided within the WT!mpact project.

the concentration of PM_{10} in the city centre (as shown for mid-May 2019 in Fig. 2). However, the observed values of NO_2 and O_3 are underestimated, in particular, at high traffic locations. A likely reason is a still too coarse horizontal resolution, but possibly also adjustments to the prescribed road traffic emissions may be needed. During the WT!mpact project, the urban air-quality forecast could already be provided to the volunteers in the project via interactive web mapping for experimental planning and the interpretation of observations (Fig. 3).

Street-level air quality modelling

Urban CFD model. In the framework of the aforementioned project WT!mpact, a new computational fluid dynamics (CFD) solver has been developed to address the combined requirements of high spatial accuracy and computational efficiency in urban air-quality forecasting.

The CFD solver is intended to bridge the gap between mesoscale and building-resolved modelling. It uses an immersed-boundary approach wherein building boundaries can be semi-permeable in a statistical sense. The governing equations, which are incompressible anelastic Euler equations, are discretised with a particular finite volume discretization. Permeability fields are used to rescale the effective cell-face areas and control volumes, which impinges on the numerical flux, potentially blocking it in any direction. The permeability fields are derived by statistical processing of detailed building geometry data within each cell volume. Thus, inside a grid cell

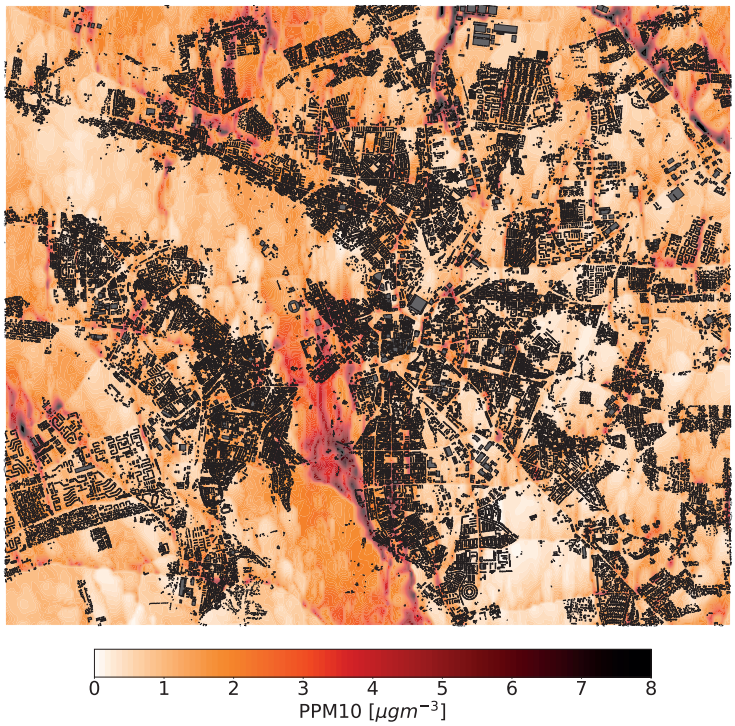

Fig. 4: 1st-layer concentration of primary PM_{10} over Leipzig on 13 May 2019, 0600 UTC from a 24-hour simulation with the new CDF model. For clarity, only a subset of the model domain is shown.

the collective effect of obstacles on the flow is represented, and not that of a single intersecting geometry. This approach allows the model to be applied for resolutions significantly lower than needed to resolve buildings, while the possibility of material exchange within narrow street canyons is retained by non-zero permeability values.

The numerical procedure to advance the equations in time consists of a pressure projection method. In a first step, the advective, diffusive, surface and turbulent tendencies are integrated explicitly in time. The advection scheme is adopted from the All Scale Atmospheric Model (ASAM) [*Jähn et al.*, 2015] and is positive and up to third order accurate in space. With the explicit tendencies, a Poisson equation for perturbation pressure is set up. Since the solver employs a multi-stage time integration scheme, at each sub-step a Poisson equation is solved, demanding an efficient Poisson solver. This is not ameliorated by the fact that the modification with the permeability fields results in a particular ill-conditioned problem. Multigrid methods belong to the most efficient solvers for hyperbolic equations. In this regard, a geometric multigrid method was developed, which uses re-discretizations of the Poisson equation on each coarse grid. The number of multigrid iterations is markedly reduced by using sparse approximate inverse smoothers instead of the more popular Gauss Seidel method, which provide additional advantages, e.g. adaptivity. Using subdomain-decomposition, the model is fully parallelised and can now be applied to simulate wind fields for entire cities at high resolution. The CFD model is supplemented with an interpolation tool, which provides initial and boundary conditions from COSMO-MUSCAT model output. A further goal in the development is a coupling to the CTM MUSCAT, as currently the applicability of the CFD solver is limited to chemically inert pollutants.

In order to test the new urban CFD solver, the dispersion of primary PM_{10} was simulated for the entire urban area of Leipzig and a period of 24 hours. The horizontal grid spacing is 50 m, and the lowest layers have a vertical resolution of 7 m. The CFD simulation is initialised and driven with COSMO-MUSCAT fields for meteorology and primary PM_{10} concentrations. The emissions are prescribed from UBA traffic emission data. The building structure is described by permeability fields, calculated from detailed building-geometry data. Figure 4 shows simulation results for 13 May 2019. The dispersion of the tracers is as expected, e.g. with channelling in narrow inner-city roads and more diluted spread in wider areas. After further successful testing, the CFD solver will be combined with the COSMO-MUSCAT model for downscaling.

PALM-4U urban climate model. TROPOS recently started testing the new urban climate model PALM-4U [*Maronga et al.*, 2015; *Resler et al.*, 2017] also for downscaling purposes and for studying relevant processes related to urban climate and air quality. PALM-4U is developed within the German-wide research project 'Model-based city planning and application in climate change' (MOSAIK) within the BMBF programme 'Urban Climate Under Change – [UC]²'. The model is based on the PArallelised Large-eddy simulation Model (PALM) initially developed by the Institute of Meteorology and Climatology (IMUK) of the Leibniz University of Hannover. The PALM for urban applications (PALM-4U) is equipped with specific components, which are suited to describe the different characteristics of the urban environment and include a range of tools and diagnostics for urban planning as well as scientific research. The PALM-4U model system is open-access software, which components will be further developed by the MOSAIK consortium. The model has a high performance and scalability and is suitable for simulations of large cities of up to 2.000 km² size with grid-resolved buildings. Its core is a set of non-hydrostatic, filtered, incompressible Navier-Stokes equations in Boussinesq-approximated form. Prognostic equations are solved for horizontal and vertical wind velocity, potential temperature, and water vapour mixing ratio on a Cartesian grid with grid spacings down to 1 m and below. A list of PALM-4U components, particularly relevant for the research at TROPOS, includes sophisticated representations of land and urban surfaces and the radiative transfer within the urban boundary layer. In addition, there is the capability of nesting from realistic meso-scale meteorological fields (e.g., COSMO-D2), a chemistry module for the transport and conversion of reactive gas species, a simple photolysis parameterization, a sectional aerosol module, as well as schemes for dry deposition of gases and particles.

Building-resolved simulations with PALM-4U were set up for a subdomain over Leipzig, spreading across the area between the parks 'Friedenspark' and 'Lene-Voigt-Park' in the south east of Leipzig. The domain has a size of 1.5 km x 1.5 km with 5 m horizontal grid spacing and 42 vertical layers of 2 m. The configuration uses very detailed information on building geometry, vegetation and street types as well as road traffic emissions, which are provided by the city of Leipzig and UBA, respectively. The model is dynamically forced by DWD COSMO-D2 analysis.

Initial 24-hour simulations were performed for summer and autumn days of recent years. The model results show a large variability in surface roughness and radiative fluxes (short- and long-wave) across the domain due to the mixed building structure including the adjacent parks with trees and lawns (Fig. 5a). As reproduced by PALM-4U, these features result in a strong differential heating and near-surface temperature gradients between vegetated and built-up areas (Fig. 5b), and cause the turbulent flow situation expected for this urban environment. The urban flow patterns affect the dispersion of air pollutants as shown for NO_2 in Fig. 5c. Traffic emission hotspots

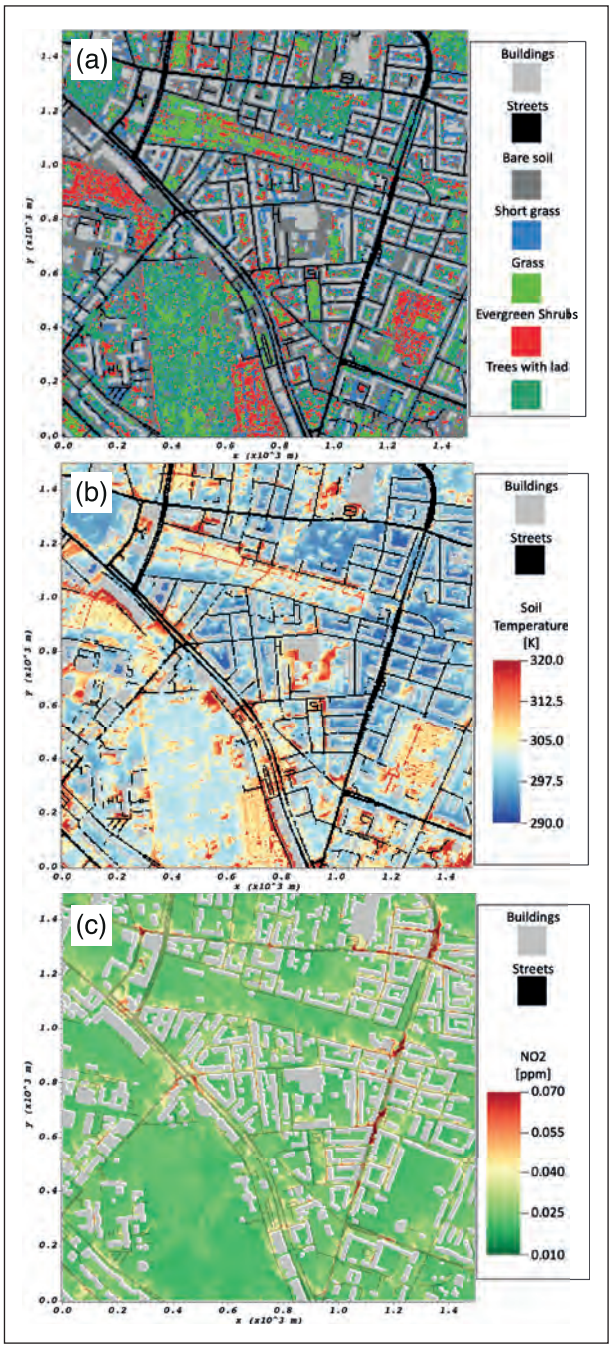

Fig. 5: Building-resolved simulations with PALM-4U for a subdomain over Leipzig, covering the area between the parks 'Friedenspark' and 'Lene-Voigt-Park' in the south east of Leipzig. Shown are (a) vegetation and buildings, (b) soil skin temperature, and (c) near-surface NO_2 concentration for 18 October 2019, 1500 UTC.

and retarded wind flow in street canyons lead to high concentration levels in some busy narrow streets while air pollution is significantly lower in the wider park areas and backyards.

As a next step, it is planned to apply this model setup to field experiments that were conducted during the exceptionally hot summers of 2018 and 2019 as part of the BMBF-funded junior research project 'Environmental-health Interactions in Cities' (GreenEquityHEALTH). Within GreenEquityHEALTH, researchers from the Humboldt University of Berlin and the Helmholtz Centre for Environmental Research – UFZ aim to assess the urban environmental processes related to climate change and urbanisation with specific focus on public health and socio-environmental justice. Here, the building-resolved simulations using PALM-4U will contribute to explore how urban vegetation can counteract extreme heat temperatures and air pollution and their negative effects on human health and well-being. The measurements of urban climate and air quality data, in turn, provide important input for model evaluation.

Both, PALM-4U and the new CFD solver are considered as approaches for downscaling the neighbourhood-scale modelling results from COSMO-MUSCAT. Further experience, however, must be gained to decide, whether the new CFD solver, which is computationally highly efficient, or the more accurate model PALM-4U is better suited to study our research questions.

Advanced urban chemistry and SOA formation

A current PhD research project funded by the German Federal Environmental Foundation (Deutsche Bundesstiftung Umwelt, DBU) investigates the interactions of biogenic emissions and urban air quality.

Particularly in times of climate warming, which will further enhance the urban heat island effect, cities and municipalities strive to take measures to ensure liveable conditions in the future. Common climate mitigation strategies include to increase the urban green as trees have a cooling effect on the cities' microclimate. Regarding their effect on air quality, which also remains a pressing concern, however, the role of trees is ambivalent. Trees adsorb and retain air pollutants, but on the other hand hinder the ventilation below their canopy and produce biogenic volatile organic compounds (BVOCs), which are ubiquitous and highly chemically reactive [*Atkinson and Arey*, 2003].

The chemical degradation of BVOCs under high urban NO_X (NO plus NO_2) conditions is known to promote the production of ground-level ozone [*Spracklen et al.*, 2011], affecting the human and environmental health as well as the level of atmospheric oxidants. Furthermore, the processing of BVOCs lowers their saturation vapour pressure, which leads to secondary organic aerosol (SOA) formation. The SOA formation might be further increased by the higher emissions of primary organic aerosol, increasing the organic matter, on which semi-volatile products can accumulate. SOA is a major constituent of $PM_{2.5}$ that is among the health-relevant air pollutants.

Therefore, the impact of BVOCs on urban air pollution is an interesting open research question that is addressed by air quality simulations for the City of Leipzig using the urbanised model framework COSMO-MUSCAT (see above for detailed information on the model setup). Specifically, it is investigated (1) the chemical processing of BVOCs under polluted conditions and the effects of air entrainment and detrainment in the urban boundary layer, as well as (2) the impact of BVOCs on the atmospheric oxidation capacity and potential feedback on anthropogenic air pollutants.

In COSMO-MUSCAT, the BVOC emission model from *Steinbrecher et al.* [2009] is implemented which, other than the widely-used scheme MEGAN-2.1 [*Guenther et al.*, 2012], was especially designed for Europe and already considers more than 100 different tree species. The considered BVOC emissions include isoprene, 17 monoterpenes (e.g., α- and β-pinene, limonene), sesquiterpene and oxygen containing BVOCs (e.g., alcohols, aldehydes). Each BVOC species has a specific reaction rate coefficient for the reaction with the radicals OH, NO_3 and O_3 and thus can influence the atmospheric oxidizing potential. The strength and composition of BVOC emissions vary considerably between tree species. It is parameterised by a BVOC and tree-species dependent standard emission potential, the tree-specific biomass density, the area covered by a tree species and some temperature and light-dependent correction factors. Plant stress conditions (drought, heat, O_3, nutrient scarcity, wounding, etc.) can either increase or decrease the BVOC emissions, again depending on the tree species. Most of the trees in cities are more vulnerable than rural trees [*Fitzky et al.*, 2019]. Therefore, considering these stressors in emission models is important, but has not yet been realised since the species-specific responses to stress are largely unknown.

For the description of SOA formation in COSMO-MUSCAT, the existing scheme SORGAM [*Schell et al.*, 2001] was upgraded with additional production pathways, including the reactions of monoterpene

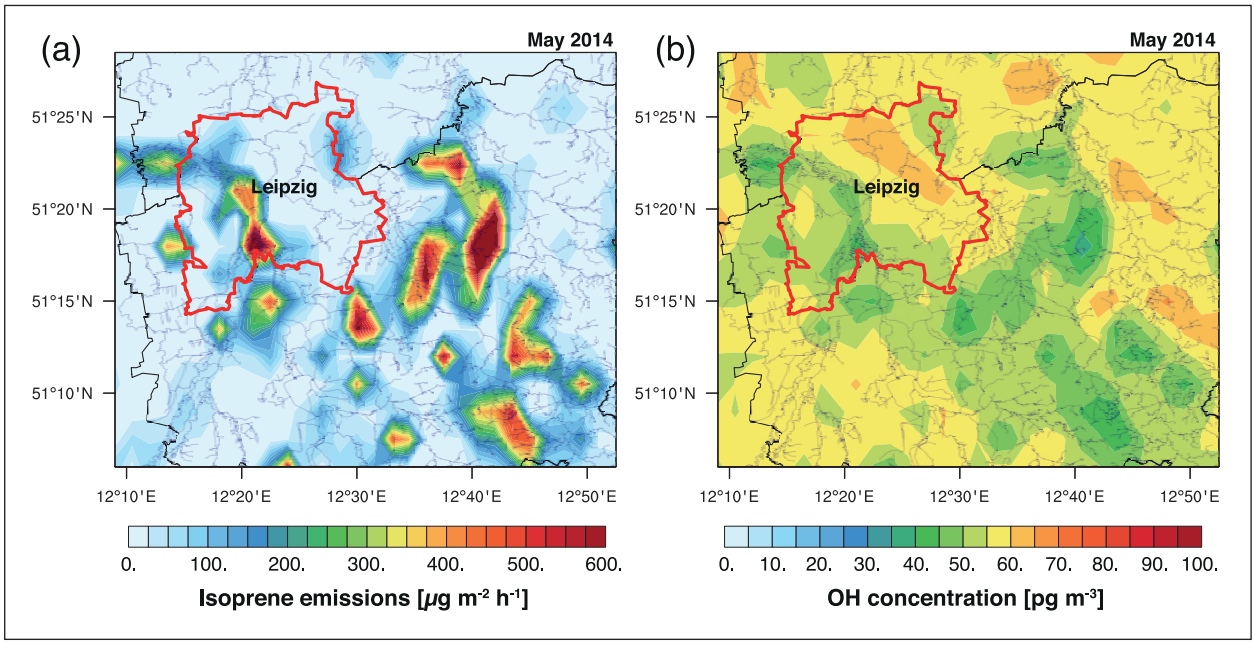

Fig. 6: Maps of (a) isoprene emissions and (b) OH radical concentration over Leipzig and surroundings in May 2014. Shown are monthly means of COSMO-MUSCAT results with 1.4 km (2.8 km) horizontal resolution in the chemistry-transport (meteorological) fields. Shown are also the administrative border of Leipzig in red colour and rivers for geographical orientation.

with the NO_3, isoprene with OH and NO_3, sesquiterpene with OH, O_3 and NO_3, as well as the formation of highly oxygenated organic molecules (HOMs) from all considered BVOCs. Tests showed that these model extensions, for example, result in up to 65% higher night-time SOA yields due to the reaction of monoterpenes with NO_3, which is in better agreement with observations at the TROPOS rural field site Melpitz (not shown).

In addition, a new, more detailed land-use dataset was implemented, which comprises 138 land-use classes with 116 tree species and 11 agricultural land types [*Köble and Seufert*, 2001] instead of the previously used dataset with only 10 land-use classes. A sensitivity study using the two setups showed that a too general model representation of land use with only a simple categorisation into coniferous, mixed and deciduous forest and agricultural land can lead to altered oxidant concentrations (e.g. a wide-spread reduction in OH by 50%) and, eventually, to an overestimation of SOA by up to 35%. Figure 6 shows the production of isoprene and the occurrence of its main oxidizing agent OH in May 2014 as simulated by COSMO-MUSCAT on the model domain for Central Germany. Isoprene is mainly emitted in the area of the Leipzig Riverside Forest and from the forests east and southeast of Leipzig. As expected, the pattern is anticorrelated with the OH distribution, with high concentrations in the inner city and lower values in the green parts. High-resolved urban simulations with a more detailed representation of building structures and vegetation, including a species-resolved tree population, will be the next step to clearly show the impact on air quality in Leipzig. For the urban setup for Leipzig, a new detailed dataset of land use including all available tree species information is developed using data from the City of Leipzig for forest, street and park tress (Fig. 7a) in combination with a high-resolved map of generalised land-use types (Fig. 7b) available from *Banzhaf and Kollai* [2018]. To further improve the representation of the chemical processing of biogenic and anthropogenic VOC, the currently used chemistry mechanism RACM-MIM2-ext will be replaced by a more recent mechanism, which is based on MOZART [*Schultz et al.*, 2018] and is currently under development. It is also planned to include a plant stress function valid for ozone and wounding (herbivory) induced stress as suggested by *Grote et al.* [2019].

Finally, using the further developed setup, the impacts of BVOCs on the atmospheric oxidation potential and air pollution in urban areas will be examined in detail. A future application is to perform model sensitivity studies in order to identify tree-specific mitigation potentials for air quality.

Summary

The latest ongoing developments in urban air pollution modelling at TROPOS are presented. The new multi-scale framework for urban air-pollution modelling presented here allows to visualise

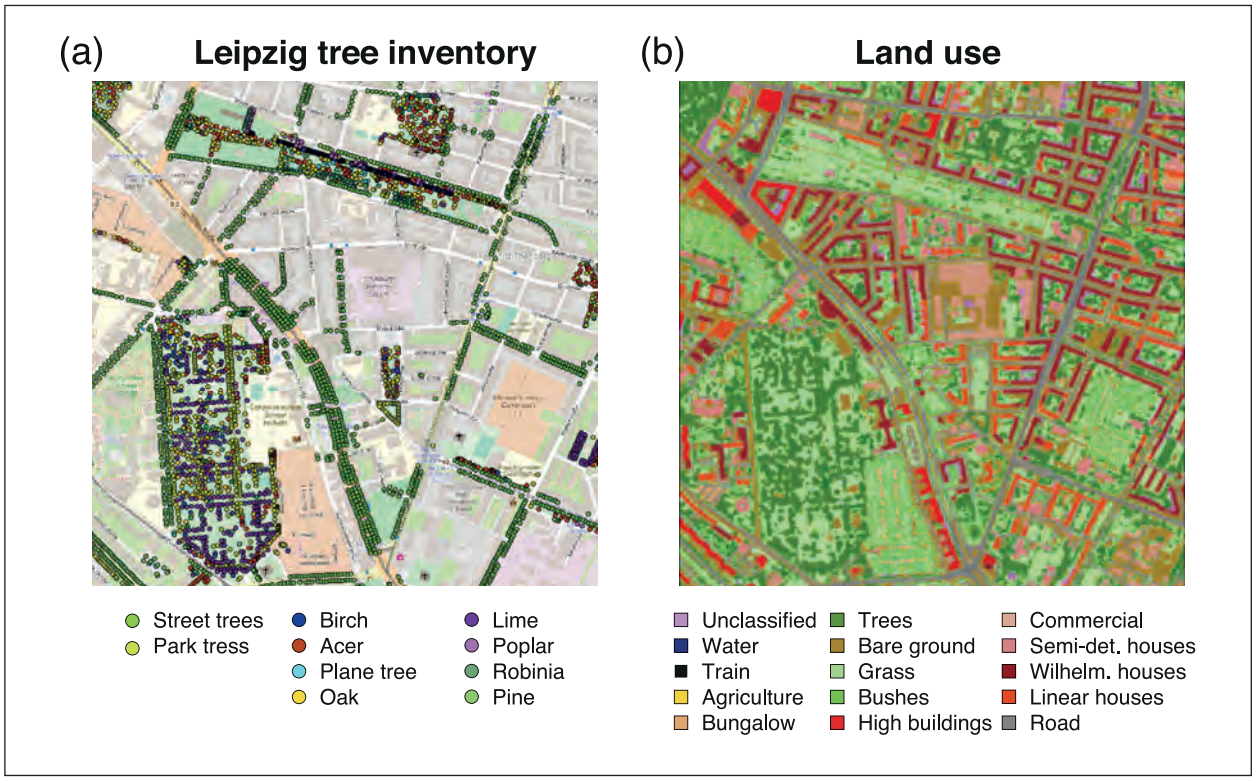

Fig. 7: Map of (a) urban tree population and (b) land-use types shown for a subdomain in the south-eastern part of Leipzig, which are planned to be integrated for the detailed, high-resolved air-pollution simulations with COSMO-MUSCAT.

air-quality issues in cities, and provides a better exposure evaluation. The model system consists of the urbanised chemistry transport model COSMO-MUSCAT, which is applied at continental to urban neighbourhood scales (< 500 m). A first application of COSMO-MUSCAT in urban air-quality forecast for the City of Leipzig is presented for a field campaign of the WT!mpact project in May 2019. For the downscaling of model results from urban-scale to street-level, two approaches are explored: A new CFD solver has been developed, which uses permeability fields to represent buildings that allow grid spacings larger than a typical street width. As shown in a first test, the CFD model can be applied to the entire urban area of Leipzig, reproducing characteristic flow patterns. As second option, the new urban climate model PALM-4U, developed within the German-wide initiative MOSAIK, has been successfully set up for building-resolved simulations for Leipzig. Near future work includes a thorough model evaluation of the coupled model framework using the unique set of mobile and stationary measurements available at Leipzig. Ultimately, the model will be used to investigate the small-scale variability of air pollutants and their controlling factors in Leipzig, as well as potentially in other cities. In a current DBU project, advanced representations of chemistry and SOA formation in the urbanised COSMO-MUSCAT are used to study the impacts of biogenic emissions from trees and plants on the atmospheric oxidation potential and urban air quality. This study shows that clean air and climate mitigation measures can have unexpected ambiguous effects and, in future, will provide tree-specific mitigation potentials for air quality.

References

Atkinson, R. and J. Arey (2003), Gas-phase tropospheric chemistry of biogenic volatile organic compounds: a review, *Atmos. Environ.*, 37, 197–219.

Banzhaf, E. and H. Kollai (2018), Land use / Land cover for Leipzig, Germany, for 2012 by an object-based image analysis (OBIA), PANGAEA
Supplement to: Banzahf, E., H. Kollai, and A. Kindler (2018), Mapping urban grey and green structures for liveable cities using a 3D enhanced OBIA approach and vital statistics, *Geocarto Int.*, 1–18, doi:10.1080/10106049.2018.1524514.

EEA (2019), Air quality in Europe – 2019 report, *EEA report No 10/2019, European Environment Agency (EEA)*, Publications Office of the European Union, Luxembourg.

Fitzky, A., C., H. Sandén, T. Karl, S. Fares, C. Calfapietra, R. Grote, A. Saunier, and B. Rewald (2019), The Interplay Between Ozone and Urban Vegetation–BVOC Emissions, Ozone Deposition,

and Tree Ecophysiology, *Front. for. glob. change*, 2, doi:10.3389/ffgc.2019.00050,

Grote R., M. Sharma, A. Ghirardo, and J-P. Schnitzler (2019), A New Modeling Approach for Estimating Abiotic and Biotic Stress-Induced de novo Emissions of Biogenic Volatile Organic Compounds From Plants, *Front. for. glob. change*, 2, doi:10.3389/ffgc.2019.00026.

Guenther, A. B., X. Jiang, C. L. Heald, T. Sakulyanontvittaya, T. Duhl, L. K. Emmons, and X. Wang (2012), The Model of Emissions of Gases and Aerosols from Nature version 2.1 (MEGAN2.1): an extended and updated framework for modeling biogenic emissions, *Geosci. Model Dev.*, 5, 1471–1492, https://doi.org/10.5194/gmd-5-1471-2012.

Huszar, P., M. Belda, J. Karlický, T. Bardachova, T. Halenka, and P. Pisoft (2018), Impact of urban canopy meteorological forcing on aerosol concentrations, *Atmos. Chem. Phys.*, 18, 14059–14078, https://doi.org/10.5194/acp-18-14059-2018.

Jähn, M., O. Knoth, M. König, and U. Vogelsberg (2015), ASAM v2.7: a compressible atmospheric model with a Cartesian cut cell approach, *Geosci. Model Dev.*, 8, 317–340, https://doi.org/10.5194/gmd-8-317-2015.

Kioutsioukis, I., U. Im, E. Solazzo, R. Bianconi, A. Badia, A. Balzarini, R. Baró, R. Bellasio, D. Brunner, C. Chemel, G. Curci, H. D. van der Gon, J. Flemming, R. Forkel, L. Giordano, P. Jiménez-Guerrero, M. Hirtl, O. Jorba, A. Manders-Groot, L. Neal, J. L. Pérez, G. Pirovano, R. San Jose, N. Savage, W. Schroder, R. S. Sokhi, D. Syrakov, P. Tuccella, J. Werhahn, R. Wolke, C. Hogrefe, and S. Galmarini (2016), Insights into the deterministic skill of air quality ensembles from the analysis of AQMEII data, *Atmos. Chem. Phys.*, 16, 15629–15652, https://doi.org/10.5194/acp-16-15629-2016.

Köble, R. and G. Seufert (2001), Novel maps for forest tree species in Europe, *Proceedings of the 8th European Symposium on the Physico-Chemical Behaviour of Air Pollutants: A Changing Atmosphere!*, Torino, Italy, 17-20 September 2001.

Maronga, B., M. Gryschka, R. Heinze, F. Hoffmann, F. Kanani-Sühring, M. Keck, K. Ketelsen, M. O. Letzel, M. Sühring, and S. Raasch (2015), The Parallelized Large-Eddy Simulation Model (PALM) version 4.0 for atmospheric and oceanic flows: model formulation, recent developments, and future perspectives, *Geosci. Model Dev.*, 8, 2515–2551, https://doi.org/10.5194/gmd-8-2515-2015.

Resler, J., P. Krč, M. Belda, P. Juruš, N. Benešová, J., Lopata, O. Vlček, D. Damašková, K. Eben, P. Derbek, B. Maronga, and F. Kanani-Sühring (2017), PALM-USM v1.0: A new urban surface model integrated into the PALM large-eddy simulation model, *Geosci. Model Dev.*, 10, 3635–3659, https://doi.org/10.5194/gmd-10-3635-2017.

Schell, B., I. J. Ackermann, H. Hass, F. S. Binkowski, and A. Ebel (2001), Modeling the formation of secondary organic aerosol within a comprehensive air quality model system, *J. Geophys. Res.*, 106(D22), 28275–28293, doi:10.1029/2001JD000384.

Schubert, S., S. Grossman-Clarke, and A. Martilli (2012), A Double-Canyon Radiation Scheme for Multi-Layer Urban Canopy Models. *Bound.-Lay. Meteorol.*, 145, 439–468, doi:10.1007/s10546-012-9728-3.

Schultz, M. G., S. Stadtler, S. Schröder, D. Taraborrelli, B. Franco, J. Krefting, A. Henrot, S. Ferrachat, U. Lohmann, D. Neubauer, C. Siegenthaler-Le Drian, S. Wahl, H. Kokkola, T. Kühn, S. Rast, H. Schmidt, P. Stier, D. Kinnison, G. S. Tyndall, J. J. Orlando, and C. Wespes (2018), The chemistry–climate model ECHAM6.3-HAM2.3-MOZ1.0, *Geosci. Model Dev.*, 11, 1695–1723, https://doi.org/10.5194/gmd-11-1695–2018.

Spracklen, D. V., J. L. Jimenez, K. S. Carslaw, D. R. Worsnop, M. J. Evans, G. W. Mann, Q. Zhang, M. R. Canagaratna, J. Allan, H. Coe, G. McFiggans, A. Rap, and P. Forster (2011), Aerosol mass spectrometer constraint on the global secondary organic aerosol budget, *Atmos. Chem. Phys.*, 11, 12109–12136, https://doi.org/10.5194/acp-11-12109-2011.

Steinbrecher, R., G. Smiatek, R. Köble, G. Seufert, J. Theloke, K. Hauff, P. Ciccioli, R. Vautard, and G. Curci (2009), Intra- and inter-annual variability of VOC emissions from natural and semi-natural vegetation in Europe and neighbouring countries, *Atmos. Environ.*, 43 (7), 1380-1391, https://doi.org/10.1016/j.atmosenv.2008.09.072.

Wolke, R., W. Schröder, R. Schrödner, and E. Renner (2012), Influence of grid resolution and meteorological forcing on simulated European air quality: a sensitivity study with the modeling system COSMO–MUSCAT. *Atmos. Environ.*, 53, 110–130, https://doi.org/10.1016/j.atmosenv.2012.02.085.

Funding

German Federal Ministry of Education and Research (BMBF), Bonn, Germany.;
German Federal Environmental Foundation (DBU), Osnabrück, Germany.

Cooperation

German Federal Environmental Agency (UBA), Dessau, Germany;
Saxon State Agency of Environment, Agriculture and Geology (LfULG), Dresden, Germany;
The Mayor of Leipzig, Environmental Office, Leipzig, Germany;
Deutscher Wetterdienst (DWD), Offenbach, Germany;
Humboldt University of Berlin, Berlin, Germany;
Helmholtz centre for environmental research (UFZ), Leipzig, Germany.

PollyNET - A growing continental-scale, fully automated, 24/7 aerosol profiling network: Latest developments and observational highlights

Holger Baars, Yin Zhenping, Ronny Engelmann, Rico Hengst, Karsten Hanbuch, Birgit Heese, Albert Ansmann, Athina Floutsi, Cristofer Jimenez, Ulla Wandinger, Johannes Bühl, Martin Radenz, Kevin Ohneiser, Hannes Griesche, Patric Seifert, Annett Skupin, Julian Hofer, Dietrich Althausen

PollyNET ist ein wissenschaftliches Netzwerk zur vertikal-aufgelösten Erfassung von Aerosoleigenschaften in der Atmosphäre. Das vom TROPOS geleitete Netzwerk besteht aus leistungsstarken, vollautomatisierten Aerosol-Lidarmesssystemen vom Typ Polly (Portable Lidar System). TROPOS entwickelt diese selbstgebauten Lidarsysteme und die dazugehörige Datenauswertung kontinuierlich weiter. So können mit der neuesten Polly-Generation jetzt z.B. neben Aerosolprofilen auch Wolkeneigenschaften abgeleitet werden. Die Messungen dieser weltweit eingesetzten Fernerkundungsgeräte werden zeitnah auf polly.tropos.de dargestellt. Um den ständig wachsenden Anforderungen gerecht zu werden, wurde eine neue Datenprozessierung entwickelt. Die Webpräsenz wurde ebenfalls erneuert, um das volle Potential des PollyNETzwerkes frei zugänglich zu machen.
Die kontinuierlichen Messungen an klimarelevanten Hotspots, gepaart mit ständiger Methodenentwicklung, haben zu mehreren wissenschaftlich bedeutenden Erkenntnissen geführt. So konnte eine Rauchfahne, die von starken Waldbränden in Westkanada verursacht wurde, über Monate in der Stratosphäre über Europa charakterisiert werden. Des Weiteren wurde erstmals eine Klimatologie der Vertikalverteilung der Massenkonzentration von Mineralstaub in Tadschikistan erstellt. Erfolgreich konnte auch ein erster Schließungsversuch von Aerosol- und Wolkeneigenschaften anhand von Polly-Lidarmessungen in Zypern abgeschlossen werden. Die langjährigen Messungen an unterschiedlichen Standorten ermöglichen außerdem eine einzigartige Charakterisierung verschiedenster Aerosoltypen.
Im Rahmen von ACTRIS wird PollyNET weiter ausgebaut. Der globale Staubgürtel und andere klimarelevante Schlüsselregionen der Erde werden dabei abgedeckt. Neben den jüngst eingeweihten Stationen in Tadschikistan und Israel bestehen konkrete Pläne für Systeme auf Zypern und den Kap Verden.

Introduction

PollyNET is a TROPOS-led network of Polly lidar systems for continuous measurements of aerosol and cloud profiles at global climate-relevant hot spots [*Baars et al.*, 2016]. Polly lidars are sophisticated, automated Raman-polarization lidar systems for scientific purpose, but with the advantage of an easy-to-use and well-characterized instrument with same design, same automated operation, and same centralized data processing delivering near-real-time data products. Polly systems have been developed and constructed at TROPOS with international partners since 2002 [*Engelmann et al.*, 2016]. All Polly lidar systems are designed for automatic and unattended operation in 24/7 mode (continuously 24 hours a day, 7 days per week). The latest standard Polly lidar system is a so-called 3+2+2+1+2+2 multi-wavelength lidar with near-range capabilities (3 elastic, 2 Raman, 2 depolarization, 1 water-vapor, 2 near-range elastic, and 2 near-range Raman channels). With such a 12-channel system, backscatter coefficients at 3 wavelengths (355, 532, 1064 nm), extinction coefficients and depolarization ratios at two wavelengths

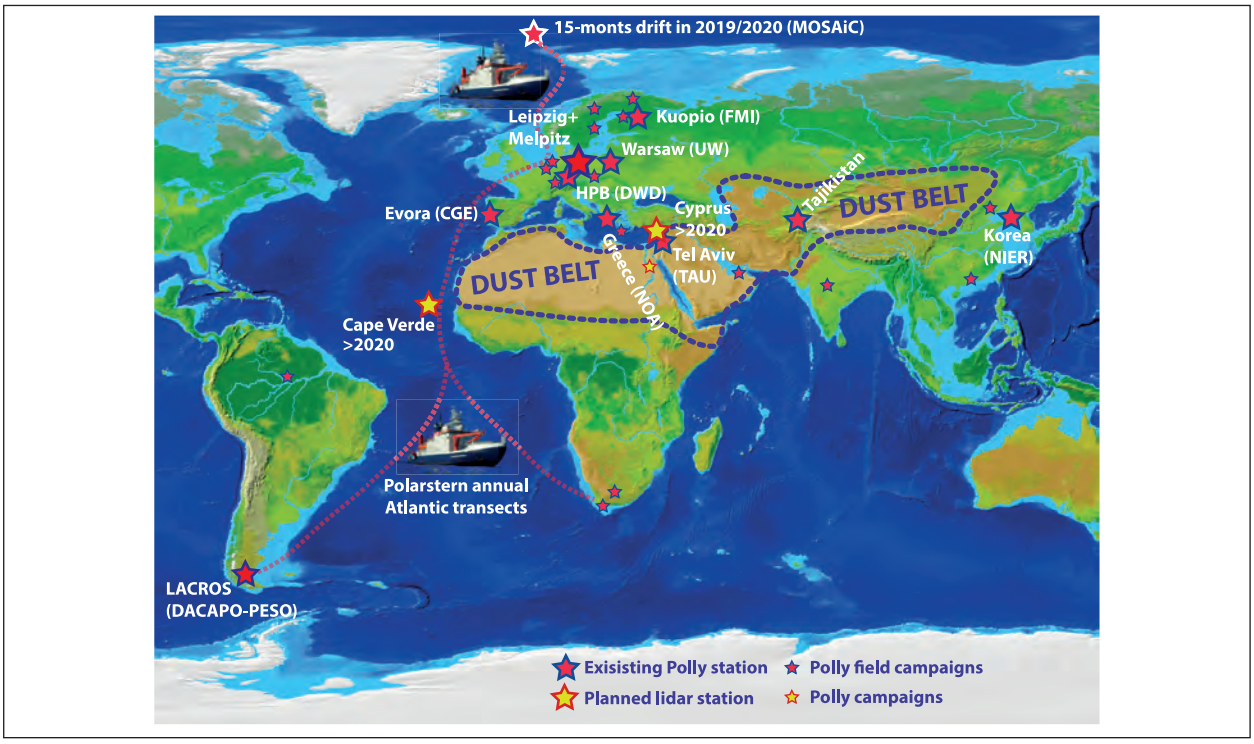

Fig. 1: Map indicating the locations of PollyNET measurements. Permanent (big stars) and field campaign (small stars) stations are shown. If the Polly lidar system is not run by TROPOS, the abbreviation of the hosting institute is given in brackets.

(355, 532 nm), and the water-vapor mixing ratio can be obtained. Combining near-range and far-range channels, the atmosphere is covered from about 80 m height above ground level (agl) up to 20-25 km agl.

Until now, 12 Polly lidar systems are in operation at various locations around the world. Five out of these 12 systems are operated by TROPOS, the other ones are operated by partner institutions. All these lidars form the PollyNET - an independent, voluntary, international network of the cooperating institutes led by TROPOS. The Polly systems are deployed at their home bases or for campaigns worldwide. For example, the Polly lidar of the Leipzig Aerosol and Cloud Remote Observations System (LACROS) has been continuously measuring at Punta Arenas, Chile, since 2018 together with the other LACROS instruments. Before, it was deployed at Cyprus for 1.5 years, in the framework of the Cyprus Clouds Aerosols and Rain Experiment (CyCARE). Another Polly of TROPOS has been operated in Haifa, Israel, for several years and is now the working horse at Leipzig. The current status of the network is shown in Fig. 1. The network is characterized by a centralized data processing with automatic lidar data analysis as well as publication of the results in near real-time on the web page polly.tropos.de. Thus, it serves as a pioneering network for ACTRIS, fully supporting the goals of this European research infrastructure. In recent years, several developments with respect to hardware, measurement locations, and processing chain as well as web presentation have been made. Some of the many interesting observations are highlighted in this report.

New developments

Aerosol-cloud interaction is one of the main research goals of TROPOS. Polly lidars are one key instrument for tackling this research field. Therefore, the so-called dual-field-of-view depolarization technology [*Jimenez et al.*, 2019] has been installed in three Polly systems. With this technique, the cloud droplet number concentration and liquid water content can be derived at the lower parts of liquid water clouds using multiple-scattering effects within the cloud droplet ensemble. For this purpose, a thirteenth channel measuring the cross-polarized light in a different (larger) field of view than the standard depolarization channel was implemented in the optical setup of Polly – see Fig. 2. This 13-channel lidar system is thus able to obtain cloud droplet properties next to aerosol profiles. This capability is a valuable addition to the methodologies developed to estimate cloud condensation nuclei concentration (CCNC) and ice-nucleating particle concentration (INPC) [*Mamouri and Ansmann*, 2016] and to derive the mass concentrations of fine-mode dust, coarse-mode dust, and pollution from lidar observations [*Mamouri and Ansmann*, 2017].

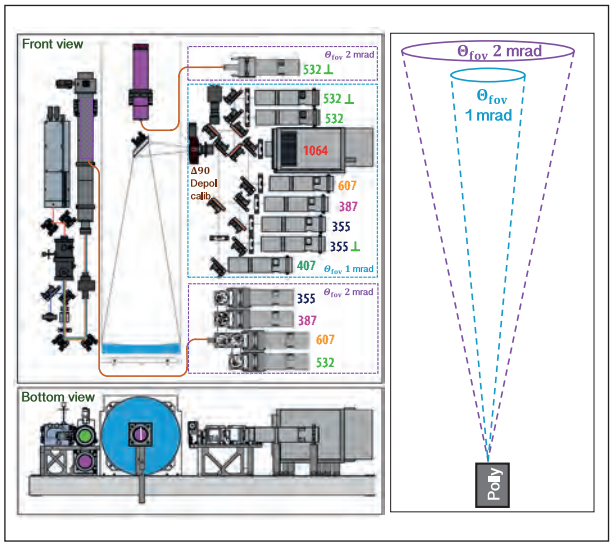

Fig. 2: Optical setup of the latest Polly lidar system emitting three wavelengths of laser light and having two telescopes and 13 channels in the receiver system.

In addition to these methodological evolutions, new Polly systems are equipped with a modern diode-pumped laser, which needs less maintenance (continuous operation up to two years) and provides more energy and a higher pulse repetition rate. First results with this new laser implemented in the Tajikistan system are very promising and show a significantly increased system performance. Beside of these two main improvements, several technical advances have been made by TROPOS pioneers, e.g., an automatic cleaning device for the roof window of the lidar to ensure accurate measurements also at very remote locations.

New processing chain and web presentation

The meanwhile 12 Polly lidar system measures continuously in 24/7 mode with 30 seconds temporal and 7.5 m vertical resolution. Data is uploaded in near real-time to the TROPOS server from all systems and published at the institute's website polly.tropos.de. Thus, an automatic processing of the data is needed to exploit the potentials of the instruments with respect to aerosol and aerosol-cloud-interaction research. The existing processing chain, which was intensively described by *Baars et al.* [2016], was completely restructured to allow the full exploitation of the large and steadily growing data input produced by the globally distributed PollyNET. The algorithms have been recoded from LABVIEW into MATLAB and PYTHON and subsequently upgraded/improved. Next to the processing itself, also a new web application was developed together with a new SQL data base structure to meet the demands of the growing user community of PollyNET. The new web application was developed as Model-View-Controller framework to separate the internal software logic and the access to the SQL data base. The application is prepared to serve the content in responsive web design to ensure

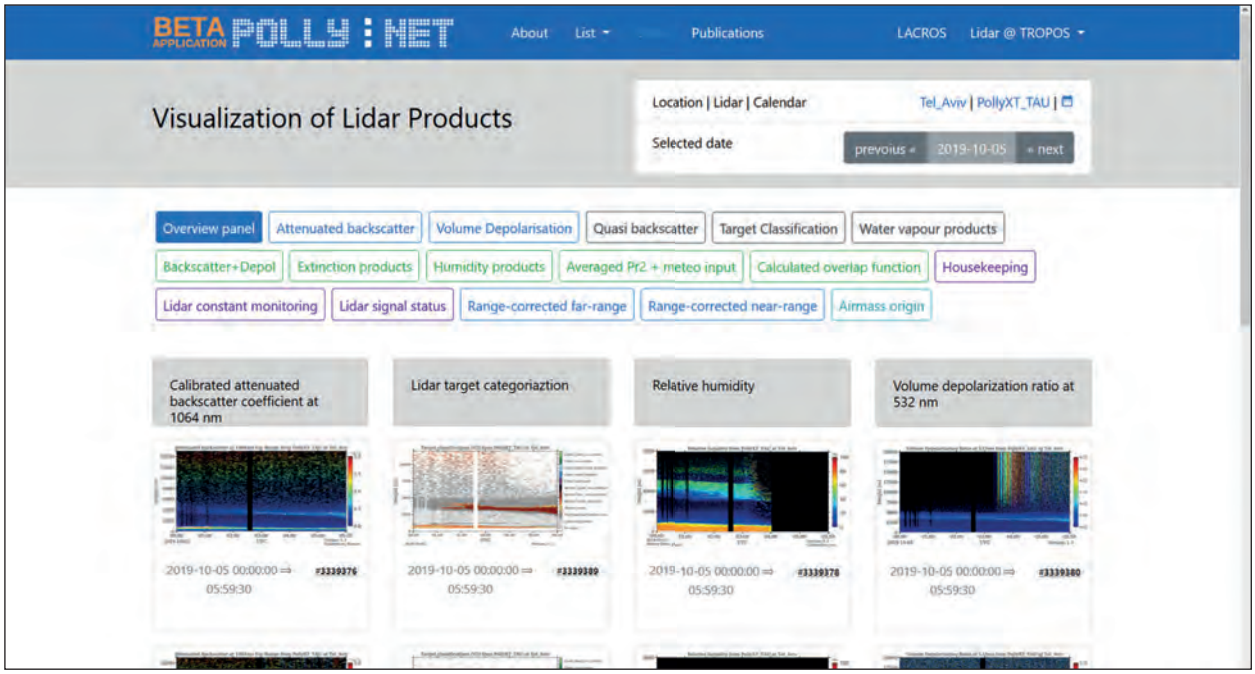

Fig. 3: Screenshot of the new PollyNET web application temporary available under picasso.tropos.de. Several new products were implemented and a significantly increased functionality was achieved. The overview page for the measurements of the lidar system at Tel Aviv on 5 October 2019 is shown.

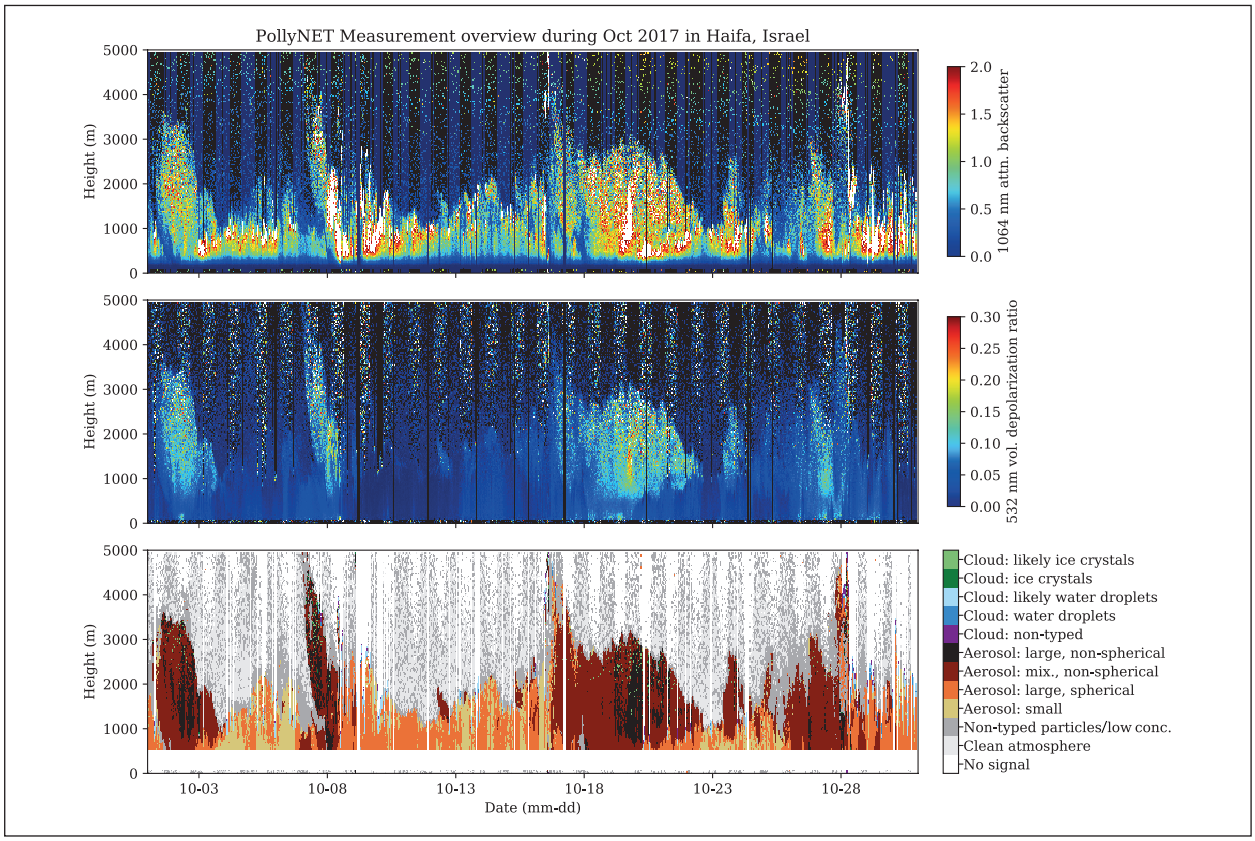

Fig. 4: One-month time series of the attenuated backscatter signal at 1064 nm (top), the volume depolarization ratio at 532 nm (middle), and the corresponding target classification at Haifa, Israel, in October 2017.

an optimal visualization on the users' end devices (pc, smartphone). A screenshot of the new webpage (currently available at picasso.tropos.de) with some of its many features is shown in Fig. 3.

Built on the well-established PollyNET processing, new products have been developed as well. An automatic calibration scheme for the signals yields to calibrated attenuated backscatter coefficients. In contrast to the formerly available range-corrected signals, which show qualitative height-time displays of the aerosol profile structure, the attenuated backscatter is a quantitative property that can be obtained with lidar and is often used for ceilometer and satellite-lidar data applications. The availability of the attenuated backscatter is a big step forward to continuous aerosol-cloud-interaction research, because the demand of a cloud-free atmosphere for calibration purposes is not needed anymore. Based on this new quantity, also the aerosol target categorization [*Baars et al.*, 2017] is now available online for most PollyNET stations. Another important example for the new features is the continuous calibration of the water-vapor observations of Polly [*Dai et al.*, 2018]. This capability leads to high-resolution profiles of the water-vapor mixing ratio and, taking model-derived temperature into account, relative humidity. Beside these atmospheric products, housekeeping variables like the lidar constant, system temperatures, and even overlap functions are determined automatically and in near real-time. All output is now written in NetCDF-4 and thus easy to use for others. A full list of all potential variables produced by the new PollyNET processing chain can be found under http://picasso.tropos.de/list/product_types, which is the temporary domain for the new web back end.

Example: Continuous Aerosol and Cloud Classification. A very interesting new PollyNET feature is the possibility to characterize the atmospheric state continuously over months. Fig. 4 shows the attenuated backscatter coefficient, the volume depolarization ratio, and the automatically retrieved aerosol target categorization of Polly in Haifa, Israel, for October 2017. Clearly visible features are phases of strong dust intrusions (high depolarization) but also periods of rather clean air (low backscatter, low depolarization ratio) with spherical aerosol particles in the boundary layer (yellow and orange in the target classification). Such plots are now available for all stations and help characterizing the atmosphere at all PollyNET locations.

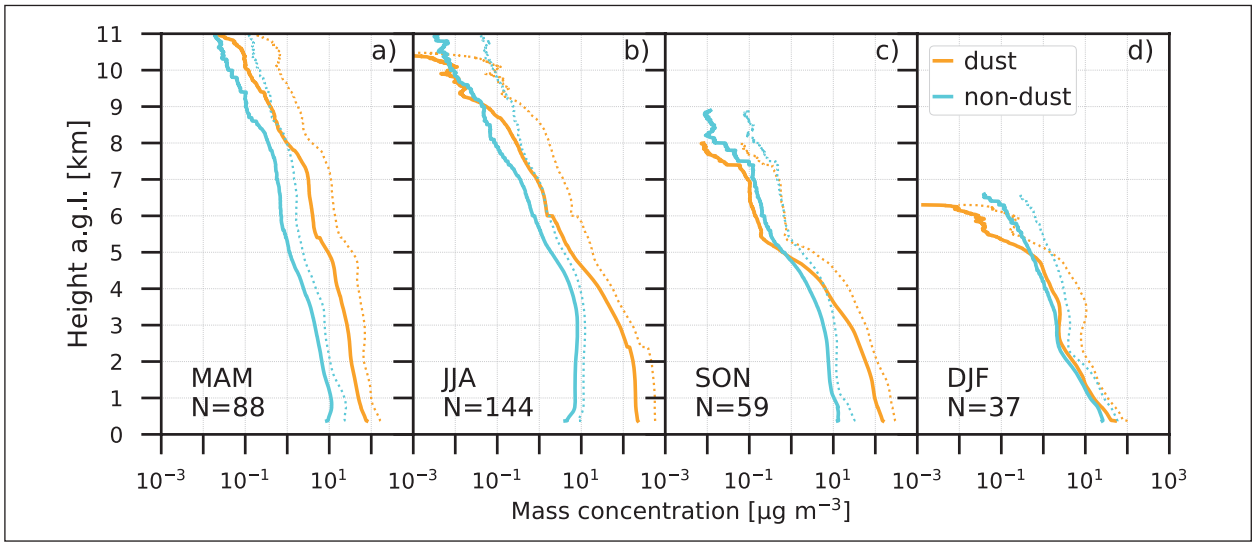

Fig. 5: Seasonal mean dust (yellow) and non-dust (cyan) mass concentration profiles for (a) spring, (b) summer, (c) autumn, and (d) winter. The dotted lines show the mean plus standard deviation values and provide an impression of the atmospheric variability. The mean minus standard deviation values are close to zero. N is the number of considered night-time observations.

Research Highlights

All the above-mentioned efforts are needed to characterize the atmospheric state with respect to aerosol and aerosol-cloud interaction as best as possible. Because of the 24/7 observations and the automatic processing, several ground-breaking findings have been made, which would have not been discovered without PollyNET. Four highlighting examples are shown below.

Aerosol characterization over Central Asia. For the first time, continuous vertically resolved long-term aerosol measurements were conducted with a state-of-the-art multiwavelength lidar over a Central Asian site. The lidar observations were performed in the framework of the Central Asian Dust Experiment (CADEX) at Dushanbe, Tajikistan, from March 2015 to August 2016 [*Hofer et al.*, 2019]. During the 18-month campaign, mixtures of continental pollution aerosol and mineral dust were frequently detected from ground to cirrus height level. Regional sources of dust and pollution as well as long-range transport of mineral dust mainly from Middle East and the Saharan deserts determine the aerosol conditions over Tajikistan. A seasonally resolved statistics regarding aerosol layering (main aerosol layer depth, lofted-layer occurrence) and optical properties (aerosol and dust optical thicknesses, vertically resolved light-extinction coefficient) was obtained. Beside these profiles of geometrical and optical aerosol properties, for the first time also a climatology of profiles of dust fraction, and dust and non-dust mass concentration was derived. As an example, Figure 5 shows the seasonal distribution of the mass concentration of dust and non-dust aerosol above Dushanbe, Tajikistan.

The highest dust mass concentrations occurred in the summer season (200–600 µg m^{-3}) and the lowest during the winter months in the main aerosol layer (20-50 µg m^{-3}). In winter, the pollution aerosol mass concentrations were 20–50 µg m^{-3}, while during the summer half year (spring to autumn) the mass concentration caused by urban haze and biomass-burning smoke decreased to 10–20 µg m^{-3} in the lower troposphere. Typical dust mass fractions were of the order of 60–80%. A considerable fraction of the aerosol load was thus related to anthropogenic pollution and biomass-burning smoke. The highest pollution levels occurred in the relatively shallow boundary layer during the winter months. The seasonal-mean 500-nm aerosol optical depth ranged from 0.15 in winter to 0.36 in summer during the CADEX period, seasonally mean particle extinction coefficients were of the order of 100–500 Mm^{-1} in the main aerosol layer during the summer half year and about 100–150 Mm^{-1} in winter. The main aerosol layer over Dushanbe reached typically up to 4–5 km height in spring to autumn. Apart from the microphysical and optical properties, also profiles of particle parameters relevant for liquid-water, mixed-phase cloud, and cirrus formation such as cloud condensation nuclei (CCN) and ice-nucleating particle (INP) concentrations were obtained. According to these observations, the CCN concentration levels were always controlled by pollution aerosol whereas lofted dust-containing aerosol layers indicated a high potential to influence cloud ice formation.

Stratospheric Smoke over Europe. In summer 2017, enormous amounts of smoke were injected into the upper troposphere and lower stratosphere over fire areas in western Canada during strong thunderstorm–pyrocumulonimbus activity. The stratospheric fire plumes spread over the entire Northern Hemisphere in the following weeks and months. One of the first observations of this phenomenon in Europe was made with a Polly lidar during an ACTRIS campaign in Košetice, Czech Republic. Significant and optically thick aerosol layers from the Canadian fires were observed in the troposphere and stratosphere. During the peak atmospheric perturbation over Europe, ca. 7–10 days after the fires, the total aerosol optical thickness was >0.8 and the maximum extinction in the stratosphere over Europe caused by these aerosol layers was stronger than after the Pinatubo eruption in the 1990's [*Ansmann et al.*, 2018].

The Polly lidar network could investigate the development of the smoke in the atmosphere for more than half a year [*Baars et al.*, 2019]. While the tropospheric smoke was washed out rather fast (within 2–3 weeks), signals of smoke have been observed in the stratosphere up to 23 km for more than 6 months. Fig. 6 shows the development of the smoke plume as observed with PollyNET in 2017 and 2018. The main smoke layer had been found at heights between 15 and 20 km since September 2017 (about 2 weeks after entering the stratosphere). Ascending aerosol layer features over the most southern European stations, especially over the eastern Mediterranean at 32–35 N, were observed. These features started at heights of about 18–19 km in the beginning of October and reached altitudes of 22–23 km in the beginning of December 2017. The stratospheric aerosol optical thickness at 532 nm decreased from values >0.25 on 21–23 August 2017 to 0.005–0.03 around 5–10 September and 0.003–0.004 from October to December 2017, when it was still significantly above the stratospheric background (0.001–0.002). Stratospheric particle extinction coefficients (532 nm) were as high as 50–200 Mm^{-1} until the beginning of September and on the order of 1 Mm^{-1} from October 2017 until the end of January 2018. The corresponding layer mean particle mass concentration was on the order of 0.05–0.5 $\mu g\ m^{-3}$ over these months. We observed a decrease of the particle linear depolarization ratio with time. It was found to be most consistent with aging of the smoke particles and related changes in the smoke particle

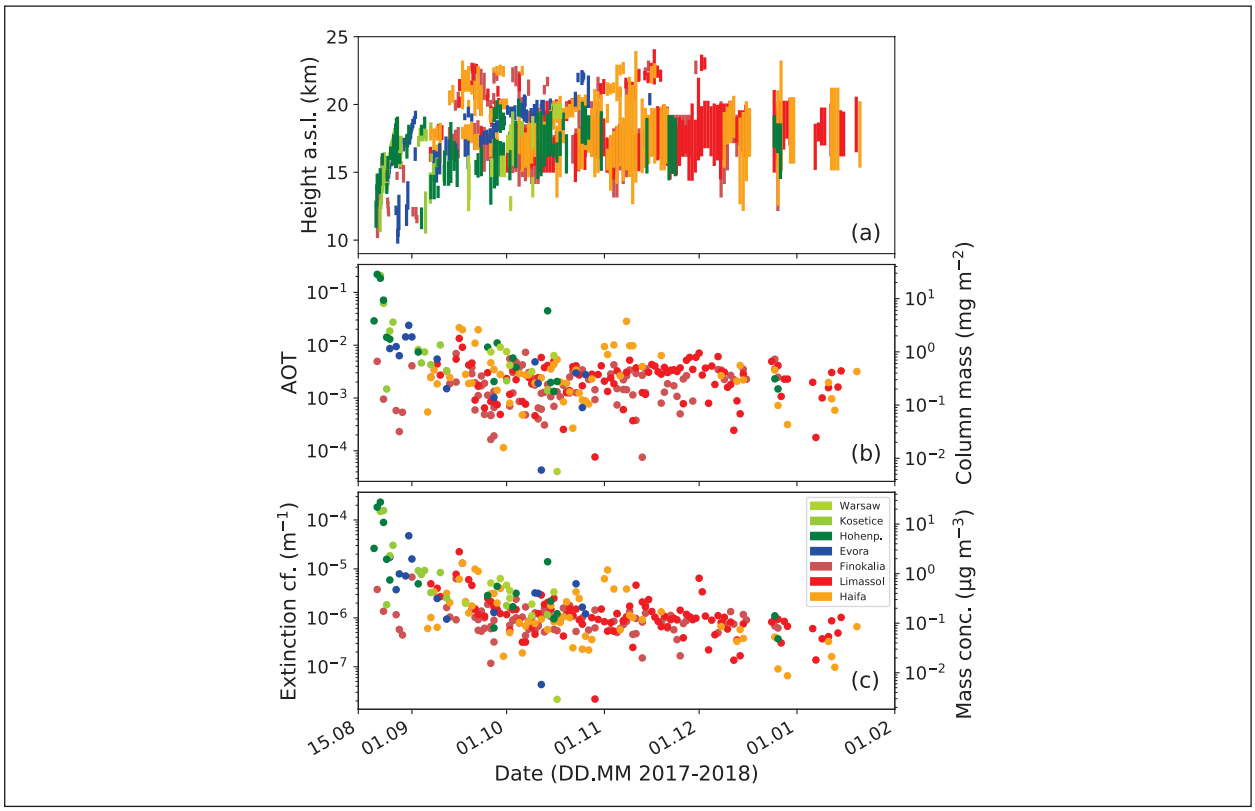

Fig. 6: (a) Overview of all Polly observations of the stratospheric smoke layer (from base to top as coloured vertical lines). For each station, one night-time observation per day is considered. (b) Corresponding smoke layer aerosol optical thickness (AOT) at 532 nm and estimated column-integrated smoke particle mass concentration, and (c) vertically averaged smoke particle extinction coefficient and corresponding mean particle mass concentration.

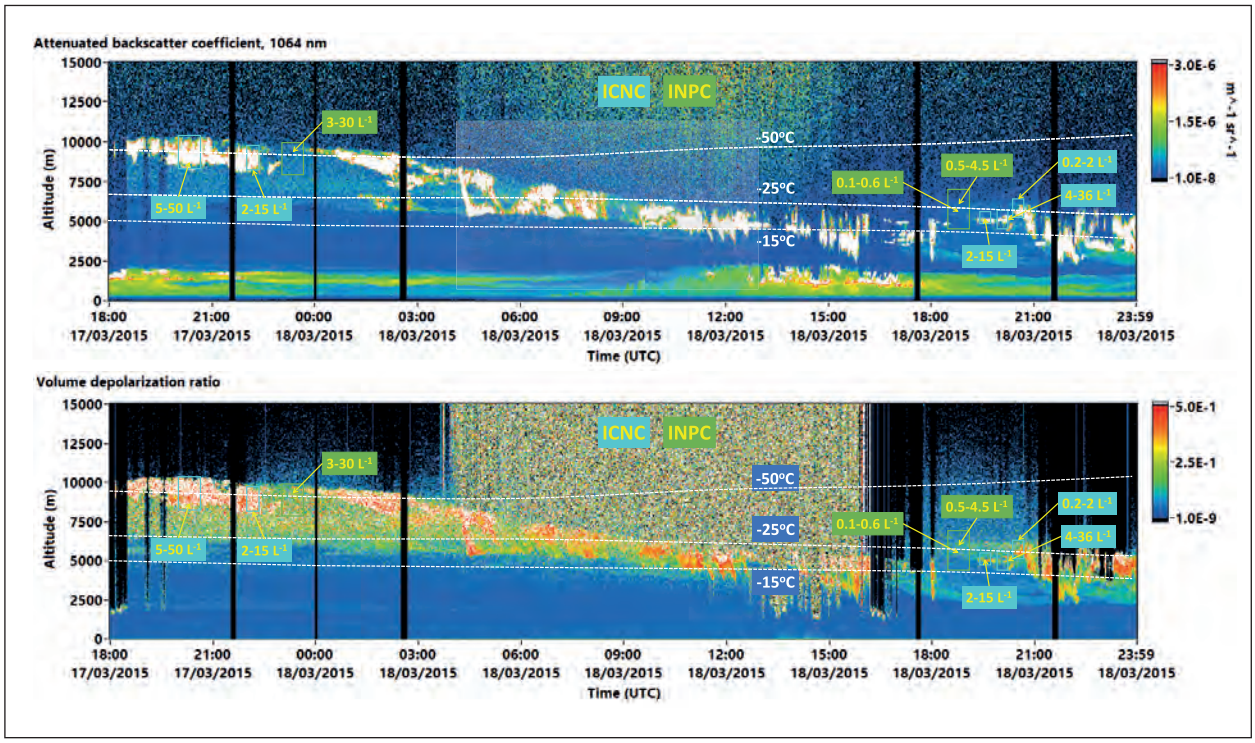

Fig. 7: Continuous cirrus and mixed-phase cloud observations over 30 h at Nicosia on 17–18 March 2015. Top: Range-corrected signal. Bottom: Volume depolarization ratio. Several INPC (orange) and ICNC (blue) values estimated from the lidar observations are given as numbers in boxes. Dashed white lines show the temperature isolines with a 3 h resolution derived from model.

shape properties (from non-spherical to spherical particle shape). Soot particles (light-absorbing carbonaceous particles) are efficient ice-nucleating particles at upper tropospheric (cirrus) temperatures and available to influence cirrus formation when entering the tropopause region from above. The estimated INP concentration levels were significantly enhanced for several months, and thus the smoke plumes served as a long-lasting INP reservoir able to trigger heterogeneous ice nucleation and in this way to influence cirrus formation at the tropopause level. This record-breaking stratospheric smoke event is the second major event after the Eyjafjallajökull volcanic eruption highlighting the importance, need, and usefulness of a ground-based aerosol profiling network of advanced lidars. Without having continuous measurements, the smoke layering details and properties as presented would widely remain undetected.

INP profiles over the Eastern Mediterranean. For the first time, a closure of the relationship between the ice-nucleating particle concentration (INPC) and the ice crystal number concentration (ICNC) in altocumulus and cirrus layers, solely based on ground-based active remote sensing was achieved. The observations were conducted at Nicosia and Limassol, Cyprus, during a 6-week field campaign in March–April 2015 and during the 18-month CyCARE campaign from October 2016 to March 2018, respectively. The focus was on cloud evolution in pronounced Saharan dust layers at heights from 5 to 11 km. The INPC was estimated from Polly measurements [*Ansmann et al.*, 2019], whereas the ICNC was retrieved from combined observations of Polly with either Doppler lidar (Nicosia campaign) or Doppler lidar and cloud radar (CyCARE). In the latter case, the ICNC is calculated in a sophisticated way from the terminal velocity of falling ice crystals, radar reflectivity, and lidar backscatter in combination with the modelling of backscattering at the lidar and radar wavelengths of 532 nm and 8.5 mm, respectively [*Bühl et al.*, 2019].

Figure 7 shows the Polly observations during a long-lasting cirrus event in March 2015. All clouds (white areas in Fig. 7, top) developed in Saharan dust laden air. Cloud top temperatures ranged from –20 to –57 °C. A good to acceptable agreement between the INPC and ICNC values (retrieved from aerosol and Doppler lidar observations) was found. INPC values ranged from 0.1 to 10 L^{-1} in the altocumulus layers and 1 to 50 L^{-1} in the cirrus layers observed between 8 and 11 km height. The observed long-lasting cirrus event could be fully explained by the presence of dust, i.e., without a need for homogeneous ice nucleation processes. In view of a potential consideration and implementation of complex aerosol–cloud

interaction in numerical weather forecast models and the assimilation of measured INPC profiles into those models, there is no alternative to continuous lidar-based INPC profiling and monitoring techniques as demonstrated with PollyNET.

Aerosol climatology. The PollyNET systems have been deployed for vertical profiling of aerosol and clouds at measurement sites from 88 N to 53 S and from 71 W to 125 E (Fig. 1). The observations cover Arctic conditions, mid-latitudes, tropical conditions, and the Antarctic regime at the southern peak of South America. Notable measurement sites are also the two research vessels *Meteor* and *Polarstern*, which allow longitudinal and latitudinal cross-section observations over the Atlantic Ocean [*Bohlmann et al.*, 2018]. The long-term observations together with their wide spatial distribution provide a very valuable data set for the characterization of predominant global aerosol types.

Figure 8 gives an overview of optical properties for different aerosol types and their mixtures as observed with PollyNET. This unique data set, which is exemplarily shown for 355 nm, is a valuable input for aerosol typing approaches and can be used for, e.g., data analysis algorithms of the new generation of space-borne lidars (ALADIN onboard Aeolus and ATLID onboard EarthCARE), harmonization of long-term space-borne observations, or the development of a near real-time and state-of-the-art aerosol typing product for PollyNET. To our knowledge, no other ground-based network covers such a range of different aerosol types and their characteristic optical properties. Thus, the heritage of PollyNET is a valuable source not only for satellite and model validation as well as data assimilation but also for the development of new retrieval algorithms and products.

Status of the network

In the last two years, four new Polly lidar systems have been under development, of which two have been completed until the end of 2019. A new permanent lidar station has been established at Dushanbe, Tajikistan, as a consequence of the amazing results during the CADEX campaign [*Hofer et al.*, 2019]. For this lidar station, the new diode-pumped laser and the 13-channel detector unit were implemented. The lidar is hosted in a newly designed container system (see Fig. 9, top) including air condition and an energy backup generator. Thus, the new Tajikistan Polly is one of the most sophisticated lidar systems worldwide able to measure continuously aerosol and cloud profiles in a region of low knowledge on the atmospheric state. The new system was inaugurated in Spring 2019, as shown in Fig. 9.

The next Polly system was completed in cooperation with the University of Tel Aviv. The cabin-housed lidar is now situated in Tel Aviv, Israel, for permanent measurements since autumn 2019 as shown in Fig. 9,

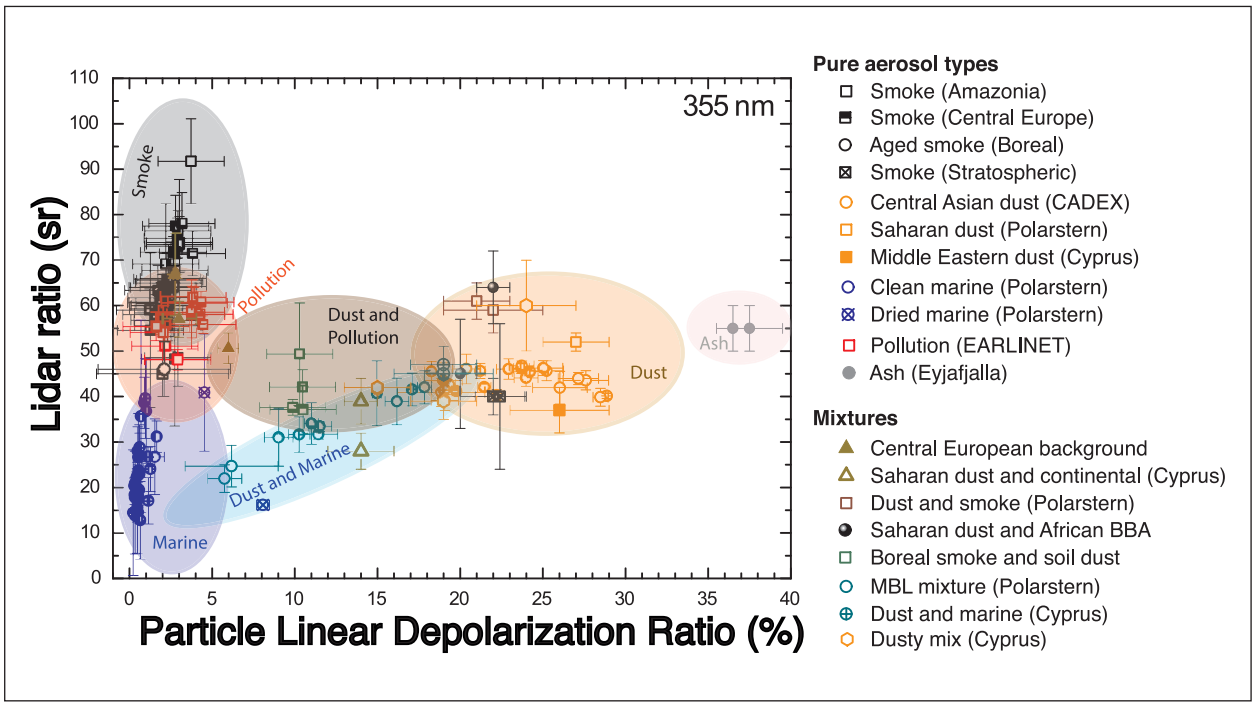

Fig. 8: Particle lidar ratio versus particle linear depolarization ratio at 355 nm for different aerosol types measured with Polly (locations and campaigns indicated in brackets in the legend).

Fig. 9: Impressions from the new PollyNET lidar systems: Top: Tajikistan Polly in Leipzig (left) and in Dushanbe (right). Bottom, left: Inauguration at Dushanbe with representatives from the governments. Bottom, right: Tel Aviv Polly at its final location on the rooftop of a building of Tel Aviv University.

bottom, right. For 2020, the installation of TROPOS-owned systems at Cyprus and on Cape Verde is planned. The Cape Verde Polly will be a specially designed lidar for dust observations including three channels for near-infrared detection to obtain backscatter, depolarization and extinction at 1064 nm [*Haarig et al.*, 2018]. Thus, it will be the first automatic 3+3+3+1+2+2 lidar system in the world, emphasizing the leading role and expertise of TROPOS in ground-based lidar remote sensing.

In summary, Europe as key area of ACTRIS and the dust belt as a hot spot for climate change will be well covered with high-performance Polly lidar systems for long-term, sustainable observations, while other atmospheric key regions are in the focus of dedicated campaign activity. For example, the OCEANET Polly is currently deployed aboard the RV Polarstern during the MOSAiC campaign, gathering a unique data set near the North Pole.

Summary

A powerful global network of automated and continuously measuring Raman-polarization lidar systems has been established with PollyNET. Permanent as well as temporary sites form the network of Polly instruments. Developments in terms of, both, hardware and software are continuously ongoing and make PollyNET a pioneering subnetwork of ACTRIS. The continuous observations at various sites worldwide together with the steady development of new techniques and methods have led to a number of research highlights and publication activities in the reporting period. Furthermore, the automatic processing chain and online presentation has been significantly upgraded to meet the demands of big data from PollyNET and serve the needs of the PollyNET users.

References

Ansmann, A., H. Baars, A. Chudnovsky, I. Mattis, I. Veselovskii, M. Haarig, P. Seifert, R. Engelmann, and U. Wandinger (2018), Extreme levels of Canadian wildfire smoke in the stratosphere over central Europe on 21–22 August 2017, Atmos. Chem. Phys., 18(16), 11831-11845, doi:10.5194/acp-18-11831-2018.

Ansmann, A., R. E. Mamouri, J. Bühl, P. Seifert, R. Engelmann, J. Hofer, A. Nisantzi, J. D. Atkinson, Z. A. Kanji, B. Sierau, M. Vrekoussis, and J. Sciare (2019), Ice-nucleating particle versus ice crystal number concentrationin altocumulus and cirrus layers embedded in Saharan dust:a closure study, Atmos. Chem. Phys., 19(23), 15087-15115, 10.5194/acp-19-15087-2019.

Baars, H., T. Kanitz, R. Engelmann, D. Althausen, B. Heese, M. Komppula, J. Preißler, M. Tesche, A. Ansmann, U. Wandinger, J.-H. Lim, J. Y. Ahn, I. S. Stachlewska, V. Amiridis, E. Marinou, P. Seifert, J. Hofer, A. Skupin, F. Schneider, S. Bohlmann, A. Foth, S. Bley, A. Pfüller, E. Giannakaki, H. Lihavainen, Y. Viisanen, R. K. Hooda, S. N. Pereira, D. Bortoli, F. Wagner, I. Mattis, L. Janicka, K. M. Markowicz, P. Achtert, P. Artaxo, T. Pauliquevis, R. A. F. Souza, V. P. Sharma, P. G. van Zyl, J. P. Beukes, J. Sun, E. G. Rohwer, R. Deng, R.-E. Mamouri, and F. Zamorano (2016), An overview of the first decade of PollyNET: An emerging network of automated Raman-polarization lidars for continuous aerosol profiling, Atmos. Chem. Phys., 16(8), 5111-5137, doi:10.5194/acp-16-5111-2016.

Baars, H., P. Seifert, R. Engelmann, and U. Wandinger (2017), Target categorization of aerosol and clouds by continuous multiwavelength-polarization lidar measurements, Atmos. Meas. Tech., 10(9), 3175-3201, doi:10.5194/amt-10-3175-2017.

Baars, H., A. Ansmann, K. Ohneiser, M. Haarig, R. Engelmann, D. Althausen, I. Hanssen, M. Gausa, A. Pietruczuk, A. Szkop, I. S. Stachlewska, D. Wang, J. Reichardt, A. Skupin, I. Mattis, T. Trickl, H. Vogelmann, F. Navas-Guzmán, A. Haefele, K. Acheson, A. A. Ruth, B. Tatarov, D. Müller, Q. Hu, T. Podvin, P. Goloub, I. Veselovskii, C. Pietras, M. Haeffelin, P. Fréville, M. Sicard, A. Comerón, A. J. Fernández García, F. Molero Menéndez, C. Córdoba-Jabonero, J. L. Guerrero-Rascado, L. Alados-Arboledas, D. Bortoli, M. J. Costa, D. Dionisi, G. L. Liberti, X. Wang, A. Sannino, N. Papagiannopoulos, A. Boselli, L. Mona, G. D'Amico, S. Romano, M. R. Perrone, L. Belegante, D. Nicolae, I. Grigorov, A. Gialitaki, V. Amiridis, O. Soupiona, A. Papayannis, R. E. Mamouri, A. Nisantzi, B. Heese, J. Hofer, Y. Y. Schechner, U. Wandinger, and G. Pappalardo (2019), The unprecedented 2017–2018 stratospheric smoke event: decay phase and aerosol properties observed with the EARLINET, Atmos. Chem. Phys., 19(23), 15183-15198, 10.5194/acp-19-15183-2019.

Bohlmann, S., H. Baars, M. Radenz, R. Engelmann, and A. Macke (2018), Ship-borne aerosol profiling with lidar over the Atlantic Ocean: From pure marine conditions to complex dust-smoke mixtures, Atmos. Chem. Phys., 18(13), 9661-9679, doi:10.5194/acp-18-9661-2018.

Bühl, J., P. Seifert, M. Radenz, H. Baars, and A. Ansmann (2019), Ice crystal number concentration from lidar, cloud radar and radar wind profiler measurements, Atmos. Meas. Tech., 12(12), 6601-6617, 10.5194/amt-12-6601-2019.

Dai, G., D. Althausen, J. Hofer, R. Engelmann, P. Seifert, J. Bühl, R.-E. Mamouri, S. Wu, and A. Ansmann (2018), Calibration of Raman lidar water vapor profiles by means of AERONET photometer observations and GDAS meteorological data, Atmos. Meas. Tech., 11(5), 2735-2748, doi:10.5194/amt-11-2735-2018.

Engelmann, R., T. Kanitz, H. Baars, B. Heese, D. Althausen, A. Skupin, U. Wandinger, M. Komppula, I. S. Stachlewska, V. Amiridis, E. Marinou, I. Mattis, H. Linné, and A. Ansmann (2016), The automated multiwavelength Raman polarization and water-vapor lidar PollyXT: The neXT generation, Atmos. Meas. Tech., 9(4), 1767-1784, doi:10.5194/amt-9-1767-2016.

Haarig, M., A. Ansmann, H. Baars, C. Jimenez, I. Veselovskii, R. Engelmann, and D. Althausen (2018), Depolarization and lidar ratios at 355, 532, and 1064 nm and microphysical properties of aged tropospheric and stratospheric Canadian wildfire smoke Atmos. Chem. Phys., 18(16), 11847-11861, doi:10.5194/acp-18-11847-2018.

Hofer, J., A. Ansmann, D. Althausen, R. Engelmann, H. Baars, S. F. Abdullaev, and A. N. Makhmudov (2019), Long-term profiling of aerosol light-extinction, particle mass, cloud condensation nuclei, and ice-nucleating particle concentration over Dushanbe, Tajikistan, in Central Asia, Atmos. Chem. Phys. Discuss., 2019, 1-33, 10.5194/acp-2019-963.

Jimenez, C., A. Ansmann, R. Engelmann, P. Seifert, R. Wiesen, M. Radenz, and U. Wandinger (2019), Continuos monitoring of liquid water clouds and aerosols with Dual-FOV lidar polarization technique, paper presented at 29th International Laser Radar Conference (ILRC29), Hefei, Anhui, China, 24-28 June 2019.

Mamouri, R., and A. Ansmann (2016), Potential of polarization lidar to provide profiles of CCN- and INP-relevant aerosol parameters, Atmos. Chem. Phys., 16(9), 5905-5931, doi:10.5194/acp-16-5905-2016.

Mamouri, R. E., and A. Ansmann (2017), Potential of polarization/Raman lidar to separate fine dust, coarse dust, maritime, and anthropogenic aerosol profiles, Atmos. Meas. Tech., 10(9), 3403-3427, 10.5194/amt-10-3403-2017.

Cooperation

Finnish Meteorological Institute (FMI), Finland;
National Institute of Environmental Research (NIER), Korea;
Évora University (CGE), Portugal;
University of Warsaw (UW), Poland;
German Meteorological Service (DWD), Germany;
National Observatory of Athens (NOA), Greece;
Tel Aviv University (TAU), Israel;
Academy of Sciences of Republic of Tajikistan;
Alfred Wegener Institute, Germany;
And many other national and international project partners.

Characterization and first results from LACIS-T: A moist-air wind tunnel to study aerosol-cloud-turbulence interactions

Dennis Niedermeier[1], Jens Voigtländer[1], Silvio Schmalfuß[1], Daniel Busch[1], Jörg Schumacher[2], Raymond A. Shaw[3], and Frank Stratmann[1]

[1] Leibniz Institute for Tropospheric Research (TROPOS), Leipzig, Germany
[2] Technische Universität Ilmenau, Ilmenau, Germany
[3] Michigan Technological University, Houghton, MI, USA

Die Wechselwirkungen zwischen Turbulenz und wolkenmikrophysikalischen Prozessen wurden in den letzten zehn Jahren vor allem durch numerische Simulationen und Feldmessungen untersucht. Allerdings können wir nur im Labor die Anfangs- und Randbedingungen definiert einstellen und sind in der Lage, unter statistisch stationären und wiederholbaren Bedingungen Untersuchungen durchzuführen. In diesem Beitrag stellen wir den turbulenten Feuchtluft-Windkanals LACIS-T (Turbulent Leipzig Aerosol Cloud Interaction Simulator) genauer vor, mit dem wir wolkenphysikalische Prozesse im Allgemeinen und Wechselwirkungen zwischen Turbulenz und mikrophysikalischen Prozessen im Besonderen untersuchen. Wir präsentieren Ergebnisse zu den thermodynamischen und Strömungsverhältnissen in LACIS-T, wobei wir neben den Charakterisierungsmessungen auch Ergebnisse von numerischen Simulationen mit einbeziehen. Ferner werden erste Ergebnisse zu den Einflüssen von Turbulenz auf die Tropfenbildung und das Tropfenwachstum vorgestellt. Wir beobachten dabei klare Hinweise auf den Einfluss von Turbulenz auf diese Prozesse.

Introduction

Aerosol particles can serve as cloud condensation nuclei (CCN) as well as ice nucleating particles (INP) in the atmosphere depending on their size and chemical composition. They are therefore crucial for the formation, phase state, and properties of clouds. Already the investigation and quantification of droplet activation and ice nucleation processes in laboratory studies is challenging. But to make matters worse, additional factors lead to an increase of complexity in the atmosphere. For example, aerosols and cloud particles always interact with their environment changing their properties and also affecting dynamics and thermodynamics of the atmosphere. Furthermore, clouds are turbulent, and therefore thermodynamic and compositional variables, such as water vapor or trace gas concentration fluctuate in space and time [*Chang et al.*, 2016]. Indeed, the coupling between turbulence and microphysical processes is recognized as one of the major research challenges in cloud physics [*Bodenschatz et al*., 2010].

We have developed a turbulent moist-air wind tunnel at TROPOS, called LACIS-T [Turbulent Leipzig Aerosol Cloud Interaction Simulator; *Niedermeier et al.*, 2019], in order to study cloud physical processes in general and interactions between turbulence and cloud microphysical processes, such as droplet / ice crystal formation, in particular. The investigations take place under well-defined and reproducible turbulent and thermodynamic conditions covering the temperature range of warm, mixed-phase and cold clouds (25°C > T > -40°C). The continuous-flow design of the facility allows for the investigation of processes occurring on small temporal (up to a few seconds) and spatial scales (micrometer to meter scale) under a Lagrangian perspective. A specific advantage of LACIS-T is the well-defined aerosol particle injection directly into the turbulent mixing zone as well as the precise control of the respective initial / boundary flow

velocity and thermodynamic conditions. The size and number concentration of aerosol and cloud particles can be measured at different defined locations below the aerosol injection.

The experimental studies using LACIS-T on aerosol–cloud–turbulence interactions are accompanied and complemented by Computational Fluid Dynamics (CFD) simulations which help us to design experiments, i.e., obtain suitable experimental parameters, as well as to interpret experimental results. The simulations are performed with OpenFOAM® for modeling flow, heat and mass transfer as well as particle and droplet dynamics. For modelling particle and droplet dynamics we use a Eulerian–Lagrangian approach so that the growth of individual cloud particles can be tracked along their trajectories through the simulation domain [see e.g. *Kumar et al.*, 2018].

In the following, the functionality of LACIS-T will be described. The numerical model and boundary conditions are explained afterwards. Then, we present results concerning the thermodynamic and flow conditions prevailing in LACIS-T, combining both the results from characterization measurements and numerical simulations followed by first results from droplet formation and growth experiments. Finally, we will close with a summary as well as an outlook concerning cloud microphysical processes we will address with LACIS-T in the near future.

Description of LACIS-T

The objective of the wind tunnel design is to generate a locally-homogeneous and isotropic turbulent air-flow into which aerosol particles can be injected, and in which the temperature and water vapor saturation is precisely controlled. Under suitable conditions, aerosol particles act as CCN or INP and cloud droplet formation or heterogeneous ice nucleation and subsequent growth within a turbulent environment is observed. Turbulence is created as air flows past passive grids. The primary novelty of the wind tunnel is the existence of two separate air-flows, which can be independently humidified and tempered and are then combined in the turbulent flow region. A supersaturated environment is created through the generally known process of isobaric mixing [*Bohren and Albrecht*, 1998] of the two air-flows. The exact humidity within the turbulent region depends on the temperatures and humidities within the two flows, as well as the location within the turbulent mixing layer between the two air-flows.

LACIS-T is a closed-loop wind tunnel. A schematic of the construction is shown in Fig. 1. The main components are radial blowers, particle filters, valves, flow meters, the humidification system, heat exchangers, turbulence grids, the measurement section and the adsorption dehumidifying system. The two radial blowers separately drive the two dry air-flows (flow branches 'A' and 'B'). Flow rates of up to 6.000 l/min in each flow branch are possible (mean velocity up to 2 m/s in the measurement section). Afterwards, each flow passes a particle filter (Filter class U16) to remove aerosol particles. Subsequently, a defined amount of water vapor can be added to each of the particle-free air-flows by means of a humidification system. The dew-point temperature can be adjusted between –40°C and 25°C.

The two air-flows are then redirected and passed through diffusers, changing the cross section from circular to rectangular. This is needed for the entrance

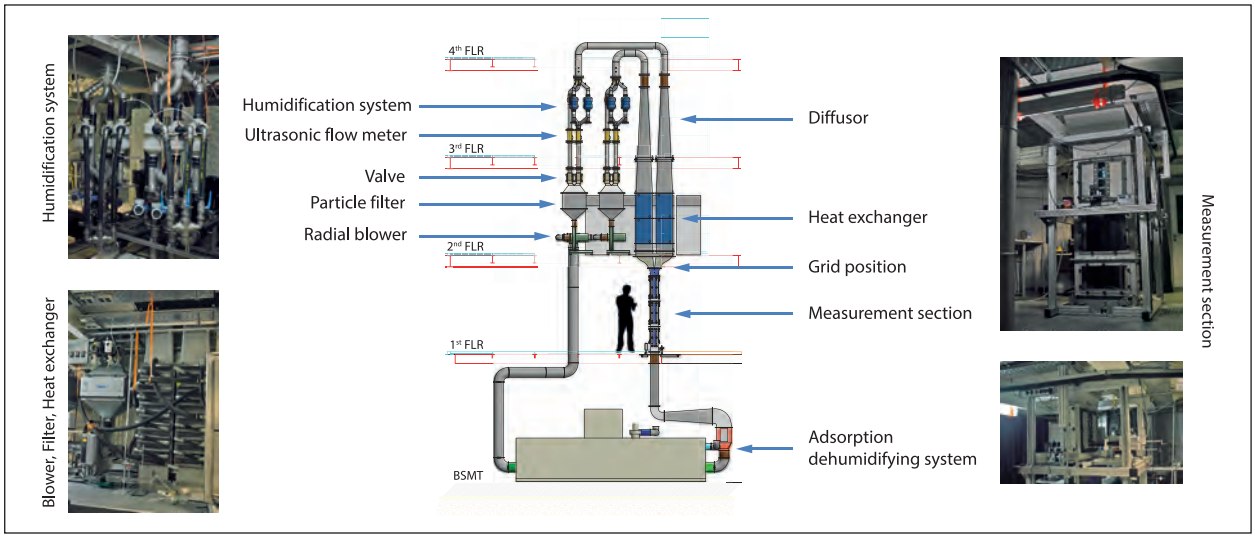

Fig. 1: A schematic of LACIS-T including photos of individual components (© by Ingenieurbüro Mathias Lippold, VDI; TROPOS).

into the heat exchangers. Each heat exchanger contains a coolant, the temperature of which can be adjusted to a defined temperature between –40°C and 25°C using thermostats. Downstream of the heat exchangers, both particle-free air-flows are precisely conditioned in terms of volume flow rate, water vapor content and temperature. Before entering the measurement section, the air-flows pass passive square-mesh grids (mesh length of 1.9 cm, rod diameter of 0.4 cm and a blockage of 30%) which are situated 20 cm above the measurement section. This configuration has been chosen to create turbulence that is approximately isotropic in the center-region of the measurement section and is homogeneous in transverse planes.

At the inlet of the measurement section, the two conditioned particle-free air-flows are merged and turbulently mixed. A wedge-shaped "cutting edge" separates both air-flows right above the inlet of the measurement section. Three rectangular feed-throughs, which represent the aerosol inlet (20 mm x 1 mm each, 1 mm separation between feed-throughs) are located in the center of this cutting edge. Here, the aerosol flow is introduced into the mixing zone of the two particle-free air-flows. Size-selected, quasi monodisperse aerosol particles of known chemical composition can be injected. The measurement section itself is a rectangular prism being Δx = 80 cm wide, Δy = 20 cm deep, and Δz = 200 cm long. It features various instruments for characterizing the prevailing thermodynamic, turbulence, and microphysical properties. This includes measurements of temperature, mean water vapor concentration, flow velocity, turbulence intensity, and dissipation rate as well as cloud particle size distributions at various locations.

After passing through the measurement section, the entire flow is dried and heated by means of the adsorption dehumidifying system. Then the flow splits up again into two branches and the whole cycle starts again.

Numerical simulations

As mentioned above, the experimental investigations are accompanied and complemented by CFD simulations performed in OpenFOAM®. In order to reduce computational effort, the computational domain comprises only a part of the wind tunnel upstream the aerosol injection, including the turbulence grid. It covers the upper 80 cm of the measurement section, and it is 11.5 cm wide and 20 cm deep (Fig. 2). This is the region of interest for the measurements carried out so far. The domain is decomposed into a grid with approximately 7.6 × 10^6 cells, with a

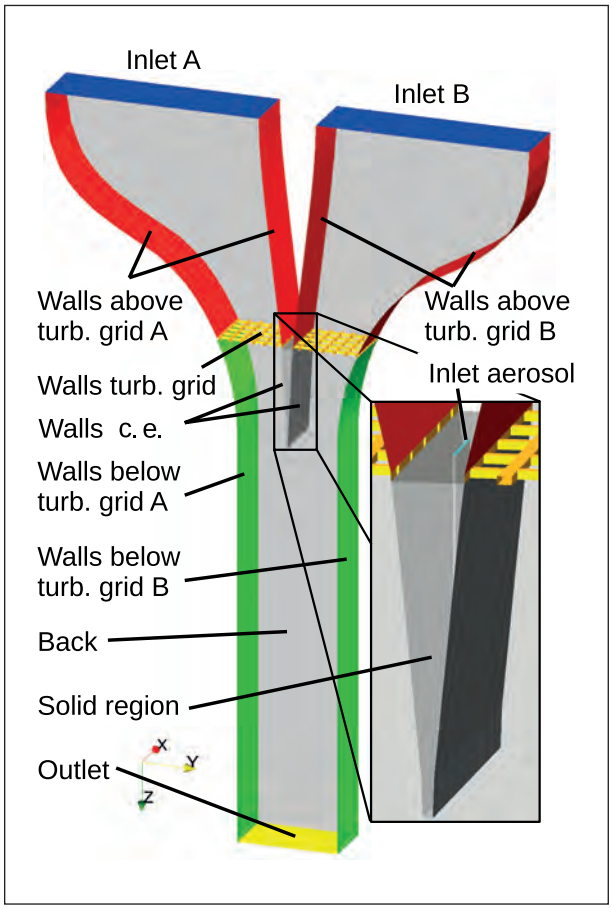

Fig. 2: Boundaries of the computational domain with detailed view of the aerosol inlet region between the two air flow branches (c.e. stands for cutting edge).

total of three inlets (two branches and aerosol), one outlet at the lower end, and cyclic boundary conditions at the front and back. All other boundaries are set as walls (see Fig. 2). Temperatures, velocities, and water vapor concentrations at the three inlets are set according to results from measurements. The flow is simulated with a solver based on OpenFOAM's chtMultiRegionFoam, which was extended to account for the transport of water vapor as a passive scalar, and a Large Eddy Simulation model (dynamic k-equation) is used for turbulence modeling.

After a spin-up of 1 s, a quasi-steady state is reached for the flow fields and particles are injected and tracked following a Lagrangian approach until they leave the domain. For this study, drag, shear lift, and gravitational forces are considered. The initial particle size distribution is derived from measurements. A growth model was implemented to calculate the mass change of the particles due to water vapor deposition from the gas phase, including both, the Raoult and the Kelvin term, as for example described by *Wilck* [1998].

Characterization of the flow and thermodynamic properties

The characterization efforts include high-resolution measurements of velocity and temperature (on the decimeter to millimeter (Kolmogorov) scale) as well as measurements of the mean relative humidity. The results will be compared to those of the Large Eddy Simulations. Overall, the characterization efforts have been performed to ensure the functionality and to investigate the performance of the wind tunnel. Note that the further down presented droplet formation and growth experiments are performed in the first meter of the measurement section for warm cloud conditions. Consequently, the presented characterization efforts will focus on $T > 0$°C conditions with $z_0 = 0$ cm corresponding to the position of the aerosol inlet which is 20 cm downstream the turbulence grid.

Flow properties in the measurement section

The flow field and the turbulent flow properties have been investigated for isothermal ($T_A = T_B$) and non-isothermal ($T_A \neq T_B$) conditions with different dew point temperature settings inside the measurement section. Here, results will be presented in detail for a dry, isothermal case, i.e. both air-flows featured the same temperature $T = 20$°C and dew-point temperature $T_d = -15$°C. Note that for the flow field and the turbulent flow properties we do not observe a significant difference between dry and moist conditions as well as for isothermal and non-isothermal conditions. Measurements were performed at various distances underneath the aerosol inlet along $\Delta y = 20$ cm at different locations by means of the hot-wire anemometer measuring the vertical velocity component at 6000 Hz for 5 minutes at each location.

Figs. 3a, b, and c show the values for the mean (vertical) velocity $\langle w \rangle$, the root-mean-square (rms) average $\sigma_w = \langle w'^2 \rangle^{1/2}$ with ($w' = w - \langle w \rangle$) and the energy dissipation rate ε for five different distances to the aerosol inlet averaged along $\Delta y = 20$ cm where the dissipation rate is homogeneous. Looking at the values determined through the measurements, it can be seen that the mean velocity remains almost constant (slight decrease with increasing distance to the aerosol inlet), while the fluctuations and thus also the energy dissipation rate decrease with increasing distance from the turbulence grid. This observed decrease of the turbulent kinetic energy, which is also presented in terms of σ_w^2 in Fig. 3b, follows a power law function $\sigma_w^2 \sim (z\text{-}z_{grid})^n$ where z_{grid} represents the grid position. The exponent n is -1.4 and is comparable with results reported in other wind tunnel investigations and depends on the initial conditions [*Lavoie* et al., 2007 and references therein]. Additionally, the simulated values for $\langle w \rangle$, σ_w and ε are given. We observe a slight decrease of $\langle w \rangle$ until $z = 0.2$ m which is similar to experimental observations. However, it is followed by a slight increase which is in contrast to the measurements. The simulations show an increase of the mean velocity close to the side walls caused by the constriction of the cross-section leading to an acceleration of the velocity field which is strongest at the side walls. These higher velocities spread slowly and also reach the inner region leading to this slight increase in the simulated $\langle w \rangle$.

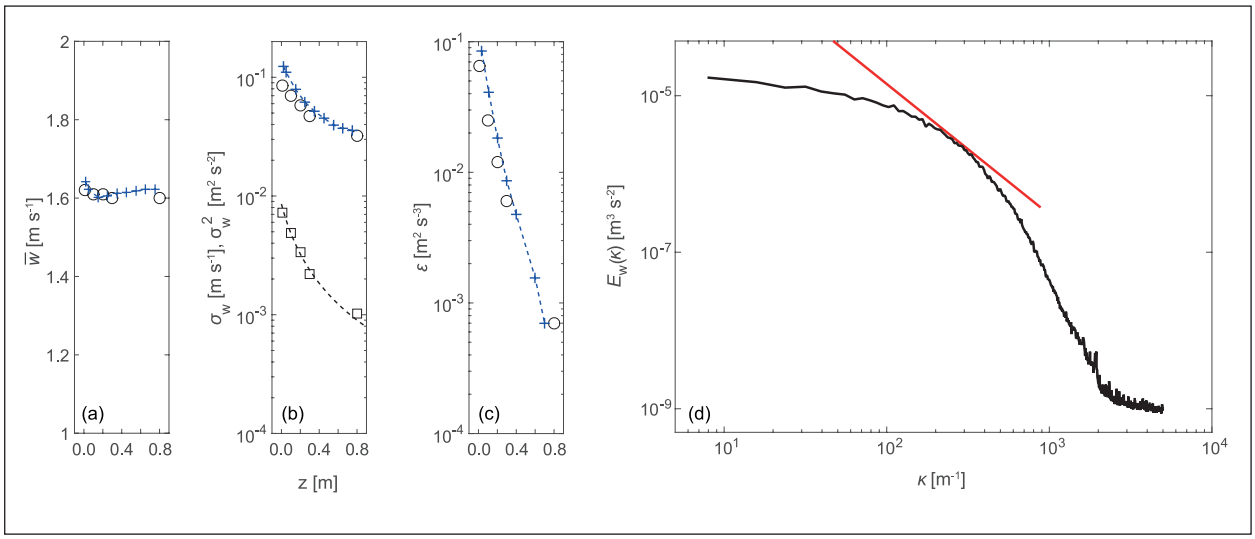

Fig. 3: The averaged values for mean velocity, rms velocity and dissipation rate are shown in (a), (b) and (c) given by the black circles. (b) further shows the drop in turbulent kinetic energy in terms of the squared rms velocity (black squares) which follows a power law function with an exponent of -1.4 (dotted black line). Additionally, the respective results from the simulations are shown (blue plus signs) being also averaged. The experimentally determined turbulent spectrum for the velocity fluctuations is shown in (d). A red line with -5/3 slope is shown as a reference.

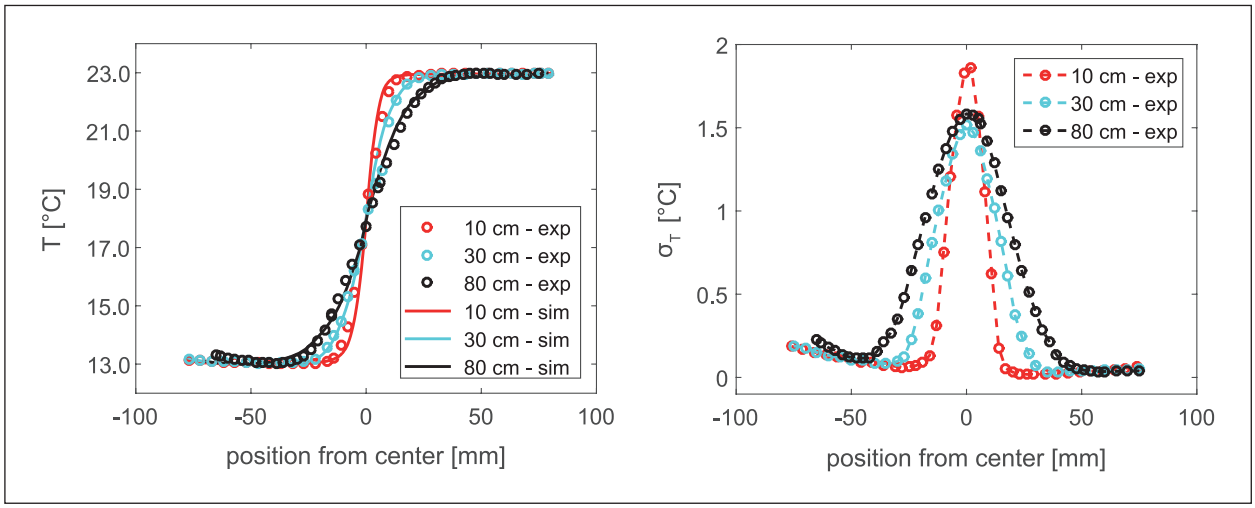

Fig. 4: Left: Comparison of experimental temperature profiles (circles) with predictions from the simulations (lines) for z = 10 cm (in red), z = 30 cm (in cyan) and z = 80 cm (in black). Right: Experimental results for temperature fluctuations for z = 10 cm (in red), z = 30 cm (in cyan) and z = 80 cm (in black).

The increase of the mean velocity close to the side walls is not visible in the measurements probably due to objects related to the turbulence grid's clamping system, which are not considered in the simulations, and which strongly reduce the acceleration at the walls. The decrease of σ_w and ε is well reproduced by the simulations.

The turbulent spectrum for the velocity fluctuations is shown as an example in Fig. 3d. A red line with -5/3 slope, which is expected for the inertial subrange of the turbulent energy cascade, is shown as a reference. This shows that the inertial subrange extends over less than an order of magnitude, which is to be expected due to the mesh length of the turbulence grid. However, this is not a limitation as turbulence on the small scales is already developed [*Schumacher et al.*, 2007] and our focus will be on small-scale interactions of cloud particles and turbulence.

Thermodynamic properties in the measurement section We performed several characterization experiments to study the turbulent transport of heat and mass in the measurement section. All related studies were performed without the insertion of aerosol particles. The measurements are again accompanied by LES where the inlet conditions corresponded to those of the respective experiments.

In the first step, the turbulent transport of heat was investigated. To do so, a temperature difference of ΔT = 10K was set between the two flow branches (T_A = 23°C and T_B = 13°C) and $T_{d,A} = T_{d,B}$ = -15°C in both air-flows (i.e., ΔT_d = 0 K). Figure 4 shows the time-averaged temperature profiles at three different locations underneath the aerosol inlet. As expected, the turbulent mixing zone widens with increasing distance from the aerosol inlet. There is a slight increase in temperature starting at about -70mm out of the center caused by heat transfer from the wall as it is in contact with ambient air on the outside which is at a temperature of 24°C. The wall on the opposite site consequently does not significantly influence the temperature measurements because here the temperature difference between wall and flow is only ΔT = 1 K. However, this wall effect, which will be eliminated in the near future by suitable heat isolation of the measurement section, has a negligible effect on the mixing zone. In addition, the results of the simulations for the mean temperature are included in Fig. 4. The simulations reproduce the measurements in an accurate manner, albeit slightly underestimating the width of the turbulent mixing zone. The rms temperatures also show the increase of the width of the mixing zone with increasing z. Again, thermal wall effects lead to an increase of the rms temperature towards the wall, however, having a negligible effect on the mixing zone.

These kind of investigations have been also performed for moist conditions with $T_{d,A} = T_{d,B}$ = 12°C and ΔT_d = 0 K as well as with $T_{d,A}$ = 12°C (water vapor mixing ratio $q_{v,A}$ = 8.68 g/kg) and $T_{d,B}$ = 8°C ($q_{v,B}$ = 6.64 g/kg) leading to ΔT_d = 4 K. In both cases, the same temperature difference of ΔT = 10 K has been set between the two flow branches (i.e., T_A = 23°C and T_B = 13°C). On the left-hand side of Fig. 5, we compare the temperature profile for the different conditions, i.e., dry with ΔT_d = 0 K; moist with ΔT_d = 0 K; and moist with ΔT_d = 4 K, exemplarily for z = 30 cm. As expected, the temperature profiles shown in the left of Fig. 5 exhibit a very similar behavior, i.e., the influence of the increased amount

of water vapor in the air-flow as well as the water vapor profile itself on the temperature curve is very low. The reasons are that still less than 1% of the total mass is water vapor which does not significantly influence the fluid properties (e.g., heat capacity). Further, there is no condensation of water vapor which could influence the temperature profile due to latent heat release.

On the right-hand side of Fig. 5 the temperature and water vapor mixing are shown for the moist case (ΔT_d = 4 K). In order to compare both quantities, the normalized water vapor mixing ratio ξ_n and the normalized temperature θ_n are depicted. The normalized water vapor mixing ratio is defined as $\xi_n = (q_v - q_{v,1})/(q_{v,2} - q_{v,1})$, where $q_{v,1}$ and $q_{v,2}$ are the lowest and highest water vapor mixing ratio set in the respective flow branch, respectively. The normalized temperature is given through $\theta_n = (T - T_1)/(T_2 - T_1)$ with T_1 being the lowest and T_2 being the highest temperature set in the respective flow branch. Both curves fall together, i.e., ξ_n and θ_n behave similarly as we would expect since turbulent transport processes dominate over laminar diffusion processes in the mixing zone.

In summary, the above described investigations and results clearly demonstrate the functionality of LACIS-T. The current setup creates sufficiently large regions of locally-homogeneous and isotropic turbulence in the measurement section. Determined dissipation rates are similar to those in atmospheric clouds. The decrease of the turbulent kinetic energy with increasing distance from the turbulence grid is comparable with other wind tunnels. Further, the turbulent mixing behavior of heat in dry air and moist air, as well as the turbulent mixing behavior of water vapor indicate that the transport of heat and mass in the mixing zone is governed by turbulent processes. Altogether, we observe a well-defined and controllable turbulent mixing process that can be simulated accurately.

Results on droplet activation and growth

The first experiments conducted at LACIS-T deal with the formation of droplets on size-selected, monodisperse aerosol particles under turbulent conditions and the subsequent growth. NaCl particles with a dry diameter $D_{p,dry}$ of 100 nm, 200 nm, 300 nm, and 400 nm were used for the experiments. A temperature difference of ΔT = 16 K was set between the two particle-free air-flows. The temperature and dew-point temperature of the air-flows were set to 20°C in branch A and 4°C in branch B, respectively, so that RH = 100% in each air-flow. Due to the mixing of both saturated air-flows in the measurement section, supersaturation conditions are reached. Based on the simulations (not shown), the mean RH was at approximately 101.5%.

For each injected $D_{p,dry}$, the particle concentration was set to 1000 cm^{-3}. A welas 2300 sensor (PALAS GmbH) was positioned at center position inside the measurement section at z = 40 cm or z = 80 cm, in order to determine the prevailing droplet size distributions.

The determined size distributions at the two positions are shown in Fig. 6. In both figures, the normalized droplet number vs. the particle diameter is displayed. The following observations can be made: a) For each $D_{p,dry}$ the formed droplets grow with increasing distance to the aerosol inlet; b) all

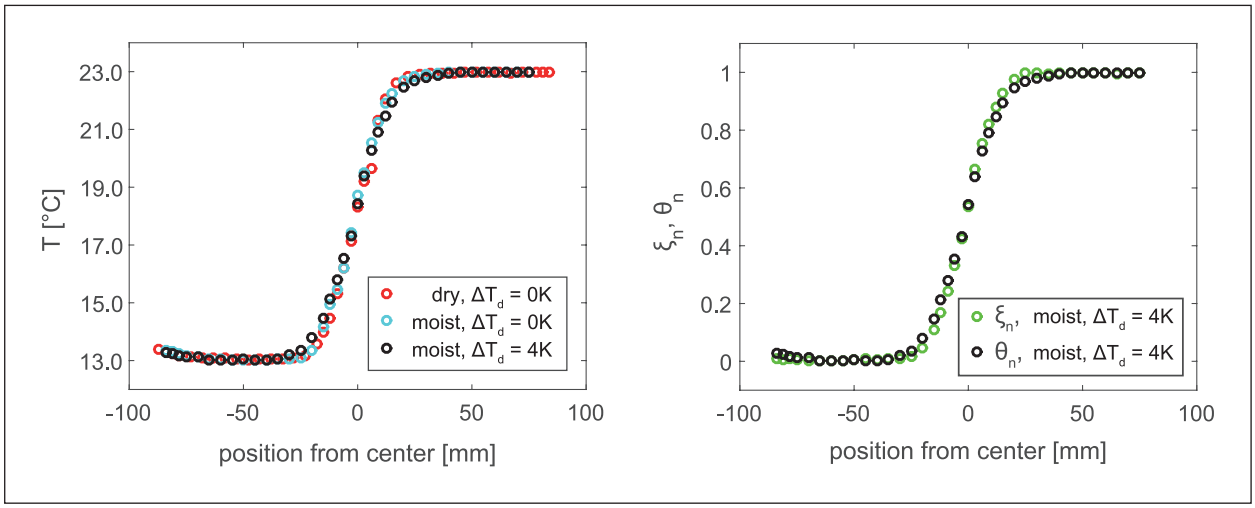

Fig. 5: Left: Mean temperature profiles for three different cases at z = 30 cm. Right: Normalized mean temperature and mean mass fraction at z = 30 cm for ΔT = 10 K and ΔT_d = 4 K.

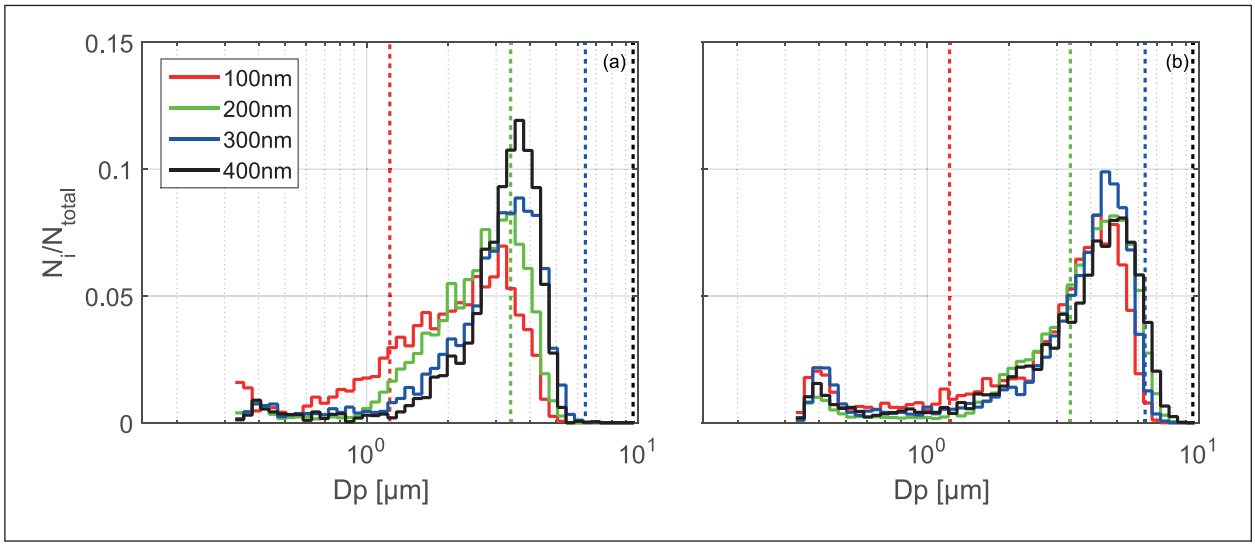

Fig. 6: Droplet formation and growth of differently size-selected, monodisperse NaCl particles ($D_{p,dry}$ = 100 nm – 400 nm) for ΔT = 16K measured at two different positions below the aerosol inlet (left figure: z = 40 cm, right figure: z = 80 cm). The dotted lines represent the critical diameters $D_{p,crit}$ for particle activation which are 1.2 µm, 3.4 µm, 6.3 µm, and 9.7 µm for $D_{p,dry}$ = 100 nm, 200 nm, 300 nm, 400 nm, respectively.

the size distributions nearly fall together at z = 80 cm (see Fig. 6b); c) the size distributions are negatively skewed and d) we also observe a significant number of particles close to D_p = 300 nm, which is approximately the welas 2300 detection limit.

To start with the interpretation of these observations, we included the critical diameters $D_{p,crit}$ for particle activation which are 1.2 µm, 3.4 µm, 6.3 µm, and 9.7 µm (dotted lines in Fig. 6) for $D_{p,dry}$ = 100 nm, 200 nm, 300 nm, 400 nm, respectively. For all dry particle sizes investigated, the supersaturation reached inside the measurement section is high enough to activate these particles to cloud droplets. However, only the grown droplets which originate from the $D_{p,dry}$ = 100 nm and $D_{p,dry}$ = 200 nm particles are almost all or mostly activated at z = 80 cm while the ones formed on the $D_{p,dry}$ = 300 nm and $D_{p,dry}$ = 400 nm particles are mostly not. The reason for this observation is the kinetic limitation of droplet growth. The time the particles are exposed to a certain level of supersaturation must be long enough to reach the respective critical diameter [*Chuang et al.*, 1997; *Nenes et al.*, 2001]. For the $D_{p,dry}$ = 300 nm and $D_{p,dry}$ = 400 nm particles and the prevailing supersaturation, it is on the order of several seconds. However, the time to reach z = 80 cm is about 0.5 s which is too short for these particles to reach their respective $D_{p,crit}$. Naturally, kinetic effects also limit the growth of the activated droplets which formed on the $D_{p,dry}$ = 100 nm and $D_{p,dry}$ = 200 nm particles as for the diffusional growth it is irrelevant whether the droplets are activated or not. In conclusion, under the prevailing conditions and the sole observation of the grown droplet distributions, it is not possible to distinguish between the activated and non-activated droplet distributions or to determine which distribution represents the activated and which the not-activated state. Droplet growth is kinetically limited regardless if the droplets are in the hygroscopic or dynamic growth regime. Further, the dry particle size has only minor influences on the observed droplet distributions, especially with increasing residence time.

In order to interpret the negative skewness of the distributions as well as the presence of a significant number of particles close to $D_{p,dry}$ = 300 nm, we consider the LES results which are shown in Fig. 7. In the left figure, a snapshot of the instantaneous saturation field in the symmetry plane as well as the respective particle diameters grown on $D_{p,dry}$ = 100 nm NaCl particles along the vertical axis are shown. For z = 40 cm and z = 80 cm, droplet size distributions are extracted from the simulations and displayed together with the measured size distributions in the right plots of Fig. 7. From the simulations, the magnitude of the RH fluctuations in terms of a standard deviation can be determined to be σ_{RH} = ~4%.

First of all, the simulations reproduce the measurements in an accurate manner. At z = 40 cm, the simulated droplet distribution is of bimodal shape where the left shoulder of the first mode was not detected by the welas 2300 due to its detection limit. Further the negative skewness can be observed in both sub-figures. From the simulation of individual particle tracks (not shown) it can be concluded that the small particles ($D_p < D_{p,crit}$) are hygroscopically grown particles that did not experience supersaturated conditions but also droplets that deactivated because they experienced sub-saturated conditions

in the fluctuating saturation field. In general, these turbulent fluctuations in RH broaden the droplet size distribution towards smaller diameters due to evaporating droplets or less-grown droplets in left tail of the droplet size distribution. In other words, the negative skewness of the obtained droplet size distributions is indicative for turbulence-influenced droplet formation and growth / evaporation. The dry particle size plays a minor role here.

Summary and outlook

Laboratory experiments, in which the turbulence and thermodynamic conditions are reliably reproducible, and long-term averaging of measurements under statistically stationary conditions can be achieved, are invaluable for increasing our quantitative understanding concerning atmospheric cloud processes. Therefore, we have developed the turbulent moist-air wind tunnel LACIS-T, specifically aiming at a better understanding of aerosol-cloud-turbulence interactions.

The investigations described here show that LACIS-T is suitable for studying the influence of turbulent temperature and water vapor fluctuations on cloud microphysical processes. We obtained indications of the influence of turbulent supersaturation fluctuations on the droplet formation. Concerning the latter, our results also suggest that kinetical effects and/or limitations may be important in inhibiting droplet formation in a turbulent environment. Our results also indicate our ability to capture the

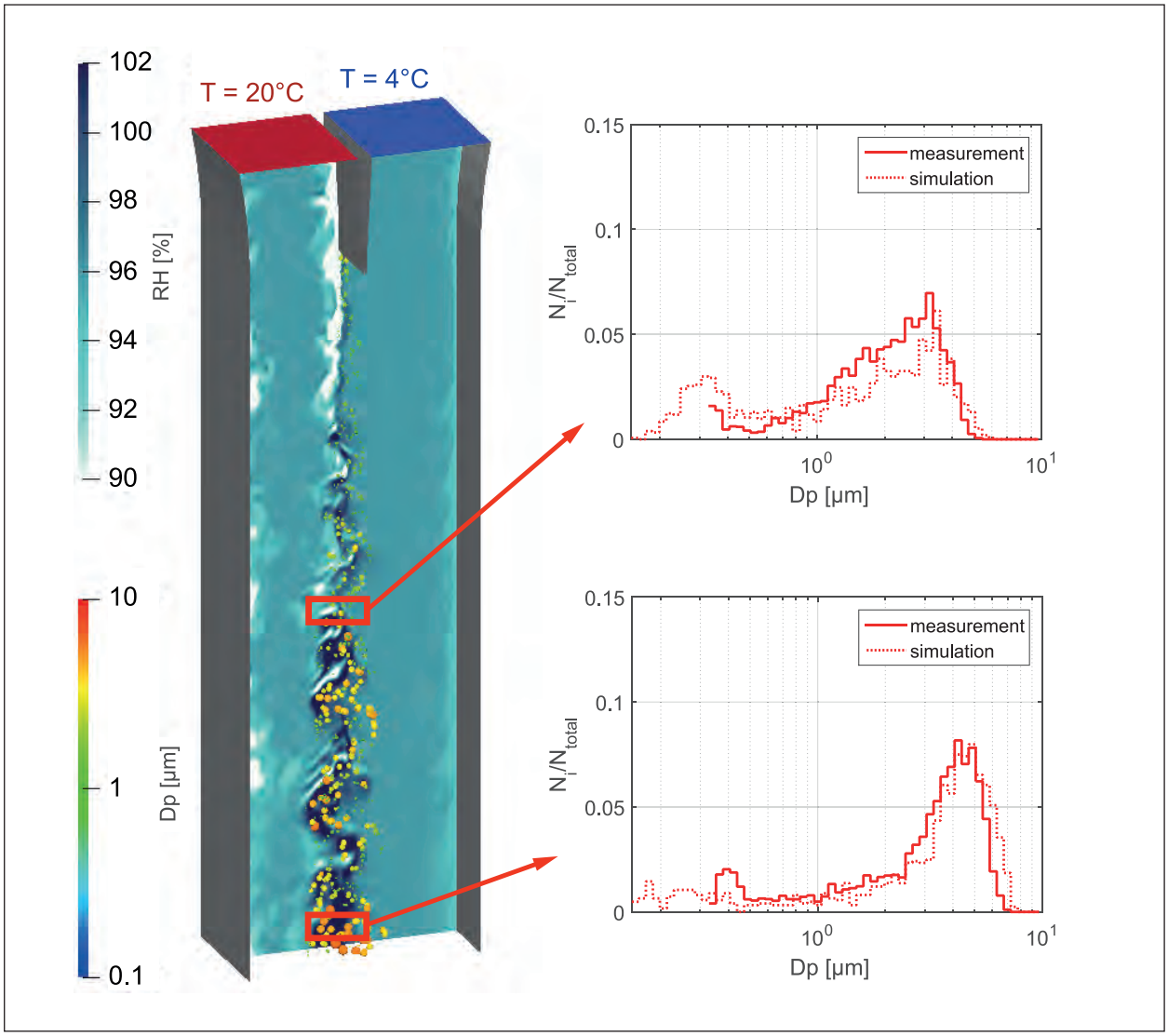

Fig. 7: Snapshot of particle simulation with fluctuating relative humidity field in the background and particles colored and sized (not to scale) according to their diameter. Right: Droplet formation and growth of monodisperse NaCl particles ($D_{p,dry}$ = 100 nm) for ΔT = 16K measured at two different positions below the aerosol inlet (upper right figure: z = 40 cm, lower right figure: z = 80 cm) for measurements (solid line) and simulations (dashed line).

investigated processes with LES. The presented results will be verified and quantified in more detail in the near future. Specifically, we will focus on the relative roles of turbulence vs. aerosol particle physical and chemical properties (particle size, number and composition) in droplet formation.

We further aim at gaining fundamental and quantitative understanding of the influences of entrainment and detrainment processes on the microphysical properties of clouds as well as the influence of turbulence on heterogeneous ice nucleation in the near future. In summary, results from LACIS-T investigations will have, among others, the potential to help interpreting and corroborating the results from related in-situ measurements in clouds [e.g., *Ditas et al.*, 2012], and therefore enhance our understanding of the interactions between cloud microphysics and turbulence, and consequently cloud processes in general.

References

Bodenschatz, E., S. P. Malinowski, R. A. Shaw, and F. Stratmann (2010), Can we understand clouds without turbulence?, *Science*, 327, 970-971, doi:10.1126/science.1185138.

Bohren, C. F. and B. A. Albrecht (1998), *Atmospheric thermodynamics*, Oxford University Press, New York.

Chang, K., J. Bench, M. Brege, W. Cantrell, K. Chandrakar, D. Ciochetto, C. Mazzoleni, L. Mazzoleni, D. Niedermeier, and R. A. Shaw (2016), A laboratory facility to study gas-aerosol-cloud interactions in a turbulent environment: The Π chamber, *Bull. Amer. Meteor. Soc.*, 97, 2343-2358, https://doi.org/10.1175/BAMS-D-15-00203.1.

Chuang, P., R. J. Charlson, and J. Seinfeld (1997), Kinetic limitations on droplet formation in clouds, *Nature*, 390, 594-596, doi:10.1038/37576.

Ditas, F., R. A. Shaw, H. Siebert, M. Simmel, B. Wehner, and A. Wiedensohler (2012), Aerosols-cloud microphysics-thermodynamics-turbulence: evaluating supersaturation in a marine stratocumulus cloud, *Atmos. Chem. Phys.*, 12, 2459–2468, https://doi.org/10.5194/acp-12-2459-2012.

Kumar, B., P. Götzfried, N. Suresh, J. Schumacher, and R. A. Shaw (2018), Scale Dependence of Cloud Microphysical Response to Turbulent Entrainment and Mixing, *J. Adv. Model Earth Sy.*, 10, 2777-2785, https://doi.org/10.1029/2018MS001487.

Lavoie, P., L. Djenidi, and R. Antonia (2007), Effects of initial conditions in decaying turbulence generated by passive grids, *J. Fluid Mech.*, 585, 395-420, https://doi.org/10.1017/S0022112007006763.

Nenes, A., S. Ghan, H. Abdul-Razzak, P. Y. Chuang, and J. H. Seinfeld (2001), Kinetic limitations on cloud droplet formation and impact on cloud albedo, *Tellus B*, 53, 133-149, https://doi.org/10.3402/tellusb.v53i2.16569.

Niedermeier, D., J. Voigtländer, S. Schmalfuß, D. Busch, J. Schumacher, R. A. Shaw, and F. Stratmann (2019), Characterization and first results from LACIS-T: A moist-air wind tunnel to study aerosol-cloud-turbulence interactions, *Atmos. Meas. Tech. Discuss.*, https://doi.org/10.5194/amt-2019-343, in review.

Schumacher, J., K. R. Sreenivasan, and V. Yakhot (2007), Asymptotic exponents from low-Reynolds-number flows, *New J. Phys.*, 9, 89, https://doi:10.1088/1367–2630/9/4/089.

Wilck, M (1999), *Modal Modelling of Multicomponent Aerosols*, VWF Verlag für Forschung GmbH, Berlin.

Funding

Leibniz-SAW-Project “Leipzig Aerosol Cloud Turbulence Tunnel (LACTT)”; number: SAW-2013-IfT-2
EUROCHAMP-2020 Infrastructure Activity (grant agreement No 730997).;
Alexander von Humboldt Foundation, Bonn, Germany.

Cooperation

Technische Universität Ilmenau, Ilmenau, Germany;
Michigan Technological University, Houghton, MI, USA.

Photosensitizers and their photochemical properties in the aqueous phase

Thomas Schaefer[1], Tamara Felber[1], Peter Alpert[2], Markus Ammann[2], Jonathan Raff[3], Hartmut Herrmann[1]

[1] Leibniz Institute for Tropospheric Research (TROPOS), Leipzig, Germany
[2] Paul Scherrer Institute, Villigen, Switzerland
[3] Indiana University, Bloomington, United States of America

Oxidative Transformationsprozesse von organischen Verbindungen sind von großer Bedeutung für die Selbstreinigung der Troposphäre. Während die Prozesse in der Gasphase gut verstanden sind, führt die Oxidation in der wässrigen Phase (Aerosolpartikel, Wolken, Dunst, Nebel und Regen) auch zur Bildung bzw. zur Prozessierung von sekundären organischen Aerosol (SOA), wobei dieser Teilaspekt weniger gut verstanden ist. Traditionelle Modelle der Beschreibung der SOA-Bildung konzentrieren sich auf die Aufnahme von nicht- bzw. weniger-flüchtigen organischen Verbindungen auf bereits existierende Aerosole. Allerdings können diese Modelle die beobachteten Eigenschaften und Konzentrationen der Aerosole nicht erklären. Neuere Erkenntnisse deuten jedoch darauf hin, dass die Aerosolalterung durch photochemische Prozesse innerhalb des Partikels ausgelöst werden. Initiiert werden diese Prozesse, durch sogenannte Photosensibilisatoren. Diese Verbindungen werden durch Licht angeregt und dadurch selbst zu reaktiven Molekülen, welche im weiteren Reaktionsverlauf oxidierend wirken können. Des Weiteren können diese photochemischen Prozesse auch zur Bildung von reaktiven Sauerstoffspezies (ROS) führen. Durch diese reaktiven Spezies kann die Aufnahme von flüchtigen Verbindungen auf existierende Aerosole und damit das Partikelwachstum gefördert werden.
In der vorliegenden Studie wurden die Eigenschaften der angeregten Photosensibilisatoren wie deren Absorptionsspektren, die Quantenausbeuten, H_2O- sowie O_2- Quenchgeschwindigkeitskonstanten und deren Lebensdauer, sowie deren Reaktivität gegenüber OH Radikalen in der wässrigen Phase untersucht.

Introduction

The description of the behavior of the atmosphere by models requires a detailed knowledge of atmospheric processes in both the gas phase and the aqueous phase (aerosol particles, clouds, fog, and rain). While the gas phase is well studied, the understanding of the aqueous- / particle-phase chemistry is still lacking. Especially the secondary organic aerosol (SOA) formation in the atmospheric aqueous- / particle phase (aqSOA) is a less understood pathway but might be significant to resolve the discrepancies between observed and modeled SOA concentrations and particulate matter (PM) properties [*Ervens et al.*, 2011]. Although, several laboratory [*McNeill*, 2015] and field studies [*Gilardoni et al.*, 2016] discover the importance of aqSOA and their data are continuously implemented into models, the discrepancies still remain. Recently, laboratory studies have shown that light-absorbing compounds can photo-induce reactions with volatile organic compounds (VOC) leading to SOA formation [*Monge et al.*, 2012]. Brown carbon (BrC) is an important chromophoric compound class with the ability to form excited triplet states and induces a new chemical pathway, the photosensitization. This compound class is defined as organic carbon which absorbs light in the near UV (λ = 300 – 400 nm) and visible spectrum

(λ > 400 nm) of the solar radiation. [*Laskin et al.*, 2015] BrC has numerous/various sources like primary emission from anthropogenic sources [*Zhang et al.*, 2011], biomass burning [*Teich et al.*, 2016] as well as secondary formation during atmospheric multiphase processes. [*Nozière et al.*, 2007] Several laboratory studies have shown that photosensitized reactions are leading to SOA formation in the absence of other oxidants [*Smith et al.*, 2015] and are a source for reactive oxygen species (ROS) such as singlet oxygen $^1O_2$ or hydroperoxyl radicals (HO_2·). [*Corral Arroyo et al.*, 2018] These ROS generated by the photochemistry within the aerosol particle might enhance reactive uptake of volatile organic compounds and promotes particle growth. During the DFG-ANR project "PHOTOSOA" a series of experiments of different photosensitizers have been conducted to describe the properties of the excited photosensitizers such as the molar attenuation coefficient, the quantum yield, H_2O - as well as O_2 - quenching rate constants and the lifetime. Besides the laboratory studies on the properties of the photosensitizers, the aerosol twin chamber ACD-C and the scanning transmission X-ray microscope (STXM) at POLLUX at the Paul Scherrer Institute (PSI) were used to examine SOA formation induced by the photochemistry in order to elaborate the importance of these photochemical processes in the tropospheric aqueous- / particle-phase.

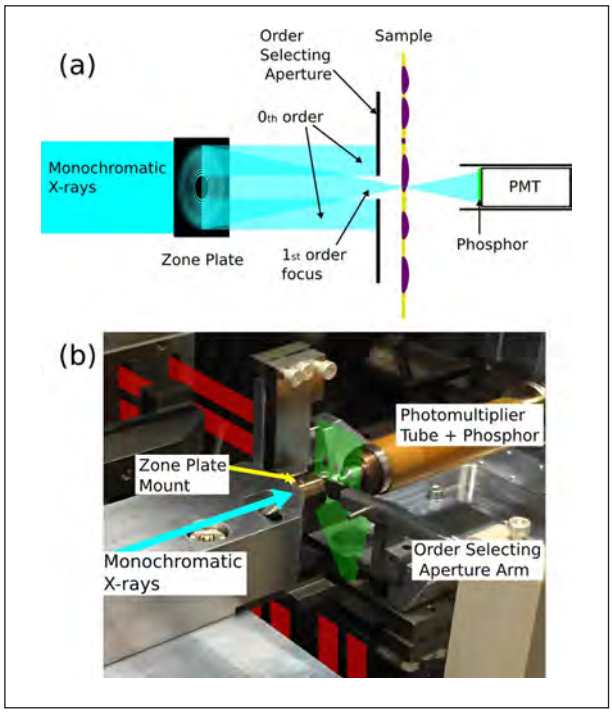

Fig. 1: a) Scheme of the STXM technique. b) Picture of the major components at the PolLux facility. Indicated in green the position and the shape of the sample holder [PSI website].

Methods

The experimental studies of the photosensitizers and their properties were performed by the laser photolysis - long path absorption (LP-LPA) setup. Briefly, the setup includes a cuboid reaction flow cell (3.5 cm long, 4 cm wide, 2 cm high), an excimer laser as photolysis light source at λ = 308 nm/ 351 nm, a light source, a White cell mirror configuration in order to increase the absorption path length, and a detector. In case of the spectroscopic broadband studies a halogen or a xenon arc lamp was used in combination with an intensified charge-coupled device (ICCD) camera. To conduct the single line experiments a continuous-wave laser at λ = 405 nm or λ = 594 nm and a photodiode as detector were applied. The concentration of O_2 in the aqueous solution was measured behind the flow cell using a Clark electrode.

The hydroxyl (OH) radical reactions were measured with the LP-LPA setup using hydrogen peroxide (H_2O_2) as OH radical precursor and thiocyanate (SCN^-) as radical scavenger. Besides the studies on the properties of the photosensitizers, the aerosol chamber ACD-C was used to examine SOA formation induced by the photochemistry. The aerosol chamber consists a 19 m^3 Teflon chamber equipped with UV-visible lights (300 < λ < 400 nm). The aerosols formed in the ACD-C chamber were also collected before and after the illumination on formvar coated copper grids to conduct further investigations at the PSI-PolLux. This facility is equipped with a scanning transmission X-ray microscope (STXM) (Figure 1), to identify particle and chemical compositions, by using high-resolution images (better than 50 nm) and soft X-ray absorption spectra (in a range of 250 - 1600 eV) of very small sample areas.

Results and Discussion

At first, the UV/Vis absorbance spectra of the photosensitizers in aqueous solution were determined to classify the absorption capabilities in the actinic region. Their molar attenuation coefficients of the ground state are necessary to describe the excitation and the associated energy transfer to generate the triplet state. Figure 2 shows the general mechanism of the photochemistry in the presence and absence of further reactants, such as O_2, H-atom donors or electron donors in the aqueous solution.

First, the ground state of the photosensitizer ($(PS)_0$) is excited to the singlet state ($^1(PS)$), which generally reacts by an intersystem crossing process (ISC) in less than a nanosecond to the triplet state ($^3(PS)$). Subsequently, the triplet state can be

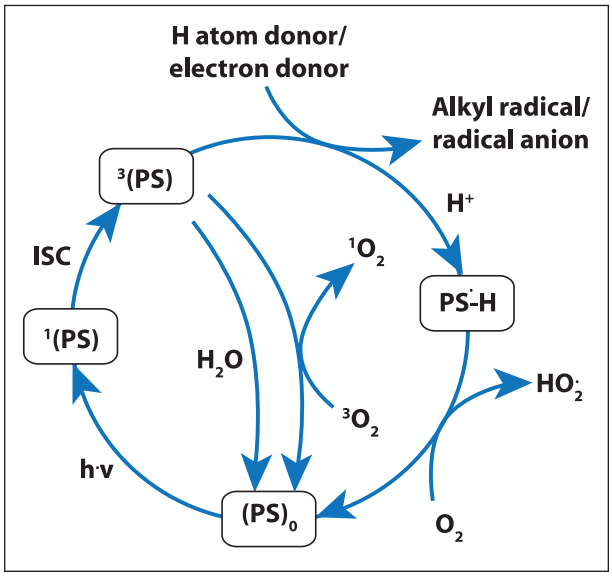

Fig. 2: General catalytic mechanism for the chemistry of photosensitizers in the aqueous solution.

deactivated by the quenching with water (H_2O), by the energy transfer with oxygen forming singlet oxygen ($^1O_2$) or the reaction with another molecule, e.g. an H atom or an electron donor to produce the reduced ketyl radical (PS-H·). The ketyl radical may transfer an H atom or electron to an acceptor such as O_2 and form an HO_2· radical.

The UV/Vis absorbance spectra of the excited state were studied to get more information about the absorbance behavior such as the position of the absorbance band that corresponds to the triplet state to conduct further kinetic investigations of the triplet state.

Imidazole-2-carboxaldehyde (2-IC)

In this section, the results of the photochemical properties of imidazole-2-carboxaldehyde (2-IC), which is a photosensitizer found in the aerosols, will be presented.

In Figure 3 two absorption bands characterize the ground state of the 2-IC. The first absorption band can be assigned to the aromatic ring system of the imidazole structure and the second band relates to the absorption of the carbonyl group, which is attached to the imidazole ring. Both absorption bands show pH-dependency, which can be explained by the protonation or deprotonation of the imidazole ring as well as the hydration of the carbonyl group. Figure 4 shows the time-resolved transient absorbance spectra of 2-IC* in degassed water at different delay times after the excitation (t_{delay}). A strong absorbance band at 338 nm characterizes the transient absorbance spectra and can be assigned to the triplet state. The results of the present study are comparable with the transient absorbance spectra from the literature [*Tinel et al.*, 2014, *Li et al.*, 2016] In a former study the transient absorbance spectrum shows the formation of a second absorbance band at around 650 nm after a delay time of 2 µs. Neither the present study nor the study of *Li et al.* [2016] showed this second absorbance band. From single laser line experiments at λ = 407 nm the decay of the triplet state, which was already visible in Figure 4, was further investigated in the absence and the presence of O_2 in the aqueous phase.

Derived from the first order rate constants at 407 nm shown in Figure 5 the second order rate constant can be calculated with $k(2\text{-IC}^* + O_2) = (2.7 \pm 0.3) \times 10^9$ L mol^{-1} s^{-1}.

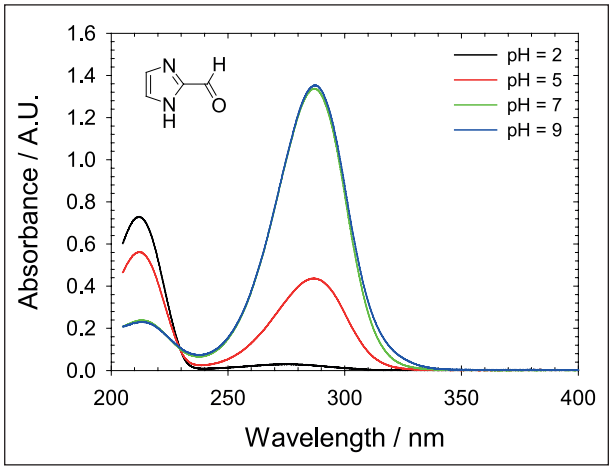

Fig. 3: pH-dependent UV/VIS absorbance spectra of the heterocycle imidazole-2-carboxaldehyde in the aqueous solution, using a concentration of c = 1.0 × 10^{-4} mol L^{-1}.

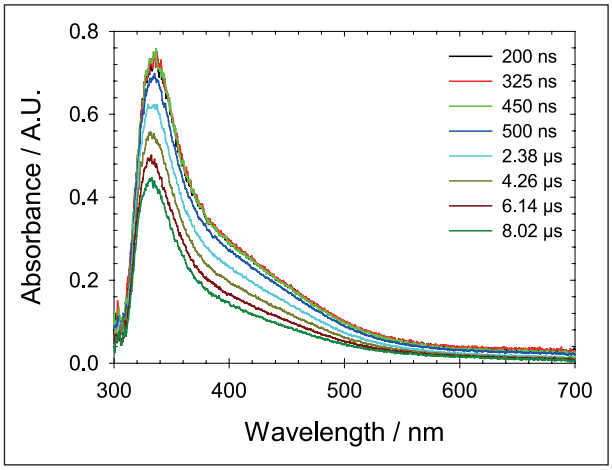

Fig. 4: Time-resolved transient absorbance spectra of the excited state of imidazole-2-carboxaldehyde (2-IC) in the absence of O_2 at pH = 6 and T = 298 K.*

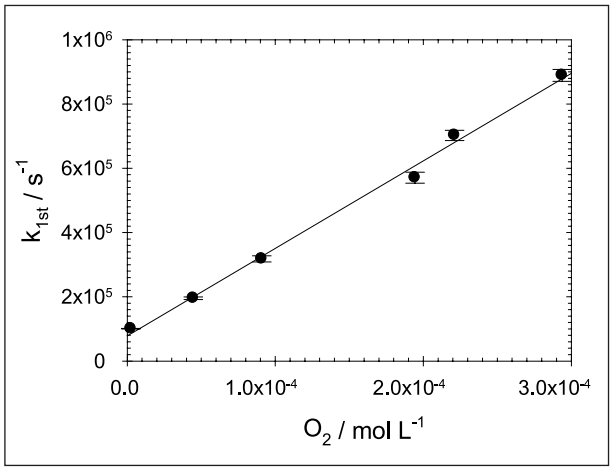

Fig. 5: Shows the decay rate of the 2-IC triplet state (k_{1st}) as function of the O_2 concentration in the aqueous solution at 407 nm.

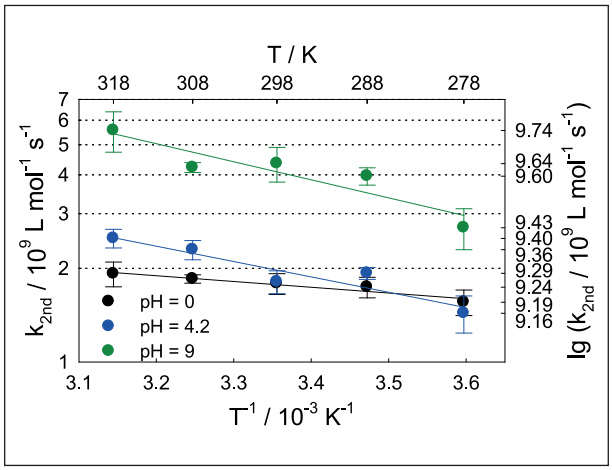

Fig. 6: Arrhenius plot of the T-dependent measurement of 2-IC with OH radicals at pH = 0 (black points), pH = 4.2 (blue points), and pH = 9.1 (green points).

The lifetimes of the triplet state can be derived from the decay first order rate constants using the following equation.

$$\tau = \frac{1}{k_{1st}}$$

In the absence and presence of O_2 the lifetime of the 2-IC* in the aqueous phase was calculated with τ = 1 µs respectively τ = 10 µs.

Beside the lifetime of the triplet state in the aqueous media, the temperature-dependent OH radical reactivity of the 2-IC ground state was also investigated, to clarify the stability of the imidazole-based photosensitizers [*Felber et al.*, 2019]. In Figure 6 the results of the pH- and T-dependent measurement of the OH radical reaction is depicted.

The derived Arrhenius expressions are shown for pH = 0, pH = 4.2, and pH = 9.1 (in unit of L mol^{-1} s^{-1}).

$$k(T, pH = 0) = (7.5 \pm 0.1) \times 10^{9} \times \exp\left(\frac{-430 \pm 80\ K}{T}\right)$$

$$k(T, pH = 4.2) = (9.0 \pm 0.4) \times 10^{10} \times \exp\left(\frac{-1140 \pm 300\ K}{T}\right)$$

$$k(T, pH = 9.1) = (3.7 \pm 0.2) \times 10^{11} \times \exp\left(\frac{-1320 \pm 360\ K}{T}\right)$$

The temperature dependency of the OH radical reaction with 2-IC can be described in the following order: pH = 0 < pH = 4.2 < pH = 9.1. Under alkaline conditions, the reaction is more T-dependent than under acidic conditions as it can be seen in the Arrhenius plot (Figure 6) and the derived Arrhenius expressions. Further compounds based on imidazole show a similar behavior of the OH radical reactivity depending on the pH value. The atmospheric aqueous-phase lifetimes (τ) of these imidazoles has been reported from only a few minutes for aerosol conditions to hours for the cloud conditions [*Felber et al.*, 2019].

In further experiments, the pseudo-halide thiocyanate (SCN^-) was used to scavenge the triplet state, in order to classify the efficiency of the excitation reaction.

Hence, the quantum yield of this process was investigated using the change of absorbance at λ = 594 nm cause by the formation of reaction product $(SCN)_2^{\cdot-}$. During the experiment, the concentration of thiocyanate was varied from c = 0.001 – 0.3 mol L^{-1} to ensure that the triplet state is completely converted to the absorbing target species $(SCN)_2^{\cdot-}$. Surprisingly, the obtained quantum yield in Figure 7 exhibits a pH-dependency even if the contribution of the different absorption behavior is considered (see Figure 3). The lower the pH value, the higher the quantum yield.

Further investigations of the scavenger reaction and the subsequent equilibrium reactions show a

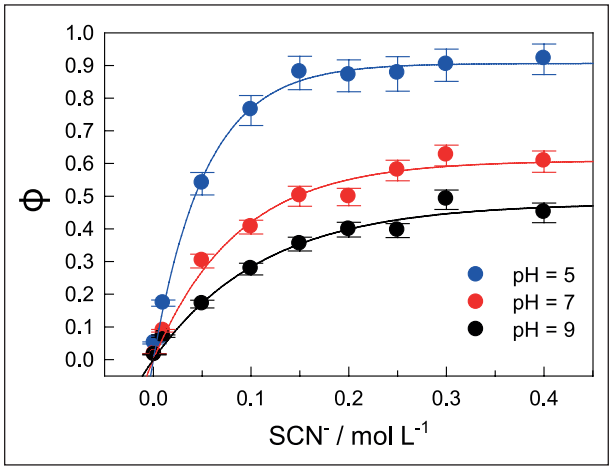

Fig. 7: Displays the obtained quantum yields ϕ of the 2-IC at T = 298 K and different pH values (blue: pH = 5, red: pH = 7, black: pH = 9).*

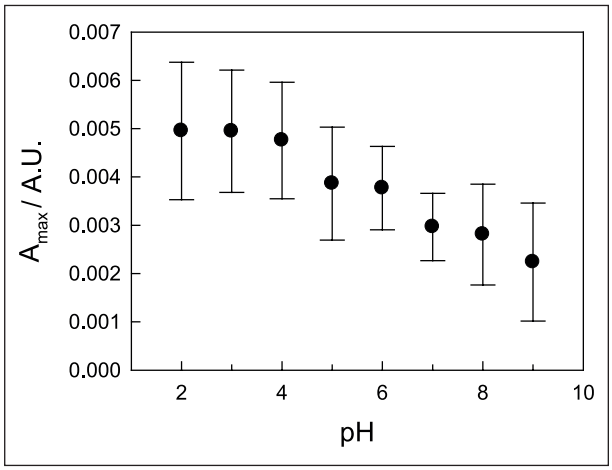

Fig. 8: The obtained absorbance at λ = 594 nm of the reaction of hydroxyl radicals (·OH) with thiocyanate at different pH values.

pH-dependency of the trapping reaction system with OH radicals.

In the range of pH = 2 – 9 the obtained absorption of $(SCN)_2^{\cdot-}$ decrease with the increase of the pH value depicted in Figure 8. However, if we consider both pH-dependent effects, first the protonation of 2-IC and second the change in the $(SCN)_2^{\cdot-}$ yield of the trapping system, the quantum yields ϕ change significantly (cf. Figure 9).

The pH value independent quantum yields of 2-IC* were obtained as ϕ(pH = 5) = 0.86 ± 0.05, ϕ(pH = 7) = 0.83 ± 0.06, and ϕ(pH = 9) = 0.83 ± 0.08. Using the obtained quantum yields and the absorption spectrum (Figure 4), the molar attenuation coefficient of the triplet state 2-IC was determined. At the absorbance maximum a value with $\varepsilon_{338nm} = 1.4 \times 10^4$ L mol^{-1} cm^{-1} was received (cf. Table 1).

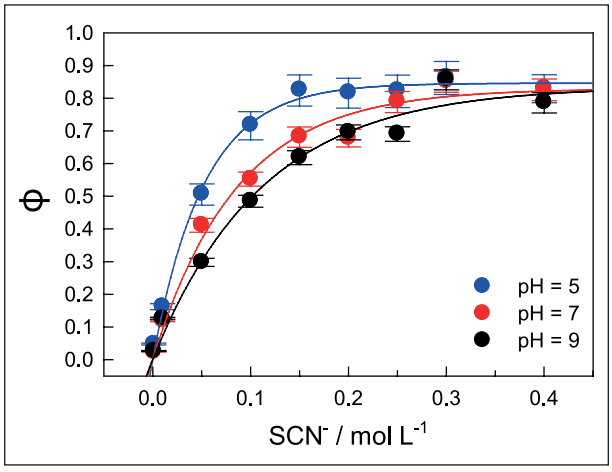

Fig. 9: Corrected quantum yields of the excited state of imidazole-2-carboxaldehyde at T = 298 K and different pH values (blue: pH = 5, red: pH = 7, black: pH = 9).

2-furaldehyde (2-FA)

Another heterocycle the 2-furaldehyde (2-FA), which is emitted by biomass burning processes, is able to act as photosensitizer.

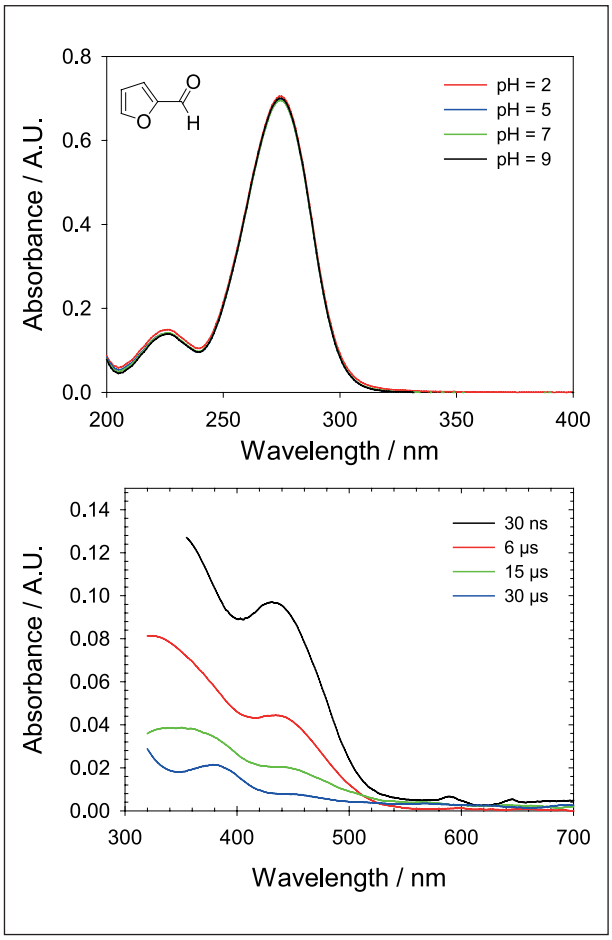

Fig. 10: Display the pH-dependency of the heterocycle 2-furaldehyde (c = 5.0 × 10^{-5} mol L^{-1}) in the UV/VIS range at the top and the time-resolved spectra of the excited state (2-FA) in the absence of O_2 at pH = 6 and T = 298 K at the bottom.*

The pH-dependent measurement of the UV/VIS absorbance in Figure 10 shows a smaller pH dependency, in comparison to the 2-IC. One reason might be that the furan ring is not affected by the protonation with the increase of H^+ concentration. Two strong absorbance bands at 320 nm and 430 nm characterize the transient absorbance spectra at different delay times and can be assigned to the triplet state. Compared to the 2-IC* extinction, the second extinction band is much more pronounced.

Benzaldehydes

Another important compound class are the benzaldehydes, which can be emitted by biomass burning processes into the atmosphere. Since they have several chromophoric groups, they have the

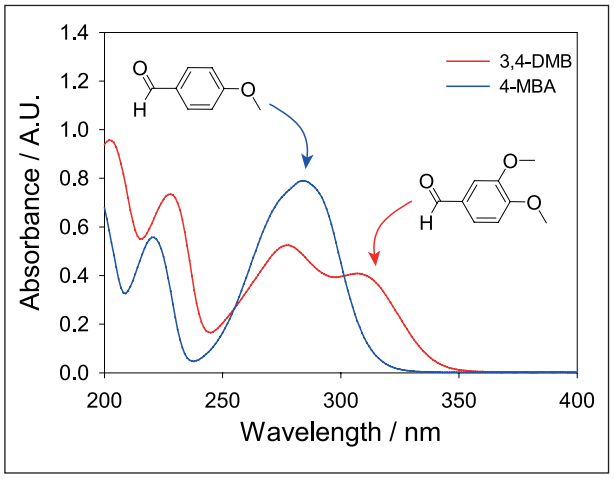

Fig. 11: UV/VIS absorbance spectra of 3,4-dimethoxy-benzaldehyde (red line) and 4-methoxy-benzaldehyde (blue line) using a concentration of c = 5.0 × 10^{-5} mol L^{-1} at pH = 5.

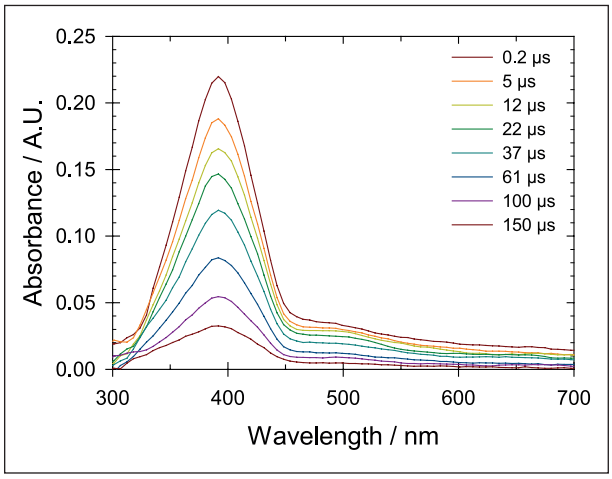

Fig. 13: Transient spectra at different delay time of 4-methoxy-benzaldehyde (c = 1.0 × 10^{-5} mol L^{-1}).

ability to absorb light in the actinic region. In these cases, the aldehyde function of these molecules reacts as photosensitizer after the excitation. The UV/VIS absorbance spectra (Figure 11) displays the 3,4-dimethoxy-benzaldehyde and 4-methoxybenz-aldehyde. The pH-dependence was investigated, but the change in the pH value shows only a small change in the absorbance, since the hydration constant of the aldehyde group is small because of the aromatic ring system.

The comparison of the spectra in Figure 11 indicates that the second methoxy group (-OCH$_3$) at the aromatic ring results in a further smaller absorbance band at around 330 nm.

However, the excitation by the excimer laser pulse at 308 nm leads to the following transient absorbance spectra shown in Figure 12 and 13.

The spectra in Figure 12 exhibits two overlapping absorbance bands at 380 nm and 450 nm. The comparison with Figure 13 shows an absorbance band at 380 nm and a second very small band at 500 nm of the excited state of the 4-methoxybenzaldehyde, which is not as pronounced as the absorbance band at 450 nm of the triplet state of 3,4-dimethoxy-benzaldehyde. In addition, the lifetime of the excited state in Figure 13 is much smaller.

Benzophenone

The most prominent photosensitizer is the benzophenone (BPh), which is used as photo initiator in organic solvents in industrial processes. The UV/VIS spectrum displays a strong absorbance band in the deep UV at λ = 260 nm (Figure 14). The pH

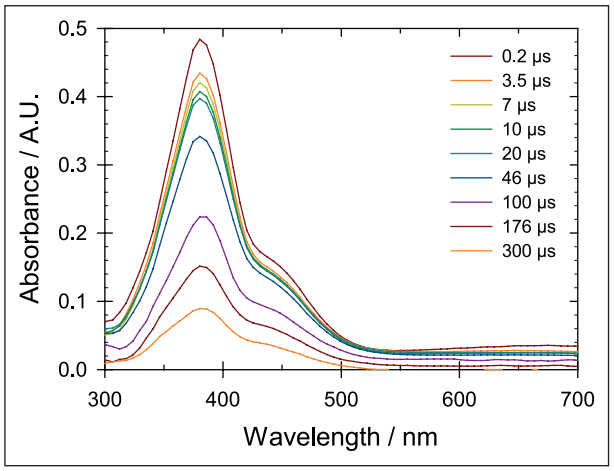

Fig. 12: Spectra of the excited state of 3,4-dimethoxybenzaldehyde (c = 1.0 × 10^{-5} mol L^{-1}) at different delay time after the laser flash excitation at 308 nm.

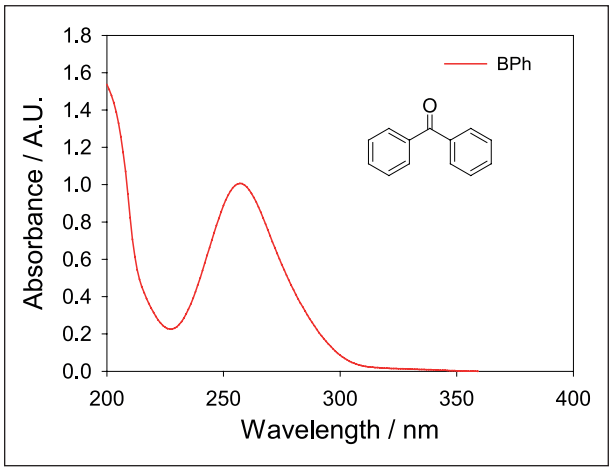

Fig. 14: UV/VIS absorbance spectra of benzophenone (BPh) (c = 5.0 × 10^{-5} mol L^{-1}) at pH = 5.

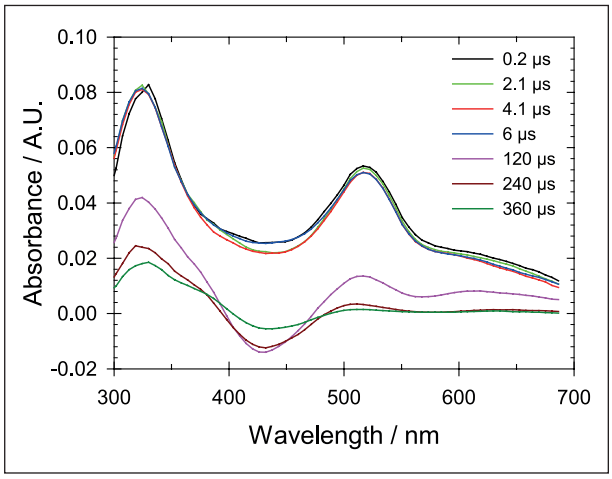

Fig. 15: Time-resolved spectra of the excited state of benzophenone (c = 1.0 × 10⁻⁵ mol L⁻¹) at pH = 5.

dependency of the absorbance of this compound is small.

The transient absorbance spectra of benzophenone (BPh) show two absorbance bands.

The first absorbance band at a wavelength of λ = 330 nm and the second at λ = 517 nm (cf. Figure 15). Furthermore, the spectra show a gap (λ = 380 – 480 nm) between these two maxima, which is resulting in negative values at higher delay times.

Phosphorescence measurements showed that triplet BPh is emitting light at this wavelength range explaining the loss of absorbance in the observed transient absorbance spectra. The Phosphorescence shown in Figure 16 has a maximum at 6 µs and disappear after 360 µs. The contribution of the emitting light to the spectrum at the delay time of 200 ns is negligible.

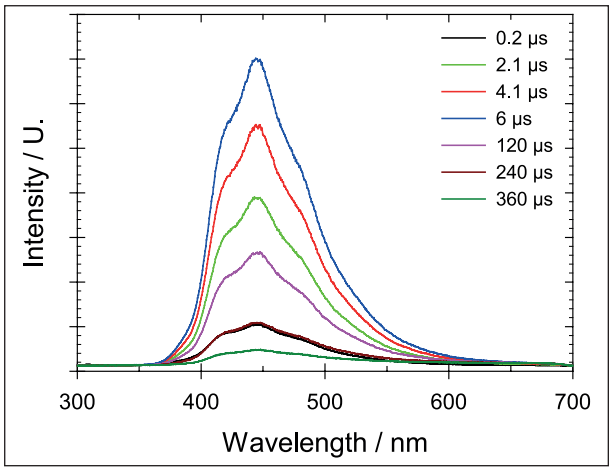

Fig. 16: Time-resolved spectra of the phosphorescence of benzophenone (c = 1.0 × 10⁻⁵ mol L⁻¹) at pH = 5.

Anthraquinone-2-sulfonate (AQ2S)

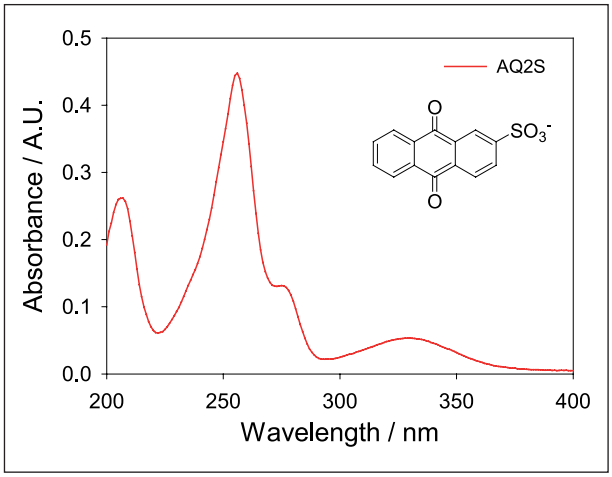

Fig. 17: UV/VIS absorbance spectra of anthraquinone-2-sulfonate (AQ2S) (c = 1.0 × 10⁻⁵ mol L⁻¹) at pH = 6.

The triplet state chromophore formed by the excitation of anthraquinone-2-sulfonate (AQ2S) is widely used as a model substance in the photochemistry of chromophoric dissolved organic matter. The UV/VIS absorbance in Figure 17 exhibit a very strong band at 257 nm, two smaller bands at

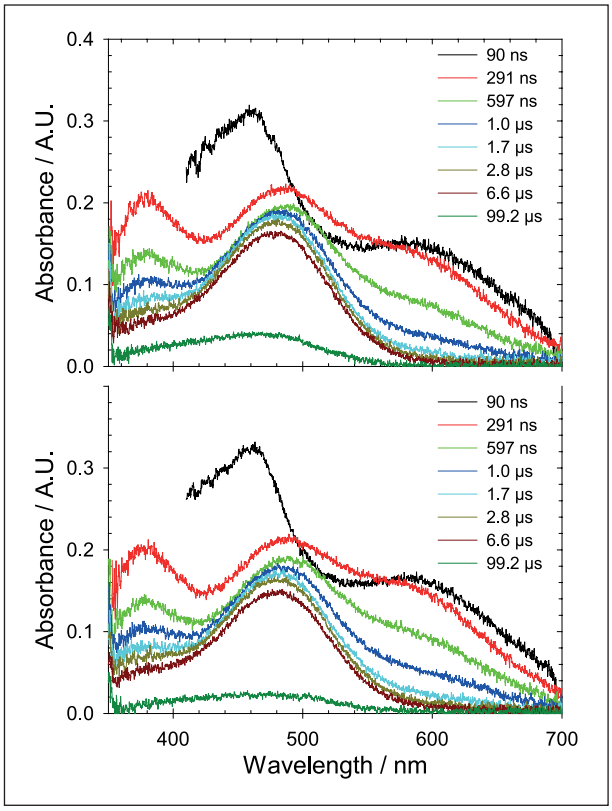

Fig. 18: Time-resolved transient absorbance spectra of the excited state anthraquinone-2-sulfonate (AQ2S) in the presence (top) and absence (bottom) of O_2 at pH = 6 and T = 298 K.

Tab. 1: Molar attenuation coefficients of the ground state ε_{308nm}(PS), the decay rate k_0 in H_2O at λ = 407 nm, the resulting lifetime τ_0, the quenching rate constant of the O_2 reaction, the quantum yield ϕ of the reaction of the excited photosensitizer with SCN^-, and the ε_{max}(PS) as well as the wavelength of the maximum of the excited state at T = 298 K.*

PS	ε_{308nm}(PS) / 10^3 L mol^{-1} cm^{-1}	k_0 x 10^{-4} / s^{-1}	τ_0 / µs	k(O_2) / L mol^{-1} s^{-1}	Φ*	ε_{308nm}(PS) / 10^3 L mol^{-1} cm^{-1}	λ_{max} / nm
2-FA	0.76	12.8 ± 0.05	7.8	(2.1 ± 0.1) × 10^9	0.96 ± 0.06	3.2	431
2-AF	0.67	14.0 ± 0.05	7.1	(2.7 ± 0.1) × 10^9	0.89 ± 0.05	6.94	392
2-IC	1.07	13.1 ± 0.3	7.7	(2.7 ± 0.3) × 10^9	0.86 ± 0.05	13.8	338
3'-MAP	2.38	1.05 ± 0.03	95	(3.9 ± 0.2) × 10^9	0.80 ± 0.04	14.6	380
4-BBA	1.7	5.84 ± 0.02	17	(1.7 ± 0.1) × 10^9	0.71 ± 0.03	22	341 / 545
2-MBA	3.13	3.03 ± 0.04	33	(4.0 ± 0.2) × 10^9	0.70 ± 0.04	13	397
3-MBA	2.46	0.43 ± 0.01	233	(3.8 ± 0.5) × 10^9	0.48 ± 0.03	545	386
Xan	1.91	0.58 ± 0.04*	172*	(2.8 ± 0.2) × 10^9 *	0.48 ± 0.03	15.4	380 / 584
BPh	0.72	1.27 ± 0.06	79	(2.4 ± 0.2) × 10^9	0.47 ± 0.03	23.7	330 / 517
DMB	8.07	0.29 ± 0.01	161	(2.7 ± 0.2) × 10^9	0.37 ± 0.02	22	380
4-MBA	3.81	0.95 ± 0.01	105	(4.4 ± 0.4) × 10^9	0.35 ± 0.02	32.5	392
1-NN	2.22	4.50 ± 0.4	22	(2.0 ± 0.1) × 10^9	0.06 ± 0.01	584	386 / 657
2-AN	2.42	0.34 ± 0.01	296	(1.1 ± 0.3) × 10^9 *	0.05 ± 0.01	24.6	375
Van	9.28	7.60 ± 0.07	13	(2.7 ± 0.1) × 10^9	0.05 ± 0.01	15.9	358
HMAP	1.5	3.09 ± 0.1	32	(2.9 ± 0.5) × 10^9	0.01 ± 0.01	517	380
AQS	3.0**	51.7***	1.9	(5.0 ± 1.1) × 10^8	/	/	380 / 490 / 610

*Observation at 594 nm, **excitation wavelength λ = 351 nm, ***observation at 380 nm

207 nm and 275 nm as well as one band at 330 nm. The very strong absorbance band corresponds to the carbonyl groups.

Figure 18 shows the time-resolved transient absorbance spectra of 1 × 10^{-5} mol L^{-1} anthraquinone-2-sulfonate excited by an excimer laser pulse (λ = 351 nm) in the presence (top) and absence (bottom) of O_2 obtained at pH = 6, T = 298 K, and different delay times after the laser pulse (t_{delay}) and a exposure time (t_{gate}) with 200 up to 300 ns.

Three strong absorbance band at 380 nm, 490 nm, and 610 nm characterizes the transient absorbance spectra at 291 ns in red of the excited state. The spectra at 90 ns in black has two absorption bands at 480 nm, and 590 nm, whereas the excimer laser pulse disturbs the absorbance below 410 nm. A comparison between the spectra in presence and absence of O_2 shows only a small contribution of the spectra. The formed absorption bands at around 380 nm, 490 nm, and 610 nm correspondence to the triplet states and two transient water complexes according to *Loeff et al.* [1983] and *Moore et al.* [1988]. The transient absorbance spectra of the present study are comparable with the transient absorbance spectra measured by *Maddigapu et al.* [2010]. Derived from the first order rate constants at 380 nm in the presence (2.6 × 10^{-4} mol L^{-1}) and absence (<1 × 10^{-6} mol L^{-1}) of O_2 the second order rate constant can be calculated with k(AQ2S* + O_2) = (5.0 ± 1.1) × 10^8 L mol^{-1} s^{-1}. In the absence and presence of O_2 the lifetime of the excited state was calculated with τ = 1.9 µs respectively τ = 1.6 µs.

In the following section, the properties of the photosensitizers as well as the excited triplet of the investigated 16 compounds will be shown. The received values such as the molar attenuation coefficient, the quantum yield, H_2O - as well as O_2 - quenching rate constants and the lifetimes are summarized in Table 1.

Some of these photosensitizers reacted quite efficient like the five membered heterocycles 2-furaldehyde (2-FA), 2-acetylfuran (2-AF),

imidazole-2-carboxaldehyde (2-IC), phenones: 3'-methoxyacetophenone (3'-MAP), 4-benzoyl-benzoic acid (4-BBA) as well as benzaldehydes: 2-methoxybenzaldehyde (2-MBA) with a quantum yield between 1.0 and 0.6.

Other investigated structure-like compounds such as 3-methoxybenzaldehyde (3-MBA), xanthone (Xan), benzophenone (BPh), 3,4-di-methoxy-benzaldehyde (DMB) or 4-methoxy-benzaldehyde (p-MBA) show a lower quantum yield in the range between 0.5 and 0.35.

Followed by a group of compounds like 1-nitronaphthalene (1-NN), 2-acetylnaphthalene (2-AN), vanillin (Van) and 2'-hydroxy-5'-methylacetophenone (HMAP) which are rather inefficient. A trend in the efficiency of the photosensitizers is not related to the molecule structure, especially when comparing the investigated benzaldehydes.

Furthermore, all photosensitizers have high molar attenuation coefficients in their ground and excited triplet state indicating that such organic compounds can initiate photochemistry in the tropospheric aerosol particles or cloud droplets.

However, all excited states have only a short lifetime in water in the absence of another reaction partner from only 2 µs to 300 µs. In contrast, the contribution of O_2 leads to an even shorter lifetime, since the quenching rate constant is in the order of 10^9 L mol^{-1} s^{-1} (Table 1). This leads to the conclusion that photochemistry only plays a significant role in higher concentrated systems, such as aerosols.

Besides the photochemistry experiments in the aqueous bulk phase further experiments in the aerosol chamber ACD-C has been conducted to address the gap of how chemistry occurring within aerosol droplets drives reactive uptake of gases into the bulk aerosol phase. Therefore, the uptake of α-pinene onto aerosols comprised of ammonium sulfate ($(NH_4)_2SO_4$) and anthraquinone-2-sulfonate (AQ2S) was studied. For that reason, a solution of $(NH_4)_2SO_4$ and AQ2S were nebulized into the ACD-C chamber containing 50 ppbV of α-pinene. After a brief equilibration time, UV-visible lights ($300 < \lambda < 400$ nm) irradiated the chamber to initiate aerosol photochemistry.

Figure 19 shows that UV-visible irradiation induces particle growth in $(NH_4)_2SO_4$ seed aerosol containing AQ2S in the presence of α-pinene. The enhanced particle growth in the presence of chromophores indicates reactive uptake of α-pinene into the aerosol phase, which is driven by ROS formed via the reaction of O_2 with excited state chromophores from the AQ2S. The addition of Fe^{3+} shuts the photochemistry of the excited state AQ2S chromophores down, by limiting effectively the particle growth. To explore this effect at the single particle level, aerosols were collected from ACD-C chamber experiments and analyzed via near edge X-ray absorption fine structure spectroscopy (NEXAFS). Figure 20 shows NEXAFS spectra of seed particles, and those particles exposed to α-pinene under UV light with a without Fe^{3+}. AQ2S shows two peaks at 284.4 and 284.8 eV associated with the quinone ring structure [*Moffet et al.*, 2010]. Another peak at 286.3 eV is associated with a phenol group [*Moffet et al.*, 2010], indicating the presence of semi- or hydroquinones [*Scharko et al.*, 2017]. After exposure to α-pinene and UV light, particles with and without Fe^{3+} were entirely

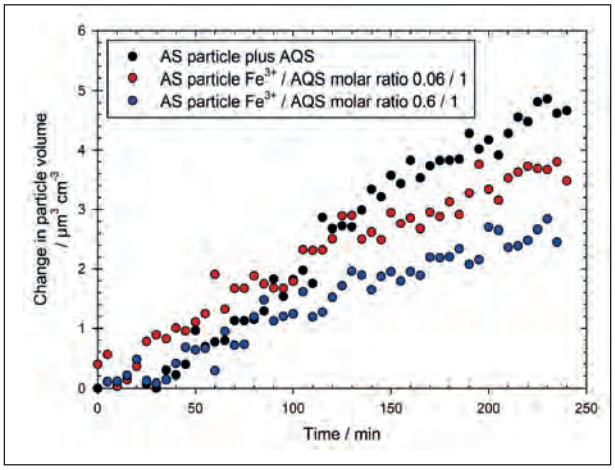

Fig. 19: Particle volume measured by mobility particle sizer during aerosol chamber experiments containing gaseous α-pinene and $(NH_4)_2SO_4$ seed aerosol comprised of the indicated components.

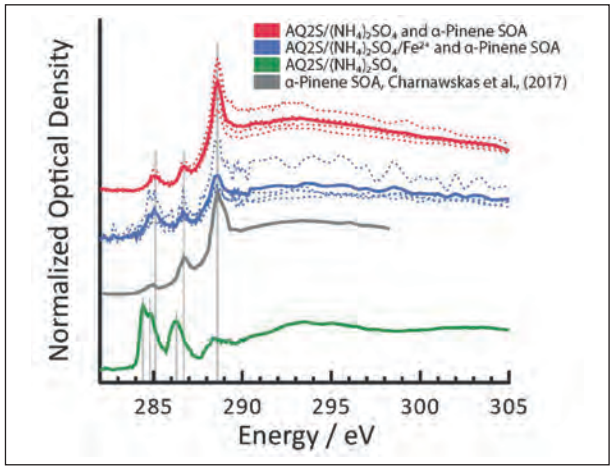

Fig. 20: Normalized NEXAFS spectra of indicated aerosol particles exposed to α-pinene under UV light. Solid lines are averages of individual particles, the latter are dotted line. Spectra are background subtracted and normalized to the area between 305-320 eV. Spectra of α-Pinene SOA from literature is shown [Charnawskas et al., 2017].

dominated by three peaks at 285.1, 286.7 and 288.6 eV indicative of unsaturated carbon, hydroxyl and carboxyl functions, respectively. Spectra are similar to those of α-pinene SOA generated from gas phase OH chemistry [*Charnawskas et al.*, 2017], indicating similar α-pinene oxidation pathways occur in the bulk aerosol phase. Consistent with chamber experiments in Figure 19, we observed significantly less SOA material on the particles containing Fe^{3+}. Together, the results show that reactive uptake is controlled by a competition between ROS sources (organic chromophores from AQ2S) and sinks (Fe^{3+} containing material), with implications for understanding the drivers of particle growth when mineral dust is present.

Summary

In the present study, the photochemical properties like the quantum yield, the lifetime, and the molar attenuation coefficient of 16 various photosensitizers were investigated. Some reacted quite efficient (e.g. five membered heterocycles), whereas other photo-sensitizers were rather inefficient (e.g. naphthalenes). Furthermore, all photo-sensitizers have high molar attenuation coefficients in their ground and excited triplet state indicating that such organic compounds can initiate photochemistry in the atmosphere. Especially, compounds emitted by biomass burning processes (e.g. five-membered heterocycles) might be important and potential photosensitizers in the aqueous and particle phase. However, all excited states have only a short lifetime in water up to several µs, which leads to the conclusion that they might only play a role in aerosol particles.

An enhanced particle growth was observed in the presence of a photosensitizer, which indicates a stronger reactive uptake into the particle phase driven by the photochemistry. Nevertheless, the addition of Fe^{3+} decreases the photochemistry of the excited state chromophores resulting in the limitation of the particle growth.

References

Charnawskas, J. C.; Alpert, P. A.; Lambe, A. T.; Berkemeier, T.; O'Brien, R. E.; Massoli, P.; Onasch, T. B.; Shiraiwa, M.; Moffet, R. C.; Gilles, M. K.; Davidovits, P.; Worsnop, D. R.; Knopf, D. A. (2017) Condensed-phase biogenic-anthropogenic interactions with implications for cold cloud formation. Faraday Discuss., 200, 165 - 194.

Corral Arroyo, P.; Bartels-Rausch, T.; Alpert, P. A.; Dumas, S.; Perrier, S.; George, C.; Ammann, M. (2018) Particle-Phase Photosensitized Radical Production and Aerosol Aging. Environ. Sci. Technol., 52, 7680-7688.

Ervens, B.; Turpin, B. J.; Weber, R. J. (2011) Secondary organic aerosol formation in cloud droplets and aqueous particles (aqSOA): a review of laboratory, field and model studies. Atmos. Chem. Phys., 11, 11069-11102.

Felber, T.; Schaefer, T; Herrmann, H. (2019) OH-Initiated Oxidation of Imidazoles in Tropospheric Aqueous-Phase Chemistry. J. Phys. Chem. A, 123, 8, 1505-1513.

Gilardoni, S.; Massoli, P.; Paglione, M.; Giulianelli, L.; Carbone, C.; Rinaldi, M.; Decesari, S.; Sandrini, S.; Costabile, F.; Gobbi, G. P.; Pietrogrande, M. C.; Visentin, M.; Scotto, F.; Fuzzi, S.; Facchini, M. C. (2016) Direct observation of aqueous secondary organic aerosol from biomass-burning emissions. Proc. Nat. Acad. Sci., 113, 10013.

Laskin, A.; Laskin, J.; Nizkorodov, S. A. (2015) Chemistry of Atmospheric Brown Carbon. Chem. Rev. 115, 4335-4382.

Li, W.-Y.; Li, X.; Jockusch, S.; Wang, H.; Xu, B.; Wu, Y.; Tsui, W. G.; Dai, H.-L.; McNeill, V. F.; Rao, Y. (2016) Photoactivated Production of Secondary Organic Species from Isoprene in Aqueous Systems. J. Phys. Chem. A, 120, 9042-9048.

Loeff, I.; Treinin, A.; Linschitz H. (1983) Photochemistry of 9,10-Anthraquinone-2-sulfonate in Solution. 1. Intermediates and Mechanism. J. Phys. Chem., 87, 2536-2544.

Maddigapu, P. R.; Bedini, A.; Minero, C.; Maurino, V.; Vione, D.; Brigante, M.; Mailhot, G.; Sarakha, M. (2010) The pH-dependent photochemistry of anthraquinone-2-sulfonate. Photochem. Photobiol. Sci., 9, 323–330.

McNeill, V. F. (2015) Aqueous Organic Chemistry in the Atmosphere: Sources and Chemical Processing of Organic Aerosols. Environ. Sci. Technol., 49, 1237-1244.

Moffet, R. C.; Tivanski, A. V.; Gilles, M. K. (2010) Scanning Transmission X-Ray Microscopy: Applications in Atmospheric Aerosol Research in Fundamentals and Applications in Aerosol Spectroscopy, 419-462.

Monge, M. E.; Rosenørn, T.; Favez, O.; Müller, M.; Adler, G.; Abo Riziq, A.; Rudich, Y.; Herrmann, H.; George, C.; D'Anna, B. (2012) Alternative Pathway for Atmospheric Particles Growth. Proc. Nat. Acad. Sci., 109, 6840-6844.

Moore, J. N.; Phillips, D.; Hester, R. E. (1988) Time-Resolved Resonance Raman Spectroscopy Applied to the Photochemistry of the Sulfonated Derivatives of 9,10-Anthraquinone. J. Phys. Chem., 92, 5619-5627.

Nozière, B.; Dziedzic, P.; Córdova, A. (2007) Formation of secondary light-absorbing "fulvic-like" oligomers: A common process in aqueous and ionic atmospheric particles? Geophys. Res. Lett., 34.

PSI website: https://www.psi.ch/de/sls/pollux/endstation

Scharko, N. K.; Martin, E. T.; Losovyj, Y.; Peters, D. G.; Raff, J. D. (2017) Evidence for Quinone Redox Chemistry Mediating Daytime and Nighttime NO2-to-HONO Conversion on Soil Surfaces. Environ. Sci. Technol., 51, 9633-9643.

Smith, J. D.; Kinney, H.; Anastasio, C. (2015) Aqueous benzene-diols react with an organic triplet excited state and hydroxyl radical to form secondary organic aerosol. Phys. Chem. Chem. Phys., 17, 10227-10237.

Teich, M.; van Pinxteren, D.; Kecorius, S.; Wang, Z.; Herrmann, H. (2016) First Quantification of Imidazoles in Ambient Aerosol Particles: Potential Photosensitizers, Brown Carbon Constituents, and Hazardous Components. Environ. Sci. Technol., 50, 1166-1173.

Tinel, L.; Dumas, S.; George, C. A (2014) Time-Resolved Study of the Multiphase Chemistry of Excited Carbonyls: Imidazole-2-carboxaldehyde and Halides. C. R. Chim., 17, 801-807.

Zhang, X.; Lin, Y.-H.; Surratt, J. D.; Zotter, P.; Prévôt, A. S. H.; Weber, R. J. (2011) Light-absorbing soluble organic aerosol in Los Angeles and Atlanta: A contrast in secondary organic aerosol. Geophys. Res. Lett., 38.

Funding

Funding for this work was provided by German Research Foundation - DFG (Project PHOTOSOA, HE 3086/32-1), the Atmospheric Chemistry Department (ACD) at the Leibniz Institute for Tropospheric Research (TROPOS), EUROCHAMP-2020 (Project LEAK-LACIS-002-2017), and the Swiss National Science Foundation (Grant 163074).

Cooperation

IRCELYON - CNRS, Lyon, France;
Indiana University, Bloomington, USA;
Paul Scherrer Institute, Villigen, Switzerland.

Clouds and their Effects in ICON Simulations

Fabian Senf

Wolken können in vielfältigen und außergewöhnlichen Formen existieren und diese Vielfalt scheint besonders wichtig zu sein. Die Art und Weise, wie sich zum Beispiel tropische Wolken anordnen, entscheidet über ihre Wirkung auf Umgebung und Klima. Wolkenpartikel streuen Sonnenlicht und absorbieren und emittieren terrestrische Wärmestrahlung. Prozesse auf der mikrophysikalischen Ebene sind somit über eine lange Skalenkaskade an die globale Wirkung gekoppelt, was eine große Herausforderung für numerische Simulationen darstellt. Aus diesem Grunde befassen sich die hier zusammengefassten Arbeiten mit der Frage, in wie weit es möglich ist, Wolkeneigenschaften und Wolkeneffekte mit den hochaufgelösten Wettermodell ICON darzustellen. Besonderes Augenmerk wird auf die räumliche Anordnung von konvektiven Wolken und Niederschlag sowie auf Wolken-Strahlungseffekte gelegt.

Introduction

The realistic representation of the emergence and impact of spatial organisation in deep moist convection is a major challenge for climate science [*Bony et al.*, 2015]. The numerical simulation of cloud formation processes without approximations is challenging because these processes occur over a vast range of spatial and temporal scales. Significant uncertainties remain in cloud parameterizations, specifically in microphysical aspects of cloud responses [*Gettelman and Sherwood*, 2016]. These aspects complicate a robust assessments of cloud feedbacks in a changing climate. Here, we consider clouds and their effects simulated with the innovative ICON model combined with a variety of atmospheric observations. The work has been performed within the framework of the project HD(CP)^2 Phase II that aimed at improving the understanding of cloud and precipitation processes and their representation in climate models. ICON is run in two different configurations: hectometre-scale simulations covering domains extending around one-thousand kilometres like the area of Germany and kilometre-scale simulations covering significant parts of the Atlantic oceans (see Fig. 1).

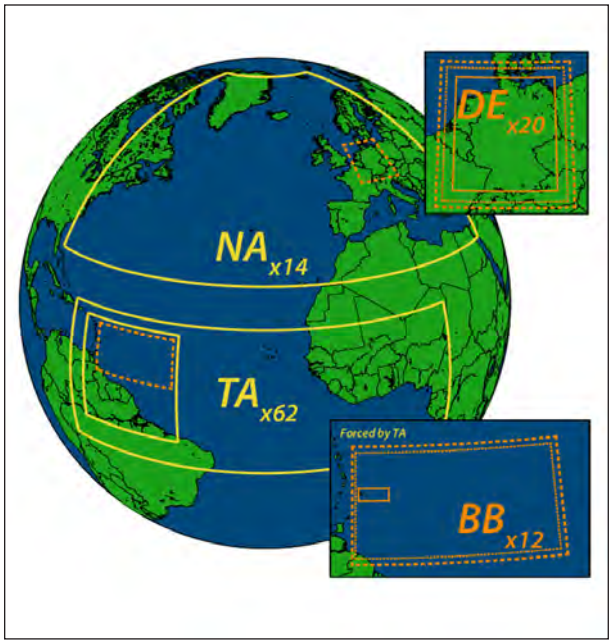

Fig. 1: Overview of different domains selected for ICON simulation experiments [taken from Stevens et al., 2020]. This report especially considers the analysis of ICON data from hectometer-scale simulations over Germany and kilometer-scale simulations over the North and Tropical Atlantic.

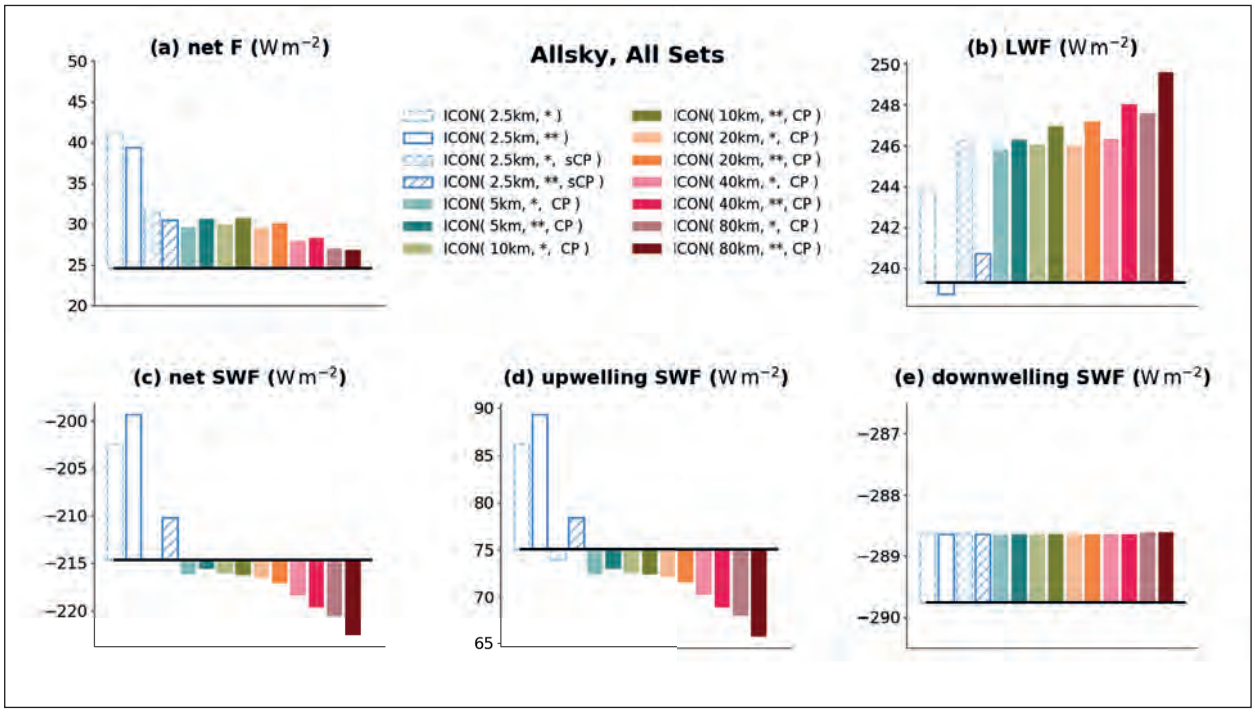

Fig. 2: Analysis of domain-average allsky radiation fluxes: (a) total net flux, (b) emitted longwave flux, (c) net shortwave flux, (d) upwelling shortwave flux, and (e) downwelling shortwave flux. The Meteosat observations (black line) were chosen as reference, and deviation of simulated fluxes are shown with colored bars. The ICON simulation experiments differ with regard to horizontal grid spacing (2.5 5, 10, 20, 40 and 80 km), and parametrization choice: one-moment (*) vs. two-moment microphysics (**), with full (CP) or just shallow convection parametrization scheme (sCP) or without any convection parameterization. All values represent time averages over a set of 11 simulated days.

Hectometre-scale simulations over Germany

Since 2013, the HD(CP)^2 consortium has carried out so-called ICON-LEM simulations with grid spacing from 600 m down to 150 m for a large set of case days [see *Stevens et al.*, 2020]. The chosen simulation domain is shown in Fig. 1 (top right). In our detailed analysis, ICON-LEM data were selected for days in which deep convection dominated the summer-time weather over Germany. Deep convection supports the development of large and very cold anvil cirrus that is easily identified in Meteosat observations. For a consistent comparison, ICON output was transferred into "observation space" using the SynSat forward operator [*Keil et al.*, 2006; *Senf and Deneke*, 2017]. The resulting ICON synthetic brightness temperatures allow for a direct comparison between simulations and observations. Furthermore, precipitation simulated with ICON-LEM has been compared to observations of the German network of scanning C-band precipitation radars.

Simulated precipitation amounts and distributions become more realistic as soon as convective motions start to be resolved (applies already to kilometre-scale simulations). Shortcomings of the simulations with convection parameterization that represent climate simulations, are especially apparent during night [*Stevens et al.*, 2020]. Improving the representation of nocturnal precipitation is important for the diurnal cycle of precipitation over land. Furthermore, the organizational state of convection over Germany has been systematically characterized using object-based methods [*Pscheidt et al.*, 2019]. Observed cloud tops and precipitation cores appear to be in a clustered organizational state for around 69% and 92% of the time, respectively. The amount of rainfall increases for increasing number of cells and their sizes, independently of the organizational state. The organizational state is reasonably well represented in ICON-LEM simulations without significant differences between different grid spacings [*Pscheidt et al.*, 2019].

Kilometre-scale simulations over the Atlantic

The kilometre-scale ICON simulations cover much larger domains (see Fig. 1) and were performed in support to different field campaigns - the Next-Generation Aircraft Remote Sensing for Validation (NARVAL) campaigns in August 2016 and December 2013 over the tropical Atlantic [*Stevens et al.*, 2016; *Klepp et al.*, 2014] and the North Atlantic Waveguide and Downstream Impact Experiment (NAWDEX) in fall 2016 over the North Atlantic [*Schäfler et al.*, 2018].

The ICON-NARVAL simulations were evaluated against Meteosat SEVIRI observations using object-based methods [*Senf et al.*, 2018]. The simulations were able to develop a well-defined intertropical convergence zone. Simulated marine convective activity was however considerably underestimated. The simulated cell size distributions were too steep, indicating too many small and too few large tropical cloud cells. The spatial arrangement of deep convective updraught cells was assessed with a pair-correlation method, which compares simulated pair numbers as a function of pair distance to an appropriately chosen reference [*Senf et al.*, 2019]. The average probability to find an updraught cell pair within 100 km is enhanced compared to a random distribution. Additionally, the spatial arrangement of larger or stronger cells deviates more from randomness compared to smaller or weaker cells, which might be related to their stronger dynamical interaction mechanisms. Using simplified equilibrium statistics of interacting cells, several spatial characteristics of the ICON simulations have been reproduced.

The sensitivity of top-of-the-atmosphere (TOA) radiation fluxes and cloud-radiative effects to parameter choices was investigated in ICON-NAWDEX simulations. Numerical experiments have been performed with varying grid spacings between 2.5 and 80 km and with different subgrid-scale parameterization approaches, switching between one-moment to two-moment microphysics and between explicit to parametrized convection. Simulations are compared to retrievals of TOA radiation fluxes and cloud-radiative effects derived from Meteosat measurements (Fig. 2). All simulated net TOA radiation fluxes are larger than the observations, and thus overestimate the net loss of radiative energy. Interestingly, the coarsest model runs which represent climate-model integrations possess the smallest net radiation biases. This is however due to an unwanted compensation between short- and longwave biases which seem to diminish with increasing resolution.

References

Bony, S. et al. (2015), Clouds, circulation and climate sensitivity, Nature Geosci, 8(4), 261–268, doi:10.1038/ngeo2398.

Gettelman, A., and S. C. Sherwood (2016), Processes Responsible for Cloud Feedback, Curr. Clim. Change Rep., 2(4), 179–189, doi:10.1007/s40641-016-0052-8.

Keil, C., A. Tafferner, and T. Reinhardt (2006), Synthetic satellite imagery in the Lokal-Modell, Atmos. Res., 82, 19–25.

Klepp, C., F. Ament, S. Bakan, L. Hirsch, and B. Stevens (2014), NARVAL Campaign Report, Max Planck Institute for Meteorology, Hamburg, Germany.

Pscheidt, I., F. Senf, R. Heinze, H. Deneke, S. Trömel, and C. Hohenegger (2019), How organized is deep convection over Germany?, Quart. J. Roy. Meteor. Soc., 145(723), 2366–2384, doi:10.1002/qj.3552.

Schäfler, A. et al. (2018), The North Atlantic Waveguide and Downstream Impact Experiment, Bull. Amer. Meteor. Soc., 99(8), 1607–1637, doi:10.1175/BAMS-D-17-0003.1.

Senf, F., and H. Deneke (2017), Uncertainties in synthetic Meteosat SEVIRI infrared brightness temperatures in the presence of cirrus clouds and implications for evaluation of cloud microphysics, Atmos. Res., 183, 113–129.

Senf, F., D. Klocke, and M. Brueck (2018), Size-Resolved Evaluation of Simulated Deep Tropical Convection, Mon. Wea. Rev., 146(7), 2161–2182.

Senf, F., M. Brueck, and D. Klocke (2019), Pair Correlations and Spatial Statistics of Deep Convection over the Tropical Atlantic, J. Atmos. Sci., 76(10), 3211–3228, doi:10.1175/JAS-D-18-0326.1.

Stevens, B. et al. (2016), The Barbados Cloud Observatory: Anchoring Investigations of Clouds and Circulation on the Edge of the ITCZ, Bull. Amer. Meteor. Soc., 97(5), 787–801.

Stevens, Bjorn and Acquistapace, C. and Hansen, A. and Coauthors incl. Senf, F. (2020), Large-eddy and Storm Resolving Models for Climate Prediction The Added Value for Clouds and Precipitation, J. Meteor. Soc. Japan, accepted.

Funding

HD(CP)^2 project is funded by the German Ministry for Education and Research (BMBF) under grant 01LK1507C and 01LK1503F.

Cooperation

Hans Ertel Center for Weather Research, Deutscher Wetterdienst, Offenbach;
Max Planck Institute for Meteorology, Germany;
Institute of Meteorology and Climate Research, Karlsruhe Institute of Technology, Karlsruhe;
Institute for Geosciences and Meteorology, University of Bonn, Bonn;
Royal Meteorological Institute of Belgium, Brussels.

Semi-direct effect of black carbon and mineral dust in a global model study

Ina Tegen, Bernd Heinold

Die Strahlungswirkung von absorbierendem Aerosol wird mit globalen Klimamodellsimulationen untersucht. Die semi-direkte Wirkung des absorbierenden Aerosols wird als Restgröße zwischen der gesamten direkten Strahlungswirkung und des direkten Strahlungsantriebs der Aerosolspezies berechnet. Während über dem Nordatlantik eine unterliegende Staubschicht den positiven Strahlungsantrieb von Rußaerosol verstärkt, reduziert die Anwesenheit einer hochliegenden Mineralstaubschicht die Strahlungswirkung von darunterliegendem Rußaerosol in Zentralasien.

Introduction

Atmospheric aerosol particles impact the atmospheric radiation budget directly and indirectly by modifying cloud properties. The effective radiative forcing of aerosols includes both the instantaneous forcing by aerosols and the so-called rapid adjustment of the atmosphere to aerosol forcing due to heating rate changes from aerosol absorption that may impact atmospheric stability or cloud cover. Such adjustments are also named “semi-direct” effects. Absorbing aerosol types that cause semi-direct effects are black carbon (BC) particles emitted by combustion of fossil fuels or biomass burning, and mineral dust. While anthropogenic BC from fossil fuel burning usually remains within the boundary layer, BC from vegetation fires can be released several kilometers high into the atmosphere and is subject to long-distance transport. BC particles are strongly absorbing in the solar spectral range and cause a positive atmospheric direct radiative forcing at the top of atmosphere (TOA). The upper limit of estimates of the overall global direct radiative effect for BC aerosol is as high as +0.9 Wm^{-2} [*IPCC*, 2013].

The effects of absorbing aerosols on cloud cover and thus on temperature changes can be opposing, thus the semi-direct effect is difficult to quantify on a global scale. Estimates of the radiative forcing due to the semi-direct effect range from -0.4 to +0.1 Wm^{-2}. Local values of -9.5 to +11 Wm^{-2} have been estimated [*Koch and Del Genio*, 2010].

We estimate the semi-direct aerosol effects by decomposing radiative forcing estimates from a global aerosol-climate model into direct, indirect and semi-direct forcing. In that study it has been shown that the positive direct instantaneous and semi-direct radiative effects of BC are more positive when forcing by mineral dust aerosol is considered together with the BC forcing, as the comparably bright dust aerosol enhances the positive BC forcing.

Method

We investigated the semi-direct effects (or rapid adjustments) of the absorbing aerosol types BC and mineral dust within the global aerosol-climate model ECHAM6-HAM2 [*Zhang et al.*, 2012], [*Tegen et al.*, 2019] (version echam6.3-ham2.3). Atmospheric radiative transfer is computed based on aerosols present in the atmosphere and their related optical properties.

The radiative effects of absorbing aerosols were evaluated with four model experiments. Each model simulation was averaged for 8 years. Sea surface temperatures were held fixed. The direct radiative and semi-direct radiative effects and radiative forcing by aerosol were computed with the method used in

Ghan et al. [2012]. Radiative fluxes at the top of the atmosphere (TOA) are diagnosed as net solar and thermal fluxes and include scattering and absorption by clouds and aerosol particles. The direct radiative effect (DRE) of BC and dust is computed as difference between the radiative fluxes at TOA for the model simulation including the aerosol species and the simulation excluding this aerosol type. The instantaneous direct radiative effect (IDR) by the individual aerosol species is computed by double calls to the radiation routine. This diagnoses the instantaneous radiative effect without influencing the atmospheric conditions. The semi-direct effect (SDE) is subsequently calculated as residual of the direct radiative and the instantaneous radiative effect. The indirect effects of the aerosol particles on cloud microphysical properties are not considered here.

Results and Discussion

The aerosol optical depth has been evaluated and the BC radiative effects including the effects of dust on this effect have been evaluated in *Tegen and Heinold* [2018, 2019].

Global average aerosol optical thicknesses are 0.09 overall, of which 0.03 is due to dust aerosol. Average absorbing optical thickness is 0.003. In comparison, *Myhre et al.* [2013] specifies absorbing aerosol optical thickness of 0.002 for multi-model median values of anthropogenic aerosols.

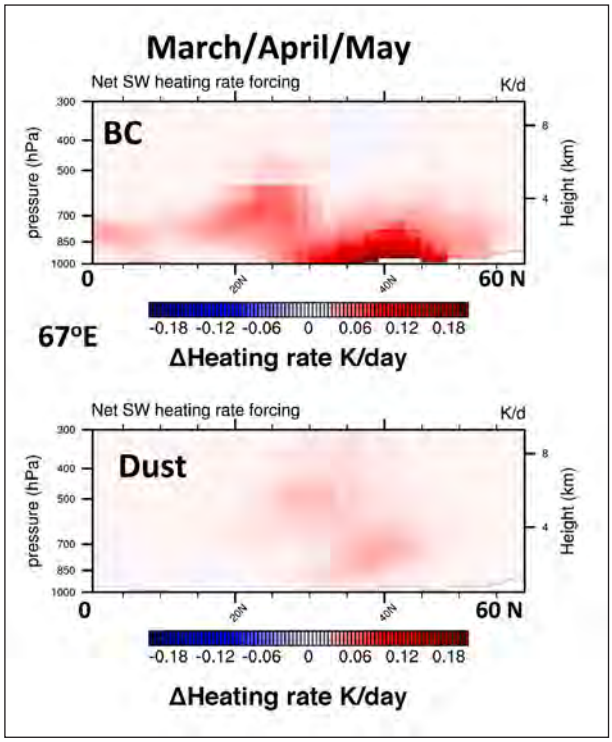

Fig. 1: Instantaneous heating differences due to simulated BC (top panels) and dust aerosol (bottom panels) at 67°E (Central Asia), averaged for 8 years, March-May.

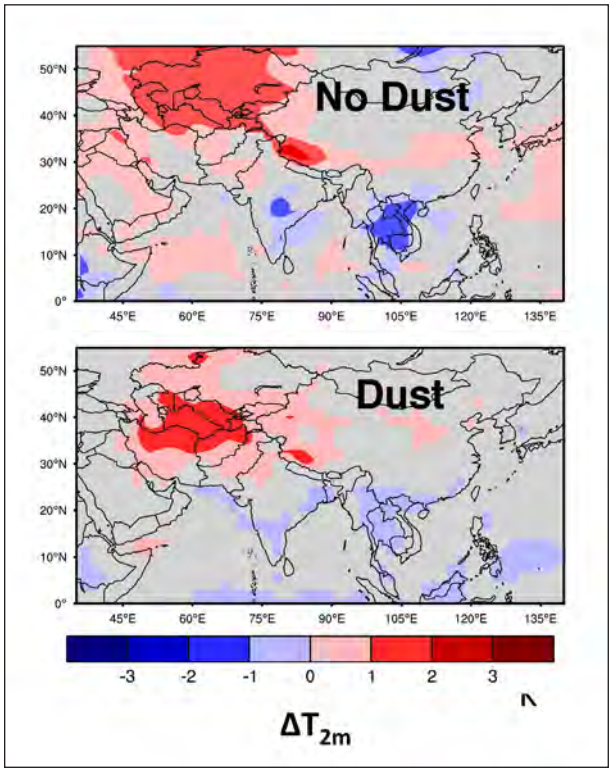

Fig. 2: 2-m temperature difference due to BC forcing without (top) and with the presence of mineral dust aerosol (bottom); 8-year average for March-May.

In the ECHAM6-HAM2 model the global annual mean of the DRE by BC aerosol is +0.5 Wm^{-2} and the IDR is +0.4 Wm^{-2}, which is close to the value in *IPCC* [2013] . The semi-direct effect computed as residual between the DRE and the IDR has the global average +0.1 Wm^{-2}, with a standard deviation of 0.5 Wm^{-2}. The regional distribution of the positive SDE is evident in the biomass burning regions in the Sahel and South American regions, but also over parts of the Sahara Desert. The SDE is mainly the consequence of changes in cloud cover due to changes in atmospheric heating rates by aerosol absorption. Decreasing cloud cover is related to a positive radiative forcing due decreased backscatter of incoming solar radiation. The linear regression coefficient between the changes in SDE to cloud cover is (–1.1Wm^{-2})/(% cloud cover) (r2=0.69). The semi-direct effect is positive for eastern Asia but negative in south India (not at the location of the maximum forcing), primarily due to an enhancement in cloud cover. The direct and semi-direct effects are positive in Central Asia, however the results for the semi-direct effect are not statistically significant in most locations.

IDR of BC is positive over the Sahara and North Atlantic. While over the Sahara the positive BC forcing

is due to the high surface albedo, the positive forcing of the BC over the Atlantic downwind of the Sahara is partly due to the reflectivity of underlying mineral dust aerosol. The direct radiative effect of BC above the comparably bright dust layer leads to additional positive forcing. Excluding dust aerosol from the model reduces BC forcing to +0.2 Wm^{-2} for DRE and to +0.3 Wm^{-2} for IDR, and the SDE is negative in the global average with –0.03 Wm^{-2}. SDE is positive in Central and East Asia particularly in spring and early summer, but is reduced if elevated mineral dust layers are present. Figure 1 shows the meridional distribution of heating rate changes at 67°E in the model due to the presence of black carbon and dust aerosol in northern hemisphere spring. The heating rate changes due to BC are as high as 0.2 K/day in the lower troposphere, while mineral dust is effective at higher altitudes. Changes in 2-m surface temperature as consequence of BC forcing with and without considering dust aerosol are shown in Figure 2. Without the presence of dust aerosol, BC causes significant warming of more than 1 K over large areas in Central Asia, co-located with reduced cloud cover. This effect is much reduced by the presence of overlying dust aerosol (Figure 2, lower panel). While the semi-direct effect and temperature change due to mineral dust itself is small in this region, the effect of BC is weaker when the shading by dust is taken into consideration.

The results of aerosol-climate model simulations suggest that the presence of mineral dust may enhance or reduce the radiative effect due to BC absorption, depending on the relative height of the aerosol layers. However, the overall effect is uncertain and may be model-dependent as simulated aerosol and cloud distributions contain uncertainties and the results may differ for different model sensitivities.

References

Ghan, S. J., X. Liu, R. C. Easter, R. Zaveri, P. J. Rasch, J.-H. Yoon, and B. Eaton (2012), Toward a Minimal Representation of Aerosols in Climate Models: Comparative Decomposition of Aerosol Direct, Semidirect, and Indirect Radiative Forcing, *Journal of Climate*, *25*(19), 6461-6476, doi: 10.1175/jcli-d-11-00650.1.

IPCC (2013), *Climate Change 2013: The Physical Science Basis. Contribution of Working Group I to the Fifth Assessment Report of the Intergovernmental Panel on Climate Change*, 1535 pp., Cambridge University Press, Cambridge, United Kingdom and New York, NY, USA.

Koch, D., and A. D. Del Genio (2010), Black carbon semi-direct effects on cloud cover: review and synthesis, *Atmos. Chem. Phys.*, *10*(16), 7685-7696, doi: 10.5194/acp-10-7685-2010.

Myhre, G., B. H. Samset, M. Schulz, Y. Balkanski, S. Bauer, T. K. Berntsen, H. Bian, N. Bellouin, M. Chin, T. Diehl, R. C. Easter, J. Feichter, S. J. Ghan, D. Hauglustaine, T. Iversen, S. Kinne, A. Kirkevåg, J. F. Lamarque, G. Lin, X. Liu, M. T. Lund, G. Luo, X. Ma, T. van Noije, J. E. Penner, P. J. Rasch, A. Ruiz, Ø. Seland, R. B. Skeie, P. Stier, T. Takemura, K. Tsigaridis, P. Wang, Z. Wang, L. Xu, H. Yu, F. Yu, J. H. Yoon, K. Zhang, H. Zhang, and C. Zhou (2013), Radiative forcing of the direct aerosol effect from AeroCom Phase II simulations, *Atmos. Chem. Phys.*, *13*(4), 1853-1877, doi: 10.5194/acp-13-1853-2013.

Tegen, I., and B. Heinold (2018), Large-Scale Modeling of Absorbing Aerosols and Their Semi-Direct Effects, *Atmosphere*, *9*(10), 380.

Tegen, I., and B. Heinold (2019), Dust impacts on radiative effects of black carbon aerosol in Central Asia, *E3S Web Conf.*, *99*, 04005.

Tegen, I., D. Neubauer, S. Ferrachat, C. Siegenthaler-Le Drian, I. Bey, N. Schutgens, P. Stier, D. Watson-Parris, T. Stanelle, H. Schmidt, S. Rast, H. Kokkola, M. Schultz, S. Schroeder, N. Daskalakis, S. Barthel, B. Heinold, and U. Lohmann (2019), The global aerosol–climate model ECHAM6.3–HAM2.3 – Part 1: Aerosol evaluation, *Geosci. Model Dev.*, *12*(4), 1643-1677, doi: 10.5194/gmd-12-1643-2019.

Zhang, K., D. O'Donnell, J. Kazil, P. Stier, S. Kinne, U. Lohmann, S. Ferrachat, B. Croft, J. Quaas, H. Wan, S. Rast, and J. Feichter (2012), The global aerosol-climate model ECHAM-HAM, version 2: sensitivity to improvements in process representations, *Atmos. Chem. Phys.*, *12*(19), 8911-8949, doi: 10.5194/acp-12-8911-2012.

Cooperation

ETH Zurich, Switzerland;
DKRZ, Hamburg.

Pyro-convectively driven emissions of mineral dust – a model approach

Robert Wagner, Kerstin Schepanski

Die Emission von Mineralstaub in die Atmosphäre wird gewöhnlich fast ausschließlich mit Winderosion infolge meteorologischer Prozesse in Verbindung gebracht. Jedoch findet man auch in den Rauchfahnen von Vegetationsbränden häufig Spuren von Mineralstaub, welcher von den feuer-induzierten Winden aufgewirbelt wird. Im Rahmen idealisierter Modelstudien wird das Potential verschiedener Arten von Vegetationsbränden hinsichtlich ihrer Staubemissionseigenschaften untersucht. Dafür werden zwei konzeptionell unterschiedlichen Parametrisierungen verwendet: Staubeintrag durch Saltation und der direkte aerodynamische Staubeintrag. Hierbei zeigt sich, dass nicht nur die Feuereigenschaften, sondern auch die Windbedingungen in der Feuerumgebung das Staubemissionspotential stark beeinflussen können. Da die feuer-induzierten Windfelder stark konvektiv geprägt sind, erscheint eine Parametrisierung des direkten Staubeintrags geeigneter, um die pyro-konvektiven Staubemissionen zu beschreiben. Um jedoch die ablaufenden Prozesse realitätsnah erfassen zu können, ist ausgehend von den gezeigten Ergebnissen die Entwicklung einer angepassten Parametrisierung erforderlich, um diesen Staubemissionsprozess in Aerosol-Klima-Modelle einbinden und dessen Auswirkungen untersuchen zu können.

Introduction

Mineral dust is an important natural aerosol type with manifold impacts on the atmosphere and our modern life. Its emission is attributed nearly exclusively to wind-driven erosion processes initiated by natural weather phenomena that are associated with strong near-surface wind velocities. However, a growing number of studies have also found admixtures of mineral dust particles in smoke plumes originating from wildfire activity [e.g., *Nisantzi et al.*, 2014; *Schlosser et al.*, 2017]. Conceptual models present in the literature indicate that the strong pyro-convective updraft, which develops above the fire, can result into the formation of a convergence at the surface, ultimately related to strongly enhanced near-surface winds. These enhanced winds are able to mobilize soil-dust particles and eventually inject them into the atmosphere through the fire's updraft as shown schematically in Fig. 1. Additionally, the fire burns and thus removes almost all soil-covering vegetation quite efficiently. It further can modify the soil properties in such a way that most likely the soil's susceptibility to wind erosion is increased. [e.g., *Ravi et al.*, 2012].

As wildfires are a major anthropogenically driven component of the Earth system and expected to increase in frequency and severity due to climate change, fires might represent a noteworthy source of airborne mineral dust at regional or even global scale. However, the efficiency of wildfires as a dust generating process has not been investigated so far. Thus, this process is currently not considered in state-of-the-art dust production models. To close the gap, the study presented here aims at (1) elaborating the impacts of wildfires on the near-surface wind patterns and their availability to foster dust emission; and (2) investigating the strength of the resulting dust emission fluxes and their dependency on different fire and ambient wind properties with respect to the applied dust emission parameterisation.

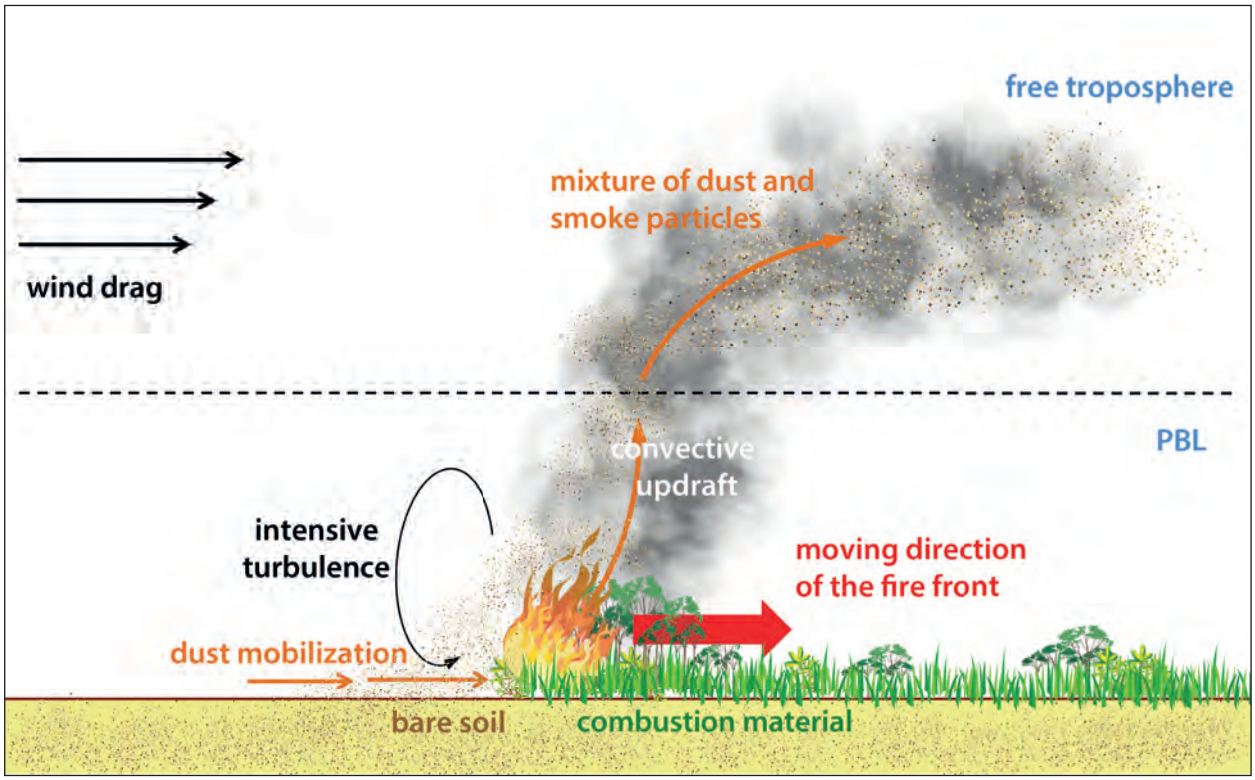

Fig. 1: Conceptional model of fire-driven emissions of mineral dust. Figure following Wagner et al. [2018].

Methods

Large-eddy simulation. A variety of likely fire setups is defined comprising different types of wildfires ranging from weak crop- and grassland fires to more intense shrubland fires including different sizes and changing ambient wind conditions. The impact of these fire setups onto the near-surface wind field ultimately driving dust entrainment are investigated by a simplified setup by means of large-eddy simulation (LES). The complexity of the model approach is kept low as only the fire impacts on the lower atmospheric conditions is in focus of this study. Thus, the fire can be described by a predefined sensible heat flux at the surface that represents the thermal effect of the fire.

Dust emission modelling. To investigate the dust emission potential of wildfires more closely, the fire-affected near-surface wind patterns obtained from the LES runs are used to drive two well established but conceptionally quite different dust emission parameterisation approaches: Saltation bombardment based on *Tegen et al.* [2002]; and direct aerodynamic entrainment following *Klose et al.* [2014]. To ensure a high level of comparability, both dust emission schemes are run with similar, idealized soil-surface conditions that include a complete consumption of the soil-covering vegetation, no residual soil moisture, a minimal roughness length and a sandy loam soil texture which is typical for fire-prone landscapes.

Results & Discussion

The results of the LES simulations show that the wind patterns within and around typical wildfires are strongly modulated by the fire's heat impact [*Wagner et al.*, 2018]. This is expressed by an increase in horizontal near-surface wind speed, large updraft velocities above the fire area and a significantly enhanced atmospheric turbulence. As an example for a typical medium-sized shrubland fire exposed to an ambient wind velocity of 3 m/s, Fig. 2a provides an overview of the changes of the horizontal and vertical wind velocities in the surrounding of the fire. The changes of the near-surface wind patterns follow an increase in the friction velocity (Fig. 2b) and the instantaneous momentum flux (Fig. 2c). These are two major parameters determining dust emission driven by saltation bombardment or direct aerodynamic entrainment. The effect on dust emission flux thereby is quite sensitive to the actual fire properties and the ambient wind conditions. However typical threshold wind speeds for dust emission are generally frequently exceeded in the vicinity of fires [*Wagner et al.*, 2018]. Nonetheless, the amount of emitted dust shows a strong dependency on the applied dust emission parameterization. In particular, direct aerodynamic entrainment (Fig. 2e)

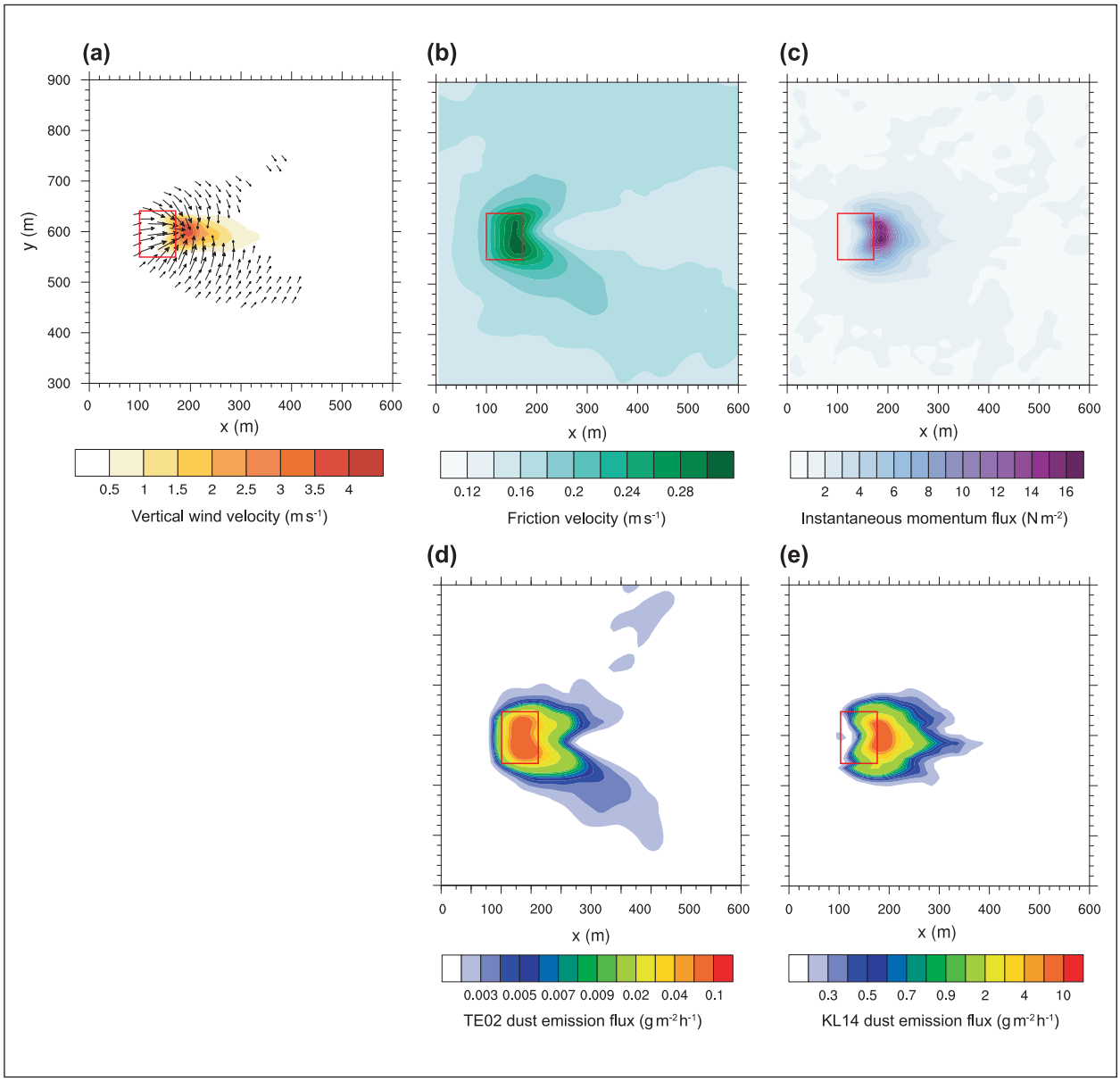

Fig. 2: Impacts of a typical wildfire on the near-surface wind patterns. Shown are (a) the major changes in the horizontal (vector deviations) and vertical (contours) wind velocity as response to the presence of the fire (represented by the red box) as well as the impacts on the (b) friction velocity and (c) the instantaneous momentum flux. Additionally, the dust emission fluxes resulting from the parameterization of (d) saltation bombardment and (e) direct aerodynamic entrainment.

is usually related to much larger dust emission fluxes than saltation bombardment (Fig. 2d), since the fire-affected wind field is strongly dominated by turbulent convective motions and thus large instantaneous momentum fluxes. In contrast, the impact on the friction velocity remains small. But saltation bombardment can still contribute to the dust emission flux during suitable circumstances such as strong ambient winds or large fires.

As no parameterisation approach is designed to handle the specific wind conditions present in the vicinity of wildfires, a sophisticated parameterization will be developed to allow for a realistic description of pyro-convectively driven dust emissions within aerosol-climate-models. The results presented here shall be seen as a first step towards the improved representation of this process.

References

Klose, M., Y. Shao, X. Li, H. Zhang, M. Ishizuka, M. Mikami, and J. F. Leys (2014), Further development of a parameterization for convective turbulent dust emission and evaluation based on field observations, *J. Geophys. Res. - Atmos.*, *119*(17), 10441-10457.

Nisantzi, A., R.-E. Mamouri, A. Ansmann, and D. Hadjimitsis (2014), Injection of mineral dust into the free troposphere during fire events observed with polarization lidar at Limassol, Cyprus, *Atmos. Chem. Phys.*, *14*(22), 12155-12165.

Ravi, S., M. C. Baddock, T. M. Zobeck, and J. Hartman (2012), Field evidence for differences in post-fire aeolian transport related to vegetation type in semi-arid grasslands, *Aeolian Res.*, *7*, 3-10.

Schlosser, J. S., R. A. Braun, T. Bradley, H. Dadashazar, A. B. MacDonald, A. A. Aldhaif, M. A. Aghdam, A. H. Mardi, P. Xian, and A. Sorooshian (2017), Analysis of aerosol composition data for western United States wildfires between 2005 and 2015: Dust emissions, chloride depletion, and most enhanced aerosol constituents, *J. Geophys. Res. - Atmos.*, *122*(16), 8951-8966.

Tegen, I., S. P. Harrison, K. Kohfeld, I. C. Prentice, M. Coe, and M. Heimann (2002), Impact of vegetation and preferential source areas on global dust aerosol: Results from a model study, *J. Geophys. Res. - Atmos.*, *107*(D21), AAC 14-11-AAC 14-27.

Wagner, R., M. Jähn, and K. Schepanski (2018), Wildfires as a source of airborne mineral dust–revisiting a conceptual model using large-eddy simulation (LES), *Atmos. Chem. Phys.*, *18*(16), 11863-11884.

Funding

Leibniz SAW project “InterDust - Dust at the interface”.

Classification of dust source types from space and model implementation

Stefanie Feuerstein, Kerstin Schepanski

Winderosion von mineralischen Bodenpartikeln (Mineralstaub, Wüstenstaub) in ariden und semi-ariden Regionen der Erde trägt signifikant zur Aerosolkonzentration in der Atmosphäre bei. Die Kenntnis über Bodencharakteristika liefert einen wichtigen Beitrag zur Berechnung lokaler Staubemissionsflüsse und damit zur Bestimmung von Aerosolkonzentrationen, Ausbreitung, und Wechselwirkungen. Obwohl die Erfahrung bei der Nutzung von Satellitendaten zur Identifizierung von Staubquellen umfangreich ist, werden die Unterschiede verschiedener Staubquellen hinsichtlich ihres Erosionspotentials kaum beachtet. Durch Kombination verschiedener spektraler Informationen wurde im Rahmen dieser Arbeit eine Methode entwickelt, welche die Unterscheidung verschiedener Staubquelltypen ermöglicht und somit eine differenzierte Betrachtung im Staubemissionsmodell erlaubt.

Introduction

Mineral dust is one of the most abundant aerosols types in the atmosphere [*Shao et al., 2011*]. It has manifold impacts on the Earth system as it interacts with radiation, stimulates cloud formation and precipitation processes, and affects air quality, human health and economy. The sources of mineral dust are mostly found in semi-arid and arid environments, where the soil surface is bare, sparsely covered by vegetation, and the soil moisture is low. However, a general determination of characteristics that make a surface particularly susceptible to wind erosion cannot be given. One dust source type that has gained increasing attention in recent years is related to the presence of alluvial sediments [e.g., *Ginoux et al.,* 2012; *Schepanski et al.,* 2013]. These sediments are formed and influenced by surface water runoff. They provide a large amount of fine-grained material particularly prone to wind erosion and thus easy to entrain into the atmosphere. Although alluvial features are abundant in desert regions, they are rather small in size and are therefore generally not accounted for in dust emission models coupled into atmosphere-aerosol models. This is one reason why they are either underrepresented or completely disregarded in dust-emission models.

Method

To overcome the underrepresentation of relevant dust source types such as the alluvial sediments and, in particular, to improve their representation in dust emission models, a new dataset providing explicit information on the wind erodibility potential of individual dust source types is developed and tested in a dust emission model. To explicitly distinguish between different dust source types, which ultimately allows for treating individual source types differently in a parameterization, an approach is developed to automatically detect the two most abundant sediment types acting as dust source: Alluvial sediments and dune/sand covers [*Feuerstein & Schepanski, 2019*]. Overall, the approach is based on two characteristics allowing for identifying alluvial sediments: First, alluvial sediments are marked by a high reflectance in the visible part of the wavelength spectrum, but also at near and shortwave infrared wavelengths [*El Bastawesy et al.,* 2009]. Second, alluvial sediments accumulate where surface water deposits its sediment loads in the lower part of a river catchment [*Zender et al.*, 2003]. To account for the reflectance behaviour of alluvial sediments, a red-green-blue (RGB) false-colour image is created that consists of visible, near and shortwave infrared channels using

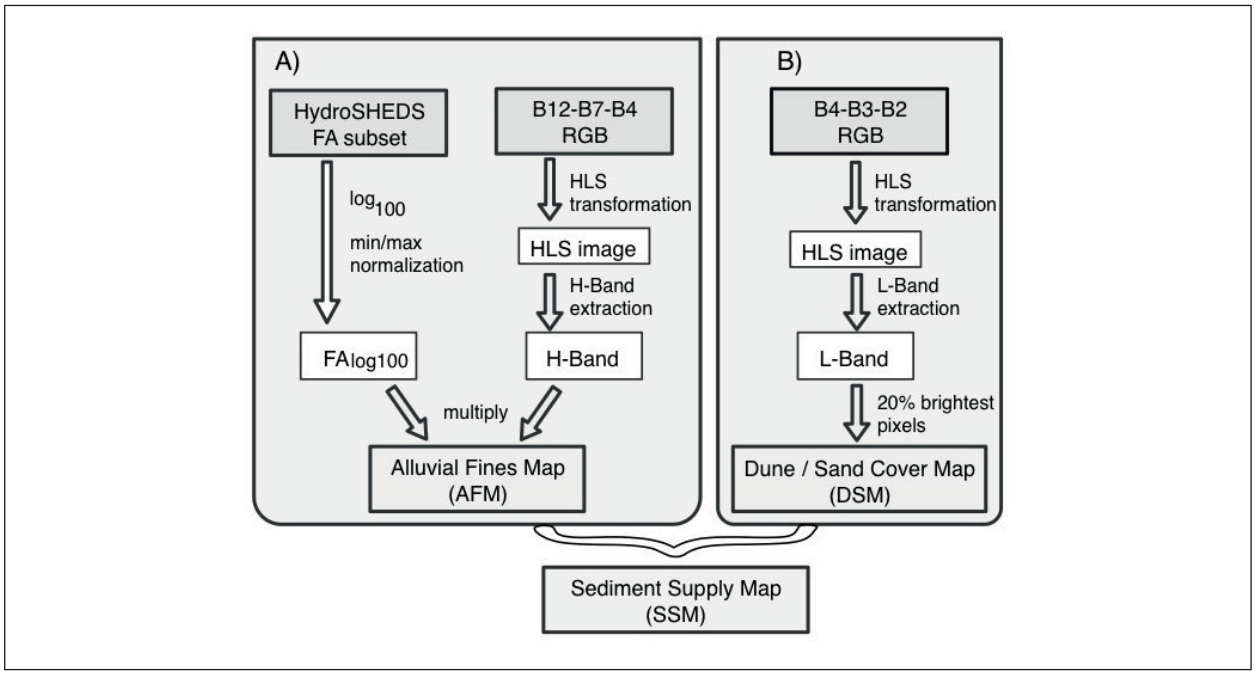

Fig. 1: Flow chart summarizing the extraction of the two components of the final Sediment Supply Map (SSM): The Alluvial Fines Map (AFM) is calculated from Sentinel-2 measurements (bands B12, B7, and B4) and combined with information on the flow accumulation provided by the HydroSHEDS dataset (A). The derivation of the Dune/Sand Cover Map (DSM) follows a similar approach but taking Sentinel-2 measurements at band B4, B3, and B2 (B). Figures taken from Feuerstein & Schepanski [2019].

measurements from the Sentinel-2 spectro-radiometer (Fig. 1A). A hue-band transformation of the RGB colour model holds particularly high values for alluvial features. The fact that the probability of alluvial sediments increases further downstream a river catchment is accounted for by using the HydroSHEDS flow accumulation dataset. This dataset provides the number of upstream pixels for each respective pixel and hence shows its location in the local digital elevation model. In essence, high flow accumulations represent strong water discharges and thus high chances for high sediment loadings that eventually will be deposited where the water flow slows down. The information derived from the hue-band and the flow accumulation are combined into a map representing the spatial distribution of alluvial fine material. Similar to the approach identifying alluvial fines, dunes and sand cover are identified (Fig. 1. B). Combined into a so-called sediment supply map (Fig. 1), this information can be used directly as information layer in dust emission models in order to assign different erodibility potentials based on the present dust source (sediment) type.

Results and concluding discussion

The new developed information layer was implemented in a dust emission model. For a known dust hot-spot region located around the Aïr Massif in the central Sahara, multi-annual simulations of dust emission fluxes were performed exemplarily and validated against (a) observed dust source activation frequencies [DSAF, *Schepanski et al., 2012*] and (b) a control run using the original model set up, which did not explicitly account for different dust source types. Generally, dust emission flux simulations using the updated model setup including an explicit representation of different dust source types reproduce well the spatial and seasonal differences characterising the main activity of the identified dust sources (Fig. 2). This becomes particularly obvious in comparison with the control model run (Fig. 2C and D), which does not include an explicit representation of alluvial sediment features. Furthermore, the control run was not able to reproduce the seasonality of dust source activation [*Feuerstein & Schepanski, 2019*].

In a nutshell, the results of this study highlight the importance of an explicit consideration of individual dust source types, in particular of alluvial features, which are a predominant dust source type [*Ginoux et al., 2012*]. Due to the global availability of the satellite data, the approach to detect alluvial features in arid environments can be implemented in regional, continental or even global studies. Long-term emission fluxes can be used to identify the influence of meteorological patterns on dust emission and can help to estimate dust fluxes under current conditions but also in a changing climate.

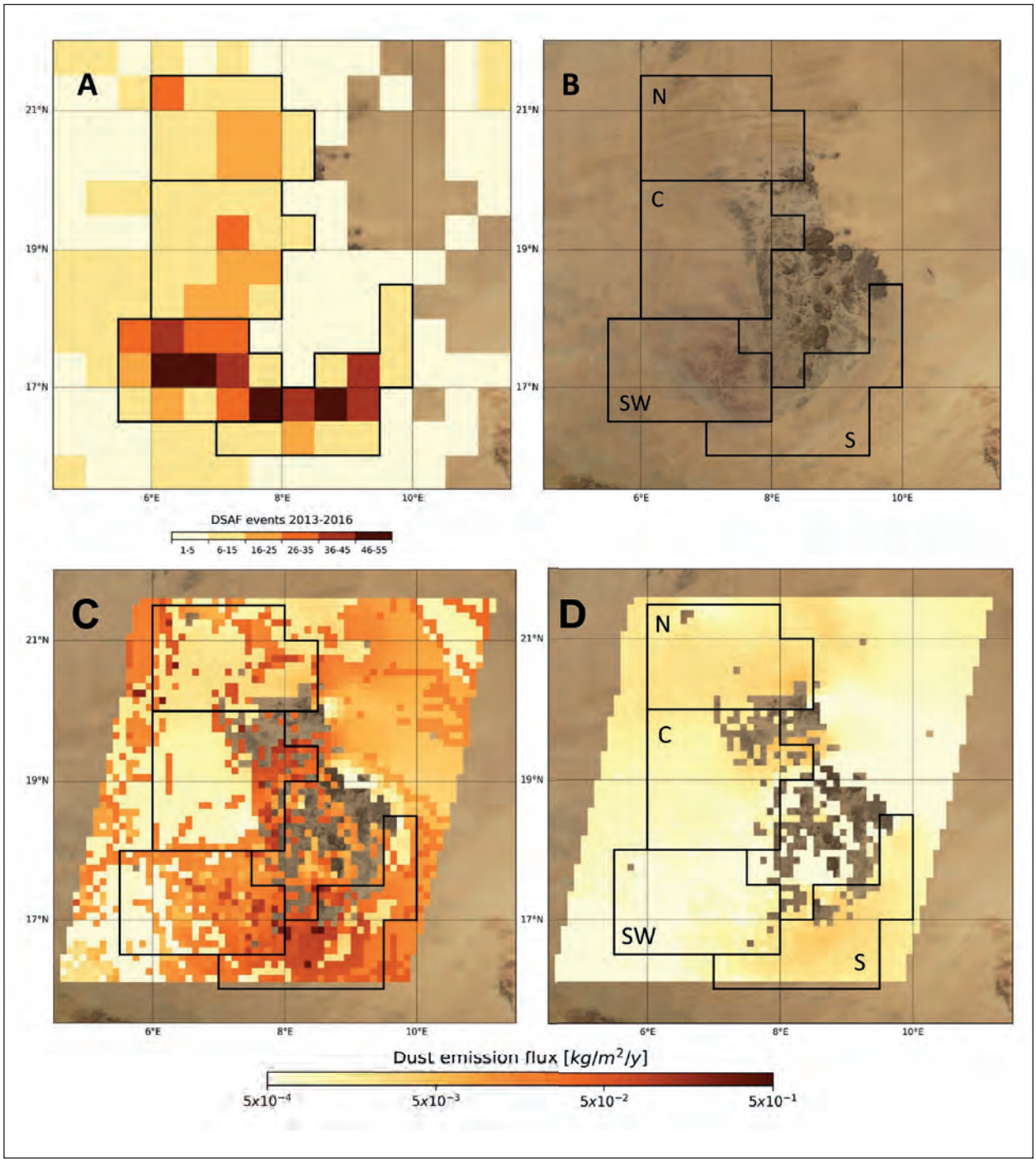

Fig. 2: Model application of the SSM. (A) shows the total number of dust events for the Air Massif identified from MSG Desert-Dust RGB images (2013-2016). Panel (B) shows a true-colour image of the study area including hot-spot zones discussed in Feuerstein & Schepanski [2019]. Panels (C, SSM run) and (D, control run) illustrate results from the model implementation. Figures taken from Feuerstein & Schepanski [2019].

References

El Bastawesy, M., K. White, and A. Nasr (2009), Integration of remote sensing and GIS for modelling flash floods in Wadi Hudain catchment, Egypt, Hydrological Processes, 23, 1359-1368, doi:10.1002/hyp.7259.

Feuerstein S., and K. Schepanski (2019), Identification of Dust sources in a Saharan Dust Hot-Spot and Their Implementation in a Dust-Emission Model, Remote Sensing, 11, 4, doi:10.3390/rs11010004.

Ginoux, P., J. M. Prospero, T. E. Gill, N. C. Hsu, and M. Zhao (2012), Global-scale attribution of anthropogenic and natural dust

sources, and their emission rates based on MODIS Deep Blue aerosol products, Reviews of Geophys., 50, RG3005, doi:10.1029/2012RG000388.

Schepanski, K., I. Tegen and A. Macke (2012), Comparison of satellite based observations of Saharan dust source areas, Remote Sensing of Environment, 123, 90-97, doi:10.1016/j.rse.2012.03.019.

Schepanski, K., C. Flamant, J.-P. Chaboureau, C. Kocha, J. R. Banks, H. E. Brindleym C. Lavaysse, F. Marnas, J. Pelon, and P. Tulet (2013), Characterization of dust emission from alluvial sources using aircraft observations and high-resolution modeling, J. Geophys. Res., 118, 7237-7259, doi:10.1002/jgrd.50538.

Shao, Y., K. H. Wyrwoll, A. Chappell, J. Huang, Z. Lin, G. H. MacTainsh, M. Mikami, T. Y. Tanaka, X. Wang, S. Yoon (2011), Dust cycle: An emerging core theme in Earth system science. Aeolian Research, 2, 181-204, doi:10.1016/J.AEOLIA.2011.01.001.

Zender, C.S., H. Bian, D. Newman (2003), Mineral Dust Entrainment and Deposition (DEAD) model: Description and 1990s dust climatology, J. Geophys. Res., 2003, 108, D17, doi:10.1029/2002JD003039.

Funding

Leibniz Association.

The Colour of Dust Aerosol in SEVIRI Composite Imagery

Jamie R. Banks[1], Anja Hünerbein[1], Bernd Heinold[1], Helen E. Brindley[2], Hartwig Deneke[1], and Kerstin Schepanski[1]

[1] Leibniz Institute for Tropospheric Research (TROPOS), Leipzig, Germany
[2] Space and Atmospheric Physics Group, and NERC National Centre for Earth Observation, Imperial College London, London, UK

Der Einfluss der atmosphärischen Zusammensetzung und der Bodeneigenschaften auf die Farbe des Staubaerosols in MSG-SEVIRI Falschfarbenbildern wurde mit dem Aerosoltransportmodell COSMO-MUSCAT und dem Strahlungstransfermodell RTTOV analysiert. Die resultierende „Staub"-Farbe in den RGB-Komposit-Bildern wurde in Bezug auf die Oberflächentemperatur, die Luftfeuchtigkeit und die Höhe der Staubschicht untersucht. Staub erscheint in den Bildern pink, bedingt durch hohe Rot-Werte im RGB-Farbschema. Dies wird besonders deutlich, wenn die Atmosphäre trocken ist, die Staubschicht optisch dick und in größere Höhen liegt.

Introduction

Desert dust aerosol may be effectively observed over the Sahara and the Middle East using "Desert Dust" [*Lensky & Rosenfeld*, 2008] false-colour infrared imagery from the SEVIRI (Spinning Enhanced Visible and InfraRed Imager) instrument onboard the Meteosat Second Generation satellites, positioned in geostationary orbit over the eastern Atlantic. Such images have been routinely used for dust identification and monitoring over the past 15 years, and are based upon brightness temperatures differences between the SEVIRI channels at 8.7, 10.8, and 12.0 µm. Fig. 1 provides an example of such an image, which clearly depicts a large Saharan dust storm over the border between Algeria and Mali, marked by characteristically deep pink colours, in clear contrast with the light blue background desert surface.

It is obvious that the atmospheric and surface environment drives dust storm activity, but it may be less obvious that the background environment also affects the capability of measuring and imaging dust activity from satellite observational data. For example, it is known that atmospheric moisture can hide the presence of dust, especially in infrared measurements and imagery [*Brindley et al.*, 2012].

Methods

Dust concentration output from the aerosol transport model COSMO-MUSCAT (COnsortium for Small-scale MOdelling, MUltiScale Chemistry Aerosol Transport Model [*Wolke et al.*, 2012]), which simulates dust emission and transport, is combined with the radiative transfer model RTTOV (Radiative Transfer for TOVs [*Saunders et al.*, 2018]) in order to simulate the SEVIRI measurements and imagery that would be produced for a given atmospheric dust distribution and atmospheric environment. This approach was used previously to simulate the effects of varying dust optical properties on the SEVIRI imagery [*Banks et al.,* 2018]. Simulations were performed at a spatial resolution of 28 km over North Africa, for the Junes and Julys of 2011-2013. The strength of this approach is that the resultant dust colours may readily be compared with co-located information on the surface and atmospheric environment, and on the properties of the dust layer.

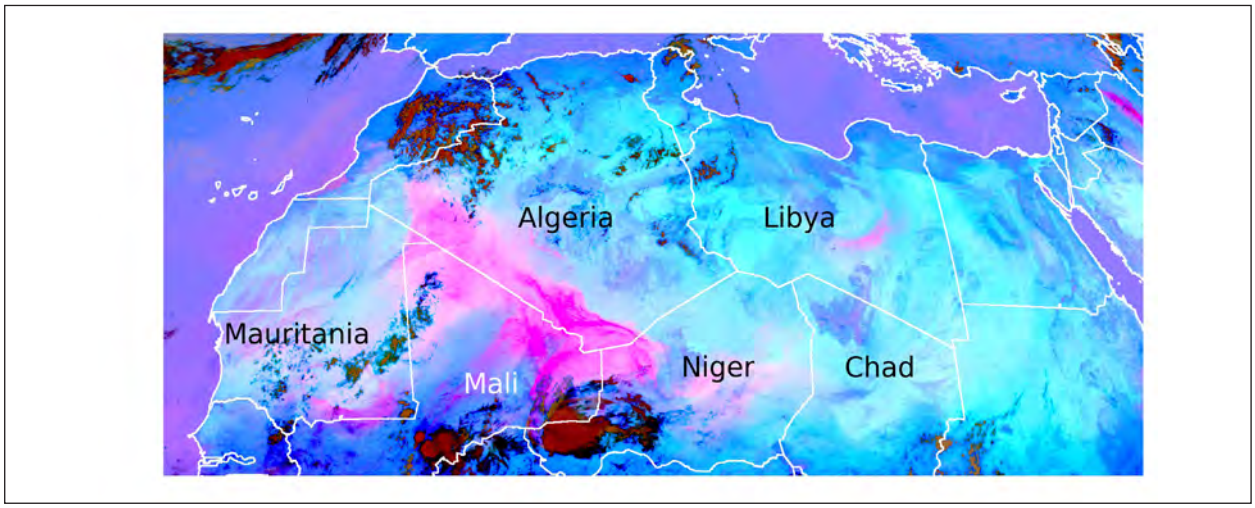

Fig. 1: SEVIRI Desert Dust RGB image from 12:00 UTC on 17th June 2012.

Results and Discussion

Simulated Desert Dust colours are depicted in Fig. 2 [*Banks et al.*, 2019], categorised by the Aerosol Optical Depth (AOD), the surface thermal emissivity, the surface skin temperature, the atmospheric column moisture, and the dust altitude. The deepest red, and hence pink, colours are apparent for the thickest dust loadings, the driest atmospheres, and for the most elevated dust layers. Conversely the bluest colours are apparent for dust-free and wet atmospheres, over hot surfaces.

Under dust-free conditions, the importance of the skin temperature is related to the differences in atmospheric transmission between the three SEVIRI channels: especially under dry conditions, the transmission at 10.8 µm is greater than for the other two channels. The red beam of the imagery is defined by the difference in the brightness temperatures between the 12.0 and 10.8 µm channels, hence, if the transmission is greater at 10.8 µm, then this brightness temperature difference will be greater when the surface is cool and lower when the surface is hot. This gives rise to redder/pinker colours when

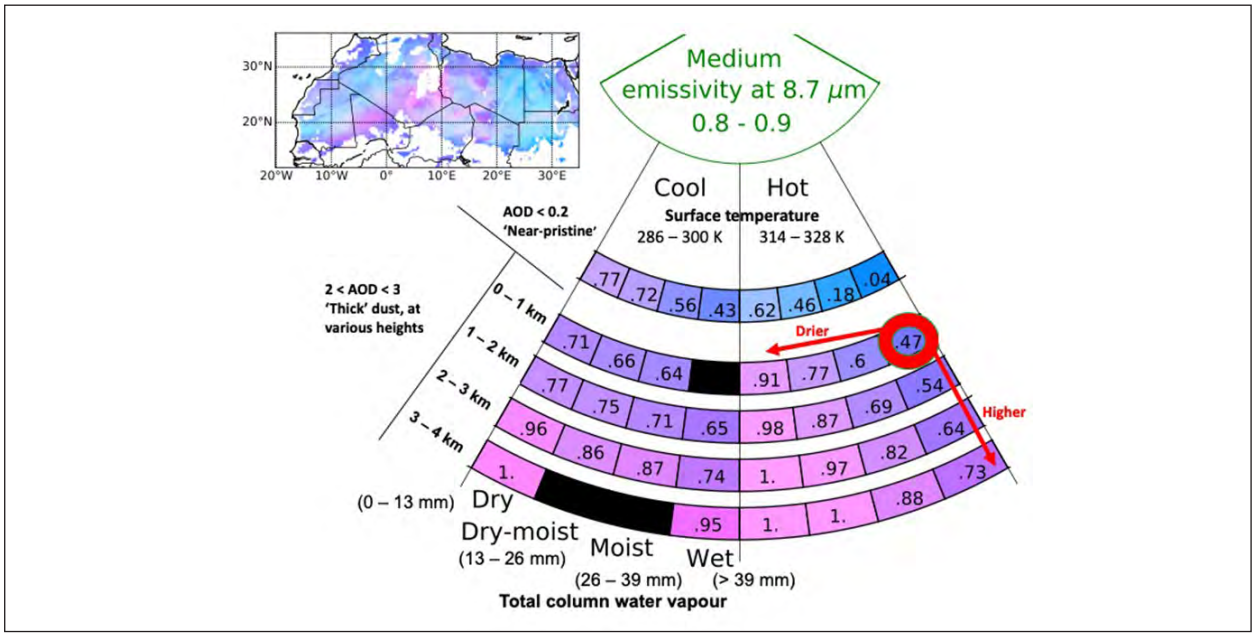

Fig. 2: Mean Desert Dust RGB colours simulated by COSMO-MUSCAT-RTTOV, subdivided into ranges of skin temperature (cool - very hot), column moisture (dry-wet), and dust altitude. Values increase in an anticlockwise direction, as indicated. The numbers marked on each segment indicate the mean red value, to two decimal places. Black segments indicate coincident conditions not contained within this data subset. Inset: Simulated SEVIRI Desert Dust RGB image, 1200 UTC, 17th June 2012.

the surface is cool, and leads also to a diurnal cycle in the apparent colour of the desert surface.

Moisture is most absorbing of atmospheric radiation in the 12.0 μm channel, which means that wet atmospheres suppress the brightness temperatures at 12.0 μm more than that at 10.8 μm, leading to weaker red colours and hence bluer resultant colours.

Introducing dust into the analysis, generally the near-pristine colours tend to appear bluer than the thick dust colours, which are redder and hence pinker. Dust has its peak in spectral extinction at 10.8 μm, which means that the brightness temperature of this channel is reduced the most in the presence of dust, giving rise to redder, pinker, colours. Considering dust and moisture, red signals for a given amount of dust are at their weakest in the wettest atmospheres, confirming that moisture acts to "hide" the presence of dust in the IR imagery. Moist dust can therefore appear more purple.

High-altitude dust layers display similar properties to dust layers in dry atmospheres. The reason for this is that the atmosphere above a high-altitude dust layer is drier than the atmosphere above a low-altitude dust layer, due to the atmospheric optical path length from the dust layer to the satellite. Hence the brightness temperature at 12.0 μm is reduced the least for dry atmospheres and/or for high altitude dust layers, and hence dry and/or high dust displays the deepest red and pink colours.

Users of the imagery may find this analysis helpful when assessing the strengths and weaknesses of the imagery as a dust identification and tracking tool. In particular, users should be aware of the environmental properties that affect the appearance of the dust imagery, to avoid erroneously attributing these effects to dust properties.

References

Banks, J. R., A. Hünerbein, B. Heinold, H. E. Brindley, H. Deneke, and K. Schepanski (2019), The sensitivity of the colour of dust in MSG-SEVIRI Desert Dust infrared composite imagery to surface and atmospheric conditions, *Atmos. Chem. Phys.*, *19*(10), 6893-6911, 10.5194/acp-19-6893-2019.

Banks, J. R., K. Schepanski, B. Heinold, A. Hünerbein, and H. E. Brindley (2018), The influence of dust optical properties on the colour of simulated MSG-SEVIRI Desert Dust infrared imagery, *Atmos. Chem. Phys.*, *18*(13), 9681-9703, 10.5194/acp-18-9681-2018.

Brindley, H., P. Knippertz, C. Ryder, and I. Ashpole (2012), A critical evaluation of the ability of the Spinning Enhanced Visible and Infrared Imager (SEVIRI) thermal infrared red-green-blue rendering to identify dust events: Theoretical analysis, *Journal of Geophysical Research: Atmospheres*, *117*(D7), 10.1029/2011JD017326.

Lensky, I. M., and D. Rosenfeld (2008), Clouds-Aerosols-Precipitation Satellite Analysis Tool (CAPSAT), *Atmos. Chem. Phys.*, *8*(22), 6739-6753, 10.5194/acp-8-6739-2008.

Saunders, R., J. Hocking, E. Turner, P. Rayer, D. Rundle, P. Brunel, J. Vidot, P. Roquet, M. Matricardi, A. Geer, N. Bormann, and C. Lupu (2018), An update on the RTTOV fast radiative transfer model (currently at version 12), *Geosci. Model Dev.*, *11*(7), 2717-2737, 10.5194/gmd-11-2717-2018.

Wolke, R., W. Schröder, R. Schrödner, and E. Renner (2012), Influence of grid resolution and meteorological forcing on simulated European air quality: A sensitivity study with the modeling system COSMO–MUSCAT, *Atmos. Environ.*, *53*, 110-130, https://doi.org/10.1016/j.atmosenv.2012.02.085.

Funding

The Leibniz Association provided funding for the project "Dust at the Interface - modelling and remote sensing" (grant no. P79/2014).

Validation of Aeolus wind and aerosol products utilizing PollyNET, LACROS, and radiosondes

Holger Baars, Alina Herzog, Birgit Heese, Ronny Engelmann, Johannes Bühl, Martin Radenz, Dietrich Althausen, Patric Seifert, Albert Ansmann, Ulla Wandinger

Seit dem Start der ESA Earth Explorer Mission namens Aeolus im August 2018 ist TROPOS intensiv an dessen Validierungsaktivitäten beteiligt. Dabei werden die Aerosol- und Windprodukte von Aeolus mit PollyNET-, Doppler-Wind-Lidar- und Wolkenradarmessungen sowie zusätzlich gestarteten Radiosonden evaluiert. TROPOS nutzt jede sich bietende Möglichkeit der Evaluierung des polarumlaufenden Satelliten, so zum Beispiel die Polarsternfahrt PS116 über den Atlantik kurz nach Beginn der Mission. Weitere Schwerpunkte der Aktivitäten sind die PollyNET-Beobachtungen im globalen Staubgürtel und die LACROS-Messungen in der Südhemisphäre.

Introduction

The European Space Agency (ESA) has launched the Earth Explorer Mission *Aeolus* on 22 August 2018. This mission aims to demonstrate significant improvement in weather forecasting by measuring height-resolved wind profiles in the troposphere and lower stratosphere [*ESA*, 2008]. The instrument onboard, named ALADIN (Atmospheric Laser Doppler Instrument), is the first lidar instrument on a European satellite. It is also the first space-borne instrument capable of measuring vertical profiles of wind on a global basis. Next to wind measurements, aerosol properties can be obtained as a spin-off product via the high-spectral-resolution-lidar (HSRL) technique, which is a space-borne novelty as well. Within the German initiative EVAA (Experimental Validation and Assimilation of Aeolus observations), TROPOS has been strongly involved in Calibration/Validation (Cal/Val) activities of this space mission from the beginning. The aim is to validate the wind and aerosol products of Aeolus and to quantify the benefits of these new measurements for weather forecasting. TROPOS utilized all possible instrument suites for this purpose. Namely, lidar observations with PollyNET [see long report and *Engelmann*, 2016], Doppler lidar and Doppler cloud radar measurements with LACROS, and additional radiosonde launches have been utilized for every opportunity of collocated measurements [*Baars*, 2019, LPS].

Figure 1 shows the locations which have been used for Aeolus Cal/Val by TROPOS together with the weekly Aeolus ground-tracks (magenta). Aerosol and wind lidar observations have been performed at Leipzig (Germany), Punta Arenas (Chile), and onboard Polarstern across the Atlantic Ocean. Aerosol-only observations were made at the PollyNET stations in Haifa (Israel), Dushanbe (Tajikistan), Tel Aviv (Israel), and at the United Arab Emirates (UAE) - the latter two are hosted by PollyNET partner institutions [*Baars*, 2016]. In the following, a few examples of the validation efforts are given.

Wind Cal/Val

Validation efforts of TROPOS for Aeolus started immediately after the instrument was turned on in space. One of the first opportunity measurements could be performed during the Polarstern cruise PS116 in Autumn 2018, in the framework of the TROPOS OCEANET activities. Thanks to the Polarstern crew flexibility, the course was adjusted so that in total seven points of intersection with the Aeolus ground track (within a radius of 150 km) were reached

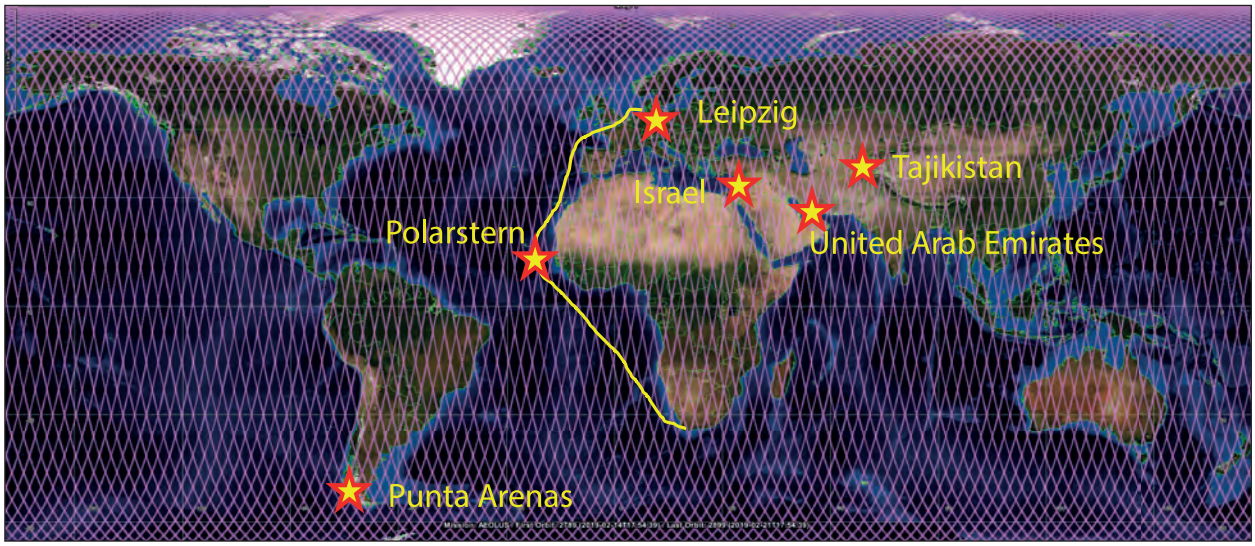

Fig. 1: Map of locations used for Cal/Val by TROPOS. The Aeolus ground track during its weekly repeat cycle is underlaid (magenta).

across the Atlantic. At these locations, additional radiosondes were launched [*Herzog et al.*, 2019].

Figure 2, left, shows wind velocity profiles measured with the radiosonde (red) and data from the closest Aeolus overpass on 29 November 2018. So-called "Rayleigh" winds (blue) are obtained with Aeolus in clear air from molecular scattering while the "Mie" (cyan) winds are obtained in clouds from scattering processes at cloud particles. The Mie measurements are in good agreement with the radiosonde measurements, even though they are only available for a limited height range. Regarding the Rayleigh clear measurements, a positive bias in the range between 7.5 and 12 km is observed. The highly resolved radiosonde profile shows a maximum wind velocity higher than 25 m/s at the tropopause level at 15 km height, whereas such wind speeds are not recognized by the Rayleigh wind measurements of Aeolus. This deviation is caused by the low vertical resolution of the Aeolus measurements of 2 km in the higher troposphere/lower stratosphere at this time of the mission. As a result of these findings, the range-bin setting was changed to a resolution of 1 km up to an altitude of 19 km in February 2019.

In addition to the continuous Doppler lidar observations in Leipzig, radiosondes have been launched

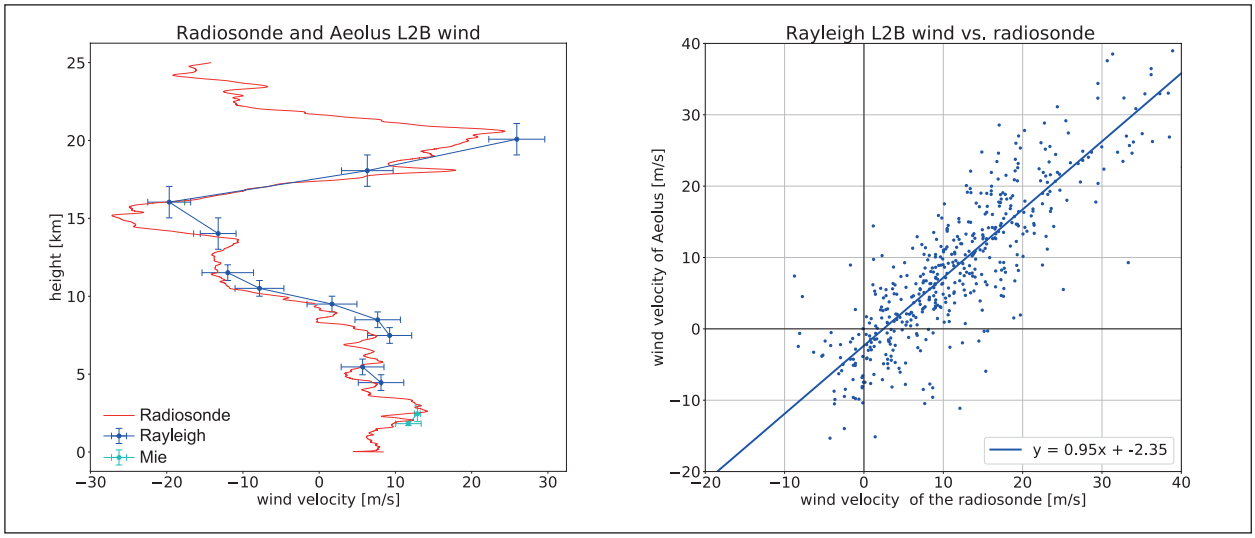

Fig. 2: Left: Wind velocity profiles measured with radiosonde (red) and the closest Aeolus Rayleigh (blue, wind obtained in clear air) and Mie data (cyan, wind obtained in clouds) over the tropical Atlantic on 29 November 2018. Polarstern had just recently passed the equator, and the distance between the research vessel and the Aeolus ground track was about 30 km. Right: Correlation between Aeolus winds and radiosonde-derived winds at Leipzig from August to November 2019. Rayleigh wind correlations are shown. As Aeolus measures only the wind along the Line-of-Sight (LOS), which is mainly the west-east wind component, the radiosonde measurements are projected to this geometry.

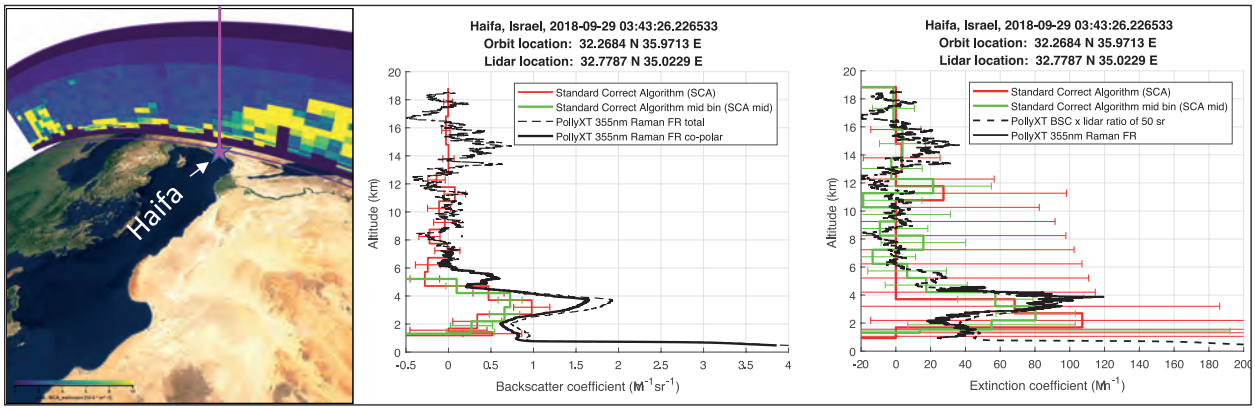

Fig. 3: Overview of the Aeolus aerosol product above the Eastern Mediterranean on 29 September 2018 and location of the PollyNET measurements at Haifa (left). Aerosol backscatter (middle) and extinction coefficients (right) for the ground-based instrument (black) in Israel and different Aeolus algorithms (red and green) during the mentioned Aeolus overpass are shown. More details in text.

during the Aeolus overpasses on each Friday since mid of May 2019 at Leipzig. Figure 2, right, shows a correlation plot between Aeolus and radiosondes at Leipzig after the switch to the second laser of Aeolus in June 2019 [*Herzog*, 2019]. A bias of ca. -2 m/s for the Rayleigh winds was observed from August to November 2019, which agrees with findings from other activities within EVAA and by ESA Cal/Val teams. Several instrumental effects are responsible for the offset. ESA is going to correct these effects in future data processing versions.

Aerosol Cal/Val

Concerning Aeolus aerosol data, the dusty locations of Israel and UAE are of particular interest. Especially in the beginning of the mission, no valid aerosol profiles could be retrieved by Aeolus in the lowermost 2 km. Thus, these locations close to the desert with frequent dense, lofted aerosol layers are very useful for Cal/Val purposes.

Figure 3 shows one example overpass at Haifa, Israel on 29th September 2018, i.e. shortly after launch [*Baars*, 2019, ILRC]. The PollyXT observations at 355 nm (middle plot: dashed black line) were transformed to the co-polar component of the circular-polarized light measured by Aeolus (thick black line) with the help of the measured linear depolarization ratio [*Wandinger*, 2015]. For Aeolus, the standard correction algorithm (SCA) and the SCA mid bin (using 2 bins to reduce noise) are shown. Considering the long horizontal averaging length of Aeolus (87 km) and the distance to the lidar (around 100 km), a good agreement between Aeolus and the ground-based lidar with respect to the co-polar backscatter coefficient is found. However, a slight height shift between the backscatter and extinction products is obvious. This problem has been reported to ESA, and the algorithm developers are working on a retrieval update. Beside the general good agreement in this case, also strong deviations have been found for other cases, when e.g. cirrus clouds are present or the scenes are horizontally heterogeneous. Then, the representativeness error of Aeolus has to be considered. As a consequence of these findings, TROPOS has proposed an adapted range-bin setting for Aeolus in the Eastern Mediterranean to test the effect of an aerosol-optimized range resolution. After agreement by ESA, the so-called Mediterranean range-bin setting (MARS) is operational for Aeolus since September 2019. First results show a significantly improved aerosol retrieval for this adapted instrumental setting.

Outlook

TROPOS Cal/Val activities for Aeolus will be continued in close collaboration with ESA and algorithm developers. One of the mission goals, namely the demonstration that wind observations from space by active remote sensing are possible, have been already achieved. Nevertheless, a number of instrumental corrections and algorithm updates are expected in the near future to further improve the results. Regardless of the challenges of such an explorer mission, a significant impact of the Aeolus measurements on the weather forecasts could be already shown recently by ECMWF. For aerosol products, it was demonstrated that the HSRL technique applied for Aeolus can provide independent backscatter and extinction measurements of aerosols – a spaceborne novelty as well. TROPOS will contribute with its expertise to the foreseen steady algorithm development by being part of expert teams advising ESA and the algorithm developers. Last but not least, a huge tropical validation campaign will be performed at Cabo Verde islands in summer 2020, including

aircraft and several ground-based instruments. TROPOS has a key role in this campaign with respect to the ground-based part due to its collaboration with ESA and its Cabo Verde activities in the framework of the European Aerosol, Clouds and Trace Gases Research Infrastructure (ACTRIS).

References

Baars, H., T. Kanitz, R. Engelmann, D. Althausen, B. Heese, M. Komppula, J. Preißler, M. Tesche, A. Ansmann, U. Wandinger, J.-H. Lim, J. Y. Ahn, I. S. Stachlewska, V. Amiridis, E. Marinou, P. Seifert, J. Hofer, A. Skupin, F. Schneider, S. Bohlmann, A. Foth, S. Bley, A. Pfüller, E. Giannakaki, H. Lihavainen, Y. Viisanen, R. K. Hooda, S. N. Pereira, D. Bortoli, F. Wagner, I. Mattis, L. Janicka, K. M. Markowicz, P. Achtert, P. Artaxo, T. Pauliquevis, R. A. F. Souza, V. P. Sharma, P. G. van Zyl, J. P. Beukes, J. Sun, E. G. Rohwer, R. Deng, R.-E. Mamouri, and F. Zamorano (2016), An overview of the first decade of PollyNET: An emerging network of automated Raman-polarization lidars for continuous aerosol profiling, Atmos. Chem. Phys., 16(8), 5111-5137, doi:10.5194/acp-16-5111-2016.

Baars, H., J. Bühl, R. Engelmann, P. Seifert, and U. Wandinger (2019), First Aeolus Cal/Val results from aerosol and wind lidar measurements in Leipzig, Germany and Punta Arenas, Chile, paper presented at ESA Living Planet Symposium (LPS19), European Space Agency, Milan, Italy, 13-17 May 2019.

Baars, H., A. Geiß, U.Wandinger, A. Herzog, R. Engelmann, J. Bühl, M. Radenz, P. Seifert, A. Ansmann, A. Martin, R. Leinweber, V. Lehmann, M. Weissmann, A. Cress , M. Filioglou, M. Komppula, and O. Reitebuch (2019), First results from the German Cal/Val activities for Aeolus, paper presented at 29th International Laser Radar Conference (ILRC29), Hefei, Anhui, China, 24-28 June 2019.

Engelmann, R., T. Kanitz, H. Baars, B. Heese, D. Althausen, A. Skupin, U. Wandinger, M. Komppula, I. S. Stachlewska, V. Amiridis, E. Marinou, I. Mattis, H. Linné, and A. Ansmann (2016), The automated multiwavelength Raman polarization and water-vapor lidar PollyXT: The neXT generation, Atmos. Meas. Tech., 9(4), 1767-1784, doi:10.5194/amt-9-1767-2016.

European Space Agency ESA, 2008: ADM-Aeolus Science Report, ESA SP-1311

Herzog, A., H. Baars, B. Heese, R. Engelmann, K. Ohneiser, K. Hanbuch, and U. Wandinger (2019), Aeolus Cal/Val onboard RV Polarstern during the North-South Atlantic crossing in November/December 2018, paper presented at ESA Living Planet Symposium (LPS19), European Space Agency, Milan, Italy, 13-17 May 2019.

Herzog, A. (2019), Validation of Aeolus wind and aerosol products with ground-based and shipborne, M.Sc. thesis, 73 pp, University of Leipzig, Faculty of Physics and Earth Sciences.

Wandinger, U., V. Amiridis, V. Freudenthaler, M. Komppula, P. Kokkalis, R. Engelmann, E. Marinou, and A. Tsekeri (2015), Validation of ADM-Aeolus L2 aerosol and cloud products employing advanced ground-based lidar Measurements (VADAM), edited, ADM-Aeolus Science and CAL/VAL Workshop, ESA-ESRIN, Frascati, Italy.

Funding

This work is funded by the German Federal Ministry for Economic Affairs and Energy (BMWi).

Cooperation

European Space Agency (ESA);
Deutsches Zentrum für Luft- und Raumfahrt (DLR);
Ludwig-Maximilians-Universität (LMU);
Alfred-Wegener-Institut (AWI).

Evaluation of satellite-based aerosol datasets and the CAMS reanalysis over ocean utilizing shipborne reference observations

Jonas Witthuhn, Anja Hünerbein, Hartwig Deneke

Diese Studie nutzt einen einmaligen Datensatz von Aerosol-optischen Eigenschaften für einen Vergleich mit Aerosolprodukten der satellitenbasierten MODIS- und SEVIRI-Instrumente sowie der modellbasierten CAMS Reanalyse. Der Datensatz basiert auf Messungen mit dem Microtops II Sonnenphotometer (2004 - 2018) und dem GUVis-3511 Schattenbandradiometer (2014 - 2018) über dem Atlantik. Die zugrunde liegenden Beobachtungen wurden an Bord verschiedener Forschungsschiffe gemessen, unter anderem auch auf dem Forschungsschiff Polarstern im Rahmen des OCEANET Projekts. Der Vergleich berücksichtigt dabei den Aerosoltyp zur Fehlercharakterisierung. Mit Wüstenstaub belastete Situationen führen zu den größten Abweichungen. Es konnte gezeigt werden, dass die Genauigkeit +-(0.03+0.1 AOD) des MODIS-Aerosolprodukts konsistent mit vorangegangenen Studien ist [z.B. *Levy et al.*,2013].
Im Gegensatz zum MODIS-produkt weißt die CAMS RA Modellreanalyse eine geringfügig schlechtere Genauigkeit auf. Eine erhöhte Unsicherheit wurde außerdem im untersuchten SEVIRI-basierten Aerosolprodukt, was vermutlich aus der Limitierung auf zwei spektrale Kanäle und der gröberen Pixelauflösung (3km gegenüber 1km) resultiert.

Introduction

Reliable reference data for aerosol optical properties over ocean are sparse but essential for the evaluation and improvement of satellite- and model-based aerosol datasets. Within the framework of the Maritime Aerosol Network (MAN), shipborne reference observations have been collected over the Atlantic ocean since 2004 with Microtops sun photometers [*Smirnov et al.*, 2009]. These observations have recently been complemented by measurements with the multi-spectral shadowband radiometer GUVis-3511 during five cruises (ps83, ps95, ps98, ps102, ps113) with the research vessel Polarstern operated as part of the OCEANET project. Based on these two datasets, a comprehensive evaluation of collocated aerosol products from the Moderate resolution Imaging Spectroradiometer (MODIS) flown on NASA's Earth Observing System satellites, the Spinning Enhanced Visible and Infra-Red Imager (SEVIRI) onboard the geostationary Meteosat satellite, and the Copernicus Atmosphere Monitoring Service reanalysis (CAMS RA) has been carried out and is presented here. For this purpose, focus is given to the accuracy of the aerosol optical depth (AOD) at 630 nm in combination with the Ångström exponent (AE), discussed in the context of the ambient aerosol type.

Method

The aim of the paper is to compare multiple aerosol products with different temporal and spatial resolution to the ship-based reference data, taking into account both their point-like nature and the aerosol type. To achieve comparability between the evaluation

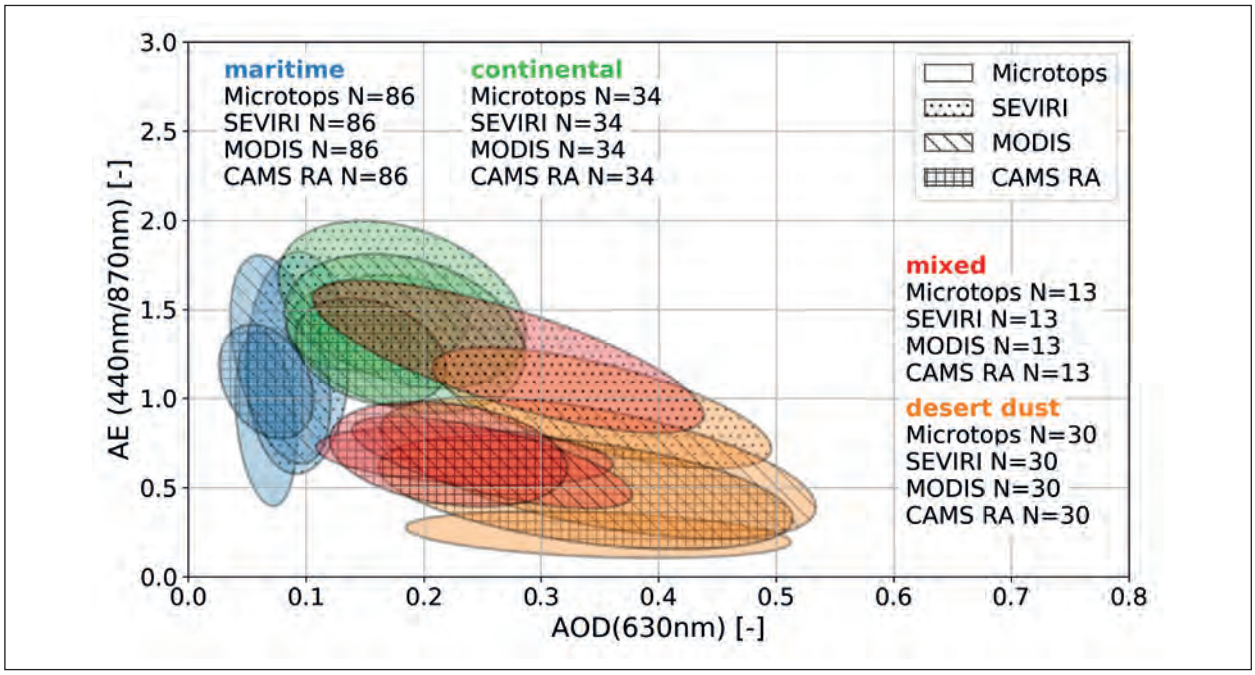

Fig. 1: Comparison of AE calculated from AOD at the wavelengths of 440 nm and 810 nm versus AOD at 630 nm, calculated from the Microtops, SEVIRI and MODIS products and CAMS RA. Simultaneous data availability from satellites, CAMS RA and Microtops is required, so that each instrumental data points has a corresponding counterpart from the other instruments. The data points are grouped by aerosol type (classified with Microtops), and visualized as covariance ellipsoids for a 67% confidence interval.

statistics, consistent methods for collocation and aerosol classification have to be applied. The applied methods are described in the next sections.

Collocation criteria. The following collocation technique is utilized here to find the corresponding satellite pixels for comparison with the shipborne data acquired at a given position. First, eligible data are selected using a time-interval of 30 min around the ship observations, and are checked if the field of view of the satellite instruments contains the ship position. The AOD is calculated as the median of all non-cloudy pixel values with a maximum angular difference to the ship position of 0.2° or less. Choosing a distance angle threshold of 0.2° for collocation assures that the shipborne observations are representative for the comparison domain, and that the same spatial extent is used in all comparisons to ensure comparability of the evaluation results. This threshold corresponds to a spatial radius of about 22 km. Model data are selected adopting the same strategy to the gridded model output.

Aerosol classification. An aerosol classification scheme is applied to the shipborne data, which is based on the empirical method presented in [*Toledano et al.*, 2007] proposed for AERONET observations. This method is also applicable to the Microtops AOD product, as it contains all required parameters. The aerosol classification is done by considering the AOD at 440 nm together with the AE calculated based on the 440 and 870 nm channels. The pair of AOD and AE values is checked against empirical thresholds to identify the aerosol type as being one of maritime, desert dust, continental, biomass burning or mixed type.

Results and Discussion

Since the data has been acquired over the Atlantic ocean, the most prominent aerosol conditions correspond to maritime or desert dust aerosol. To examine the representation of AOD and AE with respect to aerosol type, the layout presented in [*Toledano et al.*, 2007] is used in Fig. 1. Instead of the AOD at 440 nm, the wavelength of 630 nm is chosen, to match the corresponding channel of the SEVIRI instrument. Points related to a certain aerosol type are combined in the form of a covariance ellipse, which spans 67 % of the related data points.

Fig. 1 shows that in general the AOD retrieved from both satellite and model agrees well with the shipborne reference, but a slight overestimate of satellite AOD can be observed in general and especially at low AOD. This effect might be related to the coarser spatial resolution of the satellite pixels or undetected cloud contamination. The spatial-mean AOD inferred

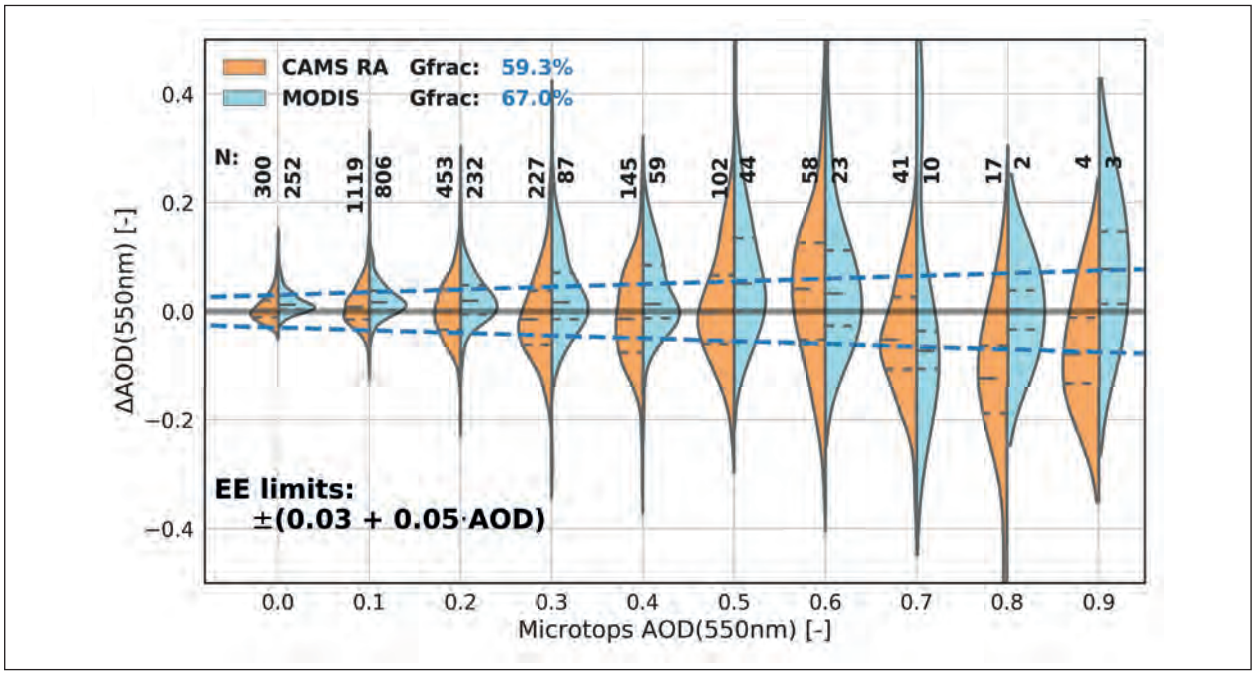

Fig. 2: Comparison of AOD at 550 nm from the Microtops reference dataset versus the CAMS RA and MODIS AOD products. The two sided violin-plots indicate the distribution of the difference for bins of 0.1 in AOD. The blue dashed lines indicate the expected error (EE) limits for the MODIS AOD products. It is expected that at least 67% of data points fall into the expected error limits. Gfrac are the actual percentage of data points lying within the error limits.

from satellite can deviate from the AOD which is retrieved from the slant transmission in case of Microtops due to the mismatch of the field of view and in the considered spatial scale. AE is found to be overestimated in particular for desert dust aerosol, showing two times larger values for the MODIS product, and more than three times larger values for the SEVIRI product. This finding suggests that likely an unrealistic mineral dust model is used in the satellite retrievals. Therefore, AOD is only accurately retrieved at the wavelengths of the native spectral channels of the satellite instruments, while the estimation of the spectral behaviour of AOD remains challenging, due to the lack of realism of the aerosol model, and the limited number of spectral channels available from SEVIRI.

Compared to the evaluation statistics found for the SEVIRI product, the CAMS RA performance is clearly superior. Further, the slight overestimation of AOD found for MODIS is not present in the CAMS RA AOD dataset. This emphasizes that although the MODIS AOD is assimilated into the CAMS RA, the overestimation of AOD is compensated in the model. This effect is clearly shown in Fig. 2, together with a tendency of CAMS RA towards an underestimation of AOD for larger values of AOD. But overall, CAMS RA AOD shows a slightly larger scatter than the MODIS products, indicating a slightly better performance of the MODIS aerosol products.

References

Levy, R. C., Mattoo, S., Munchak, L. A., Remer, L. A., Sayer, A. M., Patadia, F., and Hsu, N. C. (2013), The Collection 6 MODIS aerosol products over land and ocean, Atmos. Meas. Tech., 6, 2989–3034, doi: 10.5194/amt-6-2989-2013.

Smirnov, A., B. N. Holben, I. Slutsker, D. M. Giles, C. R. McClain, T. F. Eck, S. M. Sakerin, A. Macke, P. Croot, G. Zibordi, P. K. Quinn, J. Sciare, S. Kinne, M. Harvey, T. J. Smyth, S. Piketh, T. Zielinski, A. Proshutinsky, J. I. Goes, N. B. Nelson, P. Larouche, V. F. Radionov, P. Goloub, K. Krishna Moorthy, R. Matarrese, E. J. Robertson, and F. Jourdin (2009), Maritime Aerosol Network as a component of Aerosol Robotic Network, *J. Geophys. Res.*, 114, D06204, doi: 10.1029/2008JD011257.

Toledano, C., V. E. Cachorro, A. Berjon, A. M. de Frutos, M. Sorribas, B. A. de la Morena, and P. Goloub (2007), Aerosol optical depth and Angström exponent climatology at El Arenosillo AERONET site (Huelva, Spain), Quarterly Journal of the Royal Meteorological Society, Wiley-Blackwell, 113, 795-807, doi: 10.1002/qj.54.

Observations of the spatiotemporal variability of solar radiation introduced by clouds in the Arctic

Carola Barrientos Velasco, Hartwig Deneke, Hannes Griesche, Patric Seifert, Ronny Engelmann, and Andreas Macke

Wolken spielen eine wichtige Rolle auf die Energiebilanz der Erde. Dabei ist der Einfluss der Wolken auf die gegenwärtige Erwärmung der Arktis bisher nicht vollständig verstanden. Hierzu wurde ihre Auswirkungen auf die Sonneneinstrahlung und die Energiebilanz der Erdoberfläche besonders betrachtet. Um die relevante kleinräumige Prozesse im Detail zu untersuchen, wurde im Frühsommer die intensive Messkampagne „PASCAL“ in der zentralen Arktis durchgeführt. Mit den Messungen wurden die physikalischen Rückkopplungen zwischen der arktischen planetarischen Grenzschicht, dem Meereis, Wolken und Aerosol untersucht. Das Forschungsschiff Polarstern lag mehrere Tage an einer Eisscholle fest, dabei wurden erstmals die kleinräumige raumzeitliche Variabilität der globalen Strahlung auf einer Eisscholle mit einem engmaschigen Netz von autonomen Pyranometern gemessen. Vom 4. bis 16. Juni 2017 wurden 15 Messstationen auf einer Fläche von 0,83 km x 1,3 km betrieben. Dieser einzigartige Datensatz wird hier beschrieben, und eine Analyse der aus diesem Datensatz abgeleiteten Eigenschaften der raumzeitlichen Variabilität vorgestellt. Basierend auf zusätzlichen Beobachtungen wurden 5 Bewölkungsklassen identifiziert und verwendet, um die Werte des Mittelwerts und der Varianz der globalen atmosphärischen Transmission für diese Bedingungen zu bestimmen. Weitere Analysen der Zeitreihen, Fallstudien und eine Wavelet-basierten Multi-Skalen-Analyse finden sich in der zugrundeliegenden Veröffentlichung von *Barrientos Velasco et al.* [(2019].

Introduction

The Arctic exhibits robust features of climate change [*IPCC*, 2013]. The surface temperature in this region continues to increase at double the rate of global mean warming, a feature known as 'Arctic Amplification' [*Osborn et al.*, 2018; *Screen and Simmonds*, 2010]. This leads to thinner [*Haas et al.*, 2008; *Lindsay and Zhang*, 2005], younger [*Maslanik et al.*, 2007] and less extensive [*Serreze et al.*, 2007] sea ice. As the surface temperature increases to near or above 273.15 K, snow and sea ice melts, reducing the albedo and increasing the amount of solar radiation absorbed by the surface, a mechanism known as the ice-albedo feedback [*Curry et al.*, 1995]. Clouds add complexity to the ice-albedo feedback by alternatively increasing or reducing the amount of solar radiation reaching the surface. Here, we present the observations made with a pyranometer network in the Central Arctic to better understand the spatiotemporal variability of solar radiation induced by clouds [*Barrientos Velasco et al.*, 2019].

In order to better elucidate several mechanisms leading to the Arctic Amplification, the project ArctiC Amplification: Climate Relevant Atmospheric and SurfaCe Processes and Feedback Mechanisms (AC)^3 was initiated. As part of this project, the 'Physical feedbacks of Arctic planetary boundary layer, Sea ice, Cloud and AerosoL; PS106/1' (PASCAL) expedition on board the German research vessel Polarstern was held in early summer 2017 [*Macke and Flores*,

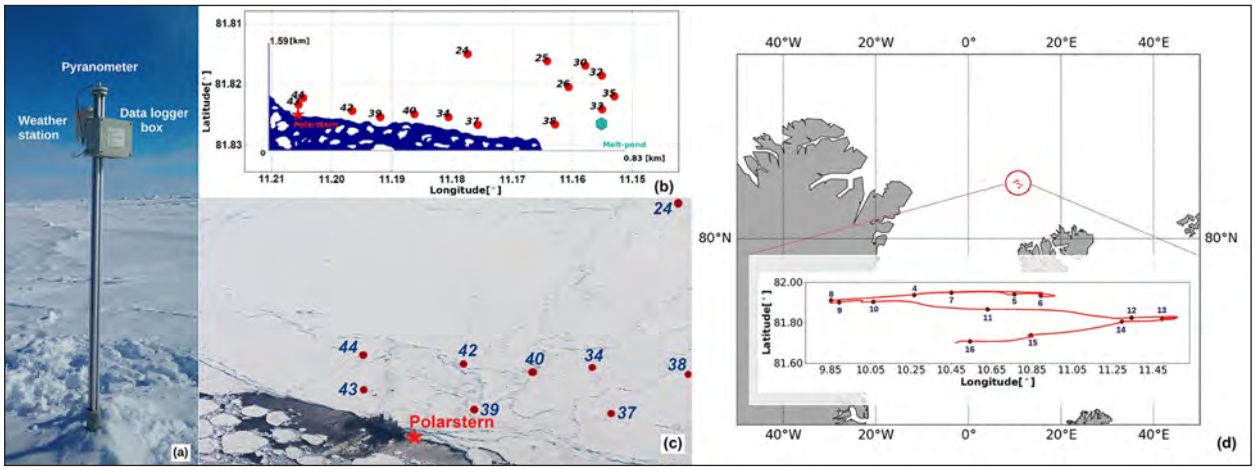

Fig. 1: (a) Photograph of a pyranometer station on the ice floe. (b) Map of the pyranometer stations. Red circles show the location on June 11, 2017, at 14:50Z, while the red star marks the position of Polarstern , and the turquoise hexagon marks the approximate position of a melt-pond. (c) Edited photograph of the ice floe station showing the approximate location of several stations (red circles) and Polarstern (red star). Photographed by Svenja Kohnemann (d) Drifting track of the ice floe from 4 to 16 of June.

2018; *Wendisch et al.*, 2019]. During PASCAL, an ice floe camp took place from June 4-16, 2017 where 15 pyranometer stations were deployed covering an area of 0.83 km x 1.3 km (See Fig. 1b and 1c). An analysis of the spatiotemporal variability of the solar radiation induced by clouds based on these observations is given here, taking into consideration meteorological and synoptic conditions.

Methods

Each pyranometer station was mounted on an aluminum rod of 1.8 m height and was equipped with a silicon photodiode pyranometer with the spectral range of 0.3-1.1 µm (EKO: ML-020VM), and a meteorological station accurately measuring the air temperature at a frequency of 1Hz [*Madhavan et al.*, 2016]. Once the network was deployed over the ice-floe, daily quality checks were performed to assure a high quality of the observations. After the campaign was finished, the data was carefully processed and checked, assigning cleanliness and leveling flags, which are important factors that could have compromised the quality of the observations.

Based on passive and active remote sensing instruments [*Griesche et al.*, 2019] and sky camera photographs taken aboard Polarstern, a classification of sky condition was made. The most frequent sky condition corresponded to overcast, with an occurrence frequency of 39.6% of the ice floe camp period, followed by multilayer clouds (32.4%), broken clouds (22.1%), thin clouds (3.5%) and cloudless conditions (2.4%). Based on the near-surface air temperature, a more general classification was made suggesting a cold period from June 4 to 9 and a warm period from June 10 to 16. Both classifications are found to be useful to interpret the observations and results.

Results

For the analysis, the atmospheric global transmittance (ATg) was calculated from the pyranometer observations, which is defined as the fraction of radiation that is transmitted by the atmosphere and reaches the surface. The time series of ATg is shown in Fig. 2a and has been color-coded in the background for the different sky conditions. It can be observed that the lowest ATg occurs under overcast and multilayer conditions, having mean values of 0.46 and 0.43, respectively. On the other hand, the highest values are found in thin cloud and cloudless conditions, with a mean value of 0.76. The transmittance for broken clouds lies in between these values with an ATg of 0.61. Fig. 2b shows the inter-station standard deviation (SD) of the operational pyranometers and it clearly indicates a higher variation of transmittance during broken cloud conditions, that goes up to values of 0.146. To quantify the temporal variability of ATg, a wavelet-based multiresolution analysis was made for 3-hourly periods in order to obtain time-localize estimates of the time-scale-dependent variance of the time series. In this analysis. broken clouds are once more found to exhibit the largest variability, while multilayer clouds show the smallest variability across all time scales. The variance for broken clouds however seem to be smaller that the ones reported during a field campaign in Jülich Germany in 2013, likely due to less convective cloud development taken place in the Arctic.

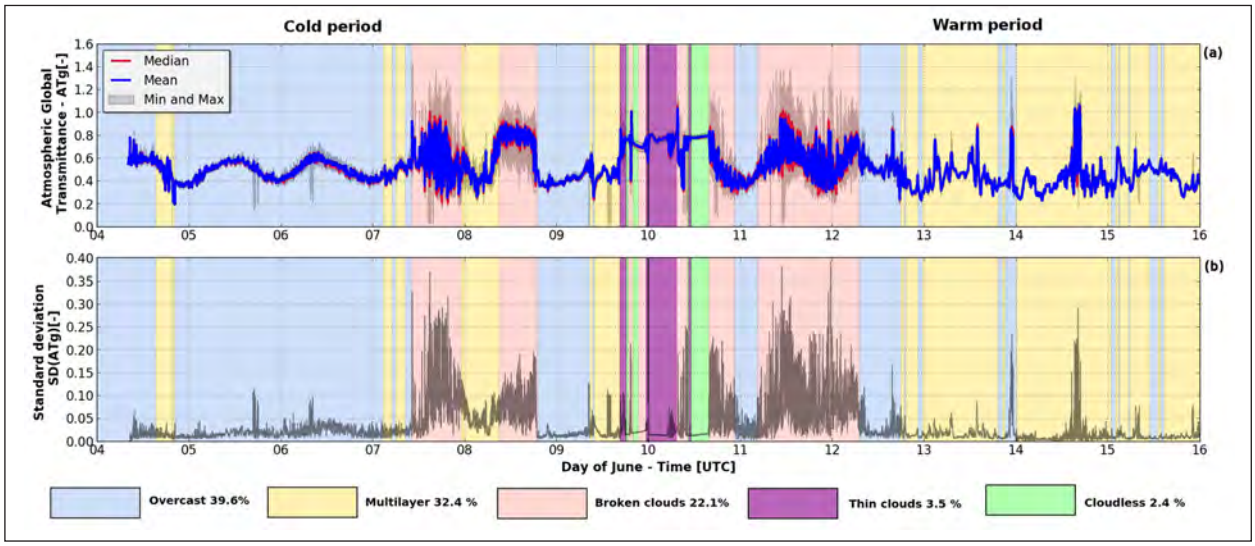

Fig. 2: (a) Time series of atmospheric global transmittance (ATg) derived from pyraronmeter network. (b) Time series of the inter-station standard deviation of ATg.

References

Barrientos Velasco, C., Deneke, H., Griesche, H., Seifert, P., Engelmann, R., and Macke, A.: Spatiotemporal variability of shortwave radiation introduced by clouds over the Arctic sea ice, Atmos. Meas. Tech. Discuss., https://doi.org/10.5194/amt-2019-231, in review, 2019.

Griesche, H. J., Seifert, P., Ansmann, A., Baars, H., Barrientos Velasco, C., Bühl, J., Engelmann, R., Radenz, M., and Zhenping, Y.: Application of the shipborne remote sensing supersite OCEANET for profiling of Arctic aerosols and clouds during Polarstern cruise PS106, Atmos. Meas. Tech. Discuss., https://doi.org/10.5194/amt-2019-434, in review, 2019.

Haas, C., A. Pfaffling, S. Hendricks, L. Rabenstein, J.-L. Etienne, and I. Rigor.: Reduced ice thickness in Arctic transpolar drift favors rapid ice retreat,Geophys. Res. Lett.,35, L17501, doi:10.1029/2008GL034457, 2008.

IPCC, 2013: Climate Change 2013: The Physical Science Basis. Contribution of Working Group I to the Fifth Assessment Report of the Intergovernmental Panel on Climate Change [Stocker, T.F., D. Qin, G.-K. Plattner, M. Tignor, S.K. Allen, J. Boschung, A. Nauels, Y. Xia, V. Bex and P.M. Midgley (eds.)]. Cambridge University Press, Cambridge, United Kingdom and New York, NY, USA, 1535 pp, doi:10.1017/CBO9781107415324.

Lindsay, R. W. and Zhang, J.: The thinning of arctic sea ice, 1988–2003: have we passed a tipping point?, J. Climate (in press), 2005.

Macke, A. and Flores, H.: PS106 cruise report: Polarstern, Tech. rep., Alfred Wegener Institute for Polar and Marine Research, Bremerhaven,Germany, report submitted for publication, 2018.

Madhavan, B. L., Kalisch, J., and Macke, A.: Shortwave surface radiation network for observing small-scale cloud inhomogeneity fields,Atmos. Meas. Tech., 9, 1153-1166, https://doi.org/10.5194/amt-9-1153-2016, 2016

Maslanik, J. A., C. Fowler, J. Stroeve, S. Drobot, J. Zwally, D. Yi, and W. Emery.: A younger, thinner Arctic ice cover: Increased potential for rapid, extensive sea-ice loss, Geophys. Res. Lett., 34, L24501, doi:10.1029/2007GL032043, 2007.

Osborne, E., J. Richter-Menge, and M. Jeffries, 2018: Arctic report card. Eds, URL https://www.arctic.noaa.gov/Report-Card.

Screen, J., Simmonds, I.: The central role of diminishing sea ice in recent Arctic temperature amplification. *Nature* 464, 1334–1337. doi:10.1038/nature09051, 2010.

Wendisch, M., A. Macke, A. Ehrlich, C. Lüpkes, M. Mech, D. Chechin, K. Dethloff, C. Barrientos Velasco, H. Bozem, M. Brückner, H.-C. Clemen, S. Crewell, T. Donth, R. Dupuy, K. Ebell, U. Egerer, R. Engelmann, C. Engler, O. Eppers, M. Gehrmann, X. Gong, M. Gottschalk, C. Gourbeyre, H. Griesche, J. Hartmann, M. Hartmann, B. Heinold, A. Herber, H. Herrmann, G. Heygster, P. Hoor, S. Jafariserajehlou, E. Jäkel, E. Järvinen, O. Jourdan, U. Kästner, S. Kecorius, E. M. Knudsen, F. Köllner, J. Kretzschmar, L. Lelli, D. Leroy, M. Maturilli, L. Mei, S. Mertes, G. Mioche, R. Neuber, M. Nicolaus, T. Nomokonova, J. Notholt, M. Palm, M. van Pinxteren, J. Quaas, P. Richter, E. Ruiz-Donoso, M. Schäfer, K. Schmieder, M. Schnaiter, J. Schneider, A. Schwarzenböck, P. Seifert, M. D. Shupe, H. Siebert, G. Spreen, J. Stapf, F. Stratmann, T. Vogl, A. Welti, H. Wex, A. Wiedensohler, M. Zanatta, and S. Zeppenfeld (2019), The Arctic cloud puzzle: Using ACLOUD/PASCAL multiplatform observations to unravel the role of clouds and aerosol particles in Arctic amplification, *Bull. Amer. Meteor. Soc.*, *100*, 841-871, doi:10.1175/bams-d-18-0072.1, 10.1175/BAMS-D-18-0072.2 (Suppl.).

Funding

Transregional Collaborative Research Centre (TR 172) "ArctiC Amplification: Climate Relevant Atmospheric and SurfaCe Processes, and Feedback Mechanisms (AC)³" funded by the German Research Foundation (DFG, Deutsche Forschungsgemeinschaft).

From ground to top of the boundary layer – optical properties retrieved with SÆMS and lidar in Košetice

Annett Skupin, Ronny Engelmann, Robert Wiesen, Holger Baars

Während der ACTRIS-Vergleichskampagne „Summer Flux campaign" Aug. – Okt. 2017 in Košetice wurde zur Bestimmung der optischen Daten im untersten Bereich der atmosphärischen Grenzschicht ein neu entwickeltes Messgerät (mobile Spectral Aerosol Extinction Monitoring System, SÆMS) eingesetzt. Mit diesem wird der Extinktionskoeffizient bei 3 Wellenlängen (405, 532 und 850 nm) auf einem ca. 2.7 km langen, horizontal verlaufenden Pfad in 5 – 20 m Höhe über dem Boden gemessen. Ebenfalls eingesetzt wurde das Lidar Polly-XT, welches kontinuierliche Messungen des Vertikalprofils der Atmosphäre liefert. Košetice ist eine rurale Hintergrundstation mit umliegenden landwirtschaftlichen Nutzflächen. Dementsprechend niedrig ist der Aerosolgehalt der Atmosphäre. Über den gesamten Verlauf der Kampagne wurden mit SÆMS bei 532 nm Tagesmittelwerte von < 0.1 km^{-1} gemessen. Es wird eine Fallstudie gezeigt, in der Lidarrückstreukoeffizient und SÆMS-Extinktionskoeffizient zur Abschätzung des Lidarverhältnisses am Boden genutzt wurden.

ACTRIS Summer Flux campaign

Measurements of vertical aerosol fluxes are often made in combination with aerosol characterization and other measurements. Simultaneous tower and remote sensing measurements were conducted for the ACTRIS Summer Flux campaign, with the lidar system Polly-XT [*Engelmann et al.*, 2016], a Halo photonics Doppler lidar, CPC and turbulence measurements at different heights (80 m, 230 m). During this campaign from Aug. – Oct. 2017 at the National Atmospheric Observatory Košetice (NAOK), CZ, the newly developed mobile SÆMS [Spectral Aerosol Extinction Monitoring System, *Skupin et al.*, 2014] for observing the extinction coefficient of atmospheric particles in the lowermost part of the boundary layer was deployed. This mobile instrument measures remotely the ambient extinction coefficient at 405, 532, and 850 nm 5 – 20 m above ground on an optical path of 2.7 km length. Furthermore, the Polly-XT multiwavelenth-Raman-lidar-system provided continuous vertical profiles of the optical properties of the atmosphere (e.g. backscatter and extinction coefficients). We performed combined measurements of SÆMS and Polly-XT to estimate the Lidar Ratio at ground level to present a solution to a long-time issue in lidar and in-situ comparison studies.

Site and instrumentation

The National Atmospheric Observatory Košetice is an ACTRIS-CZ measurement site (49°34'24" N,15°04'49" E, 534 m asl). Košetice is a hilly rural background station surrounded by agricultural countryside. The 250 m measuring tower is suitable for in-situ measurements at different heights and one of the reasons why the location was chosen for the campaign.

Simplified, the mobile SÆMS has 3 laser diodes which emit light at 405, 532, and 850 nm on

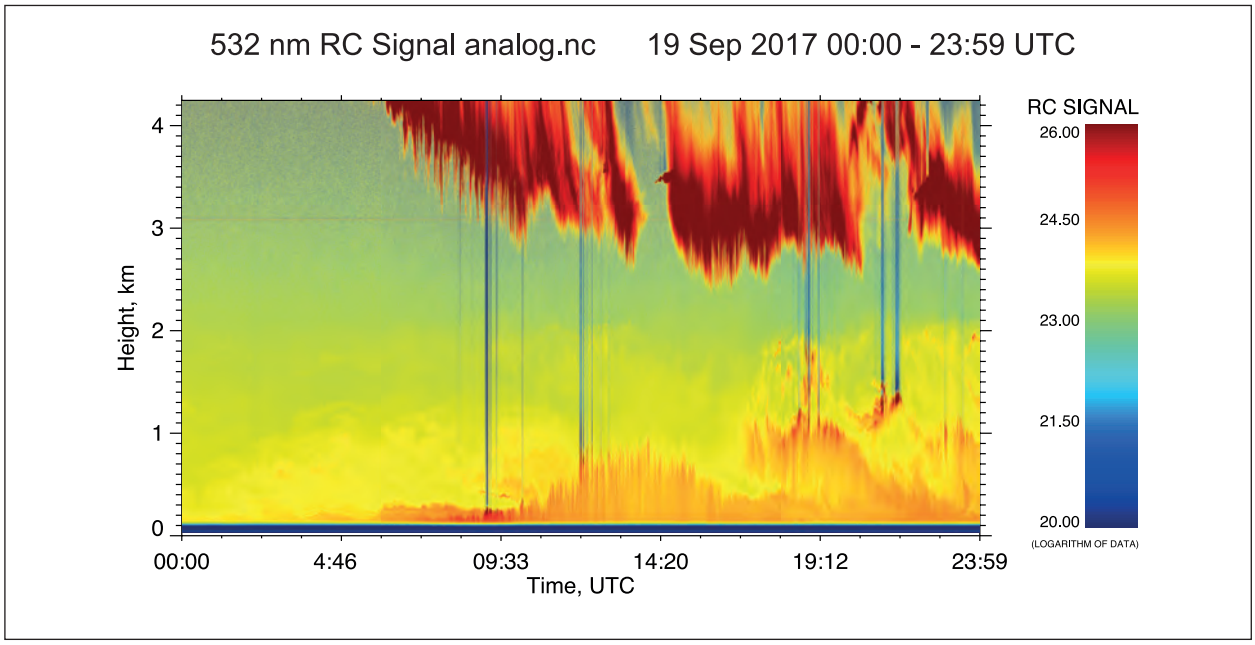

Fig. 1: High resolved time-height-plot of the range corrected lidar signal of the near-range channel at 532 nm from 19 September 2017.

a horizontal path of 2.7 km optical length, whereas 2 rotational units allow the adjustment of the light beam to the optical path. Retroreflector units are mounted at the end of the path. The receiving unit consists of a telescope, a photodiode and a lock-in amplifier. By the measurement at two different path length [*Skupin et al.*, 2014], we can calculate the extinction coefficient for the 3 wavelengths by assuming a homogeneous atmosphere along the path.

The Polly-XT was equipped with a 532-nm near-range analog channel. This channel measured high time-resolved vertical aerosol profiles with 5 s resolution in order to apply the Eddy-correlation technique [*Engelmann et al.*, 2008]. However, Polly-XT can measure the backscatter coefficient with the Raman method [*Ansmann et al.*, 1992].

Here, the mobile SÆMS measurements aim to provide a link between ground-based in-situ measurements and vertically pointed lidar measurements. The first step is the comparison between lidar and SÆMS measurements. The lidar ratio is the factor between backscatter and extinction coefficient.
We aim for a method of determining the lidar ratio (extinction-to-backscatter-ratio) close to the ground by combining extinction coefficients from SÆMS and aerosol backscatter coefficients from Raman lidar down to about 100 m height, but not the extinction coefficient because of an incomplete overlap function. The lidar ratio is a quantity commonly used for aerosol characterization because it depends on size, shape and mostly on absorption of the particles. Therefore, its knowledge is inevitable in order to link remote-sensing and in-situ measurements at the ground.

Method for the determination of the lidar ratio

Here, we want to focus on a case study of 19 September 2017. The area of Košetice on that day was influenced by a high-pressure zone with very calm westerly to south-westerly wind directions. The maximum near-surface temperature was around 16°C. Figure 1 shows the 532-nm range corrected lidar signal from which a maximum boundary-layer height of around 900 m agl. around noon is visible for this typical late-summer/early-autumn day. Above 3 km height a cirrostratus cloud was present for the entire day (c.f. polly.tropos.de). It can be seen from Fig. 1 that the lowest trustworthy lidar altitude is about 150 m height for the determination of the particle back-scatter coefficient.

Figure 2 shows the aerosol backscatter coefficient at 532 nm wavelength determined with Polly-XT at the lowest altitude of 150 m. Also, the time series of the aerosol extinction coefficients determined with SÆMS at 405, 532, and 850 nm are shown. It can be seen that in the morning and evening hours the aerosol extinction at 532 nm was in the order of 0.02 km^{-1}. During midday the extinction coefficients increased up to 0.08 km^{-1}, possibly because of some rural activity, increased photochemistry, or increased boundary-layer turbulence and thus further mobilization of surface aerosol. These increased values were also independently of SÆMS observed with Polly-XT. However, these rather low values for the aerosol concentration were very typical for the entire campaign. Most of the time, the surface aerosol extinction was below 0.1 km^{-1}.

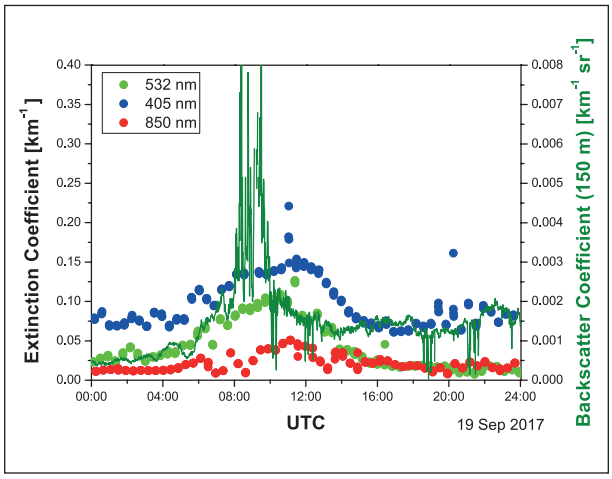

Fig. 2: Diurnal cycle of the aerosol extinction coefficients at 405, 532, and 850 nm (blue, green and red dots) obtained with SÆMS and corresponding lidar backscatter coefficient at 150 m height above ground at 532 nm from 19 September 2017.

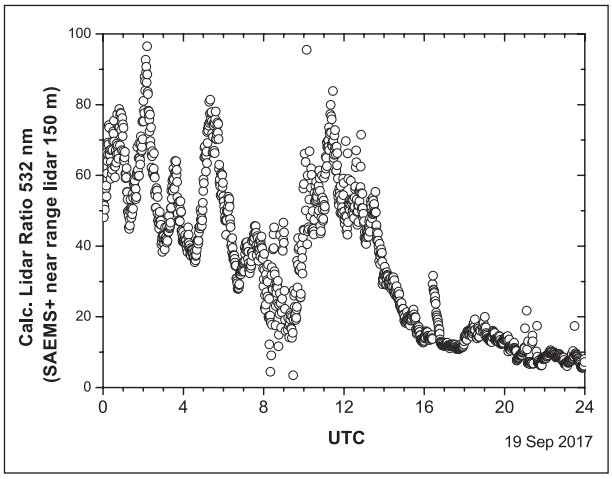

Fig. 3: Diurnal cycle of the calculated lidar ratio based on the data of Fig. 2 at ground level from 19 September 2017.

For the combined method to determine the lidar ratio at the surface we had to assume homogeneous aerosol properties between the SÆMS path at 5 – 20 m above the ground and the lowest lidar range of 150 m agl. Figure 3 shows the calculated near-surface lidar ratios at 532 nm by the combination of lidar and SÆMS. One should keep in mind, that this property can only be derived trustworthy if a certain amount of aerosol is present, i.e., preferably the extinction coefficient is > 0.1 km^{-1}. Nevertheless, the values of 40 – 70 sr derived in the early and midday hours of 19 September 2019 are very typical values for continental background aerosols and lie within the expected range. The daytime mean value was 49 sr.

Unfortunately, the very clean conditions (Extinction coefficient < 0.1 km^{-1}) during the Summer Flux campaign were connected with a high uncertainty of ± 15 sr in the lidar ratio calculation. It can be expected that the uncertainty of the lidar ratio can be as low as ± 5 sr for higher aerosol concentrations.

References

Ansmann, A., U. Wandinger, M. Riebesell, C. Weitkamp, and W. Michaelis (1992), Independent Measurement of Extinction and Backscatter Profiles in Cirrus Clouds by Using a Combined Raman Elastic-Backscatter Lidar, *Appl Optics*, *31*(33), 7113-7131, Doi 10.1364/Ao.31.007113.

Engelmann, R., U. Wandinger, A. Ansmann, D. Müller, E. Zeromskis, D. Althausen, and B. Wehner (2008), Lidar observations of the vertical aerosol flux in the planetary boundary layer, *J Atmos Ocean Tech*, *25*(8), 1296-1306, 10.1175/2007jtecha967.1.

Engelmann, R., T. Kanitz, H. Baars, B. Heese, D. Althausen, A. Skupin, U. Wandinger, M. Komppula, I. S. Stachlewska, V. Amiridis, E. Marinou, I. Mattis, H. Linne, and A. Ansmann (2016), The automated multiwavelength Raman polarization and water-vapor lidar Polly(XT): the neXT generation, *Atmos Meas Tech*, *9*(4), 1767-1784, 10.5194/amt-9-1767-2016.

Skupin, A., A. Ansmann, R. Engelmann, H. Baars, and T. Müller (2014), The Spectral Aerosol Extinction Monitoring System (SÆMS): setup, observational products, and comparisons, *Atmos Meas Tech*, *7*(3), 701-712, 10.5194/amt-7-701-2014.

Funding

German Science Foundation under grant SK 292/1-1.

Cooperation

ACTRIS-CZ;
NAOK.

Progress made in the remote sensing of aerosol effects on mixed-phase clouds

Patric Seifert, Johannes Bühl, Martin Radenz, Albert Ansmann, Holger Baars, Ronny Engelmann

Die Anwendung von Lidar, Wolkenradar und deren Kombination bietet großes Potenzial für die Beobachtung von Aerosol, Wolken und deren Interaktion unter natürlichen Umgebungsbedingungen. Neue, am TROPOS entwickelte Techniken erlauben seit kurzem die Ableitung von wolkenrelevanten Aerosoleigenschaften, wie der Konzentration von Wolkenkondensationskeimen und eisnukleierenden Partikeln, aus Lidarmessungen, sowie der Bestimmung von aerosolsensitiven Wolkeneigenschaften, wie der Konzentration und dem Massefluss von Eiskristallen, mittels Wolkenradar. Die gleichzeitige Anwendung beider Techniken auf kombinierte Lidar- und Wolkenradarmessungen ermöglicht erstmals Schließungsstudien zwischen Eiskeim- und Eiskristallkonzentrationen. Um die Techniken in Zukunft auf komplexere Mischphasenwolkensysteme anwenden zu können, wurde zudem ein Algorithmus entwickelt, verschiedene Hydrometeortypen anhand ihrer Signaturen in Wolkenradar-Dopplerspektren detektieren zu können.

Introduction

Capturing the response of the microphysical properties of mixed-phase clouds to the strongly variable characteristics of aerosol particles is a challenge. Improvement of the observational capabilities is key for the evaluation of the relevance of aerosol-cloud-interaction for meteorological processes and climate under ambient conditions. Solely the fact, that the response of mixed-phase cloud processes to aerosol perturbations is currently not considered in future climate predictions, demonstrates that further research is required in this field.

Continous, ground-based remote sensing of the properties of clouds, aerosol and atmospheric dynamics allows to gain insights into aerosol-cloud-dynamics interaction under ambient conditions. TROPOS has been intensifying its activities in using combined lidar and cloud-radar observations to gain more insights into this topic.

Instruments and Methods

To enable continuous observations of aerosols, clouds and atmospheric dynamics, TROPOS operates the mobile Leipzig Aerosol and Cloud Remote Observations System (LACROS). LACROS consists of a MIRA-35 cloud radar, a Polly^{XT} Raman lidar, a microwave radiometer, Doppler lidar, precipitation disdrometer and a radiation station. LACROS is dedicated to deployment at hot spots of climate research. Recent deployments were the 1.5 year measurement campaign Cyprus Cloud And pRecipitation Experimant (CyCARE) in Limassol, Cyprus (34° N, 33° E, 11/2016-03/2018) and the ongoing Dynamics, Aerosol, Clouds And Precipitation Observations in the Pristine Environment of the Southern Ocean (DACAPO-PESO) campaign in Punta Arenas, Chile (53° S,71° W), which started in 11/2018. When not deployed for a campaign, LACROS is operated at Leipzig, for which meanwhile also a 2-year dataset is available. The synergies of the deployed instruments

allow novel approaches for gaining insights in aerosol-clouds-dynamics relationships at mixed-phase conditions in the temperature range from 0 to -38 °C. Some aspects of recent contributions of the LACROS team to the research field regarding the interactions between aerosol and mixed-phase clouds will be reviewed in the following section.

Results

It is known that vertical air motions have an essential role for the evolution of clouds as they produce the supersaturation required for cloud formation. But measurements under ambient conditions are rare because of the complexity of the involved processes. In a combined study of Doppler-lidar and cloud-radar observations *Bühl et al.* [2019] documented the impact of vertical air motions on the ice formation rate in mixed-phase stratiform cloud layers which are known to be dominated by primary ice formation. For layers with a cloud-top temperature below –12 °C, an increase of vertical-velocity standard deviation from 0.1 to 1.0 m s^{-1} was found to lead to an increase in the mass flux of ice water by two orders of magnitude (see Fig. 1).

Even more insights into ice cloud properties were enabled by a novel algorithm of *Bühl et al.* [2019b] that allows to infer the ice crystal number concentration (ICNC) from combined lidar, cloud radar and radar wind profiler measurements. The authors exploit, for the first time, measurements of terminal fall velocity together with the radar reflectivity factor and/or the lidar-derived particle extinction coefficient

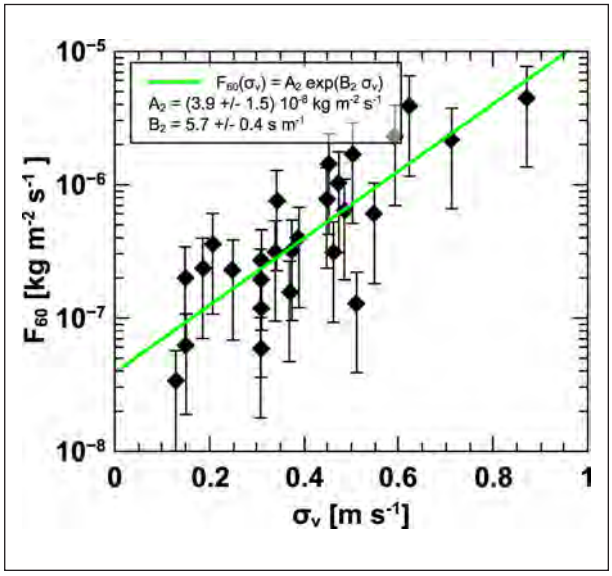

Fig. 1: Relationship between ice mass flux F_{60} and standard deviation of vertical velocity σ_v in the ice-forming mixed-phase layer.

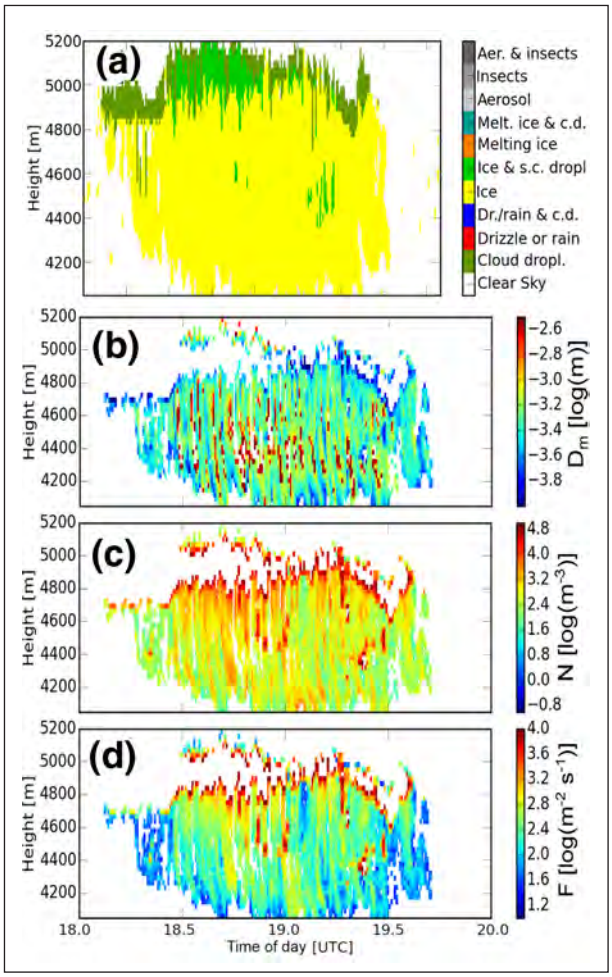

Fig. 2: Application of the ICNC retrieval scheme of Bühl et al. [2019b] to an altocumulus cloud observed on 11 Jun 2015 at Lindenberg, Germany. Shown are the hydreometeor target classification (a), mean particle diameter D_m (b), ICNC N (c) and ice particle Flux F (d).

in clouds to retrieve the number concentration of pristine ice particles with presumed particle shapes. An example of an ICNC retrieval is shown in Fig. 2.

In a study of *Ansmann et al.* [2019], the ICNC retrieval of *Bühl et al.* [2019b] was combined with the recently developed technique of *Mamouri and Ansmann* [2016] for the estimation of ice nucleating particle concentrations (INP, INPC). The combination of both approaches enabled, also for the first time, a closure study of the relationship between the INPC and ICNC in altocumulus and cirrus layers, solely based on ground-based active remote sensing.

In more complex clouds, not yet targeted by the above-mentioned studies, multiple hydrometeor populations might be present in a cloud parcel. In order to identify such scenarios, *Radenz et al.* [2019] developed the PeakTree algorithm which separates the Doppler spectra observed with vertically pointed cloud radar into its different peaks. The new technique was successfully applied to investigate particle populations

in an Arctic multilayered mixed-phase cloud, which was observed in the frame of ArctiC Amplification: Climate Relevant Atmospheric and SurfaCe Processes, and Feedback Mechanisms (AC^3) during the research vessel Polarstern expedition PS106. In that case study, dendrites and columnar-shaped ice crystal populations were separated. This is an essential requirement for the ICNC retrieval of *Bühl et al.* [2019].

Summary and Outlook

Huge progress has been made in the development of techniques for the characterization of cloud-relevant aerosol properties and related cloud microphysical properties. In the near future, the new algorithms will be deployed to infer statistics about aerosol-cloud-dynamics interaction in the datasets from the long-term field experiments CyCARE, DACAPO-PESO, and Leipzig.

References

Ansmann, A., R. E. Mamouri, J. Bühl, P. Seifert, R. Engelmann, J. Hofer, A. Nisantzi, J. D. Atkinson, Z. A. Kanji, B. Sierau, M. Vrekoussis, and J. Sciare (2019), Ice-nucleating particle versus ice crystal number concentrationin altocumulus and cirrus layers embedded in Saharan dust:a closure study, Atmos. Chem. Phys., 19(23), 15087-15115, doi: 10.5194/acp-19-15087-2019.

Bühl, J., P. Seifert, R. Engelmann, and A. Ansmann (2019), Impact of vertical air motions on ice formation rate in mixed-phase cloud layers, npj Climate and Atmospheric Science, 2(1), 36, doi: 10.1038/s41612-019-0092-6.

Bühl, J., P. Seifert, M. Radenz, H. Baars, and A. Ansmann (2019), Ice crystal number concentration from lidar, cloud radar and radar wind profiler measurements, Atmos. Meas. Tech., 12(12), 6601-6617, doi: 10.5194/amt-12-6601-2019.

Mamouri, R. E., and A. Ansmann (2016), Potential of polarization lidar to provide profiles of CCN- and INP-relevant aerosol parameters, Atmos. Chem. Phys., 16(9), 5905-5931, doi: 10.5194/acp-16-5905-2016.

Radenz, M., J. Bühl, P. Seifert, H. Griesche, and R. Engelmann (2019), peakTree: a framework for structure-preserving radar Doppler spectra analysis, Atmos. Meas. Tech., 12(9), 4813-4828, doi: 10.5194/amt-12-4813-2019.

Funding

The presented work received funding from:

- European Union's Horizon 2020 research and innovation programme ACTRIS under grant agreements No 654109 and 739530.
- Deutsche Forschungsgemeinschaft (DFG, German Research Foundation) – grant number 268020496 – TRR 172, within the Transregional Collaborative Research Center "ArctiC Amplification: Climate Relevant Atmospheric and SurfaCe Processes, and Feedback Mechanisms ($AC)^3$".
- Deutsche Forschungsgemeinschaft – grant no. 398285025 – COARSEMIX.

Cooperation

Cyprus University of Technology, Cyprus;
German Weather Service (DWD), Germany;
University of Magallanes, Chile.

Case study of humidity layers above Arctic stratocumulus and its impact on cloud evolution

Ulrike Egerer[1], Holger Siebert [1], Roel Neggers[3], André Ehrlich[2], Matthias Gottschalk[2], Manfred Wendisch[2]

[1] Leibniz Institute for Tropospheric Research (TROPOS), Leipzig, Germany

[2] Institute for Meteorology, University of Leipzig, Leipzig, Germany

[3] Institute of Geophysics and Meteorology, University of Cologne

Während der Polarstern-Expedition PASCAL wurden im Sommer 2017 Fesselballonsondierungen der bewölkten Grenzschicht in der eisbedeckten Arktis nördlich Spitzbergens durchgeführt. An mehreren Tagen konnten direkt über den Wolken Schichten mit erhöhter spezifischer Feuchte gemessen werden. Abschätzungen der turbulenten Flüsse unterstützen die Hypothese, dass diese Feuchteschichten die Wolken zusätzlich mit Wasserdampf versorgen und damit zur beobachteten Langlebigkeit arktischer Wolken beitragen.

Introduction

The Arctic atmospheric boundary layer (ABL) exhibits numerous peculiarities compared to lower latitudes such as persistent mixed-phase clouds, multiple cloud layers often decoupled from the surface and ubiquitous vertical temperature inversions. Local ABL and cloud processes are complex and not completely understood, but arean important component to explain the rapid warming of the Arctic region [*Wendisch et al., 2019*]. One of the special features frequently observed in the Arctic are specific humidity inversions (SHIs), although specific humidity is generally expected to decrease with height. The frequency of occurrence of low level SHIs in summer is estimated being around 70-90% over the Arctic ocean [*Naakka et al., 2018*]. SHIs maybe one explanation of the longevity of Arctic mixed-phase clouds [*Sedlar and Tjernström, 2009*] by providing moisture at cloud top.

Method

The observations analysed in this study were performed during the Polarstern cruise PASCAL [*Wendisch et al., 2019, Macke and Flores, 2018]*, which took place in the sea-ice covered area north of Svalbard in summer 2017. This study is based on measurements with instruments carried by the tethered balloon system BELUGA (Balloon-bornE moduLar Utility for profilinG the lower Atmosphere, *Egerer et al., 2019*). BELUGA was launched from an ice floe at around 82° N, 10° E in the period 5-14 June 2017. The balloon measurements are complemented by regular radiosoundings launched every 6 hours and ship-based remote sensing data from radar and lidar, which are processed with the Cloudnet algorithm [*Griesche et al., 2019*]

Results and Discussion

A persistent layer of increasing specific humidity above a single-layer stratocumulus deck was observed in the period between 5 and 7 June 2017, which provides the observational basis for this study. For this period, Fig. 1 shows the temporal development of the vertical specific humidity profile derived from radiosondes in combination with cloud boundaries and the time-height profile of the corresponding BELUGA flights. The BELUGA flights were conducted around noon each day. An increased specific humidity is observed on all three days with a slight diurnal cycle peaking at noon and with a maximum specific humidity on 6 June. It is noteworthy that the observations show a well-defined layer of increased specific

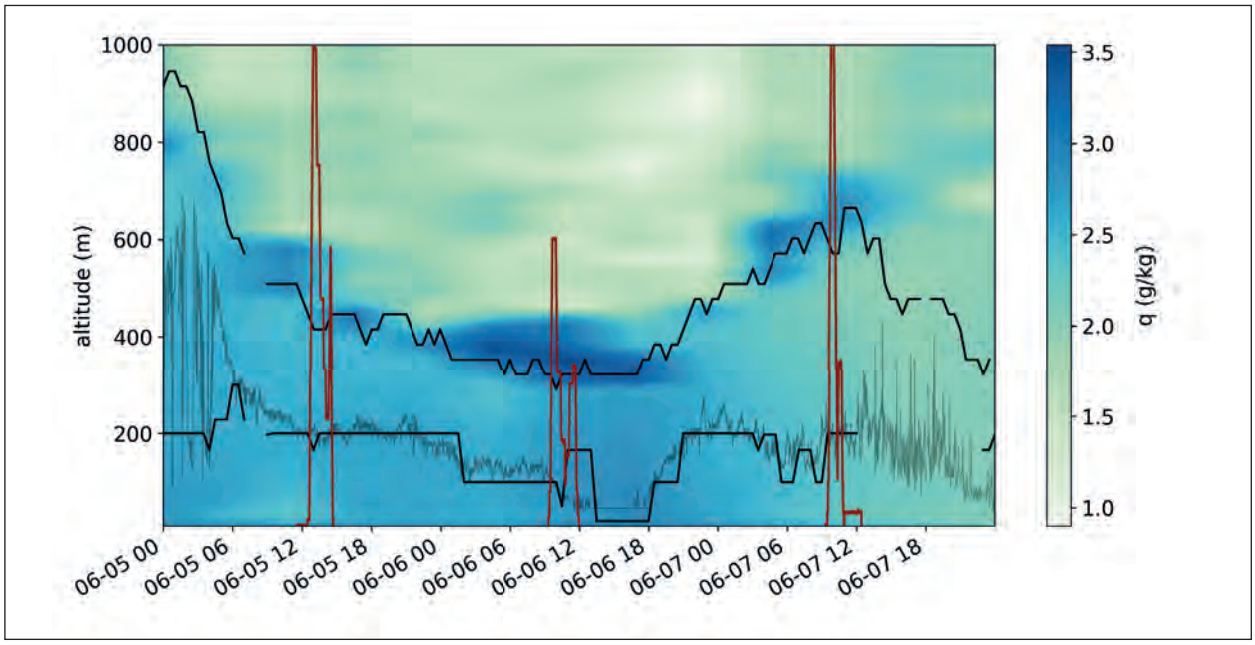

Fig. 1: Temporal development of the specific humidity vertical profile observed by radiosondes. The period 5 to 7 June 2017 exhibits a distinct layer of increased humidity above a low, single-layer stratocumulus. The cloud extent derived from Cloudnet data is depicted as black lines, the cloud base height derived from the Polarstern ceilometer data is indicated as a grey line. The red lines represent the BELUGA flight profiles.

humidity rather than a humidity inversion with only a slight decrease above.

Figure 2 shows vertical in-situ profiles as observed by BELUGA for 5 June 2017. The profile of specific humidity (Fig. 2b) clearly shows a distinct humidity layer above cloud top (shaded area). The base of this layer coincides with the base of the temperature inversion. In addition to the thermodynamic profiles in Fig. 2a & b, the terrestrial heating rate is shown with significant cooling at cloud top. This cooling and its resulting negative buoyancy is the only local source for turbulence around cloud top because wind shear is negligible (Fig. 2d). Local turbulence parameters as energy dissipation ε and turbulent kinetic energy TKE indicate almost constant

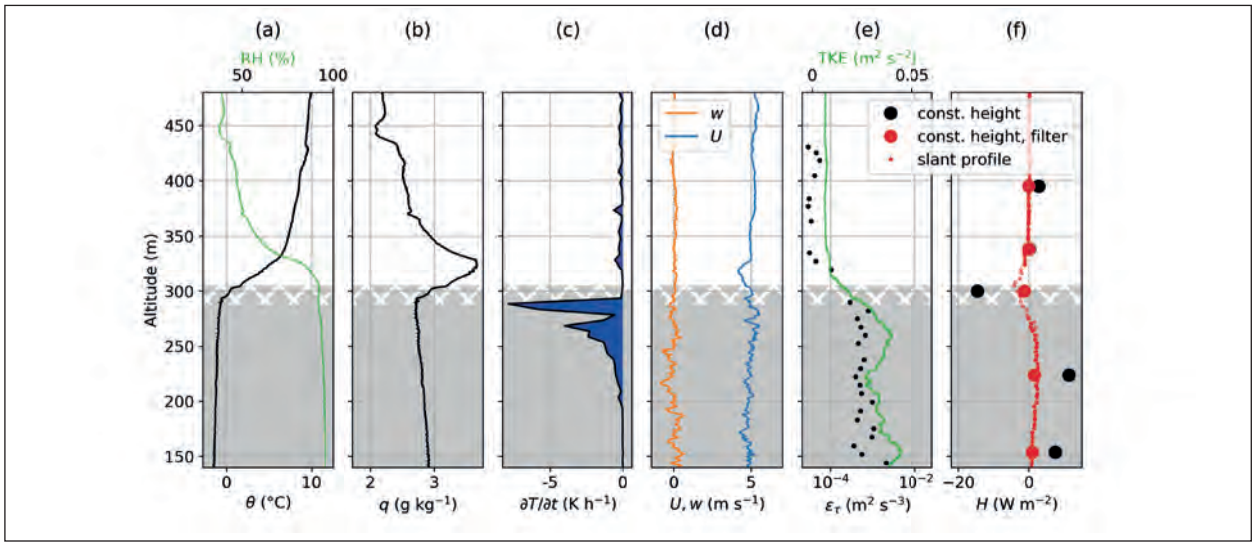

Fig. 2: Boundary layer observations around cloud top on 5 June 2017: Vertical profiles of (a) potential temperature θ and RH, (b) specific humidity q, (c) terrestrial heating rate δT/δt, (d) horizontal wind velocity U and vertical wind velocity w , (e) local dissipation rate ε and turbulent kinetic energy TKE and (f) virtual sensible heat flux H. Small red dots represent flux estimates on the slant profile, big black dots on constant altitude segments. Red big dots represent constant altitude fluxes based on high-pass filtered data. The cloud is shown as shaded area, the cloud top uncertainty as hatched area.

vales inside the cloud with some variability and gradually decrease around cloud top to lower values in the free troposphere. This gradual decrease is a clear indication that both layers – cloud and free troposphere – are not completely de-coupled and vertical exchange by turbulent mixing is possible.

The profile of the turbulent heat flux $H = \rho\, c_p \langle w' T_v' \rangle$ has been estimated by different methods and is shown in Fig. 2f. The flux has been estimated based on 10min-long time records at constant height (big circles) and from continuous profiling (red dots). For the profiling method, the flux has been calculated from height intervals. The height intervals and the low-pass filtering settings have been chosen according to the vertical extend of the cloud layer; length scales larger than the vertical cloud extend are filtered out and smaller scales are considered as fluctuations contributing to the turbulent fluxes (primed values in the turbulence flux). Due to filtering the absolute values for the different methods vary from the non-filtered values (black circles) but the negative sign for fluxes around cloud top is consistent for all methods indicating a downward flux of virtual temperature. We argue – although the flux could be calculated only for T_v – that also the moisture from the SHI will transported downward because their vertical gradients show a similar structure (increase with height) above cloud top.

This corroborates the idea that the SHI feeds the cloud layer, which directly contributes to the longevity of Arctic cloud layers. Large-Eddy Simulations (LES) performed by the University of Cologne have confirmed the evolution of SHIs under the boundary layer conditions observed on 5 June 2017. LES will help to evaluate the details of the development of SHIs and its influence on cloud lifetime.

References

Griesche, H. J., Seifert, P., Ansmann, A., Baars, H., Barrientos Velasco, C., Bühl, J., Engelmann, R., Radenz, M., and Zhenping, Y. (2019), Application of the shipborne remote sensing supersite OCEANET for profiling of Arctic aerosols and clouds during Polarstern cruise PS106, *Atmos. Meas. Tech. Discussions,* doi.org/10.5194/amt-2019-434.

Macke, A. and Flores, H.: The expeditions PS106/1 and 2 of the research vessel POLARSTERN to the Arctic ocean in 2017, (2018) *Reports on polar and marine research, Bremerhaven, Alfred Wegener Institute for Polar and Marine Research*, 719, doi.org/10.2312/BzPM_0719_2018.

Naakka, T., Nygård, T., and Vihma, T. (2018), Arctic Humidity Inversions: Climatology and Processes, *J. Climate*, 31, 3765 – 3787, doi.org/DOI:10.1175/JCLI-D-17-0497.1.

Sedlar, J. and Tjernström, M. (2009), Stratiform Cloud—Inversion Characterization During the Arctic Melt Season, *Bound.-Lay. Meteorol.*, 132, 455–474, doi.org/10.1007/s10546-009-9407-1.

Wendisch, M., Macke, A., Ehrlich, A., Lüpkes, C., Mech, M., Chechin, D., Dethloff, K., Velasco, C. B., Bozem, H., Brückner, M., Clemen, H.-C., Crewell, S., Donth, T., Dupuy, R., Ebell, K., Egerer, U., Engelmann, R., Engler, C., Eppers, O., Gehrmann, M., Gong, X.,Gottschalk, M., Gourbeyre, C., Griesche, H., Hartmann, J., Hartmann, M., Heinold, B., Herber, A., Herrmann, H., Heygster, G., Hoor, P., Jafariserajehlou, S., Jäkel, E., Järvinen, E., Jourdan, O., Kästner, U., Kecorius, S., Knudsen, E. M., Köllner, F., Kretzschmar, J., Lelli, L., Leroy, D., Maturilli, M., Mei, L., Mertes, S., Mioche, G., Neuber, R., Nicolaus, M., Nomokonova, T., Notholt, J., Palm, M., van Pinxteren, M., Quaas, J., Richter, P., Ruiz-Donoso, E., Schäfer, M., Schmieder, K., Schnaiter, M., Schneider, J., Schwarzenböck, A., Seifert, P., Shupe, M. D., Siebert, H., Spreen, G., Stapf, J., Stratmann, F., Vogl, T., Welti, A., Wex, H., Wiedensohler, A., Zanatta, M., and Zeppenfeld, S. (2019), The Arctic Cloud Puzzle: Using ACLOUD/PASCAL Multiplatform Observations to Unravel the Role of Clouds and Aerosol Particles in Arctic Amplification, *Bull. Am. Meteor. Soc.*, 100, 841–871, doi.org/10.1175/BAMS-D-18-0072.1.

Cooperation

Institute for Meteorology, University of Leipzig, Leipzig;
Institute of Geophysics and Meteorology, University of Cologne.

Ice nucleating particles around the world

Heike Wex, Xianda Gong, Markus Hartmann, Christian Tatzelt, Conrad Jentzsch, Silvia Henning, Manuela van Pinxteren, Nadja Triesch, Sebastian Zeppenfeld, Frank Stratmann*

* as a number of studies is summarized here, please refer to the cited literature for external co-operating scientists

In den letzten Jahren wurden neu implementierte Instrumente zur Offline-Analyse von atmosphärischen Konzentrationen von INP (ice nucleating particles) eingesetzt, um neue Informationen über atmosphärische INPs, ihre Quellen und Häufigkeiten zu erhalten. Die untersuchten Proben waren weltweit gesammelt worden. Ergebnisse zeigten wiederholt, dass atmosphärische INP, die im Temperaturbereich bis -25°C eisaktiv sind nicht anthropogenen Ursprungs sind. Es wurden höhere INP Konzentrationen in Verbindung mit Landmassen gefunden, verglichen mit solchen über Ozeanen, und ein Großteil der z.B. auf den Cap Verden beobachteten INP kann nicht marinen Ursprungs gewesen sein. Andererseits wurden im Arktischen Ozean direkt über offenen Stellen im Meereis in niedrigen Höhen erhöhte INP Konzentrationen beobachtet, so dass vermutet werden kann, dass INP marinen Ursprungs in abgelegenen marinen Regionen zu atmosphärischen Hintergrundkonzentrationen von INP merklich beitragen.

Introduction

In the past years, newly implemented instrumentation for the off-line analysis of number concentrations of INP (ice nucleating particles) were used for obtaining unprecedented information concerning the abundances, properties and sources of atmospheric INPs. This short article will give an overview of our recent achievements.

Methods

Examined samples were taken worldwide and include samples from the Arctic as well as the Antarctic region, Beijing as an example for anthropogenic pollution, Puy de Dome in France as a European background site and Cyprus and the Cabo Verde islands (São Vicente) as examples for regions close to desert dust sources. Most of the examined samples were atmospheric samples collected on filters, occasionally amended with sea and cloud water samples.

Two different measurement set-ups were used, LINA (Leipzig Ice Nucleation Array) and INDA (Ice Nucleation Droplet Array). Detailed explanations on LINA and INDA can be found in e.g., *Chen et al.* [2018] and *Hartmann et al.* [2019a]. In short, for one measurement both methods examine ~ 90 separate droplets (droplet volume LINA: 1µL, INDA: 50µL), where those droplets are either the sample itself (e.g., a cloud water sample) or samples for which particles collected on a polycarbonate filter are washed off into ultra-clean water. If quartz fiber filters were used for the sampling, filter stances of 1 mm in diameter from these filters are immersed in 50µL droplets of ultra-clean water in the INDA set-up. The examined droplets sit on a hydrophobic glass slide in LINA, or in the separate tubes of a PCR-tray in INDA. They are cooled at a rate of 1 K/min and it is observed how many droplets freeze at which temperature. From that, INP concentrations (N_{INP}) can be determined. Measurements are feasible down to ~ -25°C, thus the herein presented results are only valid for this temperature range.

Results

In the following, results obtained from a range of samples in a range of studies are summarized:

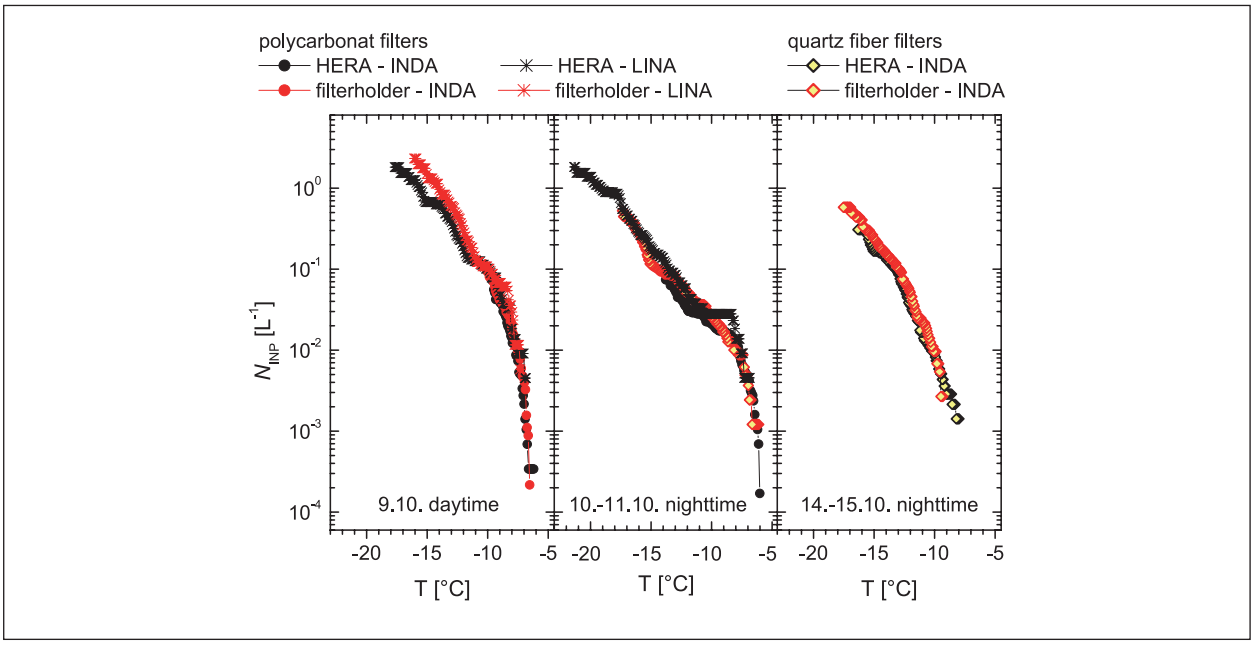

Fig. 1: Spectra of INP number concentrations for three exemplary sampling periods (8 hours each) are shown. Samples were taken in October 2018 on Puy de Dome in France. Generally, measured values agreed well, independent of the filter material that was used (polycarbonate or quartz fiber), of the sampler in which the sample was taken (HERA or a simple filter holder) and (in the temperature region in which overlapping data are obtained) independent of the use of either LINA or INDA.

- Different samplers (HERA, a sampler developed for air-craft sampling, and a simple filter holder), different filter materials (quartz fiber and polycarbonate) and the two different measurement set-ups INDA and LINA all were applied to evaluate N_{INP} collected on Puy de Dome in France in October 2018. Data agreed across both samplers, both filter materials and both set-ups (Fig. 1), corroborating the feasibility to use all of these different materials and methods for INP measurements. This work was done within the framework of a broader inter-comparison campaign [*Freney et al.*, 2019].
- Measurements of N_{INP} from two different Arctic ice cores (from Greenland and Svalbard) showed that N_{INP} has not increased in the past 500 years prior to the year 2000 [*Hartmann et al.*, 2019a], indicating that anthropogenic pollution does not increase N_{INP}.
- Filter samples from four different Arctic ground based stations (in Alaska, Canada, Greenland and Svalbard), collected during the course of one year at each of these stations, showed a clear yearly cycle of N_{INP}, with higher concentrations in summer, compared to winter [*Wex et al.*, 2019]. Sources of high concentrations in summer could be both, marine or terrestrial [*Wex et al.*, 2019; *Creamean et al.*, 2018]. Samples in summer were found to be heat-sensitive [*Šantl-Temkiv et al.*, 2019], while those in winter were not, pointing towards a biogenic nature of the highly ice active INP collected in summer (Fig. 2). This also corroborates that anthropogenic particles (seen

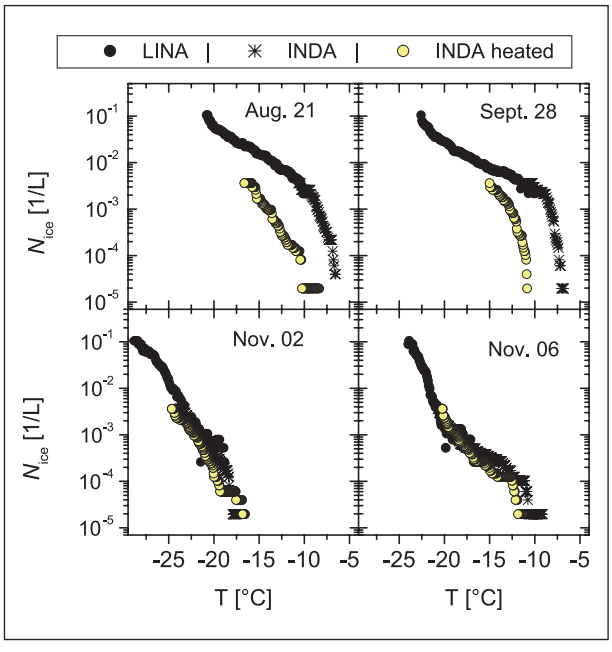

Fig. 2: Spectra of INP number concentrations for four exemplary sampling periods (3.5 days each, starting date is indicated) are shown. INDA measurements were done for both the original and a heated sample, were heating was done at 95°C for one hour. INP number concentrations were clearly higher in the summer months, and heating diminished the signals, indicating a biogenic origin of those INP that cause the higher concentrations.

as Arctic haze in this region) do not increase N_{INP}, as Arctic haze is strongest in early spring when N_{INP} are lowest.
- Increased concentrations of heat-sensitive (i.e., biogenic) INP were observed in the Arctic Ocean in late March / early April at low altitudes directly above open waters in the sea ice [*Hartmann et al.*, 2019b], suggesting that marine sources contribute to atmospheric background concentrations of INP in remote marine regions.
- The analysis of filter samples taken during ship cruises in the Arctic (PASCAL on Polarstern, summer 2017) and around Antarctica (ACE-SPACE on Tryoshnikov, winter 2016/1017) showed low N_{INP} in general, with increasing concentrations close to land [*Wendisch et al.*, 2019; *Schmale et al.*, 2019].
- Airborne N_{INP} from filter samples collected on Cyprus [*Gong et al.*, 2019a] and on São Vicente (one of the Cabo Verde islands) [*Gong et al.*, 2019b] were similar and generally in the lower half of values reported in literature for continental sites in North America and Europe in *Petters & Wright* [2015].
- A large fraction of airborne INP collected on São Vicente were supermicron in size [*Gong et al.*, 2019b], in agreement with results recently presented in literature by *Mason et al.* [2016] and *Creamean et al.* [2018], and the ice activity of these supermicron particles was related to the presence of biogenic INP.
- Altogether, on and around São Vicente N_{INP} were obtained from ocean bulk water, the ocean surface microlayer and cloud water (collected on a ~ 700 m high mountain) as well as in the air (both at sea level and at the mountain). It could be shown that the aerosol in general was well mixed within the marine boundary layer [*Gong et al.*, 2019c]; comparing N_{INP} from the different samples, we concluded that at most only a small fraction of the atmospheric INP originated from the ocean [*Gong et al.*, 2019b].
- N_{INP} in Beijing were independent of the degree of pollution ($PM_{2.5}$ and total particle number concentration varied by a factor of more than 30 during the time when the different samples were taken), again showing that in the examined temperature range (down to ~ -25°C) , anthropogenic pollution does not add INP to the atmosphere [*Chen et al.*, 2018].

Results as those described above are important pieces in the puzzle to better quantify the abundance and properties of atmospheric INP, identify their source and transport patterns, understand their role(s) in cloud glaciation and are highly valuable for driving, constraining and evaluating various kinds of atmospheric models (from large eddy to global scale).

References

Chen, J., Z. Wu, S. Augustin-Bauditz, S. Grawe, M. Hartmann, X. Pei, Z. Liu, D. Ji, and H. Wex (2018), Ice nucleating particle concentrations unaffected by urban air pollution in Beijing, China, Atmos. Chem. Phys., 18, 3523–3539, doi:10.5194/acp-18-3523-2018.

Creamean, J. M., R. M. Kirpes, K. A. Pratt, N. J. Spada, M. Maahn, G. de Boer, R. C. Schnell, and S. China (2018), Marine and terrestrial influences on ice nucleating particles during continuous springtime measurements in an Arctic oilfield location, Atmos. Chem. Phys., 18, 18023–18042, doi:10.5194/acp-18-18023-2018.

Freney, E., Y. Bras, D. Picard, J. L. Baray, P. Villani, P. Amato, M. Ribeiro, L. Lacher, B. Bertozzi, O. Möhler, P. J. DeMott, E. J. T. Levin, K. Barry, T. C. H. Hill, M. Wolf, D. J. Cziczo, M. Goodell, L. A. Ladino, C. Ramirez, C. Jentzsch, H. Wex, S. Mertes, D. Axisa, B. J. Murray, M. Adams, E. S. Thomson, D. Castarede, J. Schrod, H. Bingemer, Z. A. Kanji, and K. Sellegri (2019), Understanding how aerosol properties influence atmospheric Ice Nucleating Particle number during the Puy de Dome ICe Nucleation Intercomparison Campaign (PICNIC), presented at the European Aerosol Conference 2019.

Gong, X., H. Wex, T. Müller, A. Wiedensohler, K. Höhler, K. Kandler, N. Ma, B. Dietel, T. Schiebel, O. Möhler, and F. Stratmann (2019a), Characterization of aerosol properties at Cyprus, focusing on cloud condensation nuclei and ice nucleating particles, Atmos. Chem. Phys., 19, 10883-10900, doi:10.5194/acp-19-10883-2019.

Gong, X., H. Wex, M. van Pinxteren, N. Triesch, K. W. Fomba, J. Lubitz, C. Stolle, B. Robinson, T. Müller, H. Herrmann, and F. Stratmann (2019b), Characterization of aerosol particles at Cape Verde close to sea and cloud level heights - Part 2: ice nucleating particles in air, cloud and seawater, Atmos. Chem. Phys. Discuss., doi:10.5194/acp-2019-729.

Gong, X., H. Wex, J. Voigtländer, K. W. Fomba, K. Weinhold, M. van Pinxteren, S. Henning, T. Müller, H. Herrmann, and F. Stratmann (2019c), Characterization of aerosol particles at Cape Verde close to sea and cloud level heights - Part 1: particle number size distribution, cloud condensation nuclei and their origins, Atmos. Chem. Phys. Discuss., doi:10.5194/acp-2019-585.

Hartmann, M., K. Adachi, O. Eppers, C. Haas, A. Herber, R. Holzinger, A. Hünerbein, E. Jäkel, C. Jentzsch, M. van Pinxteren, H. Wex, S. Willmes, and F. Stratmann (2019b), A marine, biogenic source for Ice Nucleating Particles on airborne filter samples in the high Arctic, submitted to Geophys. Res. Lett..

Hartmann, M., T. Blunier, S. O. Brügger, J. Schmale, M. Schwikowski, A. Vogel, H. Wex, and F. Stratmann (2019a), Variation of ice nucleating particles in the European Arctic over the last centuries, Geophys. Res. Lett., 46, doi:10.1029/2019GL082311.

Mason, R. H., M. Si, C. Chou, V. E. Irish, R. Dickie, P. Elizondo, R. Wong, M. Brintnell, M. Elsasser, W. M. Lassar, K. M. Pierce, W. R. Leaitch, A. M. MacDonald, A. Platt, D. Toom-Sauntry, R. Sarda-Esteve, C. L. Schiller, K. J. Suski, T. C. J. Hill, J. P. D. Abbatt, J. A. Huffman, P. J. DeMott, and A. K. Bertram (2016), Size-resolved measurements of ice-nucleating particles at six locations in North America and one in Europe, Atmos. Chem. Phys., 16(3), 1637-1651, doi:10.5194/acp-16-1637-2016.

Petters, M. D., and T. P. Wright (2015), Revisiting ice nucleation from precipitation samples, Geophys. Res. Lett., 42(20), 8758-8766, doi:10.1002/2015gl065733.

Šantl-Temkiv, T., R Lange, D. Beddows, U. Rauter, S. Pilgaard, M. Dall'Osto, N. Gunde-Cimerman, A. Massling, and H. Wex (2019), Biogenic sources of Ice Nucleation Particles at the high Arctic site Villum Research Station, Environ. Sci. Technol., 53(18), 10580-10590, doi:10.1021/acs.est.9b00991.

Schmale, J., A. Baccarini, I. Thurnherr, S. Henning, A. Efraim, L. Regayre, C. Bolas, M. Hartmann, A. Welti, K. Lehtipalo, F. Aemisegger, C. Tatzelt, S. Landwehr, R. L. Modini, F. Tummon, J. S. Johnson, N. Harris, M. Schnaiter, A. Toffoli, M. Derkani, N. Bukowiecki, F. Stratmann, J. Dommen, U. Baltensperger, H. Wernli, D. Rosenfeld, M. Gysel-Beer, and K. S. Carslaw (2019), Overview of the Antarctic Circumnavigation Expedition: Study of Preindustrial-like Aerosols and their Climate Effects (ACE-SPACE), BAMS, doi:10.1175/BAMS-D-18-0187.1.

Wendisch, M., et al. (2019), The Arctic cloud puzzle: Using ACLOUD/PASCAL multi-platform observations to unravel the role of clouds and aerosol particles in Arctic Amplification, BAMS, doi:10.1175/BAMS-D-18-0072.1.

Wex, H., L. Huang, W. Zhang, H. Hung, R. Traversi, S. Becagli, R. J. Sheesley, C. E. Moffett, T. E. Barrett, R. Bossi, H. Skov, A. Hünerbein, J. Lubitz, M. Löffler, O. Linke, M. Hartmann, P. Herenz, and F. Stratmann (2019), Annual variability of ice nucleating particle concentrations at different Arctic locations, Atmos. Chem. Phys., 19, 5293–5311, doi:10.5194/acp-19-5293-2019.

Funding

German Research Foundation (DFG);
Leibniz Competition within the Leibniz Association (SAW);
Swizz Polar Institute.

Decreasing Trends of Particle Number and Black Carbon Mass Concentrations at 16 Observational Sites in Germany from 2009 to 2018

Jia Sun[1], Wolfram Birmili[2,1], Markus Hermann[1], Thomas Tuch[1], Kay Weinhold[1], Maik Merkel[1], Fabian Rasch[1], Thomas Müller[1], Alexander Schladitz[3,a], Susanne Bastian[3], Gunter Löschau[3], Josef Cyrys[4,5], Jianwei Gu[4,5,b], Harald Flentje[6], Björn Briel[6], Christoph Asbach[7], Heinz Kaminski[7], Ludwig Ries[2], Ralf Sohmer[2], Holger Gerwig[2], Klaus Wirtz[2], Frank Meinhardt[2], Andreas Schwerin[2], Olaf Bath[2], Nan Ma[8,1], Alfred Wiedensohler[1]

[1]Leibniz Institute for Tropospheric Research (TROPOS), Leipzig, Germany
[2]German Environment Agency (UBA), Dessau-Roßlau, Germany
[3]Saxon State Office for Environment, Agriculture and Geology (LfULG), Dresden, Germany
[4]Helmholtz Zentrum München (HMGU), Institute of Epidemiology II, Neuherberg, Germany
[5]University of Augsburg(UA), Wissenschaftszentrum Umwelt, Augsburg, Germany
[6]Deutscher Wetterdienst (DWD), Meteorologisches Observatorium Hohenpeißenberg, Germany
[7]Institute of Energy and Environmental Technology (IUTA), Duisburg, Germany
[8]Institute for Environmental and Climate Research, Jinan University, Guangzhou, Guangdong 511443, China
[a]now at: SICK Engineering GmbH, Ottendorf-Okrilla, Germany
[b]now at: Fraunhofer Wilhelm-Klauditz-Institut (WKI), Braunschweig, Germany

Seit den 1990er Jahren werden Minderungsmaßnahmen zur Verringerung der anthropogen verursachten Luftverschmutzung in Europa durchgeführt. Unter anderem um die Effektivität dieser Maßnahmen zu überprüfen, wurde 2008 das Deutsche Ultrafeine Aerosolpartikel Netzwerk etabliert (Englisch: German Ultrafine Aerosol Network, GUAN). GUAN hat seinen Fokus auf Ruß (black carbon) und ultrafeine Partikel (< 100 nm im Durchmesser). In der vorliegenden Studie, wurden die Trends von größenaufgelösten Partikelanzahlkonzentrationen (PNCs) und äquivalenter Rußmassenkonzentration (eBc) in einem 10 Jahreszeitraum (2009-2018) an 16 GUAN Beobachtungsstationen in verschiedenen Umgebungen untersucht. Die Ergebnisse zeigen in allen Umgebungen einen negativen Trend (Konzentrationsabnahme), sowohl für die PNCs in allen Größenklassen als auch für eBC, außer für die Nukleationsmode-Partikel (PNC, 10-30 nm) im regionalen Hintergrund und auf den Bergstationen. Der wahrscheinlichste Einflussfaktor für die negativen Trends sind die abnehmenden anthropogenen Emissionen, hervorgerufen durch die Minderungsmaßnahmen der Europäischen Union.

Introduction

To reduce the harmful effects caused by air pollution, emission mitigation policies were implemented around the world since the 1990s. In Germany, the Federal Emission Control Regulations (German: Bundes-Immissionsschutzverordnung, BImSchV) limits the emissions of industry, domestic heating, transport, etc. To evaluate the effectiveness of those emission mitigation policies, long-term observations of pollutants are crucial, especially for those health-related pollutants, such as sub-micrometer particles and black carbon (BC). This study takes Germany as an example to understand the effectiveness of emission mitigation policies on the reduction of the regional particle number concentration (PNC) and BC mass concentration. In this investigation, trend analysis was done for the sub-micrometer PNC (diameter < 1 µm) and the equivalent black carbon (eBC) mass concentration in Germany based on a unique dataset of the German Ultrafine Aerosol Network (GUAN).

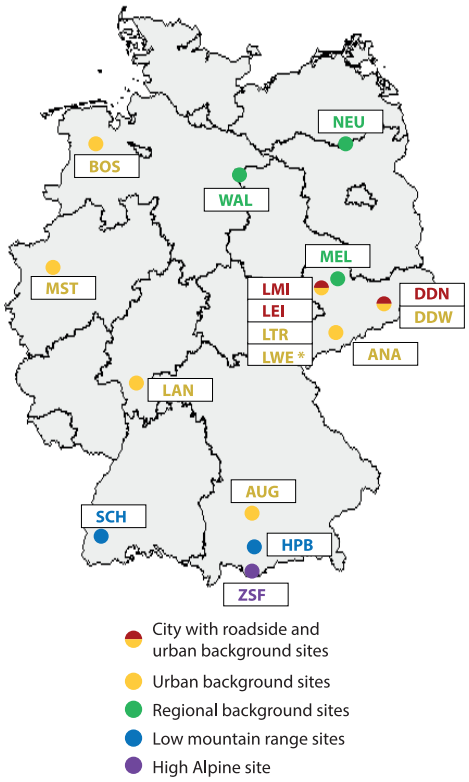

Abbreviation	Site name
ANA	Annaberg-Buchholz
AUG	Augsburg
BOS	Bösel
DDN	Dresden-Nord
DDW	Dresden-Winckelmannstraße
HPB	Hohenpeißenberg
LAN	Langen
LEI	Leipzig-Eisenbahnstraße
LMI	Leipzig-Mitte
LTR	Leipzig-TROPOS
LWE *	Leipzig-West
MEL	Melpitz
MST	Mülheim-Styrum
NEU	Neuglobsow
SCH	Schauinsland
WAL	Waldhof
ZSF	Zugspitze (Schneefernerhaus)

*Fig. 1: The map of atmospheric measurement stations in German Ultrafine Aerosol Network (GUAN). * The site LWE was not included in the trend analysis in this article due to its short data coverage.*

Method

GUAN is a specialized network in Germany, which provides continuous measurements including sub-micrometer particle number size distribution (PNSD) and eBC mass concentration, for diverse environments from roadside, urban background, regional background, low mountain range to high Alpine, as shown in Fig. 1.

The technical details of the PNSD and eBC mass concentration measurements at GUAN sites are summarized in *Birmili et al.* [2016]. Depending on individual set-up, the PNSD are measured either by Mobility Particle Size Spectrometers (MPSS) or by Dual Mobility Particle Size Spectrometers (D-MPSS). The quality of the PNSD was ensured by onsite or laboratory inter-comparisons conducted by the World Calibration Center for Aerosol Physics (WCCAP, http://www.wmo-gaw-wcc-aerosol-physics.org/) at TROPOS [*Wiedensohler et al.,* 2012]. Mass concentrations of eBC have been measured by Multi-Angle Absorption Photometers (MAAP, Thermo Scientific, model 5012), except in site Augsburg (AUG) where an Aethalometer (Type 8100, Thermo Fisher Scientific Inc.) is used.

Result

The temporal trends of the PNCs and eBC mass concentrations during 2009-2018 were evaluated by the customized Sen's estimator [*Birmili et al.*, 2015]. The relative annual slopes are shown in Table 1. Significant decreases of the eBC mass concentration or PNC can be seen for 92% evaluated stations and parameters.

Figure 2 shows the customized Sen's slopes of the PNCs and eBC mass concentration at each hour of day. BC is mainly emitted from anthropogenic sources in Europe, and traffic emission is thought to be one of the dominant contributors for anthropogenic emissions. Stronger decrease of BC is observed at daytime due to higher traffic emission reduction at roadside and urban background sites. Negative slopes can be also observed in night time and for other site categories. A plausible explanation is that a reduction of local anthropogenic emissions can also reduce the background eBC mass concentration in a larger area and longer time scale since BC has a lifetime of about one week [*Wang et al.*, 2014]. This result confirms that reduction of anthropogenic emissions plays a major role in the decreasing of eBC mass concentration in Germany. The trends of the PNCs depend on the

Tab. 1: Multi-annual trends of the eBC mass concentration and PNCs in percent per year, using the customized Sen's estimator. The bold slopes are the significant slopes at the 95% significance level. Five site categories on the left column are roadside (RS), urban background (UB), regional background (RB), low mountain range (LMT) and high Alpine (HA).

Category	Site	eBC mass concentration	$N_{[20-800]}$	$N_{[10-30]}$	$N_{[30-200]}$	$N_{[200-800]}$
RS	DDN	**-11,3%**	**-7,3%**	**-8,0%**	**-6,7%**	**-9,7%**
	LEI	**-5,0%**	**-2,9%**	**-5,0%**	**-2,9%**	**-1,2%**
	LMI	**-5,5%**	**-4,8%**	-0,2%	**-5,5%**	**-4,8%**
UB	MST	---[a]	**-2,6%**	---[b]	**-3,2%**	**-6,1%**
	LTR	**-4,1%**	**-4,3%**	**-4,7%**	**-4,1%**	**-4,6%**
	ANA	**-6,9%**	**-5,5%**	**-6,5%**	**-5,4%**	**-11,1%**
	AUG	**-2,3%**	**-6,3%**	**-6,0%**	**-6,3%**	**-3,7%**
	DDW	**-8,1%**	**-4,8%**	**-3,2%**	**-5,0%**	**-8,8%**
	LAN	---[a]	**-3,4%**	**-1,4%**	**-4,3%**	**-2,5%**
	BOS	**-4,9%**	**-5,5%**	**-1,7%**	**-5,9%**	**-6,3%**
RB	MEL	**-4,4%**	-0,2%	1,9%	-0,2%	**-2,9%**
	WAL	**-3,2%**	**-4,2%**	**-3,3%**	**-4,4%**	**-5,2%**
	NEU	**-7,8%**	-1,0%	-0,6%	-0,5%	**-3,9%**
LMT	HPB	**-2,8%**	**-1,2%**	**1,7%**	**-1,2%**	**-3,9%**
	SCH	**-1,7%**	**-1,5%**	**3,8%**	**-2,0%**	**-3,8%**
HA	ZSF	**-4,0%**	**-4,2%**	---[b]	**-4,1%**	**-4,2%**

[a] The parameter was not measured at the corresponding sites.
[b] The parameter was measured at the corresponding sites, but the time period is not long enough for the trend analysis (< 6 years).

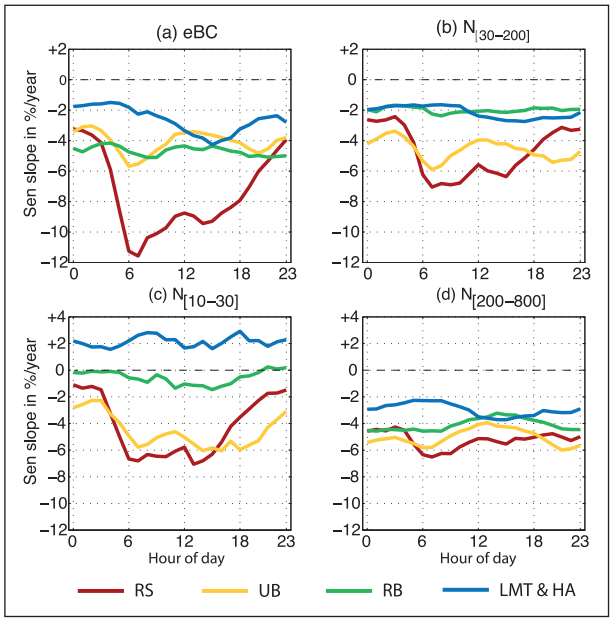

Fig. 2: Annual trends of the eBC mass concentration and PNCs for each hour of day, using the customized Sen's estimator at each site category: roadside (RS), urban background (UB), regional background (RB), low mountain range and high Alpine (LMT&HA).

particle size ranges and time of day. At roadside sites, similar diurnal patter with higher reduction rate in daytime and lower rate at nighttime can be observed for $N_{[20-800]}$, $N_{[10-30]}$ and $N_{[30-200]}$. We attribute this diurnal pattern of reduction rate to the reduced traffic emission in urban background conditions. At regional and mountain sites, $N_{[30-200]}$ and $N_{[200-800]}$ show a constant negative trend throughout the day, suggesting the decrease of PNCs in the regional background air which is likely to be the result of the reduction of anthropogenic emissions in cities, resulting from the implementation of emission mitigation strategies all over Germany.

References

Birmili, W., J. Sun, K. Weinhold, M. Merkel, F. Rasch, A. Wiedensohler, S. Bastian, G. Löschau, A. Schladitz, U. Quass, T. A. J. Kuhlbusch, H. Kaminski, J. Cyrys, M. Pitz, J. Gu, A. Peters, H. Flentje, F. Meinhardt, A. Schwerin, O. Bath, L. Ries, H. Gerwig, K. Wirtz, and S. Weber (2015), Atmospheric aerosol measurements in the German Ultrafine Aerosol Network (GUAN) – Part 3: Black Carbon mass and particle number concentrations 2009 to 2014, Gefahrst. Reinh. Luft, 75(11/12).

Birmili, W., K. Weinhold, F. Rasch, A. Sonntag, J. Sun, M. Merkel, A. Wiedensohler, S. Bastian, A. Schladitz, G. Löschau, J. Cyrys, M. Pitz, J. Gu, T. Kusch, H. Flentje, U. Quass, H. Kaminski, T. A. J. Kuhlbusch, F. Meinhardt, A. Schwerin, O. Bath, L. Ries, H. Gerwig, K. Wirtz, and M. Fiebig (2016), Long-term observations of tropospheric particle number size distributions and equivalent black carbon mass concentrations in the German Ultrafine Aerosol Network (GUAN), Earth Syst. Sci. Data, 8(2), 355-382, 10.5194/essd-8-355-2016.

Wang, Q., D. J. Jacob, J. R. Spackman, A. E. Perring, J. P. Schwarz, N. Moteki, E. A. Marais, C. Ge, J. Wang, and S. R. Barrett (2014), Global budget and radiative forcing of black carbon aerosol: Constraints from pole-to-pole (HIPPO) observations across the Pacific, Journal of Geophysical Research: Atmospheres, 119(1), 195-206.

Wiedensohler, A., W. Birmili, A. Nowak, A. Sonntag, K. Weinhold, M. Merkel, B. Wehner, T. Tuch, S. Pfeifer, M. Fiebig, A. M. Fjäraa, E. Asmi, K. Sellegri, R. Depuy, H. Venzac, P. Villani, P. Laj, P. Aalto, J. A. Ogren, E. Swietlicki, P. Williams, P. Roldin, P. Quincey, C. Hüglin, R. Fierz-Schmidhauser, M. Gysel, E. Weingartner, F. Riccobono, S. Santos, C. Grüning, K. Faloon, D. Beddows, R. Harrison, C. Monahan, S. G. Jennings, C. D. O'Dowd, A. Marinoni, H. G. Horn, L. Keck, J. Jiang, J. Scheckman, P. H. McMurry, Z. Deng, C. S. Zhao, M. Moerman, B. Henzing, G. de Leeuw, G. Löschau, and S. Bastian (2012), Mobility particle size spectrometers: harmonization of technical standards and data structure to facilitate high quality long-term observations of atmospheric particle number size distributions, Atmos. Meas. Tech., 5(3), 657-685, 10.5194/amt-5-657-2012.

Funding

The German Federal Environment Ministry (BMU) grants F&E 370343200 and F&E 371143232.

Cooperation

German Environment Agency (UBA), Berlin, Germany;
The Saxon State Office for Environment, Agriculture and Geology (LfULG), Dresden, Germany;
Helmholtz Zentrum München (HMGU), Institute of Epidemiology II, Neuherberg, Germany;
University of Augsburg(UA), Wissenschaftszentrum Umwelt, Augsburg, Germany;
Deutscher Wetterdienst (DWD), Meteorologisches Observatorium Hohenpeißenberg, Germany;
Institute of Energy and Environmental Technology (IUTA), Duisburg, Germany.

Optical properties of black carbon with changing morphology and composition: A modelling study

Baseerat Romshoo, Thomas Müller, Sascha Pfeifer, Alfred Wiedensohler

Die optischen Eigenschaften von Ruß sind von großem Interesse, weil hieraus Rückschlüsse auf die Art der Partikel gezogen kann und deren Strahlungseinflüsse untersucht werden können. Nach der Emission in die Atmosphäre erfahren BC-Aggregate verschiedene Änderungen in Form, Größe und Zusammensetzung. In dieser Studie untersuchen wir diese Veränderungen, indem wir die verschiedenen Fälle möglicher Partikelaggregate nach einem systematischen Schema simulieren. Es wird angenommen, dass die Partikel eine fraktale Morphologie aufweisen, wobei jedes Monomer in einer nicht absorbierenden Beschichtung eingeschlossen ist. Die optischen Eigenschaften dieser Aggregate werden in einem weiten Parameterraum berechnet, um Parametrisierungen der optischen Eigenschaften für beschichtete BC-Aggregate zu entwickeln.

Introduction

Black carbon (BC), also called light-absorbing carbon (LAC) is produced from various combustion processes and is pointed out to be the second-largest contributor to global warming after CO_2. The formation of BC from combustion and subsequent ageing is a process involving several stages. In the earlier stages, BC consists of fractal structures, which are formed from the aggregation of primary spherules with the sizes between 10–30nm depending on the burning conditions to the flame [*Homann*, 1967]. Depending upon the atmospheric conditions after emission, irregularly shaped spherules provide active sites for deposition of water. This causes a change in the hygroscopicity of the particles. Furthermore, different by-products of burning like organics are condensed onto the particles. These processes lead to the formation of a coating around the black carbon core [*Bond and Bergstrom*, 2006] and reshaping the black carbon aggregates into spherical structures [*Abel et al.*, 2003]. Therefore, BC particles go through changes in morphology and composition over time. As the black carbon fractal aggregates become more compact, changes in the absorption and scattering cross-sections have been seen. Laboratory studies also show changes in the optical properties of black carbon with an increasing volume of a non-absorbing organic coating [*Shiraiwa et al.*, 2010].

Method

Fractal BC containing particles are generated using a Diffusion Limited Aggregation (DLA) program developed by *Woźniak* et al. [2012]. Coated BC aggregates are further designed by taking a spherical coating around each individual monomer corresponding to the given volume fraction C_f (fraction of coating material to total volume). A Multi Sphere T Matrix Code (MSTM) [*Mackowski Mackowski and Mishchenko*, 2011] calculates the optical properties of the simulated BC aggregates. The study is divided into two parts, first focusing on the change in morphology of the aggregates, quantified by the

parameter fractal dimension (D_f). The second part focuses on the change in composition, which is quantified by the coating fraction (C_f). In both cases, the change in optical properties is studied by increasing the size of the aggregates gradually by changing the number of monomers, along with D_f or C_f. This approach covers a huge parameter space and is well suited for relating the modelled optical properties to laboratory results as well as in providing parameterization for climate modelers.

For the first part, fixing the C_f to 50%, we change the fractal dimension (D_f) from 1.6 to 2.2, representing a range of aggregate morphologies from fractal (fresh) to slightly compact (partially aged) particles. In addition to this, we take as a reference case a coated sphere (D_f=3), which is widely used by atmospheric scientists. For the second part, the coating fraction (C_f) is changed from 5 to 60% for an aggregate of D_f equal to 1.7. The radius of the black carbon monomers (a_i) is fixed to 15 nm throughout this study outer radius of the coated monomer (a_o) changes according to coating fraction C_f.

Result and Discussion

The optical properties were calculated for all cases at a wavelength of 0.66 *um*, and the refractive index was assumed to be 1.7 + 0.7*i* for BC and 1.46 + 0*i* for the coating [*Bond and Bergstrom*, 2006]. The results are discussed as follows:

- **Change in morphology**

  Figure 1 shows the different optical properties as a function of changing size (D_m) and morphology (D_f). The absorption cross-section (C_{abs}) decreases, as the aggregates become more compact (higher D_f). This is because of the shielding effect of the outer layer of monomers not allowing the electromagnetic field to penetrate. On the contrary, for the case of a single coated sphere, C_{abs} is larger than the equivalent aggregate for larger particels (D_m = 250*nm*). This may be caused by Mie resonances. The scattering cross-section (C_{sca}) is smaller at lower D_f due to decreasing scattering in loosely packed particles (Rayleigh effect). The single scattering albedo (SSA = C_{sca}/C_{ext}) was between 0.02 to 0.32, with higher values for larger particle and the more compact the particle is. Mass absorption cross-section (MAC) is defined as the ratio of C_{abs} and BC mass. The values of MAC are higher at lower D_m consistent with the larger absorption cross section for loosely packed aggregates. As the size of the aggregate increases, the MAC has a value between 5 – 7 m^2g^{-1} consistent with calculations in literature [*Bond and Bergstrom*, 2006]. It is observed that at smaller D_m, the *g* is larger for lower D_f since the scattering is tending to the Rayleigh scattering regime. The opposite effect is seen at larger D_m, this may be because of Mie resonances.

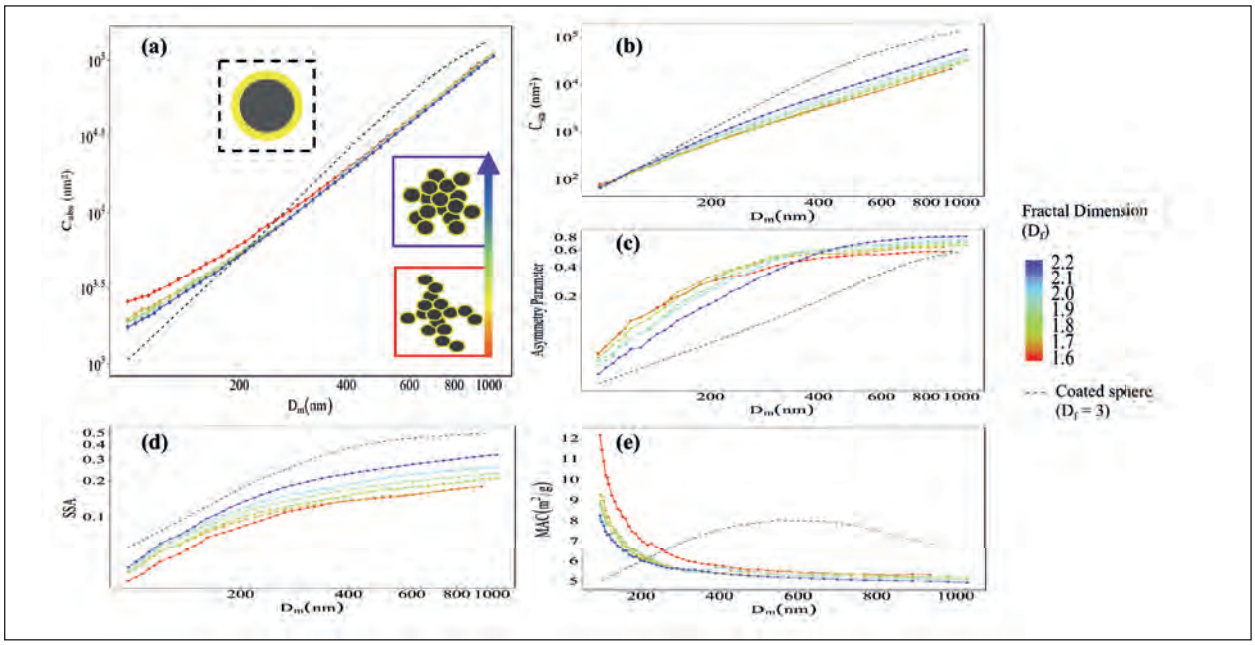

Fig. 1: Optical properties of black carbon aggregates with C_f of 50% at wavelength of 0.66 um. The particle size is given by the mobility diameter for fractal particles according to Sorensen [2011]. Absorption cross-section (a), scattering cross-section (b), asymmetry parameter (c), single scattering albedo (d) and mass absorption cross-section (e) as a function of fractal dimension (D_f) and mobility diameter (D_m). The orange line represents the case of a coated sphere shown in the orange box. The aggregate inside the yellow and blue box have a D_f equal to 2.2 and 1.6 respectively.

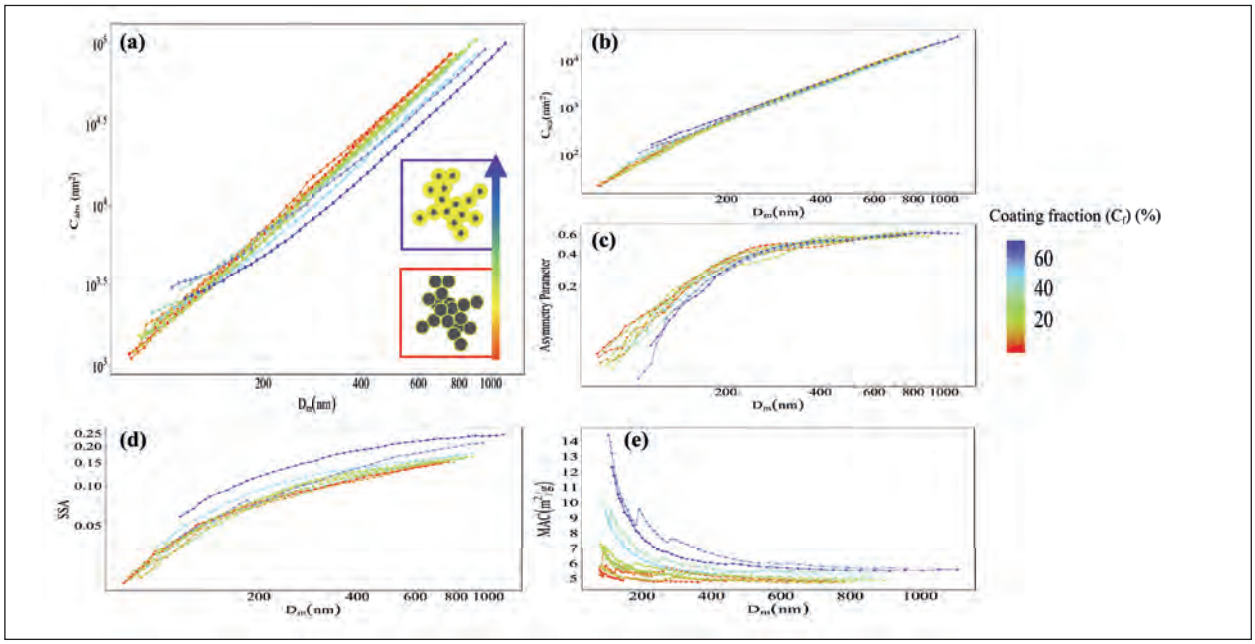

Fig. 2: Optical properties of black carbon aggregates with D_f of 1.7 at wavelength 0.66 um. Absorption cross-section (a), scattering cross-section (b), asymmetry parameter (c), single scattering albedo (d) and mass absorption cross-section (e) as a function of coating fraction (C_f) and mobility diameter (D_m). The aggregate inside the yellow and blue box has a C_f equal to 15% and 60% respectively.

- **Change in composition**
  The various optical properties with respect to increasing coating fraction (C_f) and size (D_m) are shown in Figure 2. As expected, C_{abs} decreases at higher values of C_f due to increasing volume of non-absorbing coating material. This decrease in C_{abs} rises after C_f > 70% because of the increase in the coating filling up the voids between BC monomers. Therefore, this design might not be representative of aggregates above a certain C_f. Even though, C_{sca} increases with higher C_f, the increase in C_{sca} due size is more pronounced.

  The values of MAC go up to 14 m^2g^{-1} for C_f > 60% at lower D_m. In the results of *g,* a converging behaviour is observed after a certain size for all C_f.

The optical properties were also calculated at wavelengths of 0.47 *um* and 0.55 *um.* With help of this large dataset covering a large parameter space, parameterizations will be developed. This will help to understand the relationships between morphology and optical properties, and to facilitate access to scattering calculations for a wide range of users.

References

Abel, S. J., Haywood, J. M., Highwood, E. J., Li, J., & Buseck, P. R. (2003), Evolution of biomass burning aerosol properties from an agricultural fire in southern Africa, *Geophysical Research Letters*, *30*(15).

Bond, Tami C. and Bergstrom, Robert W. (2006) ‚Light Absorption by Carbonaceous Particles: An Investigative Review', *Aerosol Science and Technology*, 40:1, 27 – 67.

Homann, K. H.: 1967, *Combust Flame* 11, 265.

D. W. Mackowski and M. I. Mishchenko (2011), "A multiple sphere T-matrix fortran code for use on parallel computer clusters," *J. Quant. Spectrosc. Radiat. Transf*. 112(13), 2182–2192.

M. Shiraiwa, Y. Kondo, T. Iwamoto & K. Kita (2010), Amplification of Light Absorption of Black Carbon by Organic Coating, *Aerosol Science and Technology*, 44:1, 46-54.

Sorensen CM (2011), The mobility of fractal aggregates: A review, *Aerosol Science and Technology*, 45, 755–769.

Woźniak M., Onofri F., Barbosa S., Yon J., Mroczka J. (2012), Comparison of methods to derive morphological parameters of multifractal samples of particle aggregates from TEM images, *Journal of Aerosol Science*, 47,12-26.

Funding

European Metrology Programme for Innovation and Research (EMPIR): Project 16ENV02.

Indoor and outdoor sources' contribution to indoor particle number concentration in 40 German homes

Jiangyue Zhao[1], Birgit Wehner[1], Wolfram Birmili[2], Kay Weinhold[1], Simonas Kecorius[1], Tareq Hussein[3], and Alfred Wiedensohler[1]

[1] Leibniz Institute for Tropospheric Research (TROPOS), Leipzig, Germany
[2] German Environment Agency (UBA), Berlin, Germany
[3] University of Jordan, Amman, Jordan

Menschen sind in Innenräumen Aerosolpartikeln ausgesetzt, die entweder aus Innenraumquellen stammen oder von außen eingetragen werden. In Deutschland wurden bislang keine Innenraum-Belastungen ultrafeiner Partikel und der Beitrag verschiedener Quellen untersucht. Im Rahmen eines vom Umweltbundesamt geförderten Projektes wurden jetzt in Leipzig und Berlin zwei Jahre lang Messungen der Partikelanzahlkonzentration sowie der Partikelgrößenverteilung im Innen- und Außenbereich in 40 Haushalten durchgeführt. In dieser Untersuchung wurden Beiträge der diffusen Infiltration von Aerosolpartikeln von außen, Belüftungsaktivitäten (z.B. Öffnen von Fenstern) sowie verschiedener Innenraum-Partikelquellen in der Wohnung zur mittleren Partikelanzahlkonzentration im Innenraum quantifiziert. Die Ergebnisse zeigen, dass die diffuse Infiltration von Innen- und Außenquellen die Hauptrolle bei der Erhöhung der Partikelanzahlkonzentration in Innenräumen spielt. Innenraum-Partikelquellen sind die Hauptursachen für die Spitzenwerte der Partikelanzahl-konzentration im Tageszyklus.

Introduction

Nowadays, people spend a large fraction of their time indoors [*Brasche and Bischof*, 2005; *Kousa et al.*, 2002]. Indoor and outdoor particle concentration have been proven to be correlated in the absence of major indoor sources [*Chen and Zhao*, 2011; *Franck et al.*, 2006; *Hussein et al.*, 2006; *Talbot et al.*, 2016]. Indoor sources such as cooking, candles, open fires, cleaning, and smoking are understood to be primary drivers of increased indoor particle number and mass concentrations [*Koistinen et al.*, 2004; *Lazaridis et al.*, 2006; *Morawska et al.*, 2013; *Semple et al.*, 2012]. It is thus important to study the contribution of outdoor infiltration and residential activities to the indoor air. However, only relatively few studies have investigated the residential fine and ultrafine particle concentrations with size-resolved information, and none was performed in central Europe in the long-term in multiple homes. There is a gap in the knowledge of the source contribution in German residences.

Therefore, on behalf of the German Environment Agency (UBA), a project to study the indoor aerosol particle exposure and its relationship to the urban and rural atmosphere has been granted to the Leibniz Institute for Tropospheric Research (TROPOS). This article presents results from the two years' measurement in 40 homes in Leipzig and Berlin, including the contribution of outdoor particles' infiltration, ventilation activities (i.e. opening windows), as well as the indoor

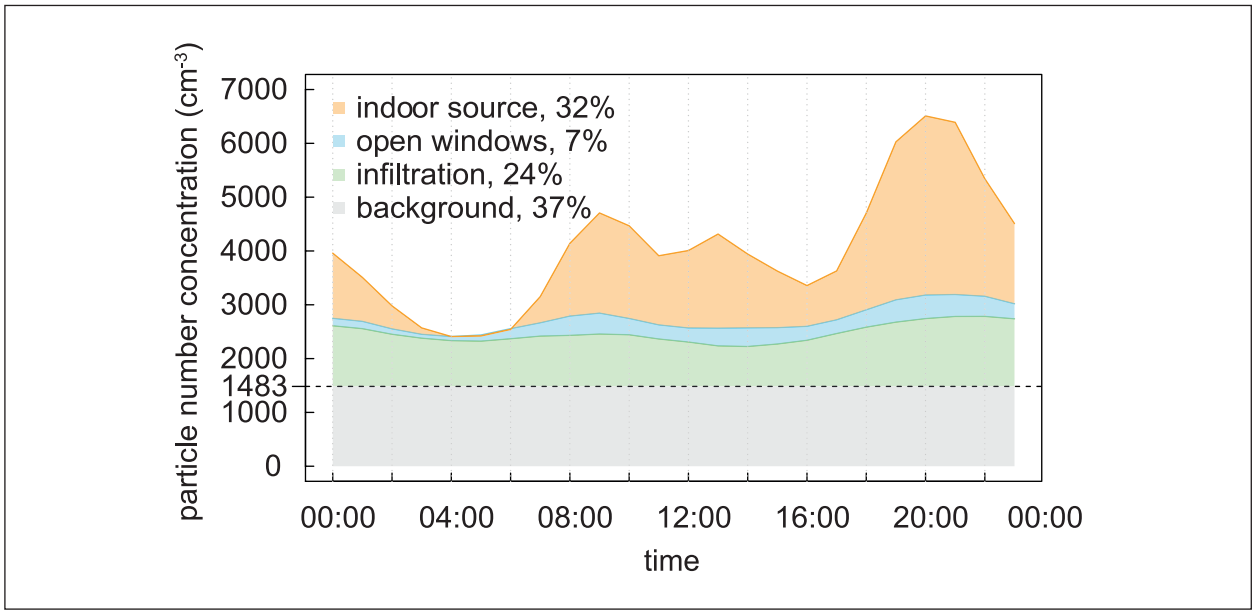

Fig. 1: Diurnal cycle of the median indoor PNC.

sources to the indoor particle number concentration (PNC). The signature particle number size distributions (PNSD) of the typical indoor sources in these 40 homes are shown exemplarily.

Method

Measurements were performed in 20 homes in Leipzig and 20 homes in Berlin. These homes are located in urban, suburban, and rural areas. Each home was probed twice for one week, covering both, the cold and warm season. In each home, indoor measurements took place in the living room and outdoor measurements took place on the balcony, terrace, or in a connected yard. Indoor and outdoor PNC and PNSD (10 - 800 nm size range) were measured simultaneously using mobility particle size spectrometers (build by TROPOS). Additionally, indoor CO_2 concentration was measured (CO_2 sensor, GMP252 Vaisala), for quantifying the ventilation rate. The measurements were accompanied by a questionnaire, which documented the room characteristics. During the measurements, the inhabitants were requested to mark their activities (e.g. open window, cooking, candle burning, and room cleaning) on a digital notebook. Therefore, the "activities log" with time-activity data could be accessed.

Results

Indoor and outdoor particle mass and number concentrations, as well as CO_2 concentrations, were measured for around 8500 to 11500 hours in total. The overall median indoor and outdoor PNC were 4100 cm^{-3} and 6000 cm^{-3}, respectively. The diurnal cycle of the median outdoor PNC was all the time higher than indoors. Through infiltration, outdoor particles were constantly transported to indoor. Moreover, when the windows were opened, indoor air quickly exchanged with outdoors, leading to rapidly increased indoor PNC. Figure 1 shows the diurnal cycle of median indoor PNC, and the colored areas mark the corresponding estimated contribution from each process during the measurements. The highest contribution is from indoor sources (32% of the total PNC), with the peak contribution to the number concentration at around 08:00, 12:00 and 19:00.

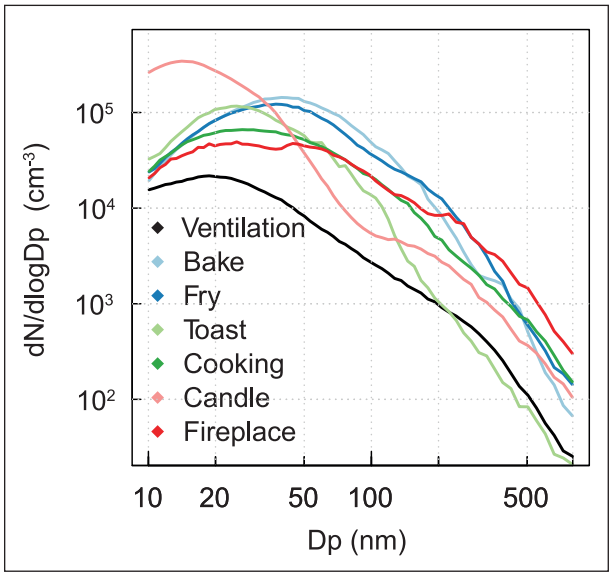

Fig. 2: Increased PNSD from single activities.

Single activities were selected according to the "activities log". Figure 2 shows the mean PNSD increased by each activity, i.e. the PNSD of each case at peak-time subtracting the background. The peak-time is defined as the time when the indoor PNC reaches a maximum during the single activity, and the background is the time before the activity start. These activities increased indoor PNC for more than four magnitudes. The highest particle number contribution of toasting, baking, frying was to 20-50 nm size-range particles. Candle burning emits particles for the entire size range, and contribute the most number to 10 - 20 nm size particles. By opening windows, outdoor sources also increase the indoor particle concentration for the entire size range, but the contribution to the ultrafine particle is much lower compared to that of indoor sources. The signature PNSD of indoor sources suggested that cooking activities and indoor combustion activities (burning candles, using fireplace) are the major contributors to the peaks of indoor PNC in the diurnal cycle.

References

Brasche, S., and W. Bischof (2005), Daily time spent indoors in German homes – Baseline data for the assessment of indoor exposure of German occupants, International Journal of Hygiene and Environmental Health, 208(4), 247-253, doi: https://doi.org/10.1016/j.ijheh.2005.03.003.

Chen, C., and B. Zhao (2011), Review of relationship between indoor and outdoor particles: I/O ratio, infiltration factor and penetration factor, Atmospheric Environment, 45(2), 275-288, doi: 10.1016/j.atmosenv.2010.09.048.

Franck, U., T. Tuch, M. Manjarrez, A. Wiedensohler, and O. Herbarth (2006), Indoor and outdoor submicrometer particles: exposure and epidemiologic relevance ("the 3 indoor Ls"), Environmental toxicology, 21(6), 606-613.

Hussein, T., T. Glytsos, J. Ondráček, P. Dohányosová, V. Ždímal, K. Hämeri, M. Lazaridis, J. Smolík, and M. Kulmala (2006), Particle size characterization and emission rates during indoor activities in a house, Atmospheric Environment, 40(23), 4285-4307.

Koistinen, K. J., R. D. Edwards, P. Mathys, J. Ruuskanen, xfc, N. nzli, and M. J. Jantunen (2004), Sources of fine particulate matter in personal exposures and residential indoor, residential outdoor and workplace microenvironments in the Helsinki phase of the EXPOLIS study, Scandinavian Journal of Work, Environment & Health, 30, 36-46.

Kousa, A., J. Kukkonen, A. Karppinen, P. Aarnio, and T. Koskentalo (2002), A model for evaluating the population exposure to ambient air pollution in an urban area, Atmospheric Environment, 36(13), 2109-2119, doi: https://doi.org/10.1016/S1352-2310(02)00228-5.

Lazaridis, M., V. Aleksandropoulou, J. Smolík, J. E. Hansen, T. Glytsos, N. Kalogerakis, and E. Dahlin (2006), Physico-chemical characterization of indoor/outdoor particulate matter in two residential houses in Oslo, Norway: measurements overview and physical properties – URBAN-AEROSOL Project, Indoor Air, 16(4), 282-295, doi: 10.1111/j.1600-0668.2006.00425.x.

Morawska, L., A. Afshari, G. N. Bae, G. Buonanno, C. Y. Chao, O. Hanninen, W. Hofmann, C. Isaxon, E. R. Jayaratne, P. Pasanen, T. Salthammer, M. Waring, and A. Wierzbicka (2013), Indoor aerosols: from personal exposure to risk assessment, Indoor Air, 23(6), 462-487, doi: 10.1111/ina.12044.

Semple, S., C. Garden, M. Coggins, K. Galea, P. Whelan, H. Cowie, A. Sánchez-Jiménez, P. Thorne, J. Hurley, and J. Ayres (2012), Contribution of solid fuel, gas combustion, or tobacco smoke to indoor air pollutant concentrations in Irish and Scottish homes, Indoor air, 22(3), 212-223.

Talbot, N., L. Kubelova, O. Makes, M. Cusack, J. Ondracek, P. Vodička, J. Schwarz, and V. Zdimal (2016), Outdoor and indoor aerosol size, number, mass and compositional dynamics at an urban background site during warm season, Atmospheric Environment, 131, 171-184.

Funding

This work was supported by the Federal Ministry for the Environment, Nature Conservation, Building and Nuclear Safety (BMUB) grant UFOPLAN FKZ 3715 61 200 (German title: „Ultrafeine Partikel im Innenraum und in der Umgebungsluft: Zusammensetzung, Quellen und Minderungsmöglichkeiten").

Cooperation

German Environment Agency (UBA), Berlin, Germany.

Impact of wood burning on rural air quality

Dominik van Pinxteren, Falk Mothes, Gerald Spindler, Khanneh Wadinga Fomba, Andrea Cuesta, Thomas Müller, Thomas Tuch, Alfred Wiedensohler, Hartmut Herrmann

Die Verbrennung von Holz zu Heizzwecken hat in den vergangenen Jahren deutlich zugenommen. Sie wird als klimafreundliche Technologie gefördert und ist aufgrund ihrer angenehmen Effekte auf das Wohngefühl beliebt. Ihre Kehrseite sind extrem hohe Emissionen, v.a. von partikulären Schadstoffen, die zu lufthygienischen Problemen in Dörfern und Städten führen können. Im vorliegenden Projekt wurde der Einfluss Holzverbrennung auf die Luftqualität im kleinen Dorf Melpitz im ländlichen Raum bei Leipzig untersucht und durch ein „twin sites" Studienkonzept quantifiziert. Inhaltsstoffe von Holzverbrennungsemissionen wie Ruß, organischer Kohlenstoff, Kalium, polyzyklische aromatische Kohlenwasserstoffe (PAK) und Anhydromonosaccharide, z.B. Levoglucosan, zeigten deutlich messbar erhöhte Konzentrationen in der Ortsmitte im Vergleich zur ca. 300 m entfernten TROPOS Forschungsstation außerhalb von Melpitz. Unter Verwendung von Levoglucosan als Macrotracer wurde die mittlere örtliche Zusatzbelastung von PM10 aus Holzverbrennung im Winter als 1,0 µg m^{-3} berechnet, was für den relativ warmen Winter 2018/19 einer Zunahme von ca. 60 % der Hintergrundbelastung entsprach. Die Ergebnisse der Studie belegen ein weiteres Mal, dass die Verbrennung von Holz zu Heizzwecken die Luftqualität deutlich verschlechtert. Weitere Anstrengungen hinsichtlich Regulierung der Emissionen erscheinen notwendig und das erfolgreich erprobte „twin site" Konzept in Melpitz könnte diese messtechnisch sinnvoll begleiten.

Introduction

Burning wood for residential heating has become increasingly popular in Europe and Germany due to its climate benefits and cozy heat. This has, however, led to severe impacts on local and regional air quality, as the emission factors especially of particulate matter (PM) from wood stoves are extremely high [*Vicente and Alves*, 2018]. High concentrations of wood burning markers, including toxic ones, have been observed both in urban [*van Pinxteren et al.*, 2016] and in rural areas [*Poulain et al.*, 2011]. Most studies, however, do not differentiate between local and regional or even long-range transported emissions. In the present study, a twin site measurement strategy was implemented to quantify local contributions of wood burning on top of the regional background in the small rural village of Melpitz.

Methods

The study concept is based on two stations with identical instrumentation and parallel measurements, i.e. twin sites. One station was implemented in the centre of the small village of Melpitz, approx. 300 m east of the TROPOS research station, which is situated just outside the village and represented the reference background station. Measurements were performed for one year from 1 November 2018 to 31 October 2019 and included time-resolved measurements of particle number size distributions using mobility and aerodynamic particle spectrometers (MPSS, APSS), equivalent black carbon (eBC) concentrations using multi-angle absorption photometers (MAAP) and multi-wavelength aethalomters, oxides of nitrogen (NO, NO_2, NO_x) using gas monitors and meteorological parameters, as well as daily measurements of PM10 mass and chemical composition using high-volume filter samplers. The filters were analysed for inorganic ions, organic carbon (OC), elemental carbon (EC), water-soluble carbon (WSOC), trace metals (every third day) and organic constituents including toxic polycyclic aromatic hydrocarbons (PAH) as well as anhydromonosaccharides as wood burning markers.

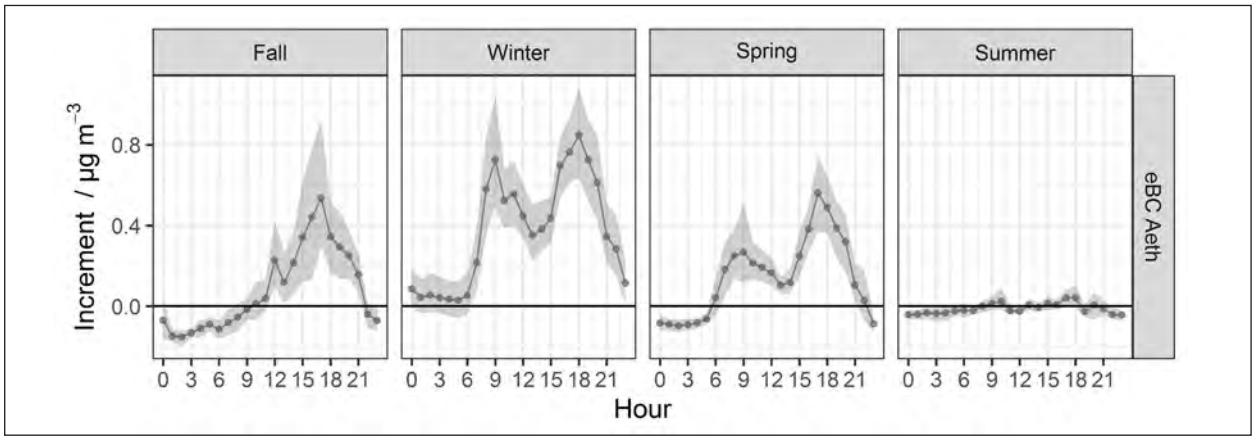

Fig. 1: Hourly means (dots) of local eBC increment in the village of Melpitz from aethalometer measurements with 95% confidence interval (shaded area).

Results

Despite a comparably warm winter 2018/19, clear indications of wood burning contributions could be observed at both sites from the time profiles of all biomass burning related species, i.e. particle number concentrations, eBC, EC, OC, PAHs and monosaccharides. Concentrations were highest during fall and winter months and diurnal variations typically showed peaks in the morning and evening hours. To quantify the local contributions of wood burning emissions, increment concentrations at the village station were calculated by subtracting the outside village concentrations obtained at the TROPOS research site from the village centre concentrations. This increment represents the local immission in addition to the regional background concentration. Its diurnal variation in different seasons is shown for eBC in Figure 1. In order to ensure that the reference background station was not influenced by local emissions, concentrations during eastern wind directions with wind speeds > 2 m s^{-1} were excluded from the increment calculations.

Equivalent BC increments from both the aethalometers and the MAAPs showed very similar diurnal profiles. Especially during winter, but to some extent also during fall and spring, considerable local increments were observed, peaking at ~0.8 µg m^{-3} during morning and evening hours. Similar increment profiles were observed for number concentrations of 50–150 nm and 150–800 nm sized particles and for PM1 and PM10 hourly mass concentrations, calculated from MPSS and APSS number concentrations. In contrast, NO and NO_2 showed increments close to zero during the heating season, which corroborates the critical role especially particulate emissions play in the burning of wood for residential heating.

To quantify the total PM10 contribution of particulate wood burning emissions, the levoglucosan mactrotracer approach was applied, which calculates PM10 originating from biomass burning, i.e. PM(BB), by multiplying measured levoglucosan concentrations with a constant factor. A factor of 10.95 was used, which in previous studies had led to good agreement between the mactrotracer estimation and more advanced source apportionment by positive matrix factorization (PMF) [*van Pinxteren et al.*, 2016]. In Figure 2, the monthly mean increments of PM(BB) estimated by the mactrotracer approach are shown.

The local additional wood burning contribution was highest during winter and lowest during summer. It peaked in February with ~1.3 µg m^{-3} and was ~1.0 µg m^{-3} on average during winter. Total PM(BB) at the reference background station was 1.8 µg m^{-3} and represented ~9% of total PM10 on winter average, which is on the lower end of typical winter BB contributions reported for Germany. The mean winter increment translates to an increase of background PM(BB) concentrations by ~60%, which – considering the small size of the village of Melpitz – is considered a relevant contribution. The total PM10 increment, obtained from gravimetric mass measurements of the daily filter samples at both sites, was 1.2 µg m^{-3} as winter mean and thus only slightly larger than the mactrotracer-estimated PM(BB) increment, which confirms the study hypothesis of wood burning being the only relevant PM10 source in the village of Melpitz and suggests the measured PM10 mass increment to fully represent the wood burning contribution during winter in this rural village.

The study is ongoing and further data analyses are underway, including correlations of increment concentrations with meteorological conditions and more detailed source apportionment using PMF.

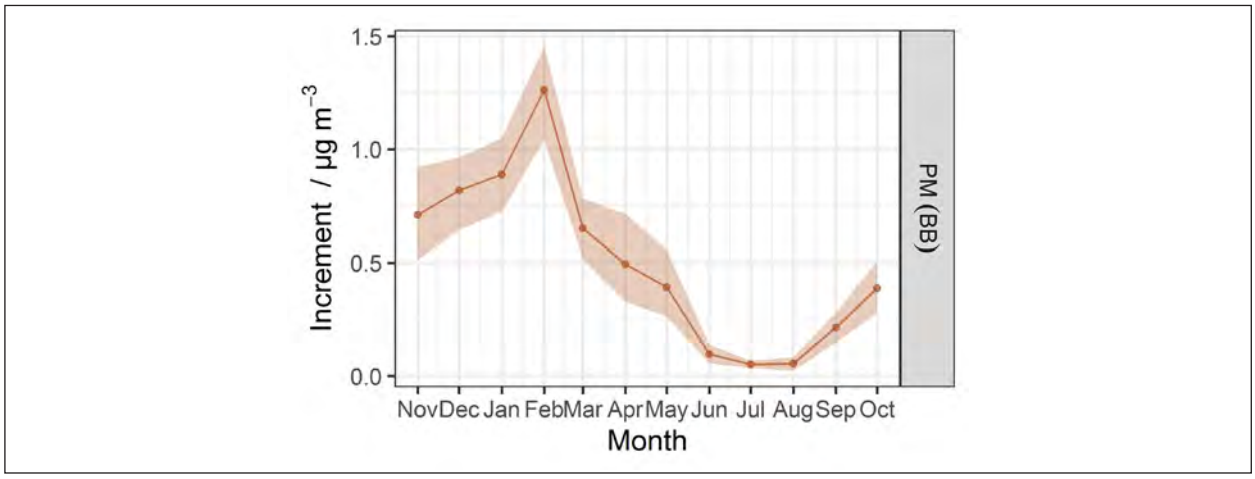

Fig. 2: Monthly means (dots) of local biomass burning derived PM increment in the village of Melpitz with 95% confidence interval (shaded area).

Conclusions

Wood burning emits large amounts of particulate matter and leads to clearly measurable deterioration of air quality not only in large urban agglomerations with often limited air exchange or rural alpine areas with long traditions of wood heating, but also in small villages in low-land rural areas of Germany. A local contribution of ~1 µg m^{-3} PM10 mass was measured in the small village of Melpitz, which together with similar contributions from other villages and cities can easily build up significant wood burning pollution in the area, especially during favourable meteorological conditions that were not too often observed in the present study. Given the harmful effects of PM to human health, it seems necessary to further develop emission regulation and mitigation measures. The twin sites implemented in Melpitz could provide a good possibility to monitor the effects of future legislation efforts on local air quality in the rural area.

References

Poulain, L., Y. Iinuma, K. Muller, W. Birmili, K. Weinhold, E. Brueggemann, T. Gnauk, A. Hausmann, G. Loschau, A. Wiedensohler, and H. Herrmann (2011), Diurnal variations of ambient particulate wood burning emissions and their contribution to the concentration of Polycyclic Aromatic Hydrocarbons (PAHs) in Seiffen, Germany, *Atmos. Chem. Phys.*, *11*(24), 12697-12713, doi: 10.5194/acp-11-12697-2011.

van Pinxteren, D., K. W. Fomba, G. Spindler, K. Müller, L. Poulain, Y. Iinuma, G. Löschau, A. Hausmann, and H. Herrmann (2016), Regional air quality in Leipzig, Germany: detailed source apportionment of size-resolved aerosol particles and comparison with the year 2000, *Faraday Discuss.*, *189*, 291-315, doi: 10.1039/c5fd00228a.

Vicente, E. D., and C. A. Alves (2018), An overview of particulate emissions from residential biomass combustion, *Atmos. Res.*, *199*, 159-185, doi: 10.1016/j.atmosres.2017.08.027.

Cooperation

Saxon State Office for the Environment, Agriculture, and Geology (LfULG).

Using LC-Orbitrap MS to Quantify Terpenoid Organosulphates in PM_{10} from Rural Germany and the North China Plain

Martin Brüggemann[1], Dominik van Pinxteren[1], Yuchen Wang[2], Jian Zhen Yu[2], Hartmut Herrmann[1]

[1] Atmospheric Chemistry Department (ACD), Leibniz Institute for Tropospheric Research (TROPOS), Germany

[2] Department of Chemistry & Division of Environment, Hong Kong University of Science & Technology, Hong Kong

Organisch gebundener Schwefel kommt ubiquitär in Form von Organosulfaten in atmosphärischen Aerosolpartikeln vor und kann deren Eigenschaften maßgeblich beeinflussen. Eine detaillierte Quantifizierung dieser Substanzen ist jedoch schwierig, da sie typischerweise in einer großen Bandbreite an unbekannten Strukturen vorliegen. Durch den Einsatz hochauflösender LC-Orbitrap Massenspektrometrie und der Entwicklung eines kombinierten *target/non-target* Ansatzes, konnten erstmals Konzentrationen von terpenoiden Organosulfaten in PM_{10} aus Deutschland (Melpitz) und der nordchinesischen Ebene ermittelt und verglichen werden. Die Ergebnisse weisen auf eine erhöhte Bildung von Carbonsäuren bei niedrigen NOx und Sulfatkonzentrationen sowie eine entscheidende Rolle der Partikelazidität für die Bildung von terpenoiden Organosulfaten hin.

Introduction

Organic aerosol (OA) accounts for a major fraction of atmospheric particulate matter, affecting climate, air quality, and human health. Organosulphates (OSs) are a ubiquitous class of compounds in OA particles formed by reactions between reactive organic compounds and particulate sulphate [*Iinuma et al.*, 2007; *Surratt et al.*, 2008]. However, sources, formation mechanisms, and total amounts of OSs in ambient aerosol are still connected to large uncertainties. In particular, uncertainties in concentrations of specific and total OSs are commonly due to a combination of (1) a lack of authentic standards, and (2) the presence of unknown and yet unidentified OS. Nonetheless, to assess the atmospheric relevance of OSs and possible implications for underlying chemical and physical processes, a comprehensive identification and quantification in ambient aerosol particles is essential.

Results and Discussion

In the present study, we quantified for the first time total contributions of known and yet unknown terpenoid OSs to PM_{10} at a rural background site in Europe (Melpitz, MEL) and at a regional background site of the North China Plain (Wangdu, NCP) in summer 2014 [*Brüggemann et al.*, 2019]. We applied a non-target and a suspect analysis approach using LC-HR Orbitrap MS in different scan modes (i.e., full scan, data-dependent MS/MS, all-ion-fragmentation). Suspect MT-OSs and SQT-OSs were identified: 1) by their characteristic HSO_4^- fragment in all-ion-fragmentation mode, 2) their absence of aromaticity, and 3) a C_{9-10} and C_{14-15} carbon skeleton for MT-OSs and SQT-OS, respectively. Subsequent quantification of identified OS was carried out using a variety of authentic MT-OSs and SQT-OSs standards. Based on a comparison to other frequently used OS surrogates and in agreement with previous studies [*Kristensen*

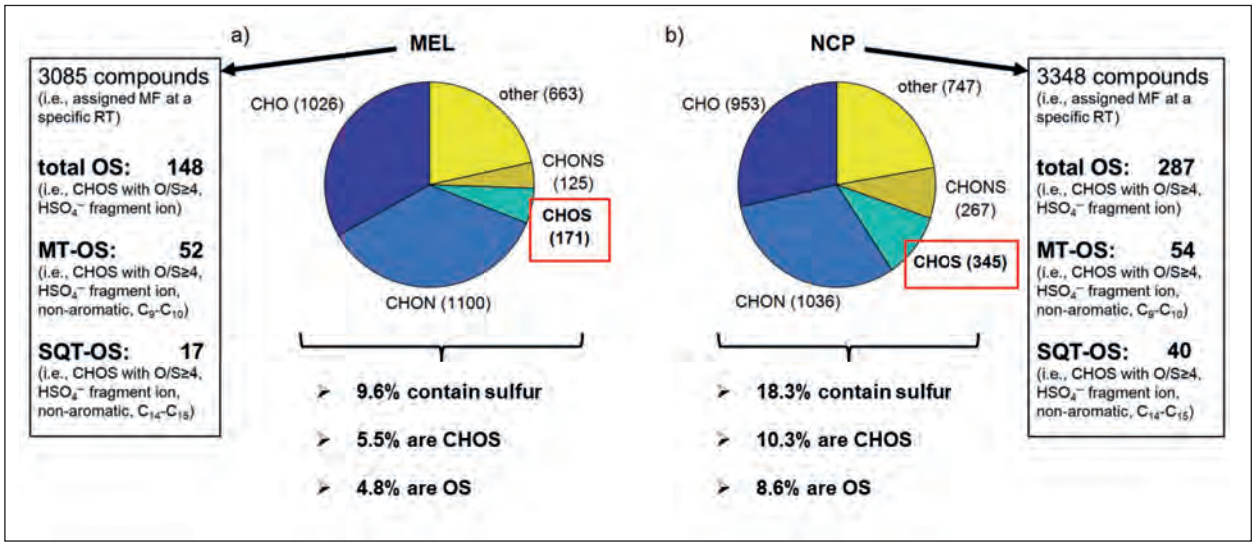

Fig. 1: Elemental composition of detected and assigned compounds by the untargeted screening of LC-Orbitrap MS data from the analysis of PM_{10} filter extracts from (a) MEL and (b) NCP.

and Glasius, 2011; *Wang et al.*, 2017], we recommend avoiding the use of octyl sulphate for terpene-derived OS quantification in future studies. Instead, camphor-10-sulfonic acid was found to be an appropriate surrogate of choice if no other authentic OSs are available.

As shown in Fig. 1, from the analysis of the MEL samples, we identified 52 compounds as MT-OSs (i.e., C_9 and C_{10}), and 17 compounds as SQT-OSs (i.e., C_{14} and C_{15}) out of 148 potential OS. For NCP, 287 compounds were identified as potential OS, 54 of which were assigned to MT-OS, and another 40 to SQT-OS. Thus, about 51% and 37% of all detected OSs were assigned to terpenoid compounds for the MEL and NCP samples, respectively. Remarkably, 13 MT-OSs were highly abundant at both sites, contributing >55% to total MT-OS concentrations. Moreover, MT-OS 267 ($C_9H_{16}O_7S$, RT = 1.07 min) was the largest single contributor with average mass concentrations of 2.23 and 6.38 ng m^{-3} for MEL and NCP, respectively. The pervasive abundance of MT-OS 267 is in agreement with previous studies [*Surratt et al.*, 2008; *Ye et al.*, 2018], suggesting limonene as potential source. Based on their large concentrations under quite different anthropogenic influences, we also assume biogenic precursors for the other 12 MT-OSs detected at both sites.

In general, we see linear correlations between MT-OS, particulate ammonium and sulphate, indicating that lower pH values and the presence of sulphate promote MT-OS formation. However, as depicted in Fig. 2, only for samples from MEL we observe a certain correlation between MT oxidation products and MT-OSs (R^2 = 0.572), whereas concentrations of such carboxylic acids are rather low for NCP and do not

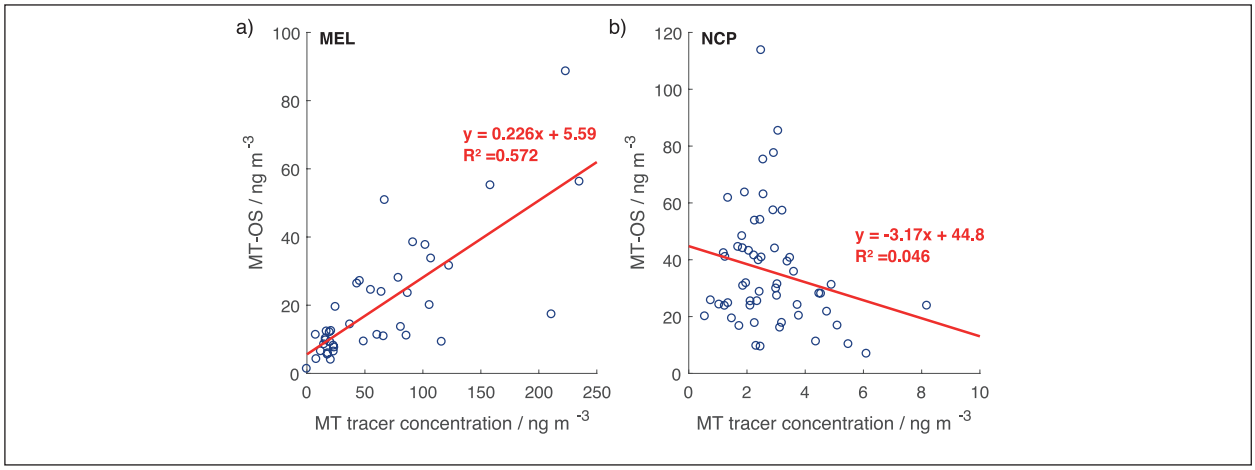

Fig. 2: Linear regression applied to the total MT-OS concentrations as a function of the summed concentrations of eight common MT oxidation products (i.e., terebic acid, MBTCA, terpenylic acid, transnorpinic acid, pinic acid, DTAA, nor-pinonic acid, pinonic acid) for (a) MEL and (b) NCP.

correlate with MT-OSs (R^2 = 0.046). This decoupled behaviour might indicate a suppression of carboxylic acid formation under high NO_X and particulate sulphate concentrations, favouring formation of OSs and other functionalized S- and N-containing compounds.

Besides potential influences from sulphate and NO_X, particle acidity was found to play a crucial role in SQT-OS formation. For MEL, median concentrations of SQT-OSs were merely 0.43 ng m^{-3}, whereas for NCP a median concentration of 3.67 ng m^{-3} was observed. Moreover, SQT-OSs exhibited no correlation to MT-OS concentration at MEL, while a clear correlation was observed for NCP samples, suggesting major differences in particle chemistry. Accordingly, only five SQT-OSs were detected at both sites. As previously reported, we find that particle acidity plays a key role in SQT-OS formation [*Chan et al.*, 2011], and was potentially not sufficient at the MEL site. In agreement, we find much stronger acidities for PM samples from NCP compared to samples from MEL. Largest single SQT-OS contributor at NCP was $C_{14}H_{28}O_6S$ (m/z 323.1539, $[M–H]^–$, RT = 10.25 min), accounting on average for 0.58 ng m^{-3}. In contrast, at MEL the largest contribution to SQT-OS concentrations was found for SQT-OS 309b ($C_{14}H_{30}O_5S$, RT = 14.98 min), accounting on average for 0.35 ng m^{-3}. Our results indicate that in particular for regions with higher aerosol particle acidity SQT-OS concentrations can account for a substantial, yet rather underestimated, fraction of total OS.

References

Brüggemann, M., D. van Pinxteren, Y. Wang, J. Z. Yu, and H. Herrmann (2019), Quantification of known and unknown terpenoid organosulfates in PM10 using untargeted LC–HRMS/MS: contrasting summertime rural Germany and the North China Plain, *Environ. Chem.*, *16*(5), 333-346, 10.1071/EN19089.

Chan, M. N., J. D. Surratt, A. W. H. Chan, K. Schilling, J. H. Offenberg, M. Lewandowski, E. O. Edney, T. E. Kleindienst, M. Jaoui, E. S. Edgerton, R. L. Tanner, S. L. Shaw, M. Zheng, E. M. Knipping, and J. H. Seinfeld (2011), Influence of aerosol acidity on the chemical composition of secondary organic aerosol from beta-caryophyllene, *Atmos. Chem. Phys.*, *11*(4), 1735-1751, 10.5194/acp-11-1735-2011.

Iinuma, Y., C. Müller, T. Berndt, O. Böge, M. Claeys, and H. Herrmann (2007), Evidence for the Existence of Organosulfates from β-Pinene Ozonolysis in Ambient Secondary Organic Aerosol, *Environ. Sci.Technol.*, *41*(19), 6678-6683, 10.1021/es070938t.

Kristensen, K., and M. Glasius (2011), Organosulfates and oxidation products from biogenic hydrocarbons in fine aerosols from a forest in North West Europe during spring, *Atmos. Environ.*, *45*(27), 4546-4556, 10.1016/j.atmosenv.2011.05.063.

Surratt, J. D., Y. Gómez-González, A. W. H. Chan, R. Vermeylen, M. Shahgholi, T. E. Kleindienst, E. O. Edney, J. H. Offenberg, M. Lewandowski, M. Jaoui, W. Maenhaut, M. Claeys, R. C. Flagan, and J. H. Seinfeld (2008), Organosulfate Formation in Biogenic Secondary Organic Aerosol, *J. Phys. Chem. A*, *112*(36), 8345-8378, 10.1021/jp802310p.

Wang, Y., J. Ren, X. H. H. Huang, R. Tong, and J. Z. Yu (2017), Synthesis of Four Monoterpene-Derived Organosulfates and Their Quantification in Atmospheric Aerosol Samples, *Environ. Sci. Technol.*, *51*(12), 6791-6801, 10.1021/acs.est.7b01179.

Ye, J., J. P. D. Abbatt, and A. W. H. Chan (2018), Novel pathway of SO2 oxidation in the atmosphere: reactions with monoterpene ozonolysis intermediates and secondary organic aerosol, *Atmos. Chem. Phys.*, *18*(8), 5549-5565, 10.5194/acp-18-5549-2018.

Cooperation

Department of Chemistry & Division of Environment, Hong Kong University of Science & Technology, Hong Kong.

Fast Peroxy Radical Isomerisation and OH Recycling in the Reaction of OH Radicals with Dimethyl Sulfide

Torsten Berndt[1], Wiebke Scholz[2], Bernhard Mentler[2], Lukas Fischer[2], Erik H. Hoffmann[1], Andreas Tilgner[1], Noora Hyttinen[3], Nonne L. Prisle[3], Armin Hansel[2], Hartmut Herrmann[1]

[1] Leibniz Institute for Tropospheric Research (TROPOS), Leipzig, Germany
[2] Institute for Ion Physics and Applied Physics, University of Innsbruck, Innsbruck, Austria
[3] Nano and Molecular Systems Research Unit, University of Oulu, Oulu, Finland

Dimethylsulfid (DMS) stellt die größte biogene Schwefelquelle in der Atmosphäre dar. Der Gasphasenabbau von DMS wird hauptsächlich über die Reaktion mit OH Radikalen initiiert, wobei zuerst $CH_3SCH_2O_2$ Radikale über den dominanten H-Abstraktionskanal gebildet werden. Es wird experimentell gezeigt, dass diese Peroxyradikale einen 2-Schritt-Isomerisierungsprozess durchlaufen, wobei $HOOCH_2SCHO$ gebildet wird. Der Isomerisierungsprozess ist mit einem Recycling von OH Radikalen verbunden. Der geschwindigkeitsbestimmende erste Isomerisierungsschritt, $CH_3SCH_2O_2 \rightarrow CH_2SCH_2OOH$, verläuft mit k = (0.23 ± 0.12) s^{-1} bei 295 ± 2 K. Die bimolekularen Folgereaktionen von $CH_3SCH_2O_2$ mit NO, HO_2 oder RO_2 Radikalen sind von untergeordneter Bedeutung für Bedingungen über den Ozeanen. Resultate von Modellrechnungen belegen die Dominanz (≥95%) der $CH_3SCH_2O_2$ Isomerisierung in der Atmosphäre.

Introduction

The emission of dimethyl sulfide (DMS: CH_3SCH_3) over the oceans is the largest natural sulfur source to the Earth´s atmosphere with an estimated rate of (10 - 35) $\times$ 10^6 metric tons of sulfur per year. Gas-phase oxidation of DMS, mainly initiated by the reaction with OH radicals, leads to the formation of sulfuric acid (H_2SO_4) and methane sulfonic acid (MSA: CH_3SO_3H) which are important for the formation of natural aerosols and clouds in the marine boundary layer [*Barnes et al*., 2006].

A series of kinetic studies in absence and presence of molecular oxygen consistently describe the occurrence of two independent channels of the OH + DMS reaction, i.e. i) the reversible OH addition forming the adduct radical $CH_3S(OH)CH_3$ and ii) the H atom abstraction pathway forming the peroxy radical $CH_3SCH_2O_2$ after subsequent O_2 addition [*Barnes et al*., 2006]. The addition / abstraction branching ratio of about 35 / 65 can be derived from kinetic measurements between 295 to 299 K at atmospheric O_2 concentration.

The knowledge regarding the 1st generation product formation from the abstraction channel is still sparse despite a large number of experimental and theoretical studies in the past. Results of a recent theoretical study propose rapid isomerisation of the $CH_3SCH_2O_2$ radical that could be able to outrun the rate of the "traditional" bimolecular $CH_3SCH_2O_2$ reactions for typical NO, HO_2 and RO_2 radical concentrations present over the oceans [*Wu et al*., 2015]. Experimental evidence for this new process and kinetic measurements of the $CH_3SCH_2O_2$ isomerisation do not exist up to now.

Here, we report on results of an experimental study of the OH + DMS reaction with focus on the 1st generation products from the abstraction channel.

Methods

Experiments have been conducted at 295 ± 2 K and 1 bar of purified air in a free-jet flow system, that allows for investigations in the absence of wall interactions for a reaction time of 7.9 s [*Berndt et al*., 2019]. The chosen reaction conditions ensured monitoring

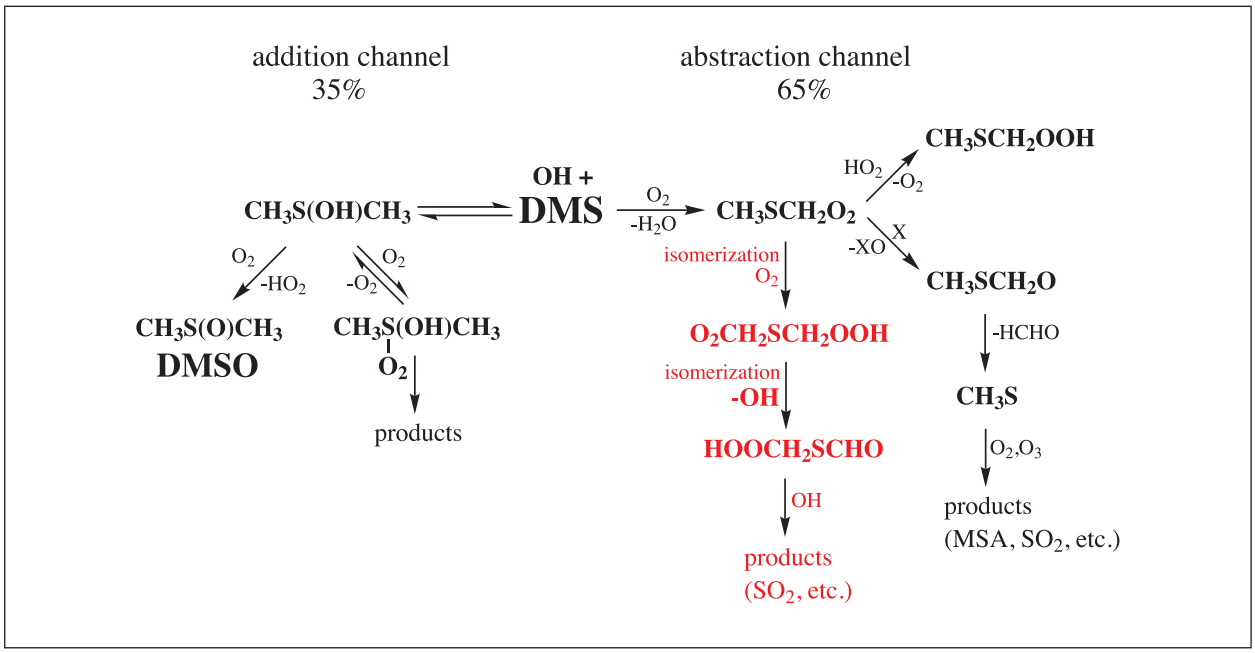

Scheme 1: First reaction steps of the OH + DMS reaction, the established scheme from the review by Barnes et al. [Barnes et al., 2006] in black and the new pathways in red. Detected products from the present study are given in bold red."X" stands for the reactants NO and RO_2 that can reduce the peroxy radical to the corresponding alkoxy radical.

of the possible $CH_3SCH_2O_2$ isomerisation products without interference from bimolecular $CH_3SCH_2O_2$ reactions. Product formation was followed by different mass spectrometric techniques using iodide (I^-), acetate (CH_3COO^-), protonated n-propylamine ($n\text{-}C_3H_7NH_3^+$), protonated acetone ($(CH_3)_2CO\text{-}H^+$) or ammonium (NH_4^+) as reagent ion. Results of quantum chemical calculations support the assessment of used ionisation schemes for product detection. Moreover, multiphase chemistry investigations with an air parcel model were carried out to validate the impact of the $CH_3SCH_2O_2$ isomerisation process for pristine ocean conditions [*Hoffmann et al*., 2016].

Results and Discussion

Sensitive detection of the sulfur containing products has been achieved using iodide-based product ionisation for a DMS conversion down to 4×10^6 molecules cm^{-3}. Observed signals in the mass spectra are consistent with the formation of the peroxyl radical $O_2CH_2SCH_2OOH$ from $CH_3SCH_2O_2$ isomerisation, pathway (1), as well as the closed-shell product $HOOCH_2SCHO$ from a subsequent isomerisation step followed by rapid decomposition of the unstable $HOOCH_2SCHOOH$ via pathway (2).

These products are in accordance with predictions from theoretical calculations [*Wu et al*., 2015]. Product analysis for elevated DMS conversion applying the other ionisation techniques confirmed the findings as observed by iodide ionisation. Scheme 1 summarises the current knowledge of the first steps of the OH + DMS reaction in the literature [*Barnes et al*., 2006] along with the new reaction pathways based on theoretical calculations [*Wu et al*., 2015] and the experimental confirmation from the present study [*Berndt et al*., 2019].

The kinetics of the $CH_3SCH_2O_2$ isomerisation relative to the $CH_3SCH_2O_2$ + NO reaction has been measured by monitoring the $CH_3SCH_2O_2$ isomerisation products for rising NO concentrations. The value $k_1 = 0.23 \pm 0.12\ s^{-1}$ at 295 ± 2 K has been obtained for the rate-limiting first isomerisation step. OH radical recycling via pathway (2) was also experimentally confirmed.

The modelling results clearly demonstrate that isomerisation dominates the chemical fate of $CH_3SCH_2O_2$. Bimolecular reactions with NO, HO_2 and RO_2 radicals are less important, contrary to the thoughts up to now. The mean contribution of $CH_3SCH_2O_2$ isomerisation ranges from 95 to 98.5% considering $k_1 = 0.23 \pm 0.12\ s^{-1}$ within its range of

$$CH_3SCH_2O_2\ (+O_2) \rightarrow O_2CH_2SCH_2OOH \quad (1)$$

$$O_2CH_2SCH_2OOH \rightarrow \{HOOCH_2SCHOOH\} \rightarrow HOOCH_2SCHO + OH \quad (2)$$

uncertainty. Average concentrations of NO, HO_2 and total RO_2 radicals in the model were 6×10^6, 1×10^8 and 4×10^8 molecules cm^{-3} resulting in pseudo first-order rate coefficients of the corresponding bimolecular $CH_3SCH_2O_2$ reactions of 7.0×10^{-5}, 1.0×10^{-3} and 1.5×10^{-3} s^{-1} at 295 K, respectively. The dominance of the isomerisation process entails consequences for the OH budget and the subsequent product formation.

References

Barnes, I., J. Hjorth, and N. Mihalopoulus, (2006), Dimethyl sulfide and dimethyl sulfoxide and their oxidation in the atmosphere, *Chem. Rev.*, 106, 940-975, doi:10.1021/cr020529+.

Berndt, T., W. Scholz, B. Mentler, L. Fischer, E. H. Hoffmann, A. Tilgner, N. Hyttinen, N. L. Prisle, A. Hansel, and H. Herrmann (2019), Fast peroxy radical isomerization and OH recycling in the reaction of OH radicals with dimethyl sulfide**,** *J. Phys. Chem. Lett.*, 10, 6478-6483, doi:10.1021/acs.jpclett.9b02567.

Hoffmann, E. H., A. Tilgner, R. Schrödner, P. Bräuer, R. Wolke, and H. Herrmann (2016), An advanced modeling study on the impacts and atmospheric implications of multiphase dimethyl sulfide chemistry, *Proc. Natl. Acad. Sci. USA*, 113, 11776-11781, doi:10.1073/pnas.1606320113.

Wu, R., S. Wang, and L. Wang (2015), New mechanism for the atmospheric oxidation of dimethyl sulfide. The importance of intramolecular hydrogen shift in a CH_3SCH_2OO radical, *J. Phys. Chem. A*, 119, 112-117, doi:10.1021/jp511616j.

Cooperation

University of Innsbruck, Austria;
University of Oulu, Finland.

Marine organic matter in the remote environment of the Cape Verde Islands - An introduction to the MarParCloud campaign

Manuela van Pinxteren[1], Khanneh Wadinga Fomba[1], Nadja Triesch[1], Heike Wex[1], Xianda Gong[1], Jens Vogtländer[1], Stefan Barthel[1], Christian Stolle[2], Enno Bahlmann[3], Tim Rixen[3], Detlef Schulz-Bull[2], Oliver Wurl[4], Frank Stratmann[1], Hartmut Herrmann[1]

[1] Leibniz Institute for Tropospheric Research (TROPOS), Leipzig, Germany
[2] Leibniz Institute for Baltic Sea Research, Warnemünde, Germany
[3] Leibniz Centre for Tropical Marine Research, Bremen, Germany
[4] Institute for Chemistry and Biology of the Marine Environment, Carl-von-Ossietzky University Oldenburg, Wilhelmshaven, Germany

Der Export von organischem Material (OM) aus den Ozeanen in die Atmosphäre stellt einen signifikanten Kohlenstoffffluss im Erdsystem dar. Die funktionellen Beziehungen von OM in der Wassersäule über den marinen Oberflächenfilm (SML) bis in die Aerosolpartikel sind jedoch noch wenig verstanden [*Cochran et al.*, 2017; *Law et al.*, 2013]. Das Projekt MarParCloud (marine biologische Produktion, organische Aerosolpartikel und marine Wolken: eine Prozesskette) zielt darauf ab, das OM in der marinen Atmosphäre besser zu charakterisieren. Dieses Projekt untersucht und beschreibt die gesamte Prozesskette der marinen biologischen OM Produktion über mikrobielle und chemische Umsetzungen an der Oberfläche der Ozeane, den Transfer des OM in atmosphärische Aerosolpartikel und den Einfluss des marinen OM auf das Eiskeim- und Wolkenkondensationskeim-Potential. Der Kern von MarParCloud bestand in einer Feldmesskampagne am kapverdischen Atmosphären Observatorium (CVAO) im Herbst 2017, bei der eine Vielzahl chemischer, physikalischer, biologischer und meteorologischer Methoden zur Anwendung kam. Dabei standen detaillierte Untersuchungen des Meerwassers und des SML, sowie umfassende Analysen von Aerosolpartikeln an der Bodenstation (30 m) und an der Bergstation (744 m) im Vordergrund (Abb. 1). Weiterhin erfolgte die Sammlung und Charakterisierung von Wolkenwasser an der Bergstation. Die in-situ Messungen werden von atmosphärenchemischen Transportmodellierungen begleitet.

Introduction

The export of organic matter (OM) from the oceans into aerosol particles establishes a significant carbon flux in the Earth system; however, the functional relationships of OM in the water column via the SML to the atmosphere are still poorly understood [*Cochran et al.*, 2017; *Law et al.*, 2013]. A better knowledge of the origin and development of marine aerosols, and in particular of the organic content, is a challenging topic and requires expertise from a wide range of disciplines.

The aim of the project MarParCloud (marine biological production, organic aerosol particles and marine clouds: a process chain) is to achieve a better understanding of the biological production of OM in the oceans, its export into marine aerosol particles and finally its ability to act as ice and cloud condensation nuclei (INP and CCN). Specifically, the focus is to elucidate (i) to what extend is seawater, and especially the SML, a source of OM in marine aerosol particles and in cloud water, (ii) the function of the marine OM as INP and CCN, (iii) what is the role of microorganism in the formation of OM, CCN and INP and (iv) how the oceanic transfer of OM can be parameterized. The core of this project comprised a field campaign at the Cape Verde Atmosphere Observatory (CVAO) in autumn 2017, which used a variety of chemical, physical, biological and meteorological approaches. The investigations included

Fig. 1: Illustration of the different sampling sites during the campaign: the Cape Verde Atmospheric Observatory (CVAO), the seawater station and the cloud station.

measurements of the bulk water, the Sea Surface Microlayer (SML), ambient aerosol particles on the ground (30 m) and in mountain heights (744 m) as well as cloud water (see Figure 1). Important aspects of the ocean atmosphere interactions focusing on marine OM have been addressed through detailed observation and modeling approaches.

Methods

Measured variables included the chemical characterization of the atmospherically relevant OM components in the ocean (in the bulk water and in the SML) and in the atmosphere using a suite of chromatographic and mass-spectrometric methods [*Triesch et al.*, 2019; *van Pinxteren et al.*, 2019]. On-line instruments and cold stage techniques were applied to measure CCN and INP concentrations [*Gong et al.*, 2019a, b]. Moreover, bacterial cell counts, trace metals and trace gases were analysed using state-of the art analytical methods [*van Pinxteren et al.*, 2019].

To interpret the results, the measurements were accompanied by various auxiliary parameters such as air mass back trajectory analysis, vertical atmospheric profile analysis, cloud observations and pigment measurements in seawater. In addition, atmospheric transport modelling studies supported the experimental analysis [*van Pinxteren et al.*, 2019].

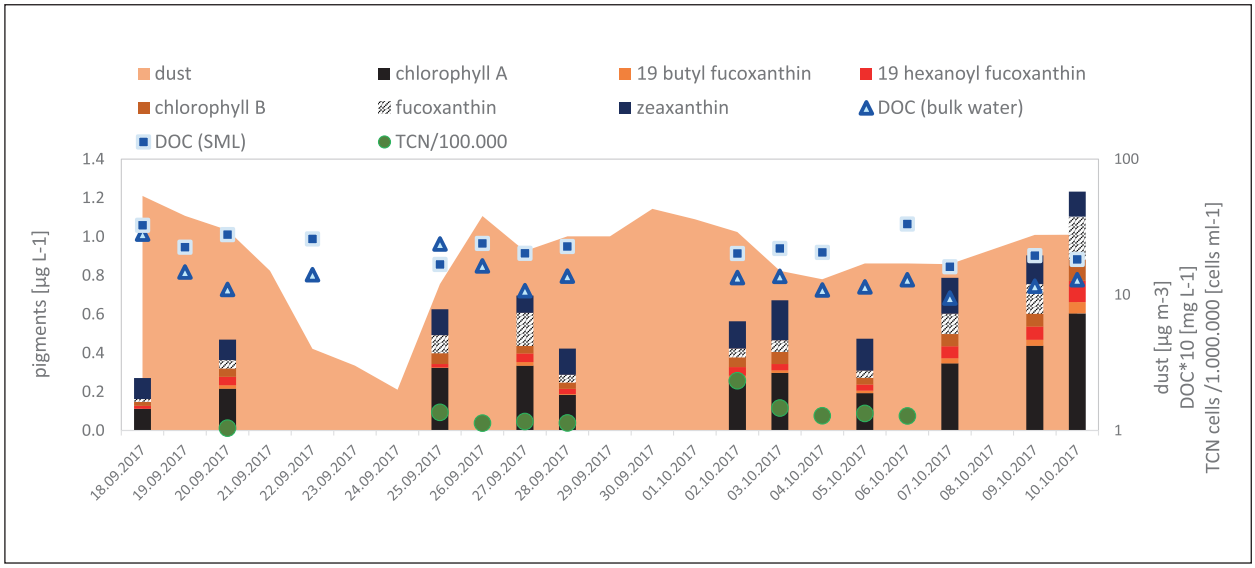

Fig. 2: Temporal evolution of DOC concentrations in the bulk water samples along the campaign together with the main pigment concentrations (chlorophyll A, chlorophyll B, zeaxanthin, fucoxanthin, 19 hexanoyl fucoxanthin and 19 butyl fucoxanthin) and total cell numbers (TCN) measured in the bulk water and dust concentrations in the atmosphere (yellow background area).

Results and Discussion

During MarParCloud, the wind direction was almost constantly from the northeast sector and the CVAO exhibited marine air masses with low and partly moderate dust influences. Based on similar particle number size distributions at the ground and mountain sites, it was found that the marine boundary layer (MBL) was generally well mixed and situated between 600 and 1100 meters. The chemical composition of the aerosol particles and the cloud water suggested that the coarse-mode particles served as efficient CCN. Most of the low-level clouds observed over the islands formed over the ocean due to local meteorological conditions. The presence of ocean-derived compounds in the cloud water at the mountain site (such as sodium, methane-sulfonic acid, amino acids and sugar-like compounds) showed a connection between ocean and clouds. However, INP measurements also showed a significant contribution of other non-marine sources to the local INP concentration.

The bulk water and SML analysis included a variety of biological and chemical components and a showed a consistent enrichment of organic compounds in the SML. The temporal evolution of the concentration of organic carbon and pigments in seawater and the atmospheric parameters (dust concentrations) is presented in Figure 2. Lipids represented an important organic compound group in the SML and a selective enrichment of surface-active lipid classes within the SML was found. The observed enrichments also indicated biotic and/or abiotic lipid degradation processing within the SML. The low chlorophyll A concentrations were typical of oligotrophic regions such as the Cape Verde islands with indications for a bloom development within the campaign. The temporal variability of bacterial abundance was investigated and provided the first concerted SML and cloud water measurements for this particular oceanic province.

In summary, when looking at the particle mass, oceanic compounds transferred to the atmospheric aerosol particles and to the cloud water were clearly observed and support the concept of ocean-atmospheric link. However, in terms of particle number concentrations, marine contributions to CCN and INP are rather limited. A clear description of possible transfer patterns and the quantification of other important sources must await a complete chemical analysis of all collected samples.

References

Cochran, R. E., O. S. Ryder, V. H. Grassian, and K. A. Prather (2017), Sea Spray Aerosol: The Chemical Link between the Oceans, Atmosphere, and Climate, *Accounts Chem. Res.*, *50*(3), 599-604, 10.1021/acs.accounts.6b00603.

Gong, X., H. Wex, M. van Pinxteren, N. Triesch, K. W. Fomba, J. Lubitz, C. Stolle, T.-B. Robinson, T. Müller, H. Herrmann, and F. Stratmann (2019), Characterization of aerosol particles at Cape Verde close to sea and cloud level heights – Part 2: ice nucleating particles in air, cloud and seawater, *Atmos. Chem. Phys. Discuss.*, https://doi.org/10.5194/acp-2019-729.

Gong, X., H. Wex, J. Voigtländer, K. W. Fomba, K. Weinhold, M. van Pinxteren, S. Henning, T. Müller, H. Herrmann, and F. Stratmann (2019), Characterization of aerosol particles at Cape Verde close to sea and cloud level heights – Part 1: particle number size distribution, cloud condensation nuclei and their origins, https://doi.org/10.5194/acp-2019-585., *Atmos. Chem. Phys. Discuss*, https://doi.org/10.5194/acp-2019-585, .

Law, C. S., E. Breviere, G. de Leeuw, V. Garcon, C. Guieu, D. J. Kieber, S. Kontradowitz, A. Paulmier, P. K. Quinn, E. S. Saltzman, J. Stefels, and R. von Glasow (2013), Evolving research directions in Surface Ocean-Lower Atmosphere (SOLAS) science, *Environmental Chemistry*, *10*(1), 1-16, 10.1071/en12159.

Triesch, N., M. van Pinxteren, A. Engel, and H. Herrmann (2019), Concerted measurements of free amino acids at the Cape Verde Islands: High enrichments in submicron sea spray aerosol particles and cloud droplets, *Atmos. Chem. Phys. Discuss.*

van Pinxteren, M., K. W. Fomba, N. Triesch, C. Stolle, O. Wurl, E. Bahlmann, X. Gong, J. Voigtländer, H. Wex, T.-B. Robinson, S. Barthel, S. Zeppenfeld, E. H. Hoffmann, M. Roveretto, C. Li, B. Grosselin, V. Daële, F. Senf, D. van Pinxteren, M. Manzi, N. Zabalegui, S. Frka, B. Gašparović, R. Pereira, T. Li, L. Wen, J. Li, C. Zhu, H. Chen, J. Chen, B. Fiedler, W. von Tümpling, K. A. Read, S. C. Punjabi, A. C. Lewis, H. J. R., C. L. J., I. Peeken, T. Rixen, D. Schulz-Bull, M. E. Monge, A. Mellouki, C. George, F. Stratmann, and H. Herrmann (2019), Marine organic matter in the remote environment of the Cape Verde Islands – An introduction and overview to the MarParCloud campaign, *Atmos. Chem. Phys. Discuss.*, https://doi.org/10.5194/acp-2019-997,.

Funding

This work was funded by Leibniz Association SAW in the project “Marine biological production, organic aerosol particles and marine clouds: a Process Chain (MarParCloud)” (SAW-2016-TROPOS-2) and within the Research and Innovation Staff Exchange EU project MARSU (69089).

Cooperation

Multiple national and international project partners.

Overview and highlights of the MARine atmospheric Science Unravelled (MARSU) project

Khanneh Wadinga Fomba[1], Manuela van Pinxteren[1], Laurent Poulain[1], Nabil Deabji[1], Tobias Otto[1], Sayf El Islam Barcha[2], Ibrahim Ouchen[2], El Mahdi Elbaramoussib[2], Rajaa Cherkaoui El Moursli[2], Mimoun Harnafi[2], Abdelwahid Mellouki[3], Luis Mendes Neves[4], Hartmut Herrmann[1]

[1]Leibniz Institute for Tropospheric Research (TROPOS), Leipzig, Germany
[2]Faculty of Science, Mohammed V University in Rabat, Morocco
[3]Institut de Combustion Aérothermique Réactivité et Environnement/ICARE-CNRS, France
[4] Instituto Nacional de Meteorologia e Geofísica (INMG), Cabo Verde

Aerosole, die aus Wechselwirkungen zwischen Luft und Meer stammen, und ihre Auswirkungen auf die Zusammensetzung der Atmosphäre und das Klima sind noch nicht gut verstanden. Im Rahmen des MARSU-Projekts bündelt ein interdisziplinäres Netzwerk von Wissenschaftlern ihre Expertise in den Bereichen Atmosphärenfeld-, Kammer-, Labor- und Modellstudien, um neue Erkenntnisse über die organische Aerosolzusammensetzung zu gewinnen und die Unsicherheit ihrer Auswirkungen auf Luftverschmutzung und Klima zu verringern. Die Aktivitäten des Projekts konzentrieren sich auf den Mitarbeiteraustausch zur Durchführung gemeinsamer Aktivitäten in den verschiedenen Bereichen, insbesondere in Feld- und Laborstudien. Es wurden Feldstudien in Berg-, Meeres- und Stadtregionen durchgeführt sowie neue Analysemethoden zur Analyse der organischen Aerosolgehalte entwickelt, um die Unterschiede in der atmosphärischen Zusammensetzung an diesen Standorten zu beurteilen. Hier werden einige Highlights vorgestellt.

Introduction

Aerosols derived from the air-sea exchange and their effects on atmospheric composition and climate are still not well understood. To reduce the uncertainty related to their properties a combination of different expertise is required. The MARSU (Marine Atmospheric Science Unravelled) project focuses on the characterization of the organic content of aerosol particles originating from the ocean surface microlayer, investigating the evolution of their chemical and physical properties, interaction with air pollution and effects on air quality and atmospheric composition. In a collaborative effort between scientific and industrial partners from seven nations, expertise in analytical method development, cutting-edge laboratory, simulation chamber, field sampling, and modelling studies are shared to gain new insights into the aerosol physicochemical properties. The activities are based on the exchange of staff within these fields of expertise to enhance the development of young scientists and improve on interdisciplinary approaches toward the analysis, quantification, and understanding of aerosol organic composition. The industrial partners are exposed to the challenges of specific research topics to which they can develop targeted solutions. Joint field campaigns were organised in marine, mountain and urban regions to investigate the variation of organic compounds at these regions and their effect on the aerosol composition. Subsequently, staff exchanges were also carried out to develop appropriate analytical methods for analysing these compounds in the different aerosol matrices.

Fig. 1: The Atlas Mohamed V atmospheric observatory (AM5) and instruments deployed at the station and other locations in the urban city of Fes during intensive field measurements.

Highlights

To achieve a broader regional understanding of the aerosol organic and chemical composition, a new site, the Atlas Mohamed V observatory (AM5, see Fig. 1), was created in the Atlas mountain region of Morocco to monitor continental background levels of aerosol constituents. The ca. 2000 m high site was one of the locations where long-term and intensive field studies were carried out. Figure 2 shows the time series of PM10 aerosol constituents in summer 2017 at the AM5 site. Averagely, during this period, mineral dust, especially Saharan dust, made up about 65% of the aerosol mass with concentrations of up to 80 µg/m³. Inorganic ions made up about 15% of the mass with organic and elemental carbon accounting for about 8% and less than 4% of the aerosol mass, respectively. Other components such as aerosol water

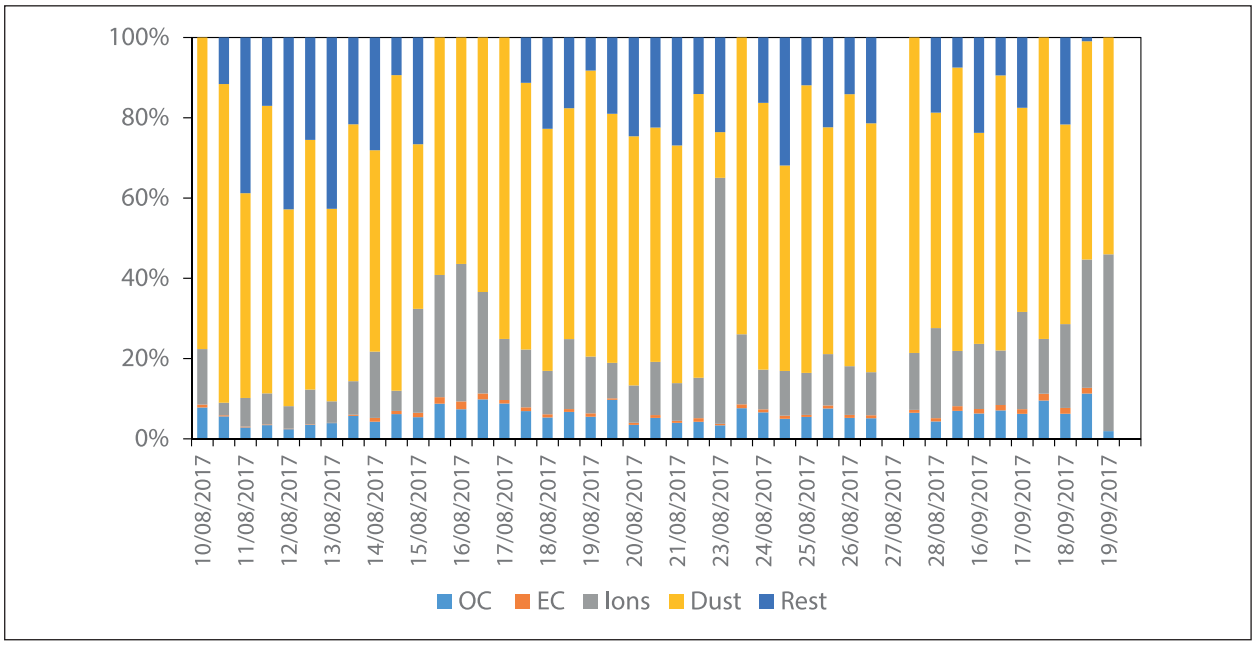

Fig. 2: Time series of the relative contribution of PM10 aerosol chemical components in summer at the AM5 site.

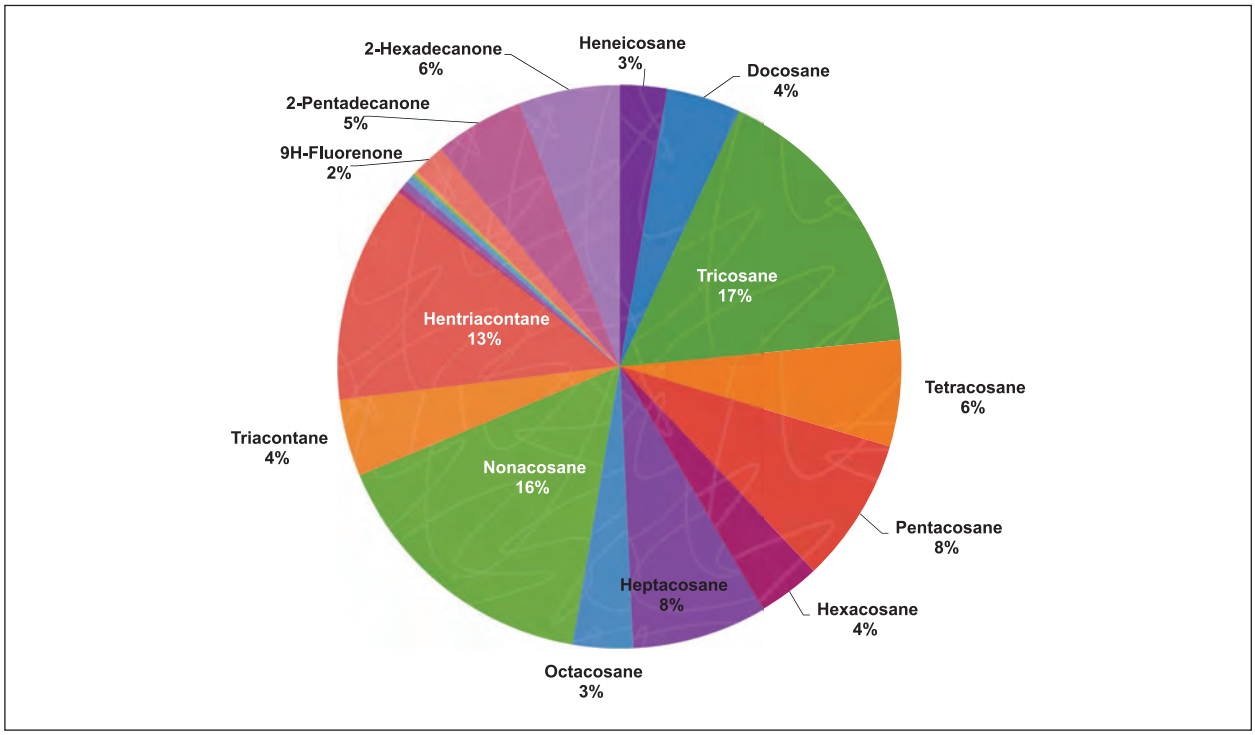

Fig. 3: Relative contribution of identified aliphatic and aromatic compounds in PM10 samples from the AM5 station.

made up the rest of the aerosol mass. Figure 3 shows the distribution of aliphatic and aromatic compounds identified in the samples revealing a diversity in the type of compounds observed in the particles. These compounds originated from both biogenic sources such as plant (e.g. Fluorenone) and insect emissions (e.g. 2-Hexadecanone) and anthropogenic sources from fuel combustion (e.g. Pentacosane, Tricosane, Nonacosane). In addition, methods were developed to quantify metals at trace concentrations in both aerosol and cloud water at such remote background sites [*Fomba et al.*, 2019], which are important parameters in the identification and quantification of aerosol sources and in assessing atmospheric multiphase chemical processes. To obtain a much broader understanding of the aerosol properties and investigate the interaction of organic aerosols with marine and polluted continental aerosols the ATLAS 2019 campaign was organised during which online and offline (filter-based, size-resolved and bulk particulate matter) aerosol in situ and remote sensing instruments (see Fig. 1) were deployed at the AM5 site and two other locations in the centre and neighbourhood of the urban city of Fes. The ongoing data analysis will provide a detailed chemical and physical characterisation of the aerosol properties as well as factors influencing the atmospheric composition at such a continental site, which is not well understood.

A second campaign was organised at the Cape Verde Atmospheric Observatory (CVAO) with the focus on elucidating the role of oceanic emissions especially from the ocean surface microlayer on marine aerosol organic matter composition. This was done together with the MarParCloud campaign, to enable a higher number of instrumentations for detailed chemical analysis. Through concerted measurements of the SML and aerosol particles, the transport and sources of ambient organic compounds such as lipids, low molecular weight, and biopolymeric substances could be identified [*van Pinxteren et al.*, 2019].

In summary, the aerosol composition at the mountain and marine sites showed different compositions in their organic carbon content and aerosol composition with particles originating from different sources including local biogenic and marine emissions as well as long-range transport of mineral dust and anthropogenic emissions. The synthesis of the spatial and temporal variability of the atmospheric composition in the targeted regions is ongoing.

The focus on field investigations in Africa developed during the MARSU project including the CVAO and the Maroccan engagements will in the future be intensified by ACDs's other African activities in Namibia in close collaboration with South Africa.

References

Fomba, K. W., Deabji, N., Barcha, S.E, Ouchen, I., Elbaramoussib, E, El Moursli, R.C., Harnafi, M., El Hajjaji, S., Mellouki, A., and Herrmann, H., Application of TXRF in monitoring trace metals in particulate matter and cloud water, Submitted, Atmos. Meas. Tech., 2019.

van Pinxteren, M., Fomba, K., Triesch, N., Stolle, C., Wurl, O., Bahlmann, E., Gong, X., Voigtländer, J., Wex, H., Robinson, T.-B., Barthel, S., Zeppenfeld, S., Hoffmann, E. H., Roveretto, M., Li, C., Grosselin, B., Daële, V., Senf, F., van Pinxteren, D., Manzi, M., Zabalegui, N., Frka, S., Gašparović, B., Pereira, R., Li, T., Wen, L., Li, J., Zhu, C., Chen, H., Chen, J., Fiedler, B., von Tümpling, W., Read, K. A., Punjabi, S., Lewis, A. C. C., Hopkins, J. R., Carpenter, L. J., Peeken, I., Rixen, T., Schulz-Bull, D., Monge, M. E., Mellouki, A., George, C., Stratmann, F., and Herrmann, H.: Marine organic matter in the remote environment of the Cape Verde Islands – An introduction and overview to the MarParCloud campaign, Atmos. Chem. Phys. Discuss., 2019.

Funding

EU Horizon 2020 Research and Innovation Staff Exchange, Grant agreement No: 69089.

Cooperation

University Mohammed V, Rabat, Morocco;
Centre National de la Recherche Scientifique – CNRS, Institut de Combustion Aérothermique Réactivité et Environnement/ICARE-CNRS, France;
Instituto Nacional de Meteorologia e Geofísica (INMG), Cabo Verde;
Centro de Investigaciones en Bionanociencias "Elizabeth Jares-Erijman", Argentina;
Institute of Urban Environment – CAS, Shandong University – Jinan, Fudan University – Shanghai, China;
IONICON Analytik Ges.m.b.H., Austria.

Appendices


Information
Enjoy it to the fullest!
EGU General Assembly
Welcome to the General Assembly
CAMECA

Publications

Publication statistics

	2018	2019
Total number of publications	**358**	**349**
Books (author, editor) *	1	1
Book sections *	2	-
Contributions to collected editions *	5	1
Articles in peer reviewed journals *	88	85
Articles (others)	32	11
Presentations (invited)	21	10
Presentations (others)	200	226
Reports/Datasets/Software *	9	15

Publications *

2018

Alas, H. D., **Müller, T.**, **Birmili, W.**, **Kecorius, S.**, Cambaliza, M. O., Simpas, J. B. B., Cayetano, M., **Weinhold, K.**, Vallar, E., Galvez, M. C. and **Wiedensohler, A.** 2018. Spatial characterization of black carbon mass concentration in the atmosphere of a Southeast Asian megacity: An air quality case study for Metro Manila, Philippines. Aerosol Air Qual. Res., **18**, 2301-2317. doi:10.4209/aaqr.2017.08.0281.

Althausen, D., Emeis, S., Flentje, H., Jäckel, S., Lehmann, V., Mattis, I., Münkel, C., Peters, G., Ritter, C., Wagner, L., Wiegner, M. and Wille, H. 2018. VDI-Richtlinie VDI 3786 / Blatt 19:2018-09: Umweltmeteorologie; Bodengebundene Fernmessung meteorologischer Parameter; Partikelrückstreulidar / Environmental meteorology; Ground-based remote sensing of meteorological parameters; Particle backscatter lidar. VDI-Verl., Düsseldorf, 65 pp. (Auch enthalten in: VDI/DIN-Handbuch Reinhaltung der Luft, Band 1b: Umweltmeteorologie).

Altstädter, B., Platis, A., **Jähn, M.**, **Baars, H.**, Lückerath, J., Held, A., Lampert, A., Bange, J., **Hermann, M.** and **Wehner, B.** 2018. Airborne observations of newly formed boundary layer aerosol particles under cloudy conditions. Atmos. Chem. Phys., **18**, 8249-8264. doi:10.5194/acp-18-8249-2018.

Andreae, M. O., Afchine, A., Albrecht, R., Holanda, B. A., Artaxo, P., Barbosa, H. M. J., Bormann, S., Cecchini, M. A., Costa, A., Dollner, M., Fütterer, D., Järvinen, E., Jurkat, T., Klimach, T., Konemann, T., Knote, C., Krämer, M., Krisna, T., Machado, L. A. T., **Mertes, S.**, Minikin, A., Pöhlker, C., Pöhlker, M. L., Pöschl, U., Rosenfeld, D., Sauer, D., Schlager, H., Schnaiter, M., Schneider, J., Schulz, C., Spanu, A., Sperling, V. B., Voigt, C., Walser, A., Wang, J., Weinzierl, B., Wendisch, M. and Ziereis, H. 2018. Aerosol characteristics and particle production in the upper troposphere over the Amazon Basin. Atmos. Chem. Phys., **18**, 921-961. doi:10.5194/acp-18-921-2018.

Ansmann, A., **Baars, H.**, Chudnovsky, A., Mattis, I., Veselovskii, I., **Haarig, M.**, **Seifert, P.**, **Engelmann, R.** and **Wandinger, U.** 2018. Extreme levels of Canadian wildfire smoke in the stratosphere over central Europe on 21–22 August 2017. Atmos. Chem. Phys., **18**, 11831-11845. doi:10.5194/acp-18-11831-2018.

Banks, J. R., **Schepanski, K.**, **Heinold, B.**, **Hünerbein, A.** and Brindley, H. E. 2018. The influence of dust optical properties on the colour of simulated MSG-SEVIRI Desert Dust infrared imagery. Atmos. Chem. Phys., **18**, 9681-9703. doi:10.5194/acp-18-9681-2018.

Appendices: Publications

Barrientos Velasco, C., **Deneke, H.** and **Macke, A.** 2018. Spatial and temporal variability of broadband solar irradiance during POLARSTERN cruise PS106.1 Ice Floe Camp (June 4th-16th 2017). *Data from:* Arctic Amplification (AC3); PS106_21-2; PS106_22-1; PS106_23-2. *PANGAEA*, doi:10.1594/PANGAEA.896710.

Belegante, L., Bravo-Aranda, J. A., Freudenthaler, V., Nicolae, D., Nemuc, A., Ene, D., Alados-Arboledas, L., Amodeo, A., Pappalardo, G., D'Amico, G., Amato, F., **Engelmann, R.**, **Baars, H.**, **Wandinger, U.**, Papayannis, A., Kokkalis, P. and Pereira, S. N. 2018. Experimental techniques for the calibration of lidar depolarization channels in EARLINET. Atmos. Meas. Tech., **11**, 1119-1141. doi:10.5194/amt-11-1119-2018.

Benedetti, A., Reid, J. S., Knippertz, P., Marsham, J. H., Di Giuseppe, F., Rémy, S., Basart, S., Boucher, O., Brooks, I. M., Menut, L., Mona, L., Laj, P., Pappalardo, G., **Wiedensohler, A.**, Baklanov, A., Brooks, M., Colarco, P. R., Cuevas, E., da Silva, A., Escribano, J., Flemming, J., Huneeus, N., Jorba, O., Kazadzis, S., Kinne, S., Popp, T., Quinn, P. K., Sekiyama, T. T., Tanaka, T. and Terradellas, E. 2018. Status and future of numerical atmospheric aerosol prediction with a focus on data requirements. Atmos. Chem. Phys., **18**, 10615-10643. doi:10.5194/acp-18-10615-2018.

Berndt, T., Mentler, B., Scholz, W., Fischer, L., **Herrmann, H.**, Kulmala, M. and Hansel, A. 2018. Accretion product formation from ozonolysis and OH radical reaction of α-pinene: Mechanistic insight and the influence of isoprene and ethylene. Environ. Sci. Technol., **52**, 11069-11077. doi:10.1021/acs.est.8b02210.

Berndt, T., Scholz, W., Mentler, B., Fischer, L., **Herrmann, H.**, Kulmala, M. and Hansel, A. 2018. Bildung von Aufbauprodukten aus den Selbst- und Kreuzreaktionen von RO_2-Radikalen in der Atmosphäre. Angew. Chem., **130**, 3882-3886. doi:10.1002/ange.201710989.

Berndt, T., Scholz, W., Mentler, B., Fischer, L., **Herrmann, H.**, Kulmala, M. and Hansel, A. 2018. Accreation product formation from self- and cross-reactions of RO_2 radicals in the atmosphere. Angew. Chem. Int. Edit., **57**, 3820-3824. doi:10.1002/anie.201710989.

Bohlmann, S., **Baars, H.**, **Radenz, M.**, **Engelmann, R.** and **Macke, A.** 2018. Ship-borne aerosol profiling with lidar over the Atlantic Ocean: From pure marine conditions to complex dust-smoke mixtures. Atmos. Chem. Phys., **18**, 9661-9679. doi:10.5194/acp-18-9661-2018.

Bucci, S., Cristofanelli, P., Decesari, S., Marinoni, A., Sandrini, S., **Größ, J.**, **Wiedensohler, A.**, Di Marco, C. F., Nemitz, E., Cairo, F., Di Liberto, L. and Fierli, F. 2018. Vertical distribution of aerosol optical properties in the Po Valley during the 2012 summer campaigns. Atmos. Chem. Phys., **18**, 5371-5389. doi:10.5194/acp-18-5371-2018.

Chappell, A., Lee, J. A., Baddock, M., Gill, T. E., Herrick, J. E., Leys, J. F., Marticorena, B., Petherick, L., **Schepanski, K.**, Tatarko, J., Telfer, M. and Webb, N. P. 2018. A clarion call for aeolian research to engage with global land degradation and climate change. Aeolian Res., **32**, A1-A3 (Editorial). doi:10.1016/j.aeolia.2018.02.007.

Chen, J., Wu, Z., **Augustin-Bauditz, S.**, **Grawe, S.**, **Hartmann, M.**, Pei, X., Liu, Z., Ji, D. and **Wex, H.** 2018. Ice nucleating particle concentrations unaffected by urban air pollution in Beijing, China. Atmos. Chem. Phys., **18**, 3523-3539. doi:10.5194/acp-18-3523-2018.

Chen, Y., Wild, O., Wang, Y., Ran, L., **Teich, M.**, **Größ, J.**, **Wang, L.**, **Spindler, G.**, **Herrmann, H.**, **van Pinxteren, D.**, McFiggans, G. and **Wiedensohler, A.** 2018. The influence of impactor size cut-off shift caused by hygroscopic growth on particulate matter loading and composition measurements. Atmos. Environ., **195**, 141-148. doi:10.1016/j.atmosenv.2018.09.049.

Chen, Y., **Wolke, R.**, Ran, L., **Birmili, W.**, **Spindler, G.**, **Schröder, W.**, Su, H., Cheng, Y., **Tegen, I.** and **Wiedensohler, A.** 2018. A parameterization of the heterogeneous hydrolysis of N_2O_5 for mass-based aerosols models: Improvement of particulate nitrate prediction. Atmos. Chem. Phys., **18**, 673-689. doi:10.5194/acp-18-673-2018.

Córdoba-Jabonero, C., Sicard, M., Ansmann, A., del Águila, A. and **Baars, H.** 2018. Separation of the optical and mass features of particle components in different aerosol mixtures by using POLIPHON retrievals in synergy with continuous polarized Micro-Pulse Lidar (P-MPL) measurements. Atmos. Meas. Tech., **11**, 4775-4795. doi:10.5194/amt-11-4775-2018.

Dai, G., **Althausen, D.**, **Hofer, J.**, **Engelmann, R.**, **Seifert, P.**, **Bühl, J.**, Mamouri, R.-E., Wu, S. and **Ansmann, A.** 2018. Calibration of Raman lidar water vapor profiles by means of AERONET photometer observations and GDAS meteorological data. Atmos. Meas. Tech., **11**, 2735-2748. doi:10.5194/amt-11-2735-2018.

Dall'Osto, M., Beddows, D. C. S., Asmi, A., **Poulain, L.**, Hao, L., Freney, E., Allan, J. D., Canagaratna, M., Crippa, M., Bianchi, F., de Leeuw, G., Eriksson, A., Swietlicki, E., Hansson, H. C., Henzing, J. S., Granier, C., Zemankova, K., Laj, P., Onasch, T., Prevot, A., Putaud, J. P., Sellegri, K., Vidal, M., Virtanen, A., Simo, R.,

Worsnop, D., O'Dowd, C., Kulmala, M. and Harrison, R. M. 2018. Novel insights on new particle formation derived from a pan-european observing system. Sci. Rep., **8**, Art. Nr. 1482. doi:10.1038/s41598-017-17343-9.

Di Ianni, A., Costabile, F., Barnaba, F., Di Liberto, L., **Weinhold, K.**, **Wiedensohler, A.**, Struckmeier, C., Drewnick, F. and Gobbi, G. P. 2018. Black carbon aerosol in Rome (Italy): Inference of a long-term (2001–2017) record and related trends from AERONET sun-photometry data. Atmosphere, **9**, 81 (24 pp.). doi:10.3390/atmos9030081.

Ditas, J., Ma, N., Zhang, Y., **Assmann, D.**, Neumaier, M., Riede, H., Karu, E., Williams, J., Scharffe, D., Wang, Q., Saturno, J., Schwarz, J. P., Katich, J. M., McMeeking, G. R., Zahn, A., **Hermann, M.**, Brenninkmeijer, C. A. M., Andreae, M. O., Pöschl, U., Su, H. and Cheng, Y. 2018. Strong impact of wildfires on the abundance and aging of black carbon in the lowermost stratosphere. Proc. Nat. Acad. Sci. (PNAS), **115**, E11595-E11603. doi:10.1073/pnas.1806868115.

Düsing, S., **Wehner, B.**, **Seifert, P.**, **Ansmann, A.**, **Baars, H.**, **Ditas, F.**, **Henning, S.**, **Ma, N.**, **Poulain, L.**, **Siebert, H.**, **Wiedensohler, A.** and **Macke, A.** 2018. Helicopter-borne observations of the continental background aerosol in combination with remote sensing and ground-based measurements. Atmos. Chem. Phys., **18**, 1263-1290. doi:10.5194/acp-18-1263-2018.

Emde, C., **Barlakas, V.**, Comet, C., Evans, F., Wang, Z., Labonnote, L. C., **Macke, A.**, Mayer, B. and Wendisch, M. 2018. IPRT polarized radiative transfer model intercomparison project: Three-dimensional test cases (Phase B). J. Quant. Spectrosc. Radiat. Transfer, **209**, 19-44. doi:10.1016/j.jqsrt.2018.01.024.

Fomba, K. W., **van Pinxteren, D.**, **Müller, K.**, **Spindler, G.** and **Herrmann, H.** 2018. Assessment of trace metal levels in size-resolved particulate matter in the area of Leipzig. Atmos. Environ., **176**, 60-70. doi:10.1016/j.atmosenv.2017.12.024.

Frey, W., Hu, D., Dorsey, J., Alfarra, M. R., Pajunoja, A., Virtanen, A., Connolly, P. and McFiggans, G. 2018. The efficiency of secondary organic aerosol particles acting as ice-nucleating particles under mixed-phase cloud conditions. Atmos. Chem. Phys., **18**, 9393–9409. doi:10.5194/acp-18-9393-2018.

Gatzsche, K., Babel, W., Falge, E., Pyles, R. D., Paw U, K. T., Raabe, A. and Foken, T. 2018. Footprint-weighted tile approach for a spruce forest and a nearby patchy clearing using the ACASA model. Biogeosciences, **15**, 2945-2960. doi:10.5194/bg-15-2945-2018.

Gatzsche, K., **Iinuma, Y.**, **Mutzel, A.**, **Berndt, T.**, **Poulain, L.**, **Tilgner, A.** and **Wolke, R.** 2018. Kinetic modeling of SOA formation for α- and β-pinene. *In: C. Mensink and G. Kallos (Eds.), Air pollution modeling and its application XXV : Proceedings of the 35th International Technical Meeting on Air Pollution Modelling and Its Application (Chania, Crete, Greece, 3-7 October 2016)*. Springer International Publishing, Cham, Switzerland, p. 559-564 (Chapter 87). doi:10.1007/978-3-319-57645-9. (Springer Proceedings in Complexity).

Glasius, M., Hansen, A. M. K., Claeys, M., Henzing, J. S., Jedynska, A. D., Kasper-Giebl, A., Kistler, M., Kristensen, K., Martinsson, J., Maenhaut, W., Nøjgaard, J., K., **Spindler, G.**, Stenström, K. E., Swietlicki, E., Szidat, S., Simpson, D. and Yttri, K. E. 2018. Composition and sources of carbonaceous aerosols in Northern Europe during winter. Atmos. Environ., **173**, 127-141. doi:10.1016/j.atmosenv.2017.11.005.

Grawe, S., **Augustin-Bauditz, S.**, Clemen, H.-C., Ebert, M., Hammer, S. E., Lubitz, J., Reicher, N., Rudich, Y., Schneider, J., Staacke, R., **Stratmann, F.**, **Welti, A.** and **Wex, H.** 2018. Coal fly ash: Linking immersion freezing behavior and physicochemical particle properties. Atmos. Chem. Phys., **18**, 13903-13923. doi:10.5194/acp-18-13903-2018.

Griesche, H., **Seifert, P.**, **Baars, H.**, **Bühl, J.**, **Barrientos, C.**, **Egerer, U.**, **Engelmann, R.**, Nomokonova, T., **Radenz, M.** and **Macke, A.** 2018. *Continuous profiling of aerosols and clouds of the Arctic during Polarstern cruise PS106*. 27th International Polar Conference 2018, Rostock, Germany, 25-29 March 2018. Berichte zur Polar- und Meeresforschung ; Reports on Polar and Marine Research ; 716/2018: Polar Systems under Pressure : 27th International Polar Conference, Rostock, 25 - 29 March 2018 (German Society for Polar Research). doi:10.2312/BzPM_0716_2018.

Größ, J., **Hamed, A.**, **Sonntag, A.**, **Spindler, G.**, Maninnen, H. E., Nieminen, T., Kulmala, M., Hõrrak, U., Plass-Dülmer, C., **Wiedensohler, A.** and **Birmili, W.** 2018. Atmospheric new particle formation at the research station Melpitz, Germany: Connection with gaseous precursors and meteorological parameters Atmos. Chem. Phys., **18**, 1835-1861. doi:10.5194/acp-18-1835-2018.

Grosvenor, D. P., Sourdeval, O., Zuidema, P., Ackerman, A., Alexandrov, M. D., Bennartz, R., Boers, R., Cairns, B., Chiu, J. C., Christensen, M., **Deneke, H.**, Diamond, M., Feingold, G., Fridlind, A., **Hünerbein, A.**, Knist, C., Kollias, P., Marshak, A., McCoy, D., **Merk, D.**, Painemal, D., Rausch, J., Rosenfeld, D., Russchenberg,

H., **Seifert, P.**, Sinclair, K., Stier, P., van Diedenhoven, B., Wendisch, M., Werner, F., Wood, R., Zhang, Z. and Quaas, J. 2018. Remote sensing of droplet number concentration in warm clouds: A review of the current state of knowledge and perspectives. Rev. Geophys., **56**, 409-453. doi:10.1029/2017RG000593.

Gualtieri, M., Grollino, M. G., Consales, C., Costabile, F., Manigrasso, M., Avino, P., Aufderheide, M., Cordelli, E., Di Liberto, L., Petralia, E., Raschellà, G., Stracquadanio, M., **Wiedensohler, A.**, Pacchierotti, F. and Zanini, G. 2018. Is it the time to study air pllution effects under environmental conditions? A case study to support the shift of *in vitro* toxicology from the bench to the field. Chemosphere, **207**, 552-564. doi:10.1016/j.chemosphere.2018.05.130.

Haarig, M., **Ansmann, A.**, **Baars, H.**, **Jimenez, C.**, Veselovskii, I., **Engelmann, R.** and **Althausen, D.** 2018. Depolarization and lidar ratios at 355, 532, and 1064 nm and microphysical properties of aged tropospheric and stratospheric Canadian wildfire smoke Atmos. Chem. Phys., **18**, 11847-11861. doi:10.5194/acp-18-11847-2018.

Hammer, S. E., **Mertes, S.**, Schneider, J., Ebert, M., Kandler, K. and Weinbruch, S. 2018. Composition of ice particle residuals in mixed-phase clouds at Jungfraujoch (Switzerland): Enrichment and depletion of particle groups relative to total aerosol Atmos. Chem. Phys., **18**, 13987-14003. doi:10.5194/acp-18-13987-2018.

Hansel, A., Scholz, W., Mentler, B., Fischer, L. and **Berndt, T.** 2018. Detection of RO_2 radicals and other products from cyclohexene ozonolysis with NH_4^+ and acetate chemical ionization mass spectrometry. Atmos. Environ., **186**, 248-255. doi:10.1016/j.atmosenv.2018.04.023.

Heintzenberg, J., **Senf, F.**, Birmili, W. and **Wiedensohler, A.** 2018. Aerosol connections between three distant continental stations. Atmos. Environ., **190**, 349-358. doi:10.1016/j.atmosenv.2018.07.047.

Hellmuth, O., Shchekin, A. K., Feistel, R., Schmelzer, J. W. P. and Abyzov, A. S. 2018. Physical interpretation of ice contact angles, fitted to experimental data on immersion freezing of kaolinite particles. Interfac. Phenom. Heat Transfer, **6**, 37-74.

Henning, S., **Welti, A.**, **Hartmann, M.**, **Löffler, M.**, Baccarini, A., Wernli, H., **Stratmann, F.**, Rosenfeld, D., Gysel, M. and Schmale, J. 2018. *Study of cloud condensation nuclei and ice nucleating particles in the Southern Ocean*. 27th International Polar Conference 2018, Rostock, Germany, 25-29 March 2018. Berichte zur Polar- und Meeresforschung ; Reports on Polar and Marine Research ; 716/2018: Polar Systems under Pressure : 27th International Polar Conference, Rostock, 25 - 29 March 2018 (German Society for Polar Research). doi:10.2312/BzPM_0716_2018.

Herenz, P., **Wex, H.**, **Henning, S.**, **Kristensen, T. B.**, Rubach, F., Roth, A., Borrmann, S., Bozem, H., Schulz, H. and **Stratmann, F.** 2018. Measurements of aerosol and CCN properties in the Mackenzie River delta (Canadian Arctic) during spring-summer transition in May 2014. Atmos. Chem. Phys., **18**, 4477-4496. doi:10.5194/acp-18-4477-2018.

Herenz, P., **Wex, H.**, **Henning, S.**, **Kristensen, T. B.**, Rubach, F., Roth, A., Borrmann, S., Bozem, H., Schulz, H. and **Stratmann, F.** 2018. Measurements of aerosol and CCN properties in the Mackenzie River delta (Arctic) during RACEPAC. *Data from:* RACEPAC; MackenzieRiver_delta. *PANGAEA*, doi:10.1594/PANGAEA.891033.

Herenz, P., **Wex, H.**, Mangold, A., Laffineur, Q., Gorodetskaya, I. V., Fleming, Z. L., Panagi, M. and **Stratmann, F.** 2018. Meteorological observations and condensation nuclei measurements at the Princess Elisabeth Antarctica Research Station during three austral summers. *Data from:* PE_Station (Princess Elisabeth Station). *PANGAEA*, doi:10.1594/PANGAEA.894841.

Hoffmann, E. H., **Tilgner, A.**, **Wolke, R.**, **Böge, O.**, Walter, A. and **Herrmann, H.** 2018. Oxidation of substituted aromatic hydrocarbons in the troposphere aqueous phase: Kinetic mechanism development and modelling. Phys. Chem. Chem. Phys., **20**, 10960-10977. doi:10.1039/C7CP08576A.

Huang, S., Wu, Z., **Poulain, L.**, **van Pinxteren, M.**, **Merkel, M.**, **Assmann, D.**, **Herrmann, H.** and **Wiedensohler, A.** 2018. Source apportionment of the organic aerosols over the Atlantic Ocean from 53° N to 53° S: Significant contributions from marine emissions and long-range transport. Atmos. Chem. Phys., **18**, 18043-18062. doi:10.5194/acp-18-18043-2018.

Huang, W. T. K., Ickes, L., **Tegen, I.**, Rinaldi, M., Ceburnis, D. and Lohmann, U. 2018. Global relevance of marine organic aerosols as ice nucleating particles. Atmos. Chem. Phys., **18**, 11423-11445. doi:10.5194/acp-18-11423-2018.

Karnezi, E., Murphy, B. N., **Poulain, L.**, **Herrmann, H.**, **Wiedensohler, A.**, **Rubach, F.**, Kiendler-Scharr, A., Mentel, T. F. and Pandis, S. N. 2018. Simulation of atmospheric organic aerosol using its volatility-oxagen-content distribution during the PEGASOS 2012 campaign. Atmos. Chem. Phys., **18**, 10759-10772. doi:10.5194/acp-18-10759-2018.

Kecorius, S., Tamayo, E. G., Galvez, M. C., Madueño, L., Betito, G., Gonzaga-Cayetano, M., Vallar, E. and **Wiedensohler, A.** 2018. Activity pattern of school/university tenants and their family members in Metro Manila – Philippines. Aerosol Air Qual. Res., **18**, 2412-2419. doi:10.4209/aaqr.2018.02.0069.

Knackstedt, K. A., Moffett, B. F., **Hartmann, S.**, **Wex, H.**, Hill, T. C. J., Glasgo, E. D., Reitz, L. A., **Augustin-Bauditz, S.**, Beall, B. F. N., Bullerjahn, G. S., Fröhlich-Nowoisky, J., **Grawe, S.**, **Lubitz, J.**, **Stratmann, F.** and McKay, R. M. L. 2018. Terrestrial origin for abundant riverine nanoscale ice-nucleating particles. Environ. Sci. Technol., **52**, 12358-12367. doi:10.1021/acs.est.8b03881.

Knudsen, E. M., **Heinold, B.**, Dahlke, S., Bozem, H., Crewell, S., Gorodetskaya, I. V., Heygster, G., Kunkel, D., Maturilli, M., Mech, M., Viceto, C., Rinke, A., Schmithüsen, H., Ehrlich, A., **Macke, A.**, Lüpkes, C. and Wendisch, M. 2018. Meteorological conditions during the ACLOUD/PASCAL field campaign near Svalbard in early summer 2017. Atmos. Chem. Phys., **18**, 17995-18022. doi:10.5194/acp-18-17995-2018.

Kokkola, H., Kühn, T., Laakso, A., Bergman, T., Lehtinen, K. E. J., Mielonen, T., Arola, A., Stadtler, S., Korhonen, H., Ferrachat, S., Lohmann, U., Neubauer, D., **Tegen, I.**, Siegenthaler-Le Drian, C., Schultz, M. G., Bey, I., Stier, P., Daskalakis, N., Heald, C. L. and Romakkaniemi, S. 2018. SALSA2.0: The sectional aerosol module of the aerosol-chemistry-climate model ECHAM6.3.0-HAM2.3-MOZ1.0. Geosci. Model Dev., **11**, 3833-3863. doi:10.5194/gmd-11-3833-2018.

Kroflič, A., Frka, S., **Simmel, M.**, **Wex, H.** and Grgić, I. 2018. Size-resolved surface active substances of atmospheric aerosol: Reconsideration of the impact on cloud droplet formation. Environ. Sci. Technol., **52**, 9179–9187. doi:10.1021/acs.est.8b02381.

Kubin, A., Merkel, U., **Schepanski, K.**, Schulz, M. and **Tegen, I.** 2018. *Verbundbericht PalMod-2-4 (Staubkreislauf)*. Bundesministerium für Bildung und Forschung (BMBF). **FKZ 01LP1508A, 01LP1508B**. p. 11.

Kumar, A., Abouchami, W., Galer, S. J. G., Singh, S. P., **Fomba, K. W.**, Prospero, J. M. and Andreae, M. O. 2018. Seasonal radiogenic isotopic variability of the African dust outflow to the tropical Atlantic Ocean and across to the Caribbean. Earth Planet. Sci. Lett., **487**, 94-105. doi:10.1016/j.epsl.2018.01.025.

Kwong, K. C., Chim, M. M., **Hoffmann, E. H.**, **Tilgner, A.**, **Herrmann, H.**, Davies, J. F., Wilson, K. R. and Chan, M. N. 2018. Chemical transformation of methansulfonic acid and sodium methanesulfonate through heterogeneous OH oxidation. ACS Earth Space Chem., **2**, 895-903. doi:10.1021/acsearthspacechem.8b00072.

Lenk, S., **Senf, F.** and **Deneke, H.** 2018. *Final Report on the Associate Scientist Activity for the validation of the Convection Initiation (CI) product of NWC SAF v2018*. Associate Scientist Activity (Dept. Nowcasting, Météo-France, Toulouse). 43.

Ling, M. L., **Wex, H.**, **Grawe, S.**, Jakobsson, J., Löndahl, J., **Hartmann, S.**, Finster, K., Boesen, T. and Šantl-Temkiv, T. 2018. Effects of ice nucleation protein repeat number and oligomerization level on ice nucleation activity. J. Geophys. Res. - Atmos., **123**, 1802-1810. doi:10.1002/2017jd027307.

Liu, J., Wu, L., Kümmel, S., Yao, J., **Schaefer, T.**, **Herrmann, H.** and Richnow, H.-H. 2018. Carbon and hydrogen stable isotope analysis for characterizing the chemical degradation of tributyl phosphate. Chemosphere, **212**, 133-142. doi:10.1016/j.chemosphere.2018.08.034.

Macke, A. and Flores, H. 2018. *The Expeditions PS106/1 und 2 of the Research Vessel POLARSTERN to the Arctic Ocean in 2017. Berichte zur Polar- und Meeresforschung - Reports on Polar and Marine Research*. Alfred-Wegener-Institut, Helmholtz-Zentrum für Polar- und Meeresforschung. Bremerhaven. **Berichte zur Polar- und Meeresforschung - Reports on Polar and Marine Research ; 719**. p. 171.

Maicher, L., Mjos, K. D. and **Tönisson, L.** 2018. Intervention opportunities for capacity building in technology transfer. *In: M. Granieri and A. Basso (Eds.), Capacity building in technology transfer : The European experience*. Springer, Cham, Switzerland, p. 29-46. doi:10.1007/978-3-319-91461-9. (SxI - Springer for Innovation ; Vol. 14).

Mamali, D., Marinou, E., Sciare, J., Pikridas, M., Kokkalis, P., Kottas, M., Binietoglou, I., Tsekeri, A., Keleshis, C., **Engelmann, R.**, **Baars, H.**, **Ansmann, A.**, Amiridis, V., Russchenberg, H. and Biskos, G. 2018. Vertical profiles of aerosol mass concentration derived by unmanned airborne in situ and remote sensing instruments during dust events. Atmos. Meas. Tech., **11**, 2897-2910. doi:10.5194/amt-11-2897-2018.

Mishra, S. K., Ahlawat, A., Khosla, D., Sharma, C., Prasad, M. V. S. N., Singh, S., Gupta, B., Tulsi, Sethi, D., Sinha, P. R., Ojha, D. K., **Wiedensohler, A.** and Kotnala, R. K. 2018. Experimental investigation of variations in morphology, composition and mixing-state of boundar layer aerosol: A balloon based study over urban environment (New Delhi). Atmos. Environ., **185**, 243-252. doi:10.1016/j.atmosenv.2018.04.053.

Moran-Zuloaga, D., Ditas, F., Walter, D., Saturno, J., Brito, J., Carbone, S., Chi, X., de Angelis, I. H., **Baars, H.**, Godoi, R. H. M., **Heese, B.**, Holanda, B. A., Lavric, J. V., Martin, S. T., Ming, J., Pöhlker, M. L., Ruckteschler,

N., Su, H., Wang, Y., Wang, Q., Wang, Z., Weber, B., Wolff, S., Artaxo, P., Pöschl, U., Andreae, M. O. and Pöhlker, C. 2018. Long-term study on coarse mode aerosols in the Amazon rain forest with the frequent intrusion of Saharan dust plumes. Atmos. Chem. Phys., **18**, 10055-10088. doi:10.5194/acp-18-10055-2018.

Mothes, F., Ifang, S., Gallus, M., Golly, B., Boréave, A., Kurtenbach, R., Kleffmann, J., George, C. and **Herrmann, H.** 2018. Bed flow photoreactor experiments to assess the photocatalytic nitrogen oxides abatement under simulated atmospheric conditions. Appl. Catal. B - Environ., **231**, 161-172. doi:10.1016/j.apcatb.2018.03.010.

Niedermeier, D., Chang, K., Cantrell, W., Chandrakar, K. K., Ciochetto, D. and Shaw, R. A. 2018. Observation of a link between energy dissipation rate and oscillation frequency of the large-scale circulation in dry and moist Rayleigh-Bénard turbulence. Phys. Rev. Fluids, **3**, 083501. doi:10.1103/PhysRevFluids.3.083501.

Nieminen, T., Kerminen, V.-M., Petäjä, T., Aalto, P. P., Arshinov, M., Asmi, E., Baltensperger, U., Beddows, D. C. S., Beukes, J. P., Collins, D., Ding, A., Harrison, R. M., Henzing, B., Hooda, R., Hu, M., Hörrak, U., Kivekäs, N., Komsaare, K., Krejci, R., Kristensson, A., Laakso, L., Laaksonen, A., Leaitch, W. R., Lihavainen, H., Mihalopoulos, N., Németh, Z., Nie, W., O'Dowd, C., Salma, I., Sellegri, K., Svenningsson, B., Swietlicki, E., Tunved, P., Ulevicius, V., Vakkari, V., Vana, M., **Wiedensohler, A.**, Wu, Z., Virtanen, A. and Kulmala, M. 2018. Global analysis of continental boundary layer new particle formation based on long-term measurements. Atmos. Chem. Phys., **18**, 14737-14756. doi:10.5194/acp-18-114737-2018.

Otto, T., **Schaefer, T.** and **Herrmann, H.** 2018. Aqueous-phase oxidation of terpene-derived acids by atmospherically relevant radicals. J. Phys. Chem. A, **122**, 9233-9241. doi:10.1021/acs.jpca.8b08922.

Palacios-Peña, L., Baró, R., Baklanov, A., Balzarini, A., Brunner, D., Forkel, R., Hirtl, M., Honzak, L., López-Romero, J. M., Montávez, J. P., Pérez, J. L., Pirovano, G., San José, R., **Schröder, W.**, Werhahn, J., **Wolke, R.**, Žabkar, R. and Jiménez-Guerrero, P. 2018. An assessment of aerosol optical properties from remote-sensing observations and regional chemistry–climate coupled models over Europe. Atmos. Chem. Phys., **18**, 5021-5043. doi:10.5194/acp-18-5021-2018.

Pandolfi, M., Alados Arboledas, L., Alastuey, A., Andrade, M., Angelov, C., Artiñano, B., Backman, J., Baltensperger, U., Bonasoni, P., Bukowiecki, N., Coen, M. C., Conil, S., Coz, E., Crenn, V., Dudoitis, V., Ealo, M., Eleftheriadis, K., Favez, O., Fetfatzis, P., Fiebig, M., Flentje, H., Ginot, P., Gysel, M., Henzing, B., Hoffer, A., Smejkalova, A. H., Kalapov, I., Kalivitis, N., Kouvarakis, G., Kristensson, A., Kulmala, M., Lihavainen, H., Lunder, C., Luoma, K., Lyamani, H., Marinoni, A., Mihalopoulos, N., Moerman, M., Nicolas, J., O'Dowd, C., Petäjä, T., Petit, J.-E., Pichon, J. M., Prokopciuk, N., Putaud, J.-P., Rodríguez, S., Sciare, J., Sellegri, K., Swietlicki, E., Titos, G., **Tuch, T.**, Tunved, P., Ulevicius, V., Vaishya, A., Vana, M., Virkkula, A., Vratolis, S., Weingartner, E., **Wiedensohler, A.** and Laj, P. 2018. A European aerosol phenomenology – 6: Scattering properties of atmospheric aerosol particles from 28 ACTRIS sites. Atmos. Chem. Phys., **18**, 7877-7911. doi:10.5194/acp-18-7877-2018.

Papagiannopoulos, N., Mona, L., Amodeo, A., D'Amico, G., Claramunt, P. G., Pappalardo, G., Alados-Arboledas, L., Guerrero-Rascado, J. L., Amiridis, V., Kokkalis, P., Apituley, A., **Baars, H.**, **Schwarz, A.**, **Wandinger, U.**, Binietoglou, I., Nicolae, D., Bortoli, D., Comerón, A., Rodríguez-Gómez, A., Sicard, M., Papayannis, A. and Wiegner, M. 2018. An automatic observation-based aerosol typing method for EARLINET. Atmos. Chem. Phys., **18**, 15879-15901. doi:10.5194/acp-18-15879-2018.

Passeport, E., Zhang, N., Wu, L., **Herrmann, H.**, Sherwood Lollar, B. and Richnow, H.-H. 2018. Aqueous photodegradation of substituted chlorobenzenes: Kinetics, carbon istotope fractionation, and reaction mechnisms. Water Res., **135**, 95-103. doi:10.1016/j.watres.2018.02.008.

Radenz, M. and **Bühl, J.** 2018. Software package for added value products from combined measurements of Radar Wind Profiler and Cloud Radar ("Spectra Mole") - Release from 2018-10-05. Zenodo, doi:10.5281/zenodo.1419486.

Radenz, M., **Bühl, J.**, Lehmann, V., Görsdorf, U. and Leinweber, R. 2018. Combining cloud radar and radar wind profiler for a value added estimate of vertical air motion and particle terminal velocity within clouds Atmos. Meas. Tech., **11**, 5925-5940. doi:10.5194/amt-11-5925-2018.

Schaefer, T. and **Herrmann, H.** 2018. Competition kinetics of OH radical reactions with oxygenated organic compounds in aqueous solution: Rate constants and internal optical absorption effects. Phys. Chem. Chem. Phys., **20**, 10939-10948. doi:10.1039/C7CP08571K.

Schepanski, K. 2018. Transport of mineral dust and its impact on climate. Geosciences, **8**, 151 (19 pp). doi:10.3390/geosciences8050151.

Schmale, J., **Henning, S.**, Decesari, S., Henzing, B., Keskinen, H., Sellegri, K., Ovadnevaite, J., Pöhlker, M. L., Brito, J., Bougiatioti, A., Kristensson, A., Kalivitis, N., Stavroulas, I., Carbone, S., Jefferson, A., Park, M.,

Schlag, P., Iwamoto, Y., Aalto, P., Äijälä, M., Bukowiecki, N., Ehn, M., Frank, G., Fröhlich, R., Frumau, A., Herrmann, E., **Herrmann, H.**, Holzinger, R., Kos, G., Kulmala, M., Mihalopoulos, N., Nenes, A., O'Dowd, C., Petäjä, T., Picard, D., Pöhlker, C., Pöschl, U., **Poulain, L.**, Prévôt, A. S. H., Swietlicki, E., Andreae, M. O., Artaxo, P., **Wiedensohler, A.**, Ogren, J., Matsuki, A., Yum, S. S., **Stratmann, F.**, Baltensperger, U. and Gysel, M. 2018. Long-term cloud condensation nuclei number concentration, particle number size distribution and chemical composition measurements at regionally representative observatories. Atmos. Chem. Phys., **18**, 2853-2881. doi:10.5194/acp-18-2853-2018.

Schrödner, R. and **Wolke, R.** 2018. *Modellierung von Luftströmung im Erzgebirge während ausgewählter Zeiträume (Abschlussbericht)*. Sächsischen Landesamtes für Umwelt, Landwirtschaft und Geologie (LfULG) Dresden. 29 p.

Schrödner, R., **Wolke, R.**, **Tilgner, A.**, **van Pinxteren, D.** and **Herrmann, H.** 2018. Modelling multiphase aerosol-cloud processing with the 3-D CTM COSMO-MUSCAT: Application for cloud events during HCCT-2010. *In: C. Mensink and G. Kallos (Eds.), Air pollution modeling and its application XXV : Proceedings of the 35th International Technical Meeting on Air Pollution Modelling and Its Application (Chania, Crete, Greece, 3-7 October 2016)*. Springer International Publishing, Cham, Switzerland, p. 587-592 (Chapter 91). doi:10.1007/978-3-319-57645-9. (Springer Proceedings in Complexity).

Schulz, C., Schneider, J., Holanda, B. A., Appel, O., Costa, A., de Sá, S. S., Dreiling, V., Fütterer, D., Jurkat-Witschas, T., Klimach, T., Knote, C., Krämer, M., Martin, S. T., **Mertes, S.**, Pöhlker, M. L., Sauer, D., Voigt, C., Walser, A., Weinzierl, B., Ziereis, H., Zöger, M., Andreae, M. O., Artaxo, P., Machado, L. A. T., Pöschl, U., Wendisch, M. and Borrmann, S. 2018. Aircraft-based observations of isoprene-epoxydiol-derived secondary organic aerosol (IEPOX-SOA) in the tropical upper troposphere over the Amazon region. Atmos. Chem. Phys., **18**, 14979-15001. doi:10.5194/acp-18-14979-2018.

Senf, F., Klocke, D. and Brueck, M. 2018. Size-resolved evaluation of simulated deep tropical convection. Mon. Wea. Rev., **146**, 2161-2183.

Slemr, F., Weigelt, A., Ebinghaus, R., Bieser, J., Brenninkmeijer, C. A. M., Rauthe-Schöch, A., **Hermann, M.**, Martinsson, B. G., van Velthoven, P., Bönisch, H., Neumaier, M., Zahn, A. and Ziereis, H. 2018. Mercury distribution in the upper troposphere and lowermost stratosphere according to measurements by the IAGOS-CARIBIC observatory: 2014–2016. Atmos. Chem. Phys., **18**, 12329-12343. doi:10.5194/acp-18-12329-2018.

Stachlewska, I. S., Samson, M., Zawadzka, O., Harenda, K. M., Janicka, L., Poczta, P., Szczepanik, D., **Heese, B.**, Wang, D., Borek, K., Tetoni, E., Proestakis, E., Siomos, N., Nemuc, A., Chojnicki, B. H., Markowicz, K. M., Pietruczuk, A., Szkop, A., **Althausen, D.**, Stebel, K., Schuettemeyer, D. and Zehner, C. 2018. Modification of local urban aerosol properties by long-range transport of biomass burning aerosol. Remote Sens., **10**, 412-439. doi:10.3390/rs10030412.

Stieger, B., **Spindler, G.**, Fahlbusch, B., **Müller, K.**, **Grüner, A.**, **Poulain, L.**, Thöni, L., Seitler, E., Wallasch, M. and **Herrmann, H.** 2018. Measurements of PM_{10} ions and trace gases with the online system MARGA at the research station Melpitz in Germany - A five-year study. J. Atmos. Chem., **75**, 33-70. doi:10.1007/s10874-017-9361-0.

Styler, S. A., Baergen, A. M., Donaldson, D. J. and **Herrmann, H.** 2018. Organic composition, chemistry, and photochemistry of urban film in Leipzig, Germany. ACS Earth Space Chem., **2**, 935-945. doi:10.1021/acsearthspacechem.8b00087.

Tatzelt, C., **Henning, S.**, **Welti, A.**, Baccarini, A., Gysel, M., Rosenfeld, D., Schmale, J., Wernli, H. and **Stratmann, F.** 2018. *Case studies concerning the air mass influence on the number concentration of cloud condensation nuclei in the Southern Ocean region during ACE*. 27th International Polar Conference 2018, Rostock, Germany, 25-29 March 2018. Berichte zur Polar- und Meeresforschung ; Reports on Polar and Marine Research ; 716/2018: Polar Systems under Pressure : 27th International Polar Conference, Rostock, 25 - 29 March 2018 (German Society for Polar Research). doi:10.2312/BzPM_0716_2018.

Tegen, I. and **Heinold, B.** 2018. Large-scale modeling of absorbing aerosols and their semi-direct effects. Atmosphere, **9**, 380 (19 p.). doi:10.3390/atmos9100380.

Tegen, I. and **Schepanski, K.** 2018. Climate feedback on aerosol emission and atmospheric concentrations. Curr. Clim. Change Rep., **4**, 1-10. doi:10.1007/s40641-018-0086-1.

Tham, Y. J., Wang, Z., Li, Q., Wang, W., Wang, X., Lu, K., **Ma, N.**, Yan, C., **Kecorius, S.**, **Wiedensohler, A.**, Zhang, Y. and Wang, T. 2018. Heterogeneous N2O5 uptake coefficient and production yield of ClNO2 in polluted northern China: Roles of aerosol water content and chemical composition. Atmos. Chem. Phys., **18**, 13155-13171. doi:10.5194/acp-18-13155-2018.

Appendices: Publications

Tilgner, A. and **Herrmann, H.** 2018. Tropospheric aqueous-phase OH oxidation chemistry: Current understanding, uptake of highly oxidized organics and its effects. *In: S. W. Hunt, A. Laskin, and S. A. Nizkorodov (Eds.), Multiphase environmental chemistry in the atmosphere*. American Chemical Society, Washington, DC, p. 49-85 (Chapter 4). doi:10.1021/bk-2018-1299.ch004. (ACS Symposium Series ; Vol. 1299).

Voigtländer, J., Chou, C., **Bieligk, H.**, **Clauss, T.**, **Hartmann, S.**, **Herenz, P.**, **Niedermeier, D.**, Ritter, G., **Stratmann, F.** and Ulanowski, Z. 2018. Surface roughness during depositional growth and sublimation of ice crystals. Atmos. Chem. Phys., **18**, 13687-13702. doi:10.5194/acp-18-13687-2018.

Wagner, R., **Jähn, M.** and **Schepanski, K.** 2018. Wildfires as a source of airborne mineral dust – revisiting a conceptual model using large-eddy simulation (LES). Atmos. Chem. Phys., **18**, 11863-11884. doi:10.5194/acp-18-11863-2018.

Wang, H., Xiang, Z., **Wang, L.**, Jing, S., Lou, S., Tao, S., Liu, J., Yu, M., Li, L., Lin, L., **Chen, Y.**, **Wiedensohler, A.** and Chen, C. 2018. Emissions of volatile organic compounds (VOCs) from cooking and their speciation: A case study for Shanghai with implications for China. Sci. Total Environ., **621**, 1300-1309. doi:10.1016/j.scitotenv.2017.10.098.

Wang, Y., Wu, Z., **Ma, N.**, Wu, Y., Zeng, L., Zhao, C. and **Wiedensohler, A.** 2018. Statistical analysis and parameterization of the hygroscopic growth of the sub-micrometer urban background aerosol in Beijing. Atmos. Environ., **175**, 184-191. doi:10.1016/j.atmosenv.2017.12.003.

Weger, M., **Heinold, B.**, **Engler, C.**, Schumann, U., Seifert, A., Fößig, R., Voigt, C., **Baars, H.**, Blahak, U., Borrmann, S., Hoose, C., Kaufmann, S., Krämer, M., **Seifert, P.**, **Senf, F.**, Schneider, J. and **Tegen, I.** 2018. The impact of mineral dust on cloud formation during the Saharan dust event in April 2014 over Europe. Atmos. Chem. Phys., **18**, 17545-17572. doi:10.5194/acp-18-17545-2018.

Welti, A., **Müller, K.**, Fleming, Z. L. and **Stratmann, F.** 2018. Concentration and variability of ice nuclei in the subtropical maritime boundary layer. Atmos. Chem. Phys., **18**, 5307-5320. doi:10.5194/acp-18-5307-2018.

Welti, A., **Müller, K.**, Fleming, Z. L. and **Stratmann, F.** 2018. Time series of ice nuclei concentration at Cape Verde. *Data from:* Surface Ocean Processes in the Anthropocene (SOPRAN); CVAO (Cape Verde Atmospheric Observatory). *PANGAEA*, doi:10.1594/PANGAEA.887029.

Wiedensohler, A., Andrade, M., **Weinhold, K.**, **Müller, T.**, **Birmili, W.**, Velarde, F., Moreno, I., Forno, R., Sanchez, M. F., Laj, P., Ginot, P., Whiteman, D. N., Krejci, R., Sellegri, K. and Reichler, T. 2018. Black carbon emission and transport mechanisms to the free troposphere at the La Paz/El Alto (Bolivia) metropolitan area based on the Day of Census (2012). Atmos. Environ., **194**, 158-169. doi:10.1016/j.atmosenv.2018.09.032.

Wiedensohler, A., **Wiesner, A.**, **Weinhold, K.**, **Birmili, W.**, **Hermann, M.**, **Merkel, M.**, **Müller, T.**, **Pfeifer, S.**, **Schmidt, A.**, **Tuch, T.**, Velarde, F., Quincey, P., Seeger, S. and Nowak, A. 2018. Mobility particle size spectrometers: Calibration procedures and measurement uncertainties. Aerosol Sci. Technol., **52**, 146-164. doi:10.1080/02786826.2017.1387229.

Wu, L., Chládková, B., Lechtenfeld, O. J., Lian, S., **Schindelka, J.**, **Herrmann, H.** and Richnow, H. H. 2018. Characterizing chemical transformation of organophosphorus compounds by ^{13}C and ^{2}H stable isotope analysis. Sci. Total Environ., **615**, 20-28. doi:10.1016/j.scitotenv.2017.09.233.

Zhang, D., Wu, L., Yao, J., **Herrmann, H.** and Richnow, H.-H. 2018. Carbon and hydrogen isotope fractionation of phthalate esters during degradation by sulfate and hydroxyl radicals. Chem. Eng. J., **347**, 111-118. doi:10.1016/j.cej.2018.04.047.

Zhang, K., Chai, F. H., Zheng, Z. L., Yang, Q., Zhong, X. C., **Fomba, K. W.** and Zhou, G. Z. 2018. Size distribution and source of heavy metals in particulate matter on the lead and zinc smelting affected area. J. Environ. Sci. (China), **71**, 188-196. doi:10.1016/j.jes.2018.04.018.

Zhang, Y., Su, H., Ma, N., Li, G., **Kecorius, S.**, **Wang, Z.**, Hu, M., Zhu, T., He, K., **Wiedensohler, A.**, Zhang, Q. and Cheng, Y. 2018. Sizing of ambient particles from a single-particle soot photometer measurement to retrieve mixing state of black carbon at a regional site of the North China plain. J. Geophys. Res. - Atmos., **123**, 12778-12795. doi:10.1029/2018JD028810.

Zhao, J., **Weinhold, K.**, **Merkel, M.**, **Kecorius, S.**, **Schmidt, A.**, **Schlecht, S.**, **Tuch, T.**, **Wehner, B.**, Birmili, W. and **Wiedensohler, A.** 2018. Concept of high quality simultaneous measurements of the indoor and outdoor aerosol to determine the exposure to fine and ultrafine particles in private homes. Gefahrst. Reinhalt. L., **78**, 73-78.

Zhu, Y., Yang, L., Chen, J., Kawamura, K., Sato, M., **Tilgner, A.**, **van Pinxteren, D.**, **Chen, Y.**, Xue, L., Wang, X., Simpson, I. J., **Herrmann, H.**, Blake, D. R. and Wang, W. 2018. Molecular distributions of dicarboxylic acids, oxocarboxylic acids and α-dicarbonyls in PM2.5 collected at the top of Mt. Tai, North China, during the wheat burning season of 2014. Atmos. Chem. Phys., **18**, 10741-10758. doi:10.5194/acp-18-10741-2018.

2019

Ahlawat, A., Mishra, S. K., Goel, V., Sharma, C., Singh, B. P. and **Wiedensohler, A.** 2019. Modelling aerosol optical properties over urban environment (New Delhi) constrained with balloon observation. Atmos. Environ., **205**, 115-124. doi:10.1016/j.atmosenv.2019.02.006.

Ahlawat, A., Mishra, S. K., Gumber, S., Goel, V., Sharma, C. and **Wiedensohler, A.** 2019. Performance evaluation of light weight gas sensor system suitable for airborne applications against co-location gas analysers over Delhi. Sci. Total Environ., **697**, 134016 (9 pp). doi:10.1016/j.scitotenv.2019.134016.

Alas, H. D., **Pfeifer, S.**, **Wiesner, A.**, **Wehner, B.**, **Weinhold, K.**, **Merkel, M.**, Löschau, G., Bastian, S., Hausmann, A. and **Wiedensohler, A.** 2019. Representativeness and variability of $PM_{2.5}$ mass concentrations and black carbon near traffic and urban background monitoring stations. Gefahrst. Reinhalt. L., **79**, 217-226.

Andrade, M. d. F., Artaxo, P., El Khouri Miraglia, S. G., Gouveia, N., Krupnick, A. J., Krutmann, J., Landrigan, P. J., Langerman, K., Makonese, T., Mathee, A., Piketh, S., Ritz, B., Saldiva, P. H. N., Samet, J., Schikowski, T., Schneider, A., Smith, K. R., Traidl-Hoffmann, C., **Wiedensohler, A.**, Wright, C., Boyd, D. R., Foltescu, V., Fuller, R., Jarosińska, D., McGlade, J. M., Shindell, D., Barnsley Scheuenstuhl, M. C., Boright, J. P., Bulani, S., Hamburg, M., Happe, K., Nissen, J. and Scheer, I. 2019. Air Pollution and health – A science-policy initiative. Annals of Global Health, **85**, 140 (1-9). doi:10.5334/aogh.2656.

Ansmann, A., Mamouri, R.-E., **Bühl, J.**, **Seifert, P.**, **Engelmann, R.**, **Hofer, J.**, Nisantzi, A., Atkinson, J. D., Kanji, Z. A., Sierau, B., Vrekoussis, M. and Sciare, J. 2019. Ice-nucleating particle versus ice crystal number concentrationin altocumulus and cirrus layers embedded in Saharan dust: A closure study. Atmos. Chem. Phys., **19**, 15087–15115. doi:10.5194/acp-19-15087-2019.

Ansmann, A., Mamouri, R.-E., **Hofer, J.**, **Baars, H.**, **Althausen, D.** and Abdullaev, S. F. 2019. Dust mass, cloud condensation nuclei, and ice-nucleating particle profiling with polarization lidar: Updated POLIPHON conversion factors from global AERONET analysis. Atmos. Meas. Tech., **12**, 4849-4865. doi:10.5194/amt-12-4849-2019.

Baars, H., **Ansmann, A.**, **Ohneiser, K.**, **Haarig, M.**, **Engelmann, R.**, **Althausen, D.**, Hanssen, I., Gausa, M., Pietruczuk, A., Szkop, A., Stachlewska, I. S., Wang, D., Reichardt, J., **Skupin, A.**, Mattis, I., Trickl, T., Vogelmann, H., Navas-Guzmán, F., Haefele, A., Acheson, K., Ruth, A. A., Tatarov, B., Müller, D., Hu, Q., Podvin, T., Goloub, P., Veselovskii, I., Pietras, C., Haeffelin, M., Fréville, P., Sicard, M., Comerón, A., Fernández García, A. J., Molero Menéndez, F., Córdoba-Jabonero, C., Guerrero-Rascado, J. L., Alados-Arboledas, L., Bortoli, D., Costa, M. J., Dionisi, D., Liberti, G. L., Wang, X., Sannino, A., Papagiannopoulos, N., Boselli, A., Mona, L., D'Amico, G., Romano, S., Perrone, M. R., Belegante, L., Nicolae, D., Grigorov, I., Gialitaki, A., Amiridis, V., Soupiona, O., Papayannis, A., Mamouri, R.-E., Nisantzi, A., **Heese, B.**, **Hofer, J.**, Schechner, Y. Y., **Wandinger, U.** and Pappalardo, G. 2019. The unprecedented 2017–2018 stratospheric smoke event: Decay phase and aerosol properties observed with the EARLINET. Atmos. Chem. Phys., **19**, 15183–15198. doi:10.5194/acp-19-15183-2019.

Banks, J. R., **Hünerbein, A.**, **Heinold, B.**, Brindley, H. E., **Deneke, H.** and **Schepanski, K.** 2019. The sensitivity of the colour of dust in MSG-SEVIRI Desert Dust infrared composite imagery to surface and atmospheric conditions. Atmos. Chem. Phys., **19**, 6893-6911. doi:10.5194/acp-19-6893-2019.

Barlakas, V., **Deneke, H.** and **Macke, A.** 2019. *Abschlussbericht: HD(CP)2 II "Niedrige Wolken in klein-skaligen und globalen Modellen (Verbund S2)". Teilprojekt 2: "Evaluierung des Strahlungseffekts mittels Synergie von satelliten- und bodengestützen Beobachtungen".* **BMBF Förderkennzeichen 01LK1504B**. p. 13.

Barthel, S., **Tegen, I.** and **Wolke, R.** 2019. Do new sea spray aerosol source functions improve the results of a regional aerosol model? Atmos. Environ., **198**, 265-278. doi:10.1016/j.atmosenv.2018.10.016.

Berndt, T., Hyttinen, N., **Herrmann, H.** and Hansel, A. 2019. First oxidation products from the reaction of hydroxyl radicals with isoprene for pristine environmental conditions. Communications Chemistry, **2**, Art. No.: 21. doi:10.1038/s42004-019-0120-9.

Berndt, T., Scholz, W., Mentler, B., Fischer, L., **Hoffmann, E. H.**, **Tilgner, A.**, Hyttinen, N., Prisle, N. L., Hansel, A. and **Herrmann, H.** 2019. Fast peroxy radical isomerization and OH recycling in the reaction of OH radicals with dimethyl sulfide. J. Phys. Chem. Lett., **10**, 6478-6483. doi:10.1021/acs.jpclett.9b02567.

Bianchi, F., Kurtén, T., Riva, M., Mohr, C., Rissanen, M. P., Roldin, P., **Berndt, T.**, Crounse, J. D., Wennberg, P. O., Mentel, T. F., Wildt, J., Junninen, H., Jokinen, T., Kulmala, M., Worsnop, D. R., Thornton, J. A., Donahue, N., Kjaergaard, H. G. and Ehn, M. 2019. Highly Osygenated Organic Molecules (HOM) from gas-phase autoxidation involving peroxy radicals: A key contributor to atmospheric aerosol. Chem. Rev., **119**, 3472-3509. doi:10.1021/acs.chemrev.8b00395.

Appendices: Publications

Bräuer, P., Mouchel-Vallon, C., **Tilgner, A.**, **Mutzel, A.**, **Böge, O.**, **Rodigast, M.**, **Poulain, L.**, **van Pinxteren, D.**, **Wolke, R.**, Aumont, B. and **Herrmann, H.** 2019. Development of a protocol for the auto-generation of explicit aqueous-phase oxidation schemes of organic compounds. Atmos. Chem. Phys., **19**, 9209-9239. doi:10.5194/acp-19-9209-2019.

Brüggemann, M., **van Pinxteren, D.**, Wang, Y., Yu, J. Z. and **Herrmann, H.** 2019. Quantification of known and unknown terpenoid organosulfates in PM10 using untargeted LC–HRMS/MS: Contrasting summertime rural Germany and the North China Plain. Environ. Chem., **16**, 333-346. doi:10.1071/EN19089.

Bühl, J., **Seifert, P.**, **Radenz, M.**, **Baars, H.** and **Ansmann, A.** 2019. Ice crystal number concentration from lidar, cloud radar and radar wind profiler measurements. Atmos. Meas. Tech., **12**, 6601–6617. doi:10.5194/amt-12-6601-2019.

Chauvigné, A., Aliaga, D., Sellegri, K., Montoux, N., Krejci, R., Močnik, G., Moreno, I., **Müller, T.**, Pandolfi, M., Velarde, F., **Weinhold, K.**, Ginot, P., **Wiedensohler, A.**, Andrade, M. and Laj, P. 2019. Biomass burning and urban emission impacts in the Andes Cordillera region based on in situ measurements from the Chacaltaya observatory, Bolivia (5240 m a.s.l.). Atmos. Chem. Phys., **19**, 14805–14824. doi:10.5194/acp-19-14805-2019.

Chen, J., Fullam, D. P., Yu, S., **Böge, O.**, **Le, P. H.**, **Herrmann, H.** and Venables, D. S. 2019. Improving the accuracy and precision of broadband optical cavity measurements. Spectrochim. Acta Part A, **218**, 178-183. doi:10.1016/j.saa.2019.04.015.

Chen, Y., Xu, L., Humphry, T., Hettiyadura, A. P. S., Ovadnevaite, J., **Huang, S.**, **Poulain, L.**, Schroder, J. C., Campuzano-Jost, P., Jimenez, J. L., **Herrmann, H.**, O'Dowd, C., Stone, E. A. and Ng, N. L. 2019. Response of the aerodyne aerosol mass spectrometer to inorganic sulfates and organosulfur compounds: Applications in field and laboratory measurements. Environ. Sci. Technol., **53**, 5176-5186. doi:10.1021/acs.est.9b00884.

Düsing, S., **Wehner, B.**, **Müller, T.**, Stöcker, A. and **Wiedensohler, A.** 2019. The effect of rapid relative humidity changes on fast filter-based aerosol-particle light-absorption measurements: Uncertainties and correction schemes. Atmos. Meas. Tech., **12**, 5879-5895. doi:10.5194/amt-12-5879-2019.

Egerer, U., Gottschalk, M., **Siebert, H.**, Ehrlich, A. and Wendisch, M. 2019. The new Beluga setup for collocated turbulence and radiation measurements using a tethered balloon: First applications in the cloudy Arctic boundary layer. Atmos. Meas. Tech., **12**, 4019–4038. doi:10.5194/amt-12-4019-2019.

Ehrlich, A., Wendisch, M., Lüpkes, C., Buschmann, M., Bozem, H., Chechin, D., Clemen, H.-C., Dupuy, R., Eppers, O., Hartmann, J., Herber, A., Jäkel, E., Järvinen, E., Jourdan, O., **Kästner, U.**, Kliesch, L.-L., Köllner, F., Mech, M., **Mertes, S.**, Neuber, R., Ruiz-Donoso, E., Schnaiter, M., Schneider, J., Stapf, J. and Zanatta, M. 2019. A comprehensive in situ and remote sensing data set from the Arctic CLoud Observations Using airborne measurements during polar Day (ACLOUD) campaign. Earth Syst. Sci. Data, **11**, 1853–1881. doi:10.5194/essd-11-1853-2019.

Felber, T., **Schaefer, T.** and **Herrmann, H.** 2019. OH-initiated oxidation of Imidazoles in tropospheric aqueous-phase chemistry. J. Phys. Chem. A, **123**, 1505-1513. doi:10.1021/acs.jpca.8b11636.

Feuerstein, S. and **Schepanski, K.** 2019. Identification of dust sources in a Saharan dust hot-spot and their implementation in a dust-emission model. Remote Sens., **11**, 4-27. doi:10.3390/rs11010004.

Formenti, P., D'Anna, B., Flamant, C., Mallet, M., Piketh, S. J., **Schepanski, K.**, Waquet, F., Auriol, F., Brogniez, G., Burnet, F., Chaboureau, J.-P., Chauvigné, A., Chazette, P., Denjean, C., Desboeufs, K., Doussin, J.-F., Enguidi, N., **Feuerstein, S.**, Gaetani, M., Giorio, C., Klopper, D., Mallet, M. D., Nabat, P., Monod, A., Solmon, F., Mamwoonde, A., Chikwililwa, C., Mushi, R., Welton, E. J. and Holben, B. 2019. The aerosols, radiation and clouds in southern Africa field campaign in Namibia: Overview, illustrative observations, and way forward. Bull. Amer. Meteor. Soc., **100**, 1277–1298. doi:10.1175/BAMS-D-17-0278.1.

Foth, A., **Kanitz, T.**, **Engelmann, R.**, **Baars, H.**, **Radenz, M.**, **Seifert, P.**, Barja, B., Fromm, M., Kalesse, H. and **Ansmann, A.** 2019. Vertical aerosol distribution in the southern hemispheric midlatitudes as observed with lidar in Punta Arenas, Chile (53.2° S and 70.9° W), during ALPACA. Atmos. Chem. Phys., **19**, 6217-6233. doi:10.5194/acp-19-6217-2019.

Freney, E., Zhang, Y., Croteau, P., Amodeo, T., Williams, L., Truong, F., Petit, J.-E., Sciare, J., Sarda-Estève, R., Bonnaire, N., Arumae, T., Aurela, M., Bougiatioti, A., Mihalopoulos, N., Coz, E., Artinano, B., Crenn, V., Elste, T., Heikkinen, L., **Poulain, L.**, **Wiedensohler, A.**, **Herrmann, H.**, Priestman, M., Alastuey, A., Stavroulas, I., Tobler, A., Vasilescu, J., Zanca, N., Canagaratna, M., Carbone, C., Flentje, H., Green, D., Maasikmets, M., Marmureanu, L., Minguillón, M. C., Prevot, A. S. H., Gros, V., Jayne, J. and Favez, O. 2019. The second ACTRIS inter-comparison (2016) for Aerosol Chemical Speciation Monitors (ACSM): Calibration protocols and instrument performance evaluations. Aerosol Sci. Technol., **53**, 830-842. doi:10.1080/02786826.2019.1608901.

Gong, X., **Wex, H.**, **Müller, T.**, **Wiedensohler, A.**, Höhler, K., Kandler, K., **Ma, N.**, Dietel, B., Schiebel, T., Möhler, O. and **Stratmann, F.** 2019. Characterization of aerosol properties at Cyprus, focusing on cloud condensation nuclei and ice-nucleating particles. Atmos. Chem. Phys., **19**, 10883–10900. doi:10.5194/acp-19-10883-2019.

Gong, X., **Wex, H.**, **Müller, T.**, **Wiedensohler, A.**, Höhler, K., Kandler, K., **Ma, N.**, Dietel, B., Schiebel, T., Möhler, O. and **Stratmann, F.** 2019. Ground-based measurements on aerosol particles at Paphos, Cyprus, in March-April 2017. *Data from:* Absorbing aerosol layers in a changing climate: aging, lifetime and dynamics (A-LIFE); Paphos_ALife. *PANGAEA*, doi:10.1594/PANGAEA.904758.

Gong, X., **Wex, H.**, **van Pinxteren, M.**, **Triesch, N.**, **Fomba, K. W.**, Lubitz, J., Stolle, C., Robinson, T.-B., **Müller, T.**, **Herrmann, H.** and **Stratmann, F.** 2019. Ice nucleating particles measured in air, cloud and seawater at the Cape Verde Atmospheric Observatory (CVAO). *Data from:* Marine biological production, organic aerosol particles and marine clouds: A process chain (MarParCloud). *PANGAEA*, doi:10.1594/PANGAEA.906946.

Haarig, M., Walser, A., **Ansmann, A.**, Dollner, M., **Althausen, D.**, Sauer, D., Farrell, D. and Weinzierl, B. 2019. Profiles of cloud condensation nuclei, dust mass concentration, and ice-nucleating-particle-relevant aerosol properties in the Saharan Air Layer over Barbados from polarization lidar and airborne in situ measurements. Atmos. Chem. Phys., **19**, 13773–13788. doi:10.5194/acp-19-13773-2019.

Hartmann, M., Blunier, T., Brügger, S. O., Schmale, J., Schwikowski, M., Vogel, A., **Wex, H.** and **Stratmann, F.** 2019. Variation of ice nucleating particles in the European Arctic over the last centuries. Geophys. Res. Lett., **46**, 4007-4016. doi:10.1029/2019GL082311.

Hartmann, M., Blunier, T., Brügger, S. O., Schmale, J., Schwikowski, M., Vogel, A., **Wex, H.** and **Stratmann, F.** 2019. Measurements of Ice Nucleating Particles in ice core samples from Lomonosovfonna (Svalbard) and Summit (Greenland). *Data from:* Arctic Amplification (AC3). *PANGAEA*, doi:10.1594/PANGAEA.899048.

Hartmann, M., **Jentzsch, C.**, **Wex, H.** and **Stratmann, F.** 2019. Airborne Ice Nucleating Particle (INP) measurements in the Arctic during PAMARCMiP 2018. *Data from:* Arctic Amplification (AC3). *Leibniz-Institut für Troposphärenforschung e.V., Leipzig, PANGAEA*, doi:10.1594/PANGAEA.899635.

He, L., **Schaefer, T.**, **Otto, T.**, Kroflič, A. and **Herrmann, H.** 2019. Kinetic and theoretical study of the atmospheric aqueous-phase reactions of OH radicals with Methoxyphenolic compounds. J. Phys. Chem. A, **123**, 7828-7838. doi:10.1021/acs.jpca.9b05696.

Heikenfeld, M., Marinescu, P. J., Christensen, M., Watson-Parris, D., **Senf, F.**, van den Heever, S. C. and Stier, P. 2019. tobac 1.2: towards a flexible framework for tracking and analysis of clouds in diverse datasets. Geosci. Model Dev., **12**, 4551-4570. doi:10.5194/gmd-12-4551-2019.

Hellmuth, O., Schmelzer, J. W. P. and Feistel, R. 2019. Ice-crystal nucleation in water: Thermodynamic driving force and surface tension. Part I: Theretical foundation. Entropy, **20**, Art.-No. 50. doi:10.3390/e22010050.

Herenz, P., **Wex, H.**, Mangold, A., Laffineur, Q., Gorodetskaya, I. V., Fleming, Z. L., Panagi, M. and **Stratmann, F.** 2019. CCN measurements at the Princess Elisabeth Antarctica research station during three austral summers. Atmos. Chem. Phys., **19**, 275-294. doi:10.5194/acp-19-275-2019.

Hiranuma, N., Adachi, K., Bell, D. M., Belosi, F., Beydoun, H., Bhaduri, B., Bingemer, H., Budke, C., Clemen, H.-C., Conen, F., Cory, K. M., Curtius, J., DeMott, P. J., Eppers, O., **Grawe, S.**, **Hartmann, S.**, Hoffmann, N., Höhler, K., Jantsch, E., Kiselev, A., Koop, T., Kulkarni, G., Mayer, A., Murakami, M., Murray, B. J., Nicosia, A., Petters, M. D., Piazza, M., Polen, M., Reicher, N., Rudich, Y., Saito, A., Santachiara, G., Schiebel, T., Schill, G. P., Schneider, J., Segev, L., Stopelli, E., Sullivan, R. C., Suski, K., Szakáll, M., Tajiri, T., Taylor, H., Tobo, Y., Ullrich, R., Weber, D., **Wex, H.**, Whale, T. F., Whiteside, C. L., Yamashita, K., Zelenyuk, A. and Möhler, O. 2019. A comprehensive characterization of ice nucleation by three different types of cellulose particles immersed in water. Atmos. Chem. Phys., **19**, 4823-4849. doi:10.5194/acp-19-4823-2019.

Hoffmann, E. H., **Tilgner, A.**, **Vogelsberg, U.**, **Wolke, R.** and **Herrmann, H.** 2019. Near-explicit multiphase modeling of halogen chemistry in a mixed urban and maritime coastal area. ACS Earth Space Chem., **3**, 2452-2471. doi:10.1021/acsearthspacechem.9b00184.

Hoffmann, E. H., **Tilgner, A.**, **Wolke, R.** and **Herrmann, H.** 2019. Enhanced chlorine and bromine atom activation by hydrolysis of halogen nitrates from marine aerosols at polluted coastal areas. Environ. Sci. Technol., **53**, 771-778. doi:10.1021/acs.est.8b05165.

Jimenez, C., **Ansmann, A.**, **Engelmann, R.**, **Haarig, M.**, Schmidt, J. and **Wandinger, U.** 2019. Polarization lidar: An extended three-signal calibration approach. Atmos. Meas. Tech., **12**, 1077-1093. doi:10.5194/amt-12-1077-2019.

Appendices: Publications

Karl, M., Leck, C., Mashayekhy Rad, F., Bäcklund, A., Lopez-Aparicio, S. and **Heintzenberg, J.** 2019. New insights in sources of the sub-micrometre aerosol at Mt. Zeppelin observatory (Spitsbergen) in the year 2015. Tellus B, **71**, 1-29. doi:10.1080/16000889.2019.1613143.

Karpińska, K., Bodenschatz, J. F. E., Malinowski, S. P., Nowak, J. L., Risius, S., **Schmeissner, T.**, Shaw, R. A., **Siebert, H.**, Xi, H., Xu, H. and Bodenschatz, E. 2019. Turbulence-induced cloud voids: observation and interpretation. Atmos. Chem. Phys., **19**, 4991-5003. doi:10.5194/acp-19-4991-2019.

Kecorius, S., **Madueño, L.**, Löndahl, J., Vallar, E., Galvez, M. C., Idolor, L. F., Gonzaga-Cayetano, M., **Müller, T.**, **Birmili, W.** and **Wiedensohler, A.** 2019. Respiratory tract deposition of inhaled roadside ultrafine refractory particles in a polluted megacity of South-East Asia. Sci. Total Environ., **663**, 265-274. doi:10.1016/j.scitotenv.2019.01.338.

Kecorius, S., **Vogl, T.**, Paasonen, P., Lampilahti, J., Rothenberg, D., **Wex, H.**, **Zeppenfeld, S.**, **van Pinxteren, M.**, **Hartmann, M.**, **Henning, S.**, **Gong, X.**, **Welti, A.**, Kulmala, M., **Stratmann, F.**, **Herrmann, H.** and **Wiedensohler, A.** 2019. New particle formation and its effect on cloud condensation nuclei abundance in the summer Arctic: A case study in the Fram Strait and Barents Sea. Atmos. Chem. Phys., **19**, 14339-14364. doi:10.5194/acp-19-14339-2019.

Kraas, F., Hackenbroch, K., Sterly, H., **Heintzenberg, J.**, Herrle, P. and Kreibich, V. (Eds.) 2019. Megacities - Megachallenge : Informal dynamics of global change. Insights from Dhaka, Bangladesh and Pearl River Delta, China, 227 pp., Borntraeger, Stuttgart.

Krause, A., **Zhao, J.** and Birmili, W. 2019. Low-cost sensors and indoor air quality: A test study in three residential homes in Berlin, Germany. Gefahrst. Reinhalt. L., **79**, 87-92.

Lammert, A., Hansen, A., Ament, F., Crewell, S., Dick, G., Grützun, V., Klein-Baltink, H., Lehmann, V., **Macke, A.**, Pospichal, B., Schubotz, W., **Seifert, P.**, Stamnas, E. and Stevens, B. 2019. A standardized atmospheric measurement data archive for distributed cloud and precipitation process-oriented observations in Central Europe. Bull. Amer. Meteor. Soc., **100**, 1299–1314. doi:10.1175/bams-d-18-0174.1.

Lange, R., Dall'Osto, M., **Wex, H.**, Skov, H. and Massling, A. 2019. Large summer contribution of organic biogenic aerosols to Arctic cloud condensation nuclei. Geophys. Res. Lett., **46**, 11500-11509. doi:10.1029/2019GL084142.

Leglise, J., Müller, M., Piel, F., **Otto, T.** and Wisthaler, A. 2019. Bulk organic aerosol analysis by proton-transfer-reaction mass spectrometry: An improved methodology for the determination of total organic mass, O:C and H:C elemental ratios, and the average molecular formula. Anal. Chem., **91**, 12619-12624. doi:10.1021/acs.analchem.9b02949.

Liu, J., Li, S., Zeng, J., Mekic, M., Yu, Z., Zhou, W., Loisel, G., Gandolfo, A., Song, W., Wang, X., Zhou, Z., **Herrmann, H.**, Li, X. and Gligorovski, S. 2019. Assessing indoor gas phase oxidation capacity through real-time measurements of HONO and NOx in Guangzhou, China. Environ. Sci.: Processes Impacts, **21**, 1393-1402. doi:10.1039/C9EM00194H.

Liu, W., Lv, G., Sun, X., **He, L.**, Zhang, C. and Li, Z. 2019. Theoretical study on the reaction of anthracene with sulfate radical and hydroxyl radical in aqueous solution. Ecotox. Environ. Safe, **183**, 109551 (Available online 13 August 2019.). doi:10.1016/j.envpol.2019.109551.

Madueño, L., **Kecorius, S.**, **Birmili, W.**, **Müller, T.**, Simpas, J., Vallar, E., Galvez, M. C., Cayetano, M. and **Wiedensohler, A.** 2019. Aerosol particle and black carbon emission factors of vehicular fleet in Manila, Philippines. Atmosphere, **10**, 603 (15 pp.). doi:10.3390/atmos10100603.

Madueño, L., **Kecorius, S.**, Löndahl, J., **Müller, T.**, **Pfeifer, S.**, **Haudek, A.**, Mardoñez, V. and **Wiedensohler, A.** 2019. A new method to measure real-world respiratory tract deposition of inhaled ambient black carbon. Environ. Pollut., **248**, 295-303. doi:10.1016/j.envpol.2019.02.021.

Marinou, E., Tesche, M., Nenes, A., **Ansmann, A.**, Schrod, J., Mamali, D., Tsekeri, A., Pikridas, M., **Baars, H.**, **Engelmann, R.**, Voudouri, K.-A., Solomos, S., Sciare, J., Groß, S., Ewald, F. and Amiridis, V. 2019. Retrieval of ice-nucleating particle concentrations from lidar observations and comparison with UAV in situ measurements. Atmos. Chem. Phys., **19**, 11315-11342. doi:10.5194/acp-19-11315-2019.

Martinsson, B. G., Friberg, J., Sandvik, O. S., **Hermann, M.**, van Velthoven, P. F. J. and Zahn, A. 2019. Formation and composition of the UTLS aerosol. npj Climate and Atmospheric Science, **2**, Art. Nr. 40. doi:10.1038/s41612-019-0097-1.

Mertes, S., **Kästner, U.** and **Macke, A.** 2019. Airborne in-situ measurements of the aerosol absorption coefficient, aerosol particle number concentration and size distribution of cloud particle residuals and ambient aerosol particles during the ACLOUD campaign in May and June 2017. *Data from:* Arctic Amplification (AC3). *Leibniz-Institut für Troposphärenforschung e.V., Leipzig, PANGAEA*, doi:10.1594/PANGAEA.900403.

Mircea, M., Bessagnet, B., D'Isidoro, M., Pirovano, G., Aksoyoglu, S., Ciarelli, G., Tsyro, S., Manders, A., Bieser, J., Stern, R., Vivanco, M. G., Cuvelier, C., Aas, W., Prévôt, A. S. H., Aulinger, A., Briganti, G., Calori, G., Cappelletti, A., Colette, A., Couvidat, F., Fagerli, H., Finardi, S., Kranenburg, R., Rouïl, L., Silibello, C., **Spindler, G.**, **Poulain, L.**, **Herrmann, H.**, Jimenez, J. L., Day, D. A., Tiitta, P. and Carbone, S. 2019. EURODELTA III exercise: An evaluation of air quality models' capacity to reproduce the carbonaceous aerosol. Atmos. Environ.: X, **2**, 100018. doi:10.1016/j.aeaoa.2019.100018.

Neggers, R., Chylik, J., **Egerer, U.**, **Griesche, H. J.**, Schemann, V., **Seifert, P.**, **Siebert, H.** and **Macke, A.** 2019. Local and remote controls on Arctic mixed-layer evolution. J. Adv. Model. Earth Syst., **11**, 2214-2237. doi:10.1029/2019MS001671.

Neubauer, D., Ferrachat, S., Siegenthaler-Le Drian, C., Stier, P., Partridge, D. G., **Tegen, I.**, Bey, I., Stanelle, T., Kokkola, H. and Lohmann, U. 2019. The global aerosol–climate model ECHAM6.3–HAM2.3 – Part 2: Cloud evaluation, aerosol radiative forcing, and climate sensitivity. Geosci. Model Dev., **12**, 3609-3639. doi:10.5194/gmd-12-3609-2019.

Neubauer, D., Ferrachat, S., Siegenthaler-Le Drian, C., **Stoll, J.**, Folini, D. S., **Tegen, I.**, Wieners, K.-H., Mauritsen, T., Stemmler, I., **Barthel, S.**, Bey, I., Daskalakis, N., **Heinold, B.**, Kokkola, H., Partridge, D., Rast, S., Schmidt, H., Schutgens, N., Stanelle, T., Stier, P., Watson-Parris, D. and Lohmann, U. 2019. HAMMOZ-Consortium MPI-ESM1.2-HAM model output prepared for CMIP6 AerChemMIP ssp370-lowNTCF. *Data from:* Coupled Model Intercomparison Project Phase 6 (CMIP6). *Earth System Grid Federation*, doi:10.22033/ESGF/CMIP6.5040.

Otto, T., **Schaefer, T.** and **Herrmann, H.** 2019. Aqueous-phase oxidation of *cis*-β-isoprene epoxydiol by hydroxyl radicals and its impact on atmospheric isoprene processing. J. Phys. Chem. A, **123**, 10599-10608. doi:10.1021/acs.jpca.9b08836.

Pauly, R. M., Yorks, J. E., Hlavka, D. L., McGill, M. J., Amiridis, V., Palm, S. P., Rodier, S. D., Vaughan, M. A., Selmer, P. A., Kupchock, A. W., **Baars, H.** and Gialitaki, A. 2019. Cloud Aerosol Transport System (CATS) 1064 nm calibration and validation. Atmos. Meas. Tech., **12**, 6241–6258. doi:10.5194/amt-12-6241-2019.

Proestakis, E., Amiridis, V., Marinou, E., Binietoglou, I., **Ansmann, A.**, **Wandinger, U.**, **Hofer, J.**, Yorks, J., Nowottnick, E., Makhmudov, A., Papayannis, A., Pietruczuk, A., Gialitaki, A., Apituley, A., Szkop, A., Muñoz Porcar, C., Bortoli, D., Dionisi, D., **Althausen, D.**, Mamali, D., Balis, D., Nicolae, D., Tetoni, E., Liberti, G. L., **Baars, H.**, Mattis, I., Stachlewska, I. S., Voudouri, K. A., Mona, L., Mylonaki, M., Perrone, M. R., Costa, M. J., Sicard, M., Papagiannopoulos, N., Siomos, N., Burlizzi, P., Pauly, R., **Engelmann, R.**, Abdullaev, S. and Pappalardo, G. 2019. EARLINET evaluation of the CATS Level 2 aerosol backscatter coefficient product. Atmos. Chem. Phys., **19**, 11743-11764. doi:10.5194/acp-19-11743-2019.

Pscheidt, I., **Senf, F.**, Heinze, R., Trömel, S., **Deneke, H.** and Hohenegger, C. 2019. How organized is deep convection over Germany? Q. J. Roy. Meteor. Soc., **145**, 2366-2384. doi:10.1002/qj.3552.

Radenz, M., **Bühl, J.** and **Seifert, P.** 2019. peakTree version of Aug2019. Zenodo, doi:10.5281/zenodo.2577387.

Radenz, M., **Bühl, J.**, **Seifert, P.**, **Griesche, H.** and **Engelmann, R.** 2019. peakTree: a framework for structure-preserving radar Doppler spectra analysis. Atmos. Meas. Tech., **12**, 4813–4828. doi:10.5194/amt-12-4813-2019.

Sandvik, O. S., Friberg, J., Martinsson, B. G., van Velthoven, P. F. J., **Hermann, M.** and Zahn, A. 2019. Intercomparison of *in-situ* aircraft and satellite aerosol measurements in the stratosphere. Sci. Rep., **9**, Art. Nr. 15576. doi:10.1038/s41598-019-52089-6.

Šantl-Temkiv, T., Lange, R., Beddows, D. C. S., Rauter, U., Pilgaard, S., Dall'Osto, M., Gunde-Cimerman, N., Massling, A. and **Wex, H.** 2019. Biogenic sources of ice nucleating particles at the high Arctic site Villum Research Station. Environ. Sci. Technol., **53**, 10580-10590. doi:10.1021/acs.est.9b00991.

Schaap, M., Kranenburg, R., Hendriks, C., Timmermans, R., Thürkow, M., Kirchner, I., **van Pinxteren, D.** and **Herrmann, H.** 2019. *Untersuchung der Herkunft des grenzüberschreitenden Feinstaubtransportes im Osten Deutschlands mit einem Chemie-Transportmodell*. Umweltbundesamt. **Forschungskennzahl [FKZ 3716 51 203 0]**. p. 81.

Schacht, J., **Heinold, B.**, Quaas, J., Backman, J., Cherian, R., Ehrlich, A., Herber, A., Huang, W. T. K., Kondo, Y., Massling, A., Sinha, P. R., Weinzierl, B., Zanatta, M. and **Tegen, I.** 2019. The importance of the representation of air pollution emissions for the modeled distribution and radiative effects of black carbon in the Arctic. Atmos. Chem. Phys., **19**, 11159–11183. doi:10.5194/acp-19-11159-2019.

Schacht, J., **Heinold, B.** and **Tegen, I.** 2019. ECHAM-HAM simulations for evaluation and quantification of BC effects in the Arctic under different emission data sets. *Data from:* Arctic Amplification (AC3); pan-Arctic. *Leibniz-Institut für Troposphärenforschung e.V., Leipzig; PANGAEA*, doi:10.1594/PANGAEA.903547.

Schechner, Y. and **Althausen, D.** 2019. *3D widefield sky scatterer tomography by lidar anchor (Scientific Report)*. German-Israeli Foundation for Scientific Research and Development (GIF). **GIF Grant No: I-1262-401.10/2014**. p. 12.

Schepanski, K. 2019. *Dust at the interface - modelling and remote sensing (Abschließender Sachstandsbericht Leibniz-Wettbewerb)*. Leibniz-Gemeinschaft. **Antragsnummer: P79/2014**. p. 6.

Schubotz, W., Klocke, D., Löhnert, U., **Macke, A.**, Stevens, B. and Wing, A. 2019. An international conference that presents current advances in simulating and observing atmospheric processes (Meeting summeries: UCP2019). Bull. Amer. Meteor. Soc., ES251-ES254. doi:10.1175/BAMS-D-19-0120.1.

Sellegri, K., Rose, C., Marinoni, A., Lupi, A., **Wiedensohler, A.**, Andrade, M., Bonasoni, P. and Laj, P. 2019. New particle formation: A review of ground-based observations at mountain research stations. Atmosphere, **10**, 493 (26 pp.). doi:10.3390/atmos10090493.

Senf, F., Brueck, M. and Klocke, D. 2019. Pair correlations and spatial statistics of deep convection over the Tropical Atlantic. J. Atmos. Sci., **76**, 3211-3228. doi:10.1175/JAS-D-18-0326.1.

Solomos, S., Gialitaki, A., Marinou, E., Proestakis, E., Amiridis, V., **Baars, H.**, Komppula, M. and **Ansmann, A.** 2019. Modeling and remote sensing of an indirect Pyro-Cb formation and biomass transport from Portugal wildfires towards Europe. Atmos. Environ., **206**, 303-315. doi:10.1016/j.atmosenv.2019.03.009.

Spranger, T., **van Pinxteren, D.**, Reemtsma, T., Lechtenfeld, O. J. and **Herrmann, H.** 2019. 2D liquid chromatographic fractionation with ultra-high resolution MS analysis resolves a vast molecular diversity of tropospheric particle organics. Environ. Sci. Technol., **53**, 11353-11363. doi:10.1021/acs.est.9b03839.

Stieger, B., **Spindler, G.**, **van Pinxteren, D.**, **Grüner, A.**, Wallasch, M. and **Herrmann, H.** 2019. Development of an online-coupled MARGA upgrade for the 2 h interval quantification of low-molecular-weight organic acids in the gas and particle phases. Atmos. Meas. Tech., **12**, 281-298. doi:10.5194/amt-12-281-2019.

Sun, J., **Birmili, W.**, **Hermann, M.**, **Tuch, T.**, **Weinhold, K.**, **Spindler, G.**, Schladitz, A., Bastian, S., Löschau, G., Cyrys, J., Gu, J., Flentje, H., Briel, B., Asbach, C., Kaminski, H., Ries, L., Sohmer, R., Gerwig, H., Wirtz, K., Meinhardt, F., Schwerin, A., Bath, O., **Ma, N.** and **Wiedensohler, A.** 2019. Variability of black carbon mass concentrations, sub-micrometer particle number concentrations and size distributions: Results of the German Ultrafine Aerosol Network ranging from city street to High Alpine locations. Atmos. Environ., **202**, 256-268. doi:10.1016/j.atmosenv.2018.12.029.

Tegen, I., Neubauer, D., Ferrachat, S., Siegenthaler-Le Drian, C., Bey, I., Schutgens, N., Stier, P., Watson-Parris, D., Stanelle, T., Schmidt, H., Rast, S., Kokkola, H., Schultz, M., Schroeder, S., Daskalakis, N., **Barthel, S.**, **Heinold, B.** and Lohmann, U. 2019. The global aerosol–climate model ECHAM6.3–HAM2.3 – Part 1: Aerosol evaluation. Geosci. Model Dev., **12**, 1643-1677. doi:10.5194/gmd-12-1643-2019.

Teich, M., **van Pinxteren, D.** and **Herrmann, H.** 2019. A one year study of functionalised medium-chain carboxylic acids in atmospheric particles at a rural site in Germany revealing seasonal trends and possible sources. J. Atmos. Chem., **76**, 115-132. doi:10.1007/s10874-019-09390-5.

Tesche, M., Kolgotin, A., **Haarig, M.**, Burton, S. P., Ferrare, R. A., Hostetler, C. A. and Müller, D. 2019. 3+2+*X*: what is the most useful depolarization input for retrieving microphysical properties of non-spherical particles from lidar measurements using the spheroid model of Dubovik et al. (2006)? Atmos. Meas. Tech., **12**, 4421-4437. doi:10.5194/amt-12-4421-2019.

Toledano, C., Torres, B., Velasco-Merino, C., **Althausen, D.**, Groß, S., Wiegner, M., Weinzierl, B., Gasteiger, J., **Ansmann, A.**, González, R., Mateos, D., Farrel, D., **Müller, T.**, **Haarig, M.** and Cachorro, V. E. 2019. Sun photometer retrievals of Saharan dust properties over Barbados during SALTRACE. Atmos. Chem. Phys., **19**, 14571–14583. doi:10.5194/acp-19-14571-2019.

van Pinxteren, D., **Düsing, S.**, **Wiedensohler, A.** and **Herrmann, H.** 2019. *Einfluss von Wetterlagen und Witterung auf die Stickstoffdioxid-Konzentrationen in der Außenluft 2015 bis 2018*. LfULG. **Vergabe-Nr. Z145/19, Az.: 1-0452/202/28**. p. 89.

van Pinxteren, D., **Mothes, F.**, **Spindler, G.**, **Fomba, K. W.** and **Herrmann, H.** 2019. Trans-boundary PM10: Quantifying impact and sources during winter 2016/17 in eastern Germany. Atmos. Environ., **200**, 119-130. doi:10.1016/j.atmosenv.2018.11.061.

van Pinxteren, M., **Fomba, K. W.**, **van Pinxteren, D.**, **Triesch, N.**, **Hoffmann, E. H.**, Cree, C. H. L., Fitzsimons, M. F., von Tümpling, W. and **Herrmann, H.** 2019. Aliphatic amines at the Cape Verde Atmospheric Observatory: Abundance, origins and sea-air fluxes. Atmos. Environ., **203**, 183-195. doi:10.1016/j.atmosenv.2019.02.011.

Wang, X., Ma, N., Lei, T., **Größ, J.**, Li, G., Liu, F., Meusel, H., Mikhailov, E., **Wiedensohler, A.** and Su, H. 2019. Effective density and hygroscopicity of protein particles generated with spray-drying process. J. Aerosol Sci., **137**, 105441. doi:10.1016/j.aerosci.2019.105441.

Wang, Y., **He, L.**, Lv, G., Liu, W., Liu, J., Ma, X. and Sun, X. 2019. Distribution, transformation and toxicity evaluation of 2,6-Di-tert-butyl-hydroxytotulene in aquatic environment. Environ. Pollut., **255**, 113330 (Available online 30 September 2019.). doi:10.1016/j.envpol.2019.113330.

Wendisch, M., **Macke, A.**, Ehrlich, A., Lüpkes, C., Mech, M., Chechin, D., Dethloff, K., **Barrientos Velasco, C.**, Bozem, H., Brückner, M., Clemen, H.-C., Crewell, S., Donth, T., Dupuy, R., Ebell, K., **Egerer, U.**, **Engelmann, R.**, Engler, C., Eppers, O., Gehrmann, M., **Gong, X.**, Gottschalk, M., Gourbeyre, C., **Griesche, H.**, Hartmann, J., **Hartmann, M.**, **Heinold, B.**, Herber, A., **Herrmann, H.**, Heygster, G., Hoor, P., Jafariserajehlou, S., Jäkel, E., Järvinen, E., Jourdan, O., **Kästner, U.**, **Kecorius, S.**, Knudsen, E. M., Köllner, F., Kretzschmar, J., Lelli, L., Leroy, D., Maturilli, M., Mei, L., **Mertes, S.**, Mioche, G., Neuber, R., Nicolaus, M., Nomokonova, T., Notholt, J., Palm, M., **van Pinxteren, M.**, Quaas, J., Richter, P., Ruiz-Donoso, E., Schäfer, M., **Schmieder, K.**, Schnaiter, M., Schneider, J., Schwarzenböck, A., **Seifert, P.**, Shupe, M. D., **Siebert, H.**, Spreen, G., Stapf, J., **Stratmann, F.**, **Vogl, T.**, **Welti, A.**, **Wex, H.**, **Wiedensohler, A.**, Zanatta, M. and **Zeppenfeld, S.** 2019. The Arctic cloud puzzle: Using ACLOUD/PASCAL multiplatform observations to unravel the role of clouds and aerosol particles in Arctic amplification. Bull. Amer. Meteor. Soc., **100**, 841-871. doi:10.1175/bams-d-18-0072.1, 10.1175/BAMS-D-18-0072.2 (Suppl.).

Wex, H. 2019. *Final report for Research Project 6 (RP 6) within Research Unit INUIT (Ice Nucleation research UnIT, FOR 1525)*. DFG. **WE 4722/1-1, WE 4722/1-2**. p. 13.

Wex, H., Huang, L., Sheesley, R., Bossi, R. and Traversi, R. 2019. Annual concentrations of ice nucleating particles at different Arctic stations. *Data from:* Arctic Amplification (AC3). *PANGAEA*, doi:10.1594/PANGAEA.899701.

Wex, H., Huang, L., Zhang, W., Hung, H., Traversi, R., Becagli, S., Sheesley, R. J., Moffett, C. E., Barrett, T. E., Bossi, R., Skov, H., **Hünerbein, A.**, **Lubitz, J.**, **Löffler, M.**, **Linke, O.**, **Hartmann, M.**, **Herenz, P.** and **Stratmann, F.** 2019. Annual variability of ice-nucleating particle concentrations at different Arctic locations. Atmos. Chem. Phys., **19**, 5293-5311. doi:10.5194/acp-19-5293-2019.

Wiedensohler, A., **Ma, N.**, **Birmili, W.**, **Heintzenberg, J.**, Ditas, F., Andreae, M. O. and Panov, A. 2019. Infrequent new particle formation over the remote boreal forest of Siberia. Atmos. Environ., **200**, 167-169. doi:10.1016/j.atmosenv.2018.12.013.

Wolke, R., **Schrödner, R.** and **Faust, M.** 2019. *Identification of odour sources in the Ore Mountains by COSMO-MUSCAT simulations*. 19th International Conference on Harmonisation within Atmospheric Dispersion Modelling for Regulatory Purposes (HARMO19), 3-6 June 2019, Bruges, Belgium. HARMO http://www.harmo.org/Conferences/Proceedings/_Bruges/publishedSections/H19-027%20Ralf%20Wolke.pdf

Yang, M.-R., Zhou, J., **van Pinxteren, D.**, Cao, M.-Y., Li, M. and Xiao, H. 2019. Characteristics of single aerosol particles during pollution in winter in an urban area of Ningbo, China. Aerosol Air Qual. Res., **19**, 1697-1707. doi:10.4209/aaqr.2019.01.0038.

Yin, Z., **Ansmann, A.**, **Baars, H.**, **Seifert, P.**, **Engelmann, R.**, **Radenz, M.**, **Jimenez, C.**, **Herzog, A.**, **Ohneiser, K.**, **Hanbuch, K.**, Blarel, L., Goloub, P., Dubois, G., Victori, S. and Mauping, F. 2019. Aerosol measurements with a shipborne Sun–sky–lunar photometer and collocated multiwavelength Raman polarization lidar over the Atlantic Ocean. Atmos. Meas. Tech., **12**, 5685-5698. doi:10.5194/amt-12-5685-2019.

Yttri, K. E., Simpson, D., Bergström, R., Kiss, G., Szidat, S., Cebumis, D., Eckhardt, S., Hueglin, C., Nøjgaard, J., K., Perrino, C., Pisso, I., Prevot, A. S. H., Putaud, J.-P., **Spindler, G.**, Vana, M., Zhang, Y.-L. and Aas, W. 2019. The EMEP Intensive Measurement Period campaign, 2008–2009: Characterizing carbonaceous aerosol at nine rural sites in Europe. Atmos. Chem. Phys., **19**, 4211-4233. doi:10.5194/acp-19-4211-2019.

Zeppenfeld, S., **van Pinxteren, M.**, **Hartmann, M.**, Bracher, A., **Stratmann, F.** and **Herrmann, H.** 2019. Glucose as a potential chemical marker for ice nucleating activity in Arctic seawater and melt pond samples. Environ. Sci. Technol., **53**, 8747-8756. doi:10.1021/acs.est.9b01469.

Zhang, K., Shang, X., **Herrmann, H.**, Meng, F., Mo, Z., Chen, J. and Lv, W. 2019. Approaches for identifying PM2.5 source types and source areas at a remote background site of South China in spring. Sci. Total Environ., **691**, 1320-1327. doi:10.1016/j.scitotenv.2019.07.178.

University courses

Lecturer	Course	WS 2017/ 2018	SS 2018	WS 2018/ 2019	SS 2019	WS 2019/ 2020
Ansmann, A. Althausen, D. Seifert, P. Engelmann, R.	Active Remote Measurement in Atmospheric Research (2 sh)	x		x		
	Seminar Active Remote Sensing (2 sh)	x		x		
Ansmann, A. Althausen, D. Seifert, P. Engelmann, R. Baars, H.	Lidar Remote Sensing of the Atmosphere (2sh)					x
	Seminar Lidar Remote Sensing (2 sh)					x
Brüggemann, M.	Advanced studies: Analytics and Spektroscopy (Atmospheric Chemistry)				x	
Herrmann, H.	Basic Atmospheric Chemistry + Exercises (3 sh)		x			x
	Atmospheric Chemistry, the Multiphase System + exercises (3 sh)	x		x		x
	Atmospheric Chemistry Seminar (1 sh)	x	x	x	x	x
	Atmospheric Chemistry Lab Course (1 sh)	x		x		x
	SESAC-Summer-School	x				x
	Organiser of the MARSU Summer School			x		x
Hünerbein, A.	Lecture: Advanced Training Module “Radiation Budget” of the LGS-CAR Graduate School, title: “Ice Nucleation”				x	
Macke, A.	Atmospheric Radiation (1 sh)		x		x	
Macke, A. Deneke, H. (SS18) Hünerbein, A. (SS19)	Satellite Remote Sensing + Exercises (2 sh)		x		x	
Macke, A. Stratmann, F. Niedermeier, D.	Cloud Physics + Exercises (3 sh)		x		x	
Mutzel, A.	Advanced Study Analytics and Spektroscopy		x			
Schepanski, K.	Dust in the Atmosphere (2sh)	x		x		x
	Dust in the Atmosphere Seminar (1sh)	x		x		x
Seifert, P.	Microwave remote sensing					x

Lecturer	Course	WS 2017/ 2018	SS 2018	WS 2018/ 2019	SS 2019	WS 2019/ 2020
Stratmann, F.	Lecture: Advanced Training Module "Ice crystal concentrations" of the LGS-CAR Graduate School, title: "Ice nucleation"		x			
Tegen, I.	Modeling of Atmospheric Trace Substances (2 sh)	x		x		x
	Seminar Modeling of Atmospheric Trace Substances (1 sh)	x		x		x
	Modelling of the Atmosphere (2sh)		x		x	
	Basics of Mesoscale Model Simulations + Exercises (3 sh)		x		x	
	Contribution to modul SQ15 "Energy and Environment", University of Leipzig: "Transport of Atmospheric Pollutants"	x		x		x
Wandinger, U.	Scattering and Atmospheric Optics (2 sh)		x			x
	Seminar Applied Scattering Theory (1 sh)		x			x
	ESA Advanced Courses: "Space Lidars", ESTEC, Noordwijk, The Netherlands 22-24 May 2019, title: "Lidar types and characteristics"				x	
Wiedensohler, A. Stratmann, F. Hermann, M. Müller, T.	Atmospheric Aerosols (2 sh) Master	x				x
	Seminar Atmospheric Aerosols (1 sh)	x				
Wiedensohler, A.	"Atmospheric Aerosol Physics, Measurements, and Sampling Techniques" course, Goa, India	x				
	2nd HAAR Summer School, Messinia, Greece		x			
	14th School on Atmospheric Aerosol Physics, Measurement, and Sampling, Hyytiäla, Finland		x			
van Pinxteren, M.	Guest lecture: Analysis and Spectroscopy: Gas Chromatography, Lecture in an one week course	x		x		x
	Lecturer at the Sino-European Summer School on Atmospheric Chemistry (SESAC 4)					x

Academic degrees

Completed academic qualifications 2018/2019

Academic degree*)	Name	Title	Faculty	Year
Ph. D.	Assmann, D.	On the spatio-temporal distribution of aerosol particles in the upper troposphere and lowermost stratosphere	University of Leipzig, Faculty of Physics and Earth Sciences	2019
	Feuerstein, S.	Alluvial dust sources and their implementation in a dust-emission model	University of Leipzig, Faculty of Physics and Earth Sciences	2019
	Gatzsche, K.	Investigation of gasSOA formation by parcel and 3-D modeling	University of Leipzig, Faculty of Physics and Earth Sciences	2019
	Grawe, S.	Coal fly ash: How sample properties and methodology influence immersion freezing results	University of Leipzig, Faculty of Physics and Earth Sciences	2019
	Haarig, M.	Triple-wavelength polarization lidar observations at Barbados during SALTRACE: Characterization of the optical properties of dust after long-range transport and of pure marine aerosol	University of Leipzig, Faculty of Physics and Earth Sciences	2018
	Herenz, P.	Physical Properties of Arctic and Antarctic Aerosol Particles and Cloud Condensation Nuclei	University of Leipzig, Faculty of Physics and Earth Sciences	2019
	Schmeißner, T.	Exploring mechanisms of large droplet production in trade wind cumuliu	University of Leipzig, Faculty of Physics and Earth Sciences	2018
M.Sc.	Bohrer, J.	Modeling and simulation of atmospheric cloud droplets	Albert-Ludwigs-University Freiburg im Breisgau, Faculty of Mathematics and Physics	2019
	Chevalier, K.	Aerosol processes in the marine boundary layer and free troposphere over the Eastern North Atlantic Ocean during July 2017	University of Leipzig, Faculty of Physics and Earth Sciences	2018
	Herzog, A.	Validation of Aeolus wind and aerosol products with ground-based and shipborne measurements	University of Leipzig, Faculty of Physics and Earth Sciences	2019
	Kessler, D.	Untersuchung der atmosphärischen Hydrolyse von Isoprenepoxydiol	University of Leipzig, Faculty of Chemistry and Mineralogy	2019
	Lemme, A.	Der Vergleich von beobachteten und simulierten Wolkeneigenschaften tropischer Konvektion über dem Atlantik unter Einfluss von Saharaluft	University of Leipzig, Faculty of Physics and Earth Sciences	2018

Academic degree*)	Name	Title	Faculty	Year
M.Sc.	Löffler, M.	Ice Nucleating Particles in the Atlantic Boundary Layer and around Antarctica	University of Leipzig, Faculty of Physics and Earth Sciences	2018
	Lubitz, J.	Untersuchungen zur Immersionsgefriereffizienz von Flugaschepartikeln	University of Leipzig, Faculty of Physics and Earth Sciences	2018
	Lückerath, J.	Vertical aerosol particle exchange in the marine boundary layer estimated from helicopter-borne measurements in the Azores region	University of Bayreuth, Department of Atmospheric Chemistry	2018
	Mewes, S.	Characterization of aerosol properties by lidar measurments at Haifa, Israel	University of Leipzig, Faculty of Physics and Earth Sciences	2018
	Ohneiser, K.	Relationship between aerosol properties and characteristics of supercooled clouds using lidar	University of Leipzig, Faculty of Physics and Earth Sciences	2019
	Schmidtpott, M.	Imidazole in atmosphärischen Partikeln - Untersuchungen ihrer Quellen anhand von Feldproben und Kammerexperimenten	University of Leipzig, Faculty of Chemistry and Mineralogy	2019
	Urbanneck, C.	Retrieval of aerosol optical and microphysical properties in Cyprus during A-LIFE and CyCARE by lidar and closure studies with airborne in-situ measurements - Towards aerosol-cloud interaction investigations	University of Leipzig, Faculty of Physics and Earth Sciences	2018
	Weger, M.	The impact of Saharan desert dust on cloud formation: A regional modelling study	University of Leipzig, Faculty of Physics and Earth Sciences	2018
B.Sc.	Freund, R.	Eiskeime im arktischen Aerosol: Kontrast zwischen Frühjahr und Sommer	University of Leipzig, Faculty of Physics and Earth Sciences	2018
	Estelmann, A. M.	Untersuchung der Kinetik von OH-Radikalen und Triplettzuständen in wässriger Lösung	University of Leipzig, Faculty of Chemistry and Mineralogy	2019
	Schönfeld, P.	Konzeptoptimierung eines Fluggetragenen Aerosolpartikel-Größenspektrometers zum Einsatz auf einem Forschungsflugzeug durch Versuchsaufbau und Belastungstest von Einzelkomponenten	Leipzig University of Applied Sciences	2018

** Habil.: Habilitation, Ph. D.: Doctoral theses, Dipl.: Diploma, M.Sc.: Master of Science, B.Sc.: Bachelor of Science*

Appendices: Academic degrees / Editorships

Summary of completed academic qualifications

Academical degrees	Number		Total
	2018	2019	
Habilitation	0	0	0
Doctoral theses	2	5	7
Master of Science	8	5	13
Bachelor of science	1	2	3

Editorships

Name	Journal
Deneke, H.	Section Editor "Atmospheric Remote Sensing", Remote Sensing
Frey, W.	Associate Editor "Atmospheric Measurement Techniques"
Heinold, B.	Associate Editor "Atmosphere - MDPI"
Herrmann, H.	Associate Editor "Atmospheric Measurement Techniques"
	Editorial Board Member "Atmospheric Pollution Research"
	"Atmospheric Chemistry and Physics", Special Issue Editor (HCCT-2010)
	Editorial Board Member "Aerosol and Air Quality Research" (AAQR)
	International Advisory Board "Environmental Science and Technology"
Macke, A.	Member of the Advisory Board "Meteorologische Zeitschrift"
	Associate Editor "Atmospheric Measurement Techniques"
	Member of Editing Committee "promet"
Schepanski, K.	Associate Editor "Aeolian Research"
Tegen, I.	Associate Editor "Journal of Geophysical Research"
Wandinger, U.	Editorial Board Member "Atmospheric Measurement Techniques"
Wiedensohler, A.	Editorial Board Member "Atmospheric Measurement Techniques"
	Chief Editor "Atmospheric Environment"
van Pinxteren, D.	Scientific Advisory Board of the Journal "Gefahrstoffe, Reinhaltung der Luft"
van Pinxteren, M.	"Atmospheric Chemistry and Physics", Special Issue Editor (MarParCloud)

Awards

Name	Prize	Awarding institution	Comments/Description
H. Herrmann	Double-Hundred Talent Plan	Shangdong University	
R. Wagner	IAC Student Poster Award 2018	AAAR	
H. Wex	BG Outstanding Reviewer Award	Chief Editors of Biogeosciences	outstanding commitment and the high quality of reviews
A. Herzog	Poster Price DACH 2019	DMG	
A. Luda	Sächsischer Geopreis 2018	Landesverband Sachsen des Verbands deutscher Schulgeografen	The award was obtained in the frame of the BELL work of Ardis Luda "Auswertung von Lidar-Messergebnissen zur meridionalen Wolkenverteilung zwischen 54°N und 34°S"

Memberships

Name	Board
Althausen, D.	Commission on Air Pollution Prevention of VDI and DIN - Standards Committee KRdL NA 134-02-01-22 UA "Ground-based remote sensing of meteorological parameters", Department II Environmental Meteorology
Baars, H.	Member of the Aeolus Science and Data Quality Group (Aeolus SAG)
Deneke, H.	Member of the Steering Committee of the BMWi Research Network MetPVNet
	Member of the International Radiation Comission
	Member of the Convection Working Group
	Member of the International Cloud Working Group (ICWG)
Heinold, B.	HAMMOZ Steering Comittee member
Hellmuth, O.	Membership in the International Association for the Properties of Water and Steam (IAPWS), Working Group Thermophysical Properties of Water and Steam (TPWS)
	Member of Leibniz-Sozietät der Wissenschaften zu Berlin e. V.
Hermann, M.	HALO Scientific Steering Committee (WLA)
	Member of the "Stratospheric Sulfur and its Role in Climate" (SSiRC), SPARC initiative planning committee

Appendices: Memberships

Name	Board
Herrmann, H.	Chairman of the working group "Atmospheric Chemistry" in the GDCh-division "Environmental Chemistry and Ecotoxicology (AKAC)"
	DECHEMA/GDCh/ (Bunsengesellschaft Bunsen Society); Gemeinschaftsausschuss "Chemie der Atmosphäre" (Community Committee "Chemistry of the Atmosphere")
	DECHEMA/GDCh/KRdL Division Particulate Matter - Co-Chair
	IUPAC Task Group on Atmospheric Chemical Kinetic Data Evaluation
	Advisory Board Member of ProcessNet-Fachgemeinschaft (Specialist Community) SuPER
	Fellow of International Union of Pure and Applied Chemistry
	National Co-Representative "International Surface Ocean - Lower Atmosphere Study" Projekt (SOLAS)
	Membership of the American Chemical Society (AMC)
	Member of the Second International Indian Ocean Expedition (IIOE-2)
	Distinguished Visiting Professor for Environmental Sciences and Engineering at Shandong University, Qingdao, China
	Professor for Environmental Sciences and Engineering at Fudan University, Shanghai, China
Hünerbein, A.	Member of the International Cloud Working Group (ICWG)
Macke, A.	Member od the Scientific Advisory Board "Meteorologische Zeitschrift"
	Member of the HALO Science Steering Comitee
	Member of the HALO Board of Trusties
	Member of the DFG Senate Commission Oceanography
	Member of the EU Steering Committee of the Leibniz Association
	Member of the DFG Topical Board 313 "Atmosphere and Ocean Research"
	Deputy Chair of Section E of the Leibniz Society
	Member of the Steering Committee of the Leibniz-Research Network "Crisis in a globalized World"
	Member of the Steering Committee of the BMBF Research Network HD(CP)^2
	Member of the Steering Committee Collaborative Research Cluster TR 172 "Arctic Amplification"

Name	Board
Mertes, S.	Member of the DFG-Collaborative Research Centres TR172 "Arctic Amplification: Climate Relevant Atmospheric and SurfaCe Processes, and Feedback Mechanisms (AC)[3]"
	Member of the Science Team of CIRRUS-HL: The airborne experiment on CIRRUS in High Latitudes with the highaltitude long-range research aircraft HALO
Müller, Ke.	Member of the "German Library Association (dbv)"
	Member of the "Professional Association Information Library (BIB)"
Müller T.	VDI-Comission "Assesment of dust pollution on solar energy systems."
Poulain, L.	Management Committee Member for COST-COLOSSAL
Schepanski, K.	Member of Executive Commitee Leibniz Research Alliance "INFECTIONS'21"
	Board member of the International Society for Aeolian Research (ISAR)
	Steering Commitee member of the Leibniz Research Alliance "INFECTIONS'21"
	Steering Commitee AEROCLO-sA
	Management Committee Substitute member for EU COSTaction InDust
Spindler, G.	VDI and DIN - Standards Committee KRdL, member of the working group "Measurement of aerosol particles in the outdoor air"
	Member of the KRdL working group "Spiegelgremium zu CEN/TC 264/WG 35 EC/OC in PM"
Stratmann, F.	Work Package (WP) Leader EU-Projekt EUROCHAMP 2
	Member of the EUROCHAMP 2 User Selection Panel (USP)
Tegen, I.	"SDS-WAS (WMO Sand and Dust Storm Warning Advisory and Assessment System), Member of Steering Committee"
	Member of Scientific Advisory Committee, Science Europe
	HAMMOZ Steering Comittee member
	Member of Management Committee für EU COSTaction 16202 InDust
	Member of the Steering Committee Collaborative Research Cluster TR 172 "Arctic Amplification"
	Steering Commitee member of the Leibniz Research Alliance "INFECTIONS'21"

Appendices: Memberships

Name	Board
Tilgner, A.	Member of the working group NA 134 VDI/DIN-Kommission Reinhaltung der Luft (KRdL) - Normenausschuss NA 134-02-01-08 UA Unterausschuss Umwelmetereologie - Depositionsparameter
van Pinxteren, D.	Member of the European working group CEN/TC 264/WG 44 “Source apportionment”
	Member of the KRdl National Mirror Committee of CEN/TC 264/WG 44 “Source apportionment”
Wandinger, U.	Member of the ESA-JAXA EarthCARE Joint Mission Advisory Group
	Member of the EARLINET Council
	Member Scientific Steering Committee and Work Package Leader EU Project ACTRIS-2
	Member of Executive Board od ACTRIS Prepatory Phase Project and WP Leader
Wehner, B.	Member of VDI/DIN-Kommission Reinhaltung der Luft (KRdL) - subgroup Meteorologische Messungen
	Speaker of the Working Group Chairs within the EAA (European Aerosol Assembly)
	Secretary General of GAeF (Gesellschaft für Aerosolforschung)
Wex, H.	Board-Member of the International Comission on Clouds and Precipitation (ICCP)
Wiedensohler, A.	“Scientific Advisory Group” for aerosols within the “Global Atmosphere Watch” - program of the “Meteorological Organization”
	VDI-Commission “Particle Counting in the Atmosphere”
	Scientific Steering Committee member (SSC) and Work Package (WP) leader of the EU project ACTRIS
	Guest Professor at the “Peking University”, Department of Environmental Science, China
	Head of the World Calibration Center WMO-GAW
	Head of the European Center for Aerosol Calibration (ECAC)
	Member of the Comité Européen de Normalisation, working group “CEN/TC 264/WG 32 Air quality - Determination of the particle number concentration”
	Member of the International Organization for Standardization (ISO), working group “ISO/TC 24/SC 4 particle characterization”
	Member of the International Advisory Board of the Institute of Chemical Process Fundamentals of the Czech Academy of Science and the Academy Council of the Czech Academy of Science

Reviews

Reviews	Number	
	2018	2019
Journals	148	130
Projects	28	14
Others	37	27
Total	214	171

Guest scientists

Name	Dauer	Institution
Manzi, M.	16.11.17 - 16.03.18	Centro de Investigacions en Bionanociencias Buenos Aires, Argentinia
Zhang, Z.	01.01. - 01.07.18	Chinese Academy of Sciences, Beijing, China
Raff, J.	01.01. - 30.06.18	Indiana University, Bloomington, Indiana, USA
Nabil, D.	03.01. - 01.07.18	University of Rabat, Marocco
Schneider, J.	12.01. - 02.02.18	Max Planck Institute for Chemistry, Mainz, Germany
Sayf El Islam, B.	14.01. - 24.06.18	University of Rabat, Marocco
Bingemer, H.	15.01. - 02.02.18	Goethe University Frankfurt, Germany
Kohl, R.	15.01. - 02.02.18	Goethe University Frankfurt, Germany
Hammer, S.	15.01. - 19.01.18	TU Darmstadt, Germany
Clemen, H.-Ch.	15.01. - 26.01.18	Max Planck Institute for Chemistry, Mainz, Germany
Zou, Z.	25.01. - 31.01.18	Aarhus University, Danmark
Kroflic, A.	05.02. - 09.02.18	National Institute of Chemistry, Ljubljana, Slowenia
Desai, N.	14.02. - 09.03.18	Michigan Tech, Houghton, Michigan, USA
Ziogas, K.	25.02. - 30.06.18	Democritus University of Thrace, Greece
Mendes da Costa, A.	01.04. - 31.05.18	Instituto Nacional de Meteorologia e Geofisica, Republic of Cabo Verde
Muscat, R.	03.04. - 29.06.18	University of Malta, Malta
Ren, Y.	16.04. - 30.04.18	Center National De La Recherche Scientifique Orleans, France
Grosselin, B.	16.04. - 21.04.18	Center National De La Recherche Scientifique Orleans, France

Appendices: Guest scientists

Name	Dauer	Institution
Quant, M.	28.05. - 17.08.18	University of Toronto, Canada
Barja, B.	15.06. - 10.07.18	University de Magallanes (UMAG), Chile
Teich, M.	01.07. - 31.08.18	University Fudan, China
Glojek, K.	15.07. - 30.07.18	University of Ljubljana, Slowenia
Apaza, F.	01.08. - 30.09.18	Universidad Mayor de San Andres, La Paz, Bolivia
Pavlica, D. J.	01.08. - 31.10.18	University of Ljubljana, Slowenia
Xiao, H.	12.08. - 15.09.18	Academy of Sciences Xiamen, China
Youwei, H.	12.08. - 15.09.18	Academy of Sciences Xiamen, China
Mateus, L.	10.09.18 - 01.03.19	University of Manizales, Colombia
Markwitz, C.	19.11. - 30.11.18	Georg-August University of Göttingen, Germany
Chen, H.	11.12. - 24.12.18	University Fudan, China
Afchine, A.	14.01. - 25.01.19	Forschungszentrum Jülich GmbH, IEK-7, Germany
Krämer, M.	21.01. - 25.01.19	Forschungszentrum Jülich GmbH, IEK-7, Germany
Nabil, D.	13.02. - 18.08.19	University of Rabat, Marocco
Zhang, J.	19.02. - 22.03.19	University of Cambridge, UK
Steimer, S.	19.02. - 22.03.19	University of Cambridge, UK
Habib, G.	01.03. - 31.08.19	Indian Institute of Technology, India
Arub, Z.	07.03. - 01.05.19	Indian Institute of Technology, India
Heffernan, E.	01.04. - 18.04.19	University College Cork, Ireland
Akther, T.	01.04. - 30.09.19	University of Dhaka, Bangladesh
Dong, Y.	13.04. - 15.06.19	University Qingdao, China
Scholz, W.	23.04. - 21.06.19	University of Innsbruck, Austria
Mentler, B.	23.04. - 21.06.19	University of Innsbruck, Austria
Li, L.	06.05. - 15.06.19	Fundan University, China
Stacewicz, T.	20.05. - 07.06.19	University of Warsaw, Poland
Barja, B.	25.05. - 07.06.19	University of Magallanes, Punta Arenas, Chile
Cordoba, C.	06.06. - 31.08.19	Instituto National de Tecnica Aerospacial, Spain
Raff, J.	16.06. - 06.07.19	Indiana University Bloomington, USA

Name	Dauer	Institution
Perraudin, E.	02.07. - 12.07.19	Universite de Bordeaux, France
Villenave, E.	02.07. - 12.07.19	Universite de Bordeaux, France
Vainiger, A.	08.07. - 12.07.19	Technion, Haifa, Israel
Hashino, T.	31.07. - 03.08.19	Kochi University of Technology, Japan
Brooks, I.	19.08. - 21.08.19	School of Earth & Environment, University of Leeds, UK
Malinowski, S.	19.08. - 24.08.19	University of Warsaw, Poland
Nowak, J.	19.08. - 06.09.19	University of Warsaw, Poland
Matthieu, R.	01.09. - 15.09.19	CNRS - IRCELYON, Paris, France
Song, Y.	01.09. - 31.11.19	College of Environmental and Resource Science, China
Kahn, R.	13.09. - 14.09.19	NASA Goddard Space Flight Center, Greenbelt, USA
Weinzierl, B.	17.09. - 24.09.19	University of Vienna, Austria
Sarang, K.	23.09. - 23.12.19	Environmental Chemistry Group Instytut Chemii Fizycznej, Warzaw, Poland
Rami, Y.	30.10. - 12.11.19	Pandit Deendyal Petroleum University, Gandhinagar, India
Hantschke, L.	04.11. - 15.11.19	Forschungszentrum Jülich GmbH, Germany
Loulli, M.	26.11. - 06.12.19	Cyprus University of Technology Limassol (CUT-TEPAK), Cyprus
Ellouzi, I.	01.12.19 - 31.01.20	University of Rabat, Marocco
Tukkainen, S.	02.12. - 05.12.19	Finnish Meteorological Institute, Helsinki, Finland

Visits of TROPOS scientists

Name	Period of stay	Institution
Macke, A.	02.01. - 02.04.18	University of Auckland, New Zeeland
Poulain, L.	19.02. - 02.03.18	Paul Sherrer Institut (PSI), Switzerland
Herrmann, H.	19.03. - 29.03.18	Shandong University (SDU), Qingdao, China
Herrmann, H.	13.05. - 18.05.18	Shandong University (SDU), Qingdao, China
Schepanski, K.	25.05. - 01.06.18	Loughborough University, UK

Appendices: Visits of TROPOS scientists / Meetings

Name	Period of stay	Institution
Herrmann, H.	05.07. - 19.07.18	Shandong University (SDU), Qingdao, China
Herrmann, H.	18.09. - 22.09.18	Shandong University (SDU), Qingdao, China
Herrmann, H.	23.10. - 09.11.18	Shandong University (SDU), Qingdao, China
Mutzel, A.	04.11. - 09.11.18	Weizmann Institute, Israel
Radenz, M.	18.11. - 18.01.18	University of Magallanes, Punta Arenas, Chile
Schepanski, K.	01.05. - 31.08.19	University of Maryland, College Park, MD, USA
Deneke, H.	20.05. - 26.09.19	Cooperative Institute for Meteorological Satellite Studies, University of Wisconsin/Madison, USA
Fomba, K. W.	10.06. - 12.07.19	Gobabeb training and research center,Gobabeb, Namibia
Tegen, I.	08.07. - 12.07.19	University of Vienna, Austria
Felber, T.	27.07. - 24.08.19	University of Colorado Boulder, Colorado, USA
Wen, L.	05.11. - 29.11.19	Laboratoire Interuniversitaire des Systèmes Atmosphériques (LISA), Paris, France
van Pinxteren, D.	25.11. - 01.12.19	University of the Witwatersrand, Johannesburg, South Afrika
Schaefer, T.	02.12. - 10.12.19	Shandong University (SDU), Qingdao, China
Seifert, P.	05.12.-12.12.19	University of Magallanes, Punta Arenas, Chile

Meetings

Meetings	Date	national/ international	number of participants
IAGOS-CARIBIC Workshop, Leipzig	31.01. - 02.02.18	national	28
3rd Leibniz MMS Days, Leipzig	28.02. - 02.03.18	national	51
2018 Annual Meeting of the German National Committee of the “International Association for the Properties of Water and Stream”, Prague, Czech Republic	09.03.18	national	24
12th HAMMOZ Annual Workshop, Leipzig	22.03. - 23.03.18	international	32

Meetings	Date	national/ international	number of participants
Plenary Assembly of the Leibniz Research Network INFECTIONS‘21, Leipzig	13.06.18	national	32
INFECTIONS‘21 Symposium: Interdisciplinary approaches to infectious disease research, Leipzig	14.06. - 15.06.18	international	51
MarParCloud Annual Meeting, Warnemünde	27.06.18	national	15
EVAA (Experimental Validation and Assimilation of Aeolus observations) Kick-off, Leipzig	26.07.18	national	13
JCS Workshop on Relative Humidity, “17th International Conference on the Properties of Water and Steam”, Prague, Czech Republic	02.09. - 06.09.18	international	20
General meeting of the FG Environmental Chemistry and Ecotoxicology at the conference “Environment 2018”, Münster	10.09.18	national	25
16th Workshop on Atmospheric Chemistry and Air Quality: Progress, Challenges, and Multiphase Aspects, Leipzig	09.10. - 10.10.18	international	35
“Synergy of physical, biological, and biogeochemical Arctic observations - From recent Arctic expeditions towards MOSAiC” (SynArc), Delmenhorst	22.10. - 24.10.18	international	41
Project Meeting WTimpact, Leipzig	10.12. - 11.12.18	international	21
AC³ PI meeting, Bremen	15.01. - 17.01.19	national	ca. 30
Intercomparison exercise WG3 + Meeting, Leipzig	16.01.19	international	27
MarParCloud Annual Meeting, Wilhelmshaven	21.05.19	national	12
AC³ PI trial evaluation, Leipzig	05.09. - 06.09.19	national	ca. 70
AC³ PI trial evaluation, Leipzig	11.09. - 12.09.19	national	ca. 70
18th World Clean Air Congress WCAC, Istanbul	23.09. - 27.09.19	international	100
EXCELSIOR Kickoff, Limassol, Cyprus	20.11. - 23.11.19	international	40
Turning mobility around for climate protection: battery or fuel cell - or “diesel”? Frankfurt (Main)	04.12.19	national	70
ACTRIS-D Kickoff Meeting	05.12. - 06.12.19	national	42

International and national field campaigns

Campaign	Project partner
Aerosol measurements at the Atlas mountains, Ifrane, Morocco TROPOS: ACD*	Mohammed V University in Rabat, Morocco; ICARE, IRCELYON, France
ALADINA Ny-Alesund Identification and characterization of new particle formation events in the Arctic boundary layer in Ny-Alesund TROPOS: ExAWoMp**	Technical University Braunschweig; University Tübingen; Alfred-Wegener-Institute for Polar and Marine Research, Germany; CNR Italy, University Stockholm, Sweden; University Helsinki, Finland
BC Berlin TROPOS: ExAWoMp, ACD	German Environment Agency, Senatsverwaltung Berlin, Germany; TNO, The Netherlands
CHARON (ACTRIS TNA) TROPOS: ACD	Ionicon, University Innsbruck, Austria; University Oslo, Norway
CLOUDNET (permanent experiment) Cloud Measurement Network Leipzig, Germany TROPOS: Remote Sensing Dept.	CLOUDNET Consortium
CyCARE (Cyprus Clouds, Aerosols, and Rain Experiment) TROPOS: Remote Sensing Dept.	Cyprus University of Technology, Limassol, Cyprus
DACAPO-PESO (Dynamics, Aerosol, Cloud and Precipitation Observations in the Pristine Environment of the Southern Ocean) TROPOS: Remote Sensing Dept.	University de Magallanes (UMAG), Chile; Leipzig Institute for Meteorology (LIM), Germany
EARLINET (permanent experiment) European Aerosol Research Lidar Network Leipzig, Germany TROPOS: Remote Sensing Dept.	EARLINET Consortium
Exploring performance of the Fast Infrared Hygrometer across the range of environmental conditions TROPOS: ExAWoMp	University of Warsaw, Poland
Exploring the limits of the Michigan Technological University holographic droplet detection system HoloPi TROPOS: ExAWoMp	Michigan Tech University, Houghton, USA
Formation and Properties of highly oxidized multifunctional compounds TROPOS: ACD	Weizmann Institute Rehevot, Israel

Campaign	Project partner
Gif-Projekt: 3D-Widefield Sky Scatterer Tomography by Lidar Anchor TROPOS: Remote Sensing Dept.	Technion University, Haifa, Israel
GUAN German Ultrafine Aerosol Network TROPOS: ExAWoMp, ACD	German Federal Environmental Agency Langen; German Research Center for Environmental Health, Munich; Saxon State Ministry of the Environment and Agriculture, Dresden; Institute of Energy and Environmental Technology e.V. (IUTA), Duisburg; DWD Hohenpeißenberg, Germany; ISSEP, Liège, Belgium
Hera4Halo PamArcMip-campaign March/April 2018: Testing of the sampler concerning the physical and chemical characterization of ice nucleating aerosol particles with HALO TROPOS: ExAWoMp; ACD	HALO Consortium; Alfred Wegener Institute, Germany; Aarhus University, Denmark
Hera4Halo PICNIC; INP comparison campaign on Puy de Dome TROPOS: ExAWoMp	University of Frankfurt, Karlsruhe Insitute of Technology, Germany; Colorado State University, Michigan Tech University, USA; University of Gothenburg, Sweden; University of Clerment-Ferrand, France
IAGOS-CARIBIC (monthly intercontinental measurement flights) Civil Aircraft for Remote Sensing and In situ measurement in Tropospheric and Lower Stratosphere based on the Instrumentation Container Concept TROPOS: ExAWoMp	CARIBIC Consortium
La Paz and El Alto mobile air quality measurement campaign Bolivia TROPOS: ExAWoMp	Universidad Mayor de San Andrés, La Paz, Bolivia
Low Emission Zone Leipzig TROPOS: ExAWoMp	Saxon State Ministry of the Environment and Agriculture, Dresden, Germany
MARSU Marine Atmospheric Sciences Unravel Remote vs. Urban pollution TROPOS: ACD	CNRS, ICARE, ICELYON, France; Mohamed V University of Rabat, Morocco; University of Fudan, China; PMI-Mainz, Germany
MetPVNet Development of innovative satellite based methods for improved forecasts of PV-yield, 1st field campaign TROPOS: Remote Sensing Dept.	10 national partner
MetPVNet Development of innovative satellite based methods for improved forecasts of PV-yields, 2nd field campaign. TROPOS: Remote Sensing Dept.	10 national partner

Appendices: International and national field campaigns

Campaign	Project partner
MOSAiC Multidisciplinary drifting Observatory for the Study of Arctic Climate TROPOS: all departments	Alfred-Wegener Institute (AWI), Bremerhaven, Germany
NIXE-CAPS at LACIS-T TROPOS: ExAWoMp	Forschungszentrum Jülich GmbH, IEK-7, Germany
OCEANET: PS113 Atlantic transect on Polarstern; Bremerhaven - Cape Town TROPOS: Remote Sensing Dept.	Alfred-Wegener Institute (AWI), Bremerhaven, Germany
OCEANET: PS116 Atlantic transect on Polarstern; Punta Arenas - Bremerhaven TROPOS: Remote Sensing Dept.	Alfred-Wegener Institute (AWI), Bremerhaven, Germany
PARAMOUNT: Laboratory studies for the production of aerosol particle organic matter in clouds at the CESAM cloud chamber in Paris TROPOS: ACD, ExaWomp	Laboratoire Interuniversitaire des Systèmes Atmosphériques (LISA) Paris; Laboratoire de Chimie de l'Environnement (LCE) Marseille, France
Performance of the UltraFast Thermometer 2.0 under turbulent cloudy conditions TROPOS: ExAWoMp	University of Warsaw, Poland
PHOSDMAP Phosphorus speciation in dust and marine aerosol particles TROPOS: ACD	GOBABEB, Namibia; INMG, Republic of Cabo Verde
PI-ICE Antarctic campaign TROPOS: ACD	Institut de Ciències del Mar (CSIC), Barcelona, Spain; Institut for Bioscience, Aarhus Universitet, Denmark; University of Birmingham, UK
PollyNet (permanent experiment) Network of institutions with a PollyXT TROPOS: Remote Sensing Dept.	PollyNet Consortium
ProAerosol and Gas Ex, Aerosols at the Baltic Sea TROPOS: ACD	IOW, University of Stockholm, Sweden
Pollution from domestic wood burning Melpitz research station and Melpitz villate TROPOS: ACD, ExaWomp	Saxon State Ministry of the Environment and Agriculture, Dresden, Germany
Real-time characterization of atmospheric Pollen with active remote sensing, Lidar campaign in Melpitz and Leipzig TROPOS: Remote Sensing Dept.	Finnish Meteorlogical Institute, Finland

* *Atmospheric Chemistry Department*

** *Experimental Aerosol and Cloud Microphysics Department*

Cooperations

International cooperations

Research project	Cooperation partners
3D Widefield Sky Scatterer Tomography by Lidar Anchor	Technion University, Haifa, Israel
A-CARE Technical Assistance for EarthCARE related research activities in combination with the A-LIFE field experiment	German Aerospace Center (DLR); University Vienna, Austria; National Observatory of Athens, Greece; European Space Research and Technology Center (ESTEC), The Netherlands
ACD-C Atmospheric Chemistry Chamber	University of British Columbia, Dept. of Chemistry, Canada; University College Cork, Ireland; Institute of Chemistry, Slovenia
ACLOUD Arctic CLoud Observations Using airborne measurements during polar Day	Max Planck Institute for Chemistry, Mainz; Alfred Wegener Institute, Bremerhaven; Karlsruhe Institute for Technology, Germany; University of Mainz, Germany; University of Clermont-Ferrand, France
ACTOS Airborne Cloud Turbulence Observation System - Interaction between turbulent mixing processes and cloud micro-physical characteristics in stratiform boundary layer clouds	Michigan Technological University, Department of Physics, Houghton, USA
ACTRIS Aerosol, Clouds and Trace Gases Research Infrastructure	more than 100 partners from 21 European countries
ACTRIS measurement station Melpitz Cooperation partners involved in research projects at the TROPOS Research Station Melpitz	Norway, United Kingdom, Italy, Switzerland, Czech Republic, Hungary, Ireland, Finland, Austria, Sweden, Bulgaria, Belgium, France, Greece, The Netherlands, Spain, Denmark, Latvia, Poland, Portugal
AerChemMip - Contribution of MPI-ESM-LR-HAM2	ETH Zurich, Switzerland; University Oxforfd, UK; DKRZ, Germany
AEROCLO-SA (Aerosol RadiatiOn and CLOuds in Southern Africa)	Institut de Recherches sur la Catalyse et l'Environnement de Lyon, Laboratoire Atmosphères, Milieux, Observations spatiales, LA Laboratoire d'Aérologie, UNIV LILLE1, Laboratoire d'Optique Atmosphérique, Laboratoire Interuniversitaire des Systèmes Atmosphériques, France
AeroCom Lagrangian Experiment Aerosol GCM Trajectory model intercomparison experiment	University of Exeter, Max Planck Institute for Meteorologie, Hamburg, Germany; ETH Zurich, Institute for Atmospheric and Climate Science, Zurich, Switzerland; Oxford University, UK and further international partners

Appendices: Cooperations

Research project	Cooperation partners
AERONET Aerosol Robotic Network, federation of ground-based remote sensing aerosol networks	Germany, Czech Republic, Denmark, Italy, France, Norway, UK, Spain, Slovenia, Sweden, Hungary, Greece, Switzerland
A-LIFE (ERC starting grant project) Absorbing aerosol layers in a changing climate: aging, lifetime and dynamics	University Vienna, Austria; German Aerospace Center (DLR); Ludwig Maximilian University, Munich, Germany
AIE Atmospheric Environmental Impacts of Aerosol in East Asia	30 partners
Analysis of DYAMOND simulations	ECWMF, Reading, UK; MPI-Met, Hamburg, Germany
Anthropogenic influence of Asian aerosol on tropical cirrus clouds	National Center for Atmospheric Research (NCAR), Boulder, Colorado, USA
APRIL Atmospheric Products from Imager and Lidar	Royal Netherlands Meteorological Institute (KNMI), The Netherlands; Institute for Space Science, Free University of Berlin (FUB), Germany
AQMEII Air Quality Model Evaluation International Initiative	Austria, Australia, Belgium, Canada, Switzerland, Cyprus, Germany, Denmark, Finland, France, Greece, Italy, Luxembourg, Malta, The Netherlands, Norway, Poland, Portugal, Sweden, UK, USA
ATTO (Amazonian Tall Tower Observatory)	Instituto Nacional de Pesquisas da Amazônia INPA, Manaus; Universidade do Estado de Amazonas, Manaus, Brazil; Max Planck Institute for Chemistry, Mainz, Germany
Azores 2017 Measurements on clouds, aerosols, and radiation at the Azores	University of Leipzig, LIM, Leipzig, Germany; Michigan Technological University, Department of Physics, Houghton, USA; Max-Planck-Institute for Chemistry, Mainz, Germany; Brookhaven National Laboratory, Upton, NY, USA; University of Warsaw, Poland
BBComp Biomass burning organic aerosol in Europe and Asia: Molecular composition and impact on air quality	Chubu University, Japan
BC Berlin Orientierende Erfassung von Black Carbon in Deutschland und Identifikation relevanter Quellen mit Chemie-Transport-Modellen	German Environment Agency, Senatsverwaltung Berlin, Germany; TNO, The Netherlands
Central European Air Quality Cooperation Harmonization of aerosol sampling and measurement; exchange of measurement data; comparison of PM transport models	Poland, Czech Republic

Research project	Cooperation partners
ChArMEx / ADRIMED Chemistry-Aerosol Mediterranean Experiment / Aerosol Direct Radiative Impact on the regional climate in the Mediterranean region	France, Italy, Germany
CLOUD Cosmics Leaving OUtdoor Droplets	16 partners from Germany, Switzerland, Finland, Austria, Portugal, Russia, UK, USA
CLOUD – motion Cosmics leaving OUtdoor Droplets - International Training Network	Germany, Switzerland, Finland, Austria, UK
Comparsion of Earth System Models (NorESM, ECHAM, EC-Earth)	Lund University, Sweden; University of Oslo, Norway
COST Chemistry transport model intercomparison	Germany, Denmark, Finland, France, Bulgaria, Estonia, Italy, Malta, Spain, The Netherlands, Norway, Poland, Switzerland, UK, Greece, Israel
COST Action COLOSSAL Chemical On-Line cOmpoSition and Source Apportionment of fine aerosoL	partners from 24 European countries, USA
CyCare Cyprus Clouds, Aerosols, and Rain Experiment	Cyprus University of Technology, Limassol, Cyprus
DACAPO-PESO (Dynamics, Aerosol, Cloud and Precipitation Observations in the Pristine Environment of the Southern Ocean)	University de Magallanes (UMAG), Punta Arenas, Chile; Leipzig Institute for Meteorology (LIM), Germany
EARLINET European Aerosol Research Network	Germany, Italy, Spain, Greece, Switzerland, Sweden, Portugal, Poland, Belarus, France, Bulgaria, Romania, Norway, The Netherlands, Finland, Ireland, Cyprus
EMPIR-BC European Metrology Programme for Innovation and Research - Black Carbon	Germany, France, UK, Finland, Greece, Switzerland
ESA-Aeolus European Space Agency, Atmospheric Dynamics Mission	European Space Research and Technology Center (ESTEC), The Netherlands
ESA-EarthCARE European Space Agency, Earth Clouds, Aerosol and Radiation Explorer	European Space Research and Technology Center (ESTEC), The Netherlands; Japan Aerospace Exploration Agency
EUROCHAMP-2020 Integration of European Simulation Chambers for Investigating Atmospheric Processes – Towards 2020 and beyond	Germany, France, Switzerland, Spain, Ireland, Finland, Greece, Italy, Romania, UK

Appendices: Cooperations

Research project	Cooperation partners
EXCELSIOR ERATOSTHENES: EXcellence Research Centre for Earth SurveiLlance and Space-Based MonItoring Of the EnviRonment	Cyprus, Germany, Greece
Generalized Definition of Relative Humidity	IAPWS/ Joint Committee on Seawater (JCS), Vancouver, Canada
HAMMOZ hosting	ETH Zürich, C2SM Zurich, Switzerland; University Oxford, UK; FMI, Geomar, MPI Hamburg, Germany
Heterogeneous ice and salt crystallisation in aqueous electrolyte and polymeric solutions	State University St. Petersburg, Russia; University Rostock; IOW Warnemünde, Germany; Institute of Thermomechanics AS, Czech Republic; University of Odessa, Ukraine; Kharkov Institute of Technology, Ukraine
IAGOS-CARIBIC In-service Aircraft for a Global Observing System - Civil Aircraft for Remote Sensing and In situ measurement in Tropospheric and Lower Stratosphere based on the Instrumentation Container Concept	Germany, UK, France, The Netherlands, Sweden
ICON-HAMMOZ Development Model development	Max Planck Institute for Meteorologie, Hamburg, Germany; ETH Zurich, Institute for Atmospheric and Climate Science, Zurich, Switzerland; Oxford University, UK; University of Leipzig, Germany
Impact of stochastic shallow cumulus parameterizations on the representation of marine cloud cover	Hans Ertel Center for Weather Reseach, German Weather Service (DWD); Max Planck Institut for Meteorology in Hamburg, Germany
Improved coupling of microphysics and radiation: Internal consistencies in ICON and the external forward operator RTTOV	German Weather Service (DWD)
InDust Cost Action International Network to Encourage the Use of Monitoring and Forecasting Dust Products	29 Cost countries
INP activity of oceanic microorganisms	University of Tromsoe, Norway
Intercomparison of Satellite Derived Wind Observations	EUMETSAT, Darmstadt, Germany
Laboratory investigations in the field of liquid phase chemistry	National Institute of Chemistry Ljubljana, Slovenia; Université de Lyon; Université de Marseilles, France; Semenov Institute of Chemical Physics, Moscow, Russia
LACIS Leipzig Aerosol Cloud Interaction Simulator	USA, UK, Denmark, Germany, Finland, Austria, Switzerland

Research project	Cooperation partners
LACIS-T Turbulent Leipzig Aerosol Cloud Interaction Simulator	University of Ilmenau, Germany; Michigan Technological University, Houghton, USA; University of Utah, Salt Lake City, USA; University of Warsaw, Poland
Lagrangian turbulence in clouds	Max Planck Institute for Dynamics and Self-Organization, Göttingen, Germany; Ilmenau University of Technology, Germany; Michigan Technological University, USA; University of Warsaw, Poland
MACE Manila Aerosol Characterization Experiment	De La Salle University, Manila, Philippines
MARSU Marine Atmospheric Science Unravelled: Analytical and Mass Spectrometric Techniques Development and Application	8 partners from Marocco, Republic of Cabo Verde, France, Austria, Argentina, China
MelCol Charaterization of aerosol particles and their properties in the column above the research station Melpitz	Germany, Switzerland, Greece
Mobile Landstation Determining aerosol and cloud microphysical processes at distinct land-based sites	Lindenberg Meteorological Observatory, Germany; Delft University of Technology, Delft, The Netherlands; University of Cologne, Germany
Mobile Seestation Autonomous measurement platform for the determination of the material and energy exchanges between ocean and atmosphere	Helmholtz Centre for Ocean Research, Kiel; Alfred Wegener Institute für Polar and Marine Research, Bremerhaven; Institute for Meteorology, University Leipzig (LIM); Max Planck Institute for Meteorology, Hamburg; University Hamburg, Germany; National Observatory Athens, Greece
Multirate Methods in CLIMA	CalTech, MIT, NavyMil Monterey
Ocean Science Center Mindelo (OSCM)	Instituto Nacional de Desenvolvimento das Pescas, Mindelo, S. Vicente, Republic of Cabo Verde; Helmholtz Centre for Ozean Research Kiel, Germany
OdCom Objektivierung der Geruchsbeschwerden im Erzgebirgskreis und Bezirk Ústí	7 partners from Germany and Czech Republic
PARAMOUNT Production of Aerosol paRticle orgAnic Matter in ClOUds: chamber and laboratory studies, mechanisms, modelling and iNTegration	University Paris-Est Créteil Val de Marne (UPEC); Institut Pierre Simon Laplace (IPSL); Laboratoire Interuniversitaire des Systèmes Atmosphériques (LISA); Aix-Marseille Université Laboratoire de Chimie de l'Environnement, France
PHOSDMAP Phosphorus speciation in dust and marine aerosol particles	GOBABEB, Namibia; Institute for Meteorology and Geophysics, Mindelo, S. Vicente, Republic of Cabo Verde

Appendices: Cooperations

Research project	Cooperation partners
PI-ICE	Institut de Ciències del Mar (CSIC), Barcelona, Spain; Institut for Bioscience, Aarhus Universitet, Denmark; University of Birmingham, UK
PollyNet Development and application of Polly systems	Finnish Meteorological Institute, Kuopio, Finland; Department of Applied Environmental Science, Stockholm University, Sweden; Institute of Geophysics, University of Warsaw, Poland; Universidade de Évora, Centro de Geofísica de Évora, Portugal; National Institute of Environmental Research, Air Quality Research Division, Korea; National Observatory of Athens, Greece, Tel-Aviv University, Tel Aviv, Israel
Properties and impacts of Secondary Organic Aerosols composed of highly oxidized multifunctional organic compounds (HOMs SOA)	Weizmann Institute, Rehovot, Israel
Regional modelling of the marine multiphase chemistry	Centre for Environmental and Climate Research, Lund University, Sweden
Theory of Ice and Salt Crystallization in Aqueous Electrolyte and Polymeric Solutions	Georgia Institute of Technology, Atlanta, Georgia, USA; IAWPS International Association for the Properties of Water and Steam; Institute for Thermal Physics, Ekaterinburg, Russia; Joint Institute for Nuclear Research Dubna; St. Petersburg State University, Saint Petersburg, Russia; SUNY at Buffalo, Buffalo, NY, USA
Tobac Development of an Open-Source-Python Software for Tracking and Object-based Analysis of Clouds in Observations and Simulations	University of Oxford, UK
WCCAP World Calibration Center for Aerosol Physics	Anmyeon, Republic of Korea; Malaysian Meteorological Service, Danum Valley, Malaysia; Bulgarian Academy of Sciences, BEO-Moussala, Bulgaria

National cooperations

Research project	cooperation partners
Absorption efficiency of Black Carbon: determining representative atmospheric values and implications for radiative transfer	Max Planck Institute for Chemistry, Mainz
$(AC)^3$ projekt A-01, DFG-SFB/Transregio 172 Arctic aerosol, cloud, and radiation characteristics from ground–based observations and modelling	Leipzig Institute for Meteorology, University Leipzig; Alfred Wegener Institute, Bremerhaven & Potsdam

Research project	cooperation partners
(AC)³ projekt A-01, DFG-SFB/Transregio 172 Radiative closure studies and cloud radiative effects	Leipzig Institute for Meteorology, University Leipzig; University of Cologne, Deutschland
(AC)³ project D-02, DFG-SFB/Transregio 172 Model–based quantification of aerosol and cloud processes and their effects in the Arctic	Leipzig Institute for Meteorology, University Leipzig; Alfred Wegener Institute, Bremerhaven & Potsdam
(AC)³ project A-02, DFG-SFB/Transregio 172 Tethered balloon-borne energy budget measurements in the cloudy central Arctic	Leipzig Institute for Meteorology, University Leipzig; Alfred Wegener Institute, Bremerhaven & Potsdam
(AC)³ project B-03, DFG-CRC/Transregio 172 Characterization of Arctic mixed-phase clouds by airborne in-situ measurements and remote sensing	Leipzig Institute for Meteorology, University Leipzig; University of Cologne, Deutschland
(AC)³ project B-04, DFG-SFB/Transregio 172 Properties and sources of Arctic ice nucleating particles and cloud condensation nuclei by ship-based in-situ measurements	Leipzig Institute for Meteorology, University Leipzig; Alfred Wegener Institute, Bremerhaven & Potsdam
(AC)³ project B-04, DFG-SFB/Transregio 172: phase II Spatial distribution, sources and cloud processing of aerosol particles	Leipzig Institute for Meteorology, University Leipzig; Alfred Wegener Institute, Bremerhaven & Potsdam
ACTRIS-D Aerosol, Clouds and Trace Gases Research Infrastructure - Deutschland	13 project partners
Aging of the emissions in a smog chamber	Helmholtz Zentrum Munich; German Research Center for Environmental Health (GmbH); Cooperation Group of Comprehensive Molecular Analytics
AirShield (BMBF joint project) Airborne remote sensing for hazard inspection by network enabled lightweight drones	8 partners
ALADINA Investigating the Small-Scale Vertical and Horizontal Variability of the Atmospheric Boundary Layer Aerosol using Unmanned Aerial Vehicles	Technical University Baunschweig; University Tübingen
Azores 2017 Measurements on clouds, aerosols, and radiation at the Azores	Leipzig Institute for Meteorology, University Leipzig; Max Planck Institute for Chemistry, Mainz
BC Berlin Orientierende Erfassung von Black Carbon in Deutschland und Identifikation relevanter Quellen mit Chemie-Transport-Modellen	German Environment Agency, Senatsverwaltung Berlin, Germany; TNO, The Netherlands

Appendices: Cooperations

Research project	cooperation partners
CARIBIC-AMS An Automated Aerosol Mass Spectrometer for the Regular Chemical Characterization of Aerosol Particles in the Upper Troposphere and Lowermost Stratosphere	Max Planck Institute for Chemistry, Mainz
CLOUD-16	Goethe University Frankfurt am Main
Colrawi Combined Observations with Lidar RAdar and WInd profiler	German Weather Service (DWD), Lindenberg
ESA-Aeolus European Space Agency, Atmospheric Dynamics Mission	DLR Oberpfaffenhofen
EVAA Experimental Validation and Assimilation of Aeolus observations: Validation of aerosol and wind products with ground-based instruments of TROPOS	German Weather Service (DWD); Ludwig-Maximilians-Universität München
Extramural Research Programme Improved Nowcasting of Convective Initiation with METEOSAT SEVIRI (INCITES)	German Weather Service (DWD), Offenbach;
GUAN German Ultrafine Aerosol Network	Federal Environmental Agency, Dessau-Roßlau, Langen, Garmisch-Partenkirchen, Hofsgrund; German Weather Service (DWD), Hohenpeißenberg; IUTA Duisburg e. V.; Helmholtz Zentrum München - German Research Center for Environmental Health
HD(CP)² (BMBF) High definition clouds and precipitation for advancing climate prediction	16 partners
HuCAR Classification of HULIS carbon from different atmospheric environments via a 2-D-Off-line chromatography (HuCar)	Helmholtz Centre for Environmental Research
IAGOS-D In-situ Aircraft for a Global Observing System	Research Center Jülich; Karlsruhe Institute of Technology;Max Planck Institutes for Chemistry and Biogeochemistry, Jena; German Aerospace Center, University of Heidelberg
INFECTIONS‘21 Transmission Control of Infections in the 21st Century, Leibniz Research Cluster	14 partners
Influence of soot on air quality and climate (pilot study)	Saxon State Agency for Environment, Agriculture and Geology

Research project	cooperation partners
INUIT Ice Nuclei Research Unit, DFG Research Unit	Max Planck Institute for Chemistry, Mainz; Goethe University Frankfurt am Main; Technical University Darmstadt; University Mainz; University Bielefeld; KIT Karlsruhe
Improvement of data quality for the measurement of ultrafine particles in the outdoor air	Saxon State Agency for Environment, Agriculture and Geology
Isotope analysis of stable oxdiation products induced by radical reactions in the aqueous phase	Helmholtz Centre for Environmental Research
KLENOS Influence of a change of energy policy and climate on air quality as well as consequences for the compliance with limit values and examining further emissions	Federal Environmental Agency, Dessau-Roßlau; TU Dresden, Institut für Hydrologie und Meteorologie
Leibniz Research Alliance “Crisis in a Globalized World”	22 partners
Low Emission Zone Deep analysis to verify the effectiveness of the Leipzig Low Emission Zone	Saxon State Agency for Environment, Agriculture and Geology
MARGA Physico-chemical characterization of the dynamic behaviour of ammonium salt in particulate matter aerosol particles - testing a new high-resolutions measurement method at EMEP-Level 3-Station Melpitz	Federal Environmental Agency, Dessau-Roßlau
MarParCloud Marine biological production, organic aerosol particles and marine clouds: a Process Chain (Leibniz competition project)	Leibniz Center for Tropical Marine Ecology; Leibniz Institute for Baltic Research; Warnemünde; University of Oldenburg; University of Hamburg
MARSU: Marine Atmospheric Science Unravelled: Analytical and Mass Spectrometric Techniques Development and Application	8 partners
MetPVNet Development of innovative satellite-based methods for improved forecasts of PV-yield	11 partners
MMS Leibniz Network “Mathematical Modeling and SImulation (MMS)”	24 partners
PalMod From the Last Interglacial to the Anthropocene: Modeling a Complete Glacial Cycle	17 partners

Appendices: Cooperations

Research project	cooperation partners
Parallel coupling framework and modern time integration methods for detailed cloud processes in atmospheric models	Technical University Dresden; Centre for Information Services and High Performance Computing, Desden; Martin Luther University Halle-Wittenberg
PM-OST Source appointment of PM10 and estimation of contribution from trans-boundary air pollution	Senate Department for Urban Development and Housing, Berlin; Saxon State Agency for Environment, Agriculture and Geology; Ministry of Rural Development, Environment and Agriculture of the Federal State of Brandenburg; Ministry of Rural Development, Protection of Nature and Geology, State of Mecklenburg-Western Pomerania
PollyNet Network of institutions with a PollyXT	German Weather Service (DWD), Hohenpeißenberg
Prototype Doppler Lidar (design phase)	ABACUS-Laser Göttingen; Licel Berlin
Quantification of the secondary ice production mechanisms: droplet shattering on freezing vs. droplet-ice collision	Institute of Meteorology and Climate Research; Karlsruhe Institute of Technology
SOARiAL Spread of Antibiotic Resistance in an Agrarian Landscape	Leibniz Institute DSMZ - German Collection of Microorganisms and Cell Cultures Braunschweig; Leibniz Centre for Agricultural Landscape Research Müncheberg; Leibniz Institute for Agriculture and Bioeconomy Potsdam, FU Berlin
Statistical modelling of aerosol particle size distribution in urban and rural environment	Technical University of Braunschweig, Section of Climatology and Environmental Meteorology
Theory of ice and salt crystallisation in aqueous electrolyte and polymeric solutions	Polymer Physics, University Rostock; Leibnitz Institute for Baltic Sea Research, Warnemünde
WTimpact: Citizen Science as Transfer Instrument	Leibniz Institute for Zoo and Wildlife Research; Leibniz Institute for Science and Mathematics Education; Leibniz-Institute for Media Research

Boards

Boards of trustees

Name	Institution
Prof. Dr. R. Haak	Federal Ministry of Education and Research
RORin C. Liebner	Saxon State Ministery for Science and the Arts
Prof. Dr. A. Wahner	Forschungszentrum Jülich GmbH, Institute for Energy and Climate Research, IEK-8: Troposphere

Scientific advisory board

Name	Institution
Prof. Dr. H. Schlünzen **(Chairperson)**	University of Hamburg, Meteorological Institute
Dr. C. George	IRCELYON - Institut de Recherches sur la Catalyse et l'Environnement de Lyon, University Claud Bernard
Prof. Dr. C. Hoose	Karlsruhe Institute of Technology (KIT), Institute of Meteorology and Climate Research (IMK)
Prof. Dr. T. Koop	Bielefeld University, Faculty of Chemistry
Prof. Dr. M. Kulmala	University of Helsinki, Department of Physics
Prof. Dr. J. Quaas	University Leipzig, Leipzig Institute for Meteorology (LIM)
Prof. Dr. M. Rapp	German Aerospace Center, Institute of Atmospheric Physics
Prof. Dr. R. Shaw	Michigan Technological University, Department of Physics
Dr. F. Beyrich	Meteorological Observatory Lindenberg
Prof. Dr. A. Engel	GEOMAR Helmholtz Centre for Ocean Research Kiel

Appendices: Boards

Members of the TROPOS association

Name	Institution
Prof. Dr. C. Jacobi **(Chairman)**	Leipzig University, Leipzig Institute for Meteorology (LIM)
RORin C. Liebner	Saxon State Ministery for Science and the Arts
Prof. Dr. R. Haak	Federal Ministry of Education and Research
Prof. Dr. B. Abel	Leibniz Institute of Surface Engineering (IOM)
Prof. Dr. B. Brümmer	University of Hamburg, Meteorological Institute
Prof. Dr. W. Engewald	Leipzig University, Faculty for Chemistry and Mineralogy
Prof. Dr. J. Quaas	Leipzig University, Leipzig Institute for Meteorology (LIM)
Dr. H.-H. Richnow	Helmholtz Centre for Environmental Research (UFZ)
Prof. Dr. C. Simmer	Rhineland Friedrich Wilhelm University Bonn, Institute for Meteorology
Prof. Dr. P. Warneck	Professor emeritus
Prof. Dr. E. Renner, honorary member	Professor emeritus
Prof. Dr. J. Heintzenberg, honorary member	Professor emeritus

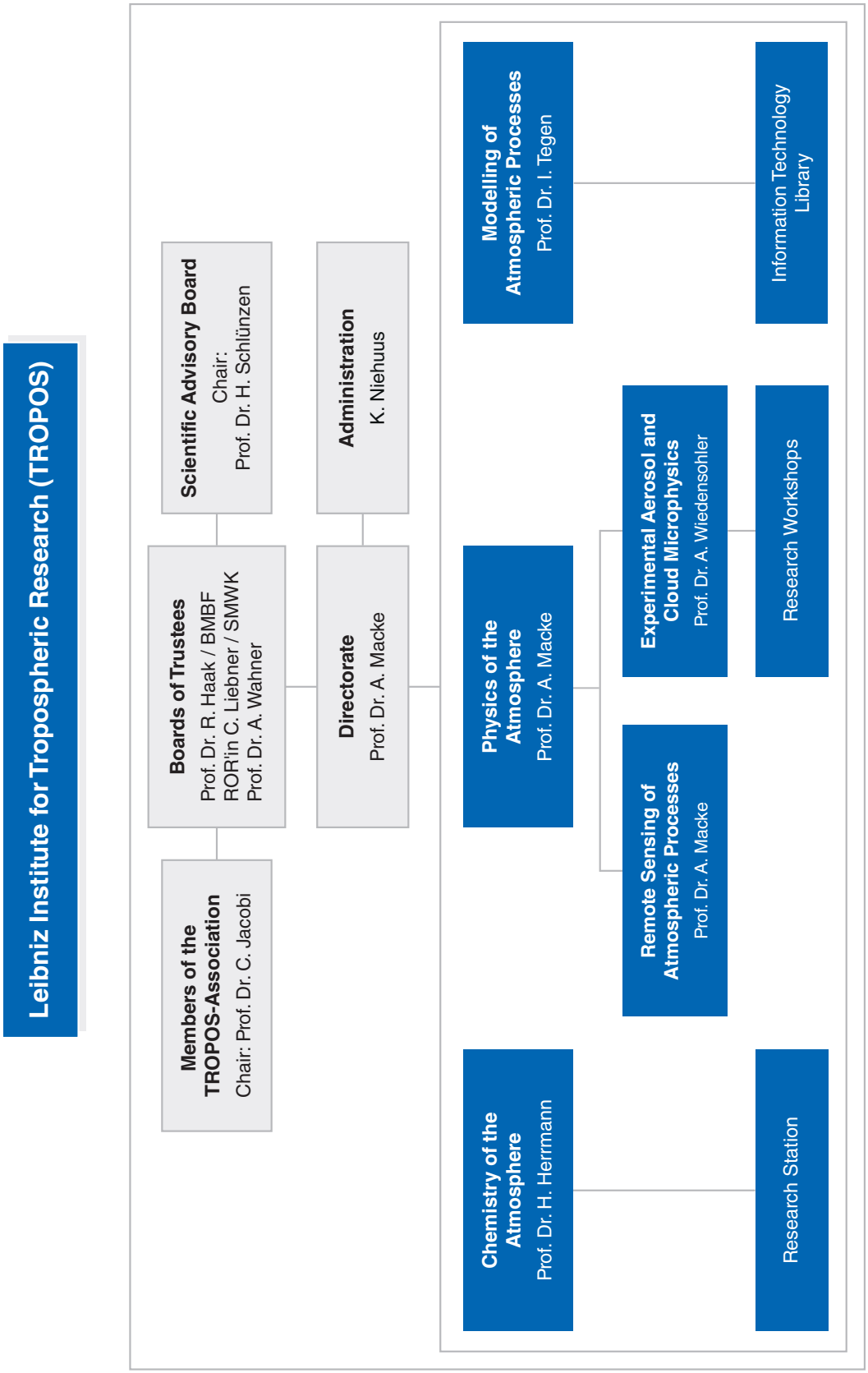
Leibniz Institute for Tropospheric Research (TROPOS)
Members of the TROPOS-Association
Chair: Prof. Dr. C. Jacobi
Boards of Trustees
Prof. Dr. R. Haak / BMBF
RORi'in C. Liebner / SMWK
Prof. Dr. A. Wahner
Scientific Advisory Board
Chair:
Prof. Dr. H. Schlünzen
Directorate
Prof. Dr. A. Macke
Administration
K. Niehuus
Chemistry of the Atmosphere
Prof. Dr. H. Herrmann
Physics of the Atmosphere
Prof. Dr. A. Macke
Modelling of Atmospheric Processes
Prof. Dr. I. Tegen
Remote Sensing of Atmospheric Processes
Prof. Dr. A. Macke
Experimental Aerosol and Cloud Microphysics
Prof. Dr. A. Wiedensohler
Research Station
Research Workshops
Information Technology
Library

TROPOS

Leibniz Institute for Tropospheric Research
Leibniz-Institut für Troposphärenforschung e.V. Leipzig
Member of the Leibniz Association (WGL)

Permoserstraße 15
04318 Leipzig
Germany

Phone: ++49 (341) 2717-7060
Fax: ++49 (341) 2717-99-7060
Email: info@tropos.de
Internet: www.tropos.de